

Organic reactions catalyzed by functionalized mesoporous silica

Thesis submitted to

Cochin University of Science and Technology

in partial fulfilment of the requirements for the degree of

Doctor of Philosophy

in

Chemistry

under the Faculty of Science

by

Sinija P. S.



DEPARTMENT OF APPLIED CHEMISTRY

COCHIN UNIVERSITY OF SCIENCE AND TECHNOLOGY

COCHIN-682 022, KERALA, INDIA

May 2016

Organic reactions catalyzed by functionalized mesoporous silica

Ph.D. Thesis under the Faculty of Science

By

Sinija P. S.

Research Fellow

Department of Applied Chemistry

Cochin University of Science and Technology

Kochi, India 682022

Email: pssinija@gmail.com

Supervising Guide

Dr. K. Sreekumar

Professor

Department of Applied Chemistry

Cochin University of Science and Technology

Kochi, India 682022

Email: ksk@cusat.ac.in

Department of Applied Chemistry

Cochin University of Science and Technology

Kochi, India 682022

May 2016



Department of Applied Chemistry
Cochin University of Science and Technology
Kochi, India 682022

Dr. K. Sreekumar
Professor

Phone-0484-2862430
Email: ksk@cusat.ac.in

Certificate

This is to certify that the thesis entitled “**Organic reactions catalyzed by functionalized mesoporous silica**” is a genuine record of original research work carried out by **Mrs. Sinija P. S.**, under my supervision, in partial fulfilment of the requirements for the award of the degree of Doctor of Philosophy in Chemistry under the Faculty of Science of Cochin University of Science and Technology, and further that no part thereof has been presented before for the award of any other degree. All the relevant corrections and modifications suggested by the audience and recommended by the doctoral committee of the candidate during the presynopsis seminar have been incorporated in the thesis.

Cochin-22
17-05-2016

Dr. K. Sreekumar
(Supervising Guide)

Declaration

I hereby declare that the work embodied in the thesis entitled **“Organic reactions catalyzed by functionalized mesoporous silica”** is based on original research work done by me under the supervision of **Dr. K. Sreekumar**, Professor, Department of Applied Chemistry, Cochin University of Science and Technology, Cochin-22, and the same has not been submitted elsewhere for the award of any other degree.

Cochin-22

17-05-2016

Mrs. Sinija P. S.

“Man needs difficulties in life, because they are necessary to enjoy the success.”

*“Those who cannot work with their hearts achieve but a hollow,
half-hearted success that breeds bitterness all around.”*

A. P. J. Abdul Kalam

Acknowledgement

I take this opportunity to convey my sincere thanks and deep appreciation to those who have supported and helped me to accomplish my dream. It is a fact that I could not have completed my thesis without their help.

First and foremost, I am deeply indebted to my supervising guide, Dr. K. Sreekumar, Professor, Department of Applied Chemistry, Cochin University of Science and Technology, whose enthusiasm, encouragement, creativity, patience and dedication to science exemplified to me what a researcher should be. It is my supreme honor to have worked as a student in his research group. He gave me complete freedom during my entire PhD studies. I thank him for his constant support, encouragement, affection and insightful suggestions throughout my work,

My sincere gratitude to Dr. K. Girish Kumar, former HOD, Department of Applied Chemistry, CUSAT is recorded. He gave me the best platform and provided opportunities in this department. I am highly thankful to Dr. N. Manoj, Head, Department of Applied Chemistry, CUSAT for rendering all the necessary facilities for the research work. I express my heartfelt gratitude to Dr. P. V. Mohanan, doctoral committee member for his support during this study. I would like to extend my sincere thanks to all faculty members and non-teaching staff of the department, for their never-ending help and support during my research work,

My research carrier was started with the most talented seniors, Dr. Rajesh Krishnan, Dr. Mangala, Dr. Kannan. Dr. Elizabeth, Dr. Maheshkumar and Dr. Anoop. I express my sincere gratitude to them at this juncture. No words of gratitude are enough to acknowledge my labmates. From the beginning to this time, I have enjoyed the benefit of their love and constant support. So I am highly indebted to Dr. Jiby, Ms. Smitha, Ms. Sherly, Ms. Anjali, Ms. Jisha, Ms. Sowmya, Ms. Anjaly Jacob, Ms. Jisha Pillai, Ms. Letcy and Ms. Shaibuna. I am also grateful to Dr. Sona, Dr. Jaimy for their valuable suggestions and support. I am

also thankful to Ms. Bhavya, Ms. Shanty, biochemistry labmates, Ms. Aswathy, Ms. Namitha and friends of the department. I recollect the memories of the support offered by the friends Ms. Jabia, Ms. Sreedevi, and Mr. Jithin during my work. I extend my gratitude to Dr. Priya and Dr. Reni for their motivation and encouragement. I thank all my friends, for their care and friendship.

I extend my sincere thanks to Dr. M. K. Jayaraj, Professor, Department of Physics, Cochin University of Science and Technology, for providing facilities for XRD analysis. I am also thankful to Mr. Vikas and Mr. Sajan, Dept. of Physics for their help in XRD analysis. I would like to express words of appreciation for the services rendered by RGCBS, TVM (MALDI-MS), AIIMS, Kochi (XPS), Dr. Bhavana Sharama from IIT, New Delhi, (solid state NMR analysis) and STIC, CUSAT, especially, Dr. Shibu for their boundless help. I remember Vishnu, Alpha Chemicals with great gratitude and condolence. Financial assistance in the form of University fellowship and UGC-BSR is acknowledged with gratitude.

Last, but not the least, I would like to thank my family. I thank my husband for his long time support, understanding, love and encouragement at all times when I met with difficulties. My lovely son, Ahsu always brings me the most happiness in my life. Words are not enough to thank my mother who has always stood with me as care taker of my child. I remember my father and grandmother, although they are no longer with us, who have encouraged me at the early stages of my studies. I thank my mother in law for her prayer and blessings. I am grateful to my brothers and sister in laws whose encouragement has provided me enormous support. I was so happy with my nephews Appu and Aman in their charming presence.

My best wishes to everyone whose entry into my life has supported and motivated me to pursue my dream.

Above all I bow my head to **God Almighty** for his blessings and gave me strength to cross the toughest situations.

Sinija P. S.

||| Preface |||

Heterogeneous catalysis plays a crucial role in modern synthetic organic chemistry as well as meets the challenges of sustainability which is an integral part of green chemistry. Solid supported catalysts have wide applicability in both academic and industrial areas due to their recyclability, enhanced catalytic reactivity, and selectivity. Periodic mesoporous silica with high surface area, narrow pore size distribution and tunable pore diameters, have attracted much attention in recent years due to their promising properties and applications in various areas including adsorption, separation, drug delivery, sensing and catalysis. Catalytic applications of such materials have been extended to numerous organic reactions. In this thesis, our aim was to develop catalysts with high density of active sites on mesoporous silica, because conventional routes to synthesize functionalized silica materials resulted in low amount of organic functionality. We have aimed to utilize functionalized mesoporous silica in heterogeneous catalysis, with special emphasis on multicomponent reactions and C-C bond forming reactions.

The thesis is structured into seven chapters, a brief summary of which is given here.

Chapter 1 deals with a brief introduction on different types of periodic mesoporous silica, their synthesis and organically modified silica through diverse functionalization methods. A survey of literature on organic reactions catalyzed by functionalized mesoporous silica and objectives of the present work are also described in this chapter.

Chapter 2 describes the synthesis and characterization of N,N-dialkylated polyamine mesoporous silica catalyst. Ring opening polymerization of epichlorohydrin by thiol functionalized mesoporous silica (MS) is

described. Lewis base site was created on silica surface and catalytic activity was studied in the synthesis of α -amino nitriles in water. Various factors which control the reaction was studied and the mechanism is also presented in this chapter.

Chapter 3 demonstrates the synthesis and characterization of Ti-grafted polyamidoamine dendritic silica hybrid catalyst. A simple, highly efficient and eco-friendly approach for the preparation of biologically potent pyranopyrazoles and 3, 4-dihydropyrimidin-2(*1H*)-ones are discussed in this chapter. The experimental parameters are optimized, scope of substrates and reusability of the catalyst are studied. The dual activation mechanism of the hybrid catalyst is also proposed.

Chapter 4 demonstrates the synthesis and characterization of polyamine and chiral amine functionalized mesoporous silica (MS I). Novel N-alkylated polyamine functionalized mesoporous silica was synthesized via radical polymerization of α -methyl styrene within silica framework followed by post-functionalization method. The catalyst was found to be active for the synthesis of flavanone by the Claisen-Schmidt condensation of benzaldehyde and 2-hydroxyacetophenone under solvent free condition. Chiral amine functionalized silica catalyst was employed for asymmetric Mannich reaction. Various factors which control the reactions are studied and the mechanisms of both reactions are also proposed.

Chapter 5 deals with the synthesis and characterization of mesoporous silica (MS)-supported N-heterocyclic carbene (NHC)-Pd complex. Catalytic application of the catalyst in Suzuki coupling and direct arylation reactions is described. The experimental parameters are optimized, scope of substrates, reusability of the catalyst and mechanism are studied.

Chapter 6 discusses the synthesis and characterization of polypeptide functionalized mesoporous silica (MS). Ring opening polymerization (ROP)

of N-carboxyanhydride (NCA) chemistry was applied in this chapter. The prepared material was used as Lewis base catalyst in aminolysis of epoxides. The experimental parameters are optimized, scope of substrates, reusability of the catalyst and mechanism are studied.

Chapter 7 comprises the summary of the present work and conclusions drawn from the earlier chapters.

Contents

Chapter 1

FUNCTIONALIZED MESOPOROUS SILICA AS CATALYSTS 01 - 56

1.1	Introduction	02
1.2	Choice of inorganic support: mesoporous silica	02
1.3	Mesoporous silica with organically modified surface	10
1.4	Polymer brushes on silica surface	20
1.5	Silica-supported dendrimer	26
1.6	Polypeptide brushes on silica	27
1.7	Silica-supported metal complexes	28
1.8	Organically functionalized silica materials as catalyst	30
1.9	Scope of the present study`	42
1.10	Main objectives of the work	42
1.11	Analysis and characterization	43
	References	46

Chapter 2

MESOPOROUS SILICA SUPPORTED N,N-DIALKYLATED POLYAMINE AS CATALYST IN STRECKER AMINO ACID SYNTHESIS 57 - 89

2.1	Introduction	58
2.2	Results and Discussion	59
2.2.1	Synthesis of mesoporous silica (MS) and N,N-dialkylated polyamine@MS	59
2.2.2	Characterization of MS and N,N-dialkylated polyamine@MS	63
2.2.3	Evaluation of catalytic performance	70
2.3	Conclusion	76
2.4	Experimental	77
	References	85

Chapter 3

Ti-GRAFTED POLYAMIDOAMINE DENDRITIC SILICA HYBRID CATALYST IN BIGINELLI REACTION AND PYRANOPYRAZOLE SYNTHESIS

91 - 130

3.1	Introduction	92
3.2	Results and Discussion	93
3.2.1	Synthesis of mesoporous benzene silica and Ti-grafted polyamidoamine dendritic silica hybrid catalyst	93
3.2.2	Characterization of mesoporous benzene silica and periodic mesoporous dendritic silica hybrids	95
3.2.3	Catalytic performance	104
3.3	Conclusion	114
3.4	Experimental	114
	References	127

Chapter 4

FUNCTIONALIZED MESOPOROUS SILICA CATALYSTS IN FLAVANONE SYNTHESIS AND ASYMMETRIC MANNICH REACTION

131 - 175

4.1	Introduction	131
4.2	Results and Discussion	134
4.2.1	Post-functionalization of the polymer-MS I silica material	135
4.2.2	Physicochemical characterization of MS I and polymer functionalized MS I material	137
4.2.3	Catalytic performance	146
4.3	Conclusion	158
4.4	Experimental	159
	References	170

Chapter 5

MESOPOROUS SILICA-SUPPORTED NHC-Pd COMPLEX: SYNTHESIS AND APPLICATION IN AROMATIC COUPLING REACTIONS

177 - 207

5.1	Introduction	177
5.2	Results and Discussion	181

5.2.1	Synthesis of silica-supported NHC-Pd complex	181
5.2.2	Characterization of NHC-Pd complex and silica-supported NHC-Pd complex	182
5.2.3	Catalytic performance	190
5.3	Conclusion	198
5.4	Experimental	199
	References	204

Chapter 6

POLYPEPTIDE FUNCTIONALIZED MESOPOROUS SILICA AS CATALYST IN AMINOLYSIS OF EPOXIDES 209 - 237

6.1	Introduction	209
6.2	Results and Discussion	212
6.2.1	Synthesis of L-phenylalanine N-carboxyanhydride (Phe-NCA)	212
6.2.2	Grafting of polypeptide onto silica surface	212
6.2.3	Characterization of polypeptide functionalized mesoporous silica catalyst	214
6.2.4	Evaluation of catalytic performance	220
6.3	Conclusion	226
6.4	Experimental	227
	References	234

Chapter 7

SUMMARY AND CONCLUSION 239 - 243

PUBLICATIONS 245

Chapter 1

FUNCTIONALIZED MESOPOROUS SILICA AS CATALYSTS

Contents	1.1	Introduction
	1.2	Choice of inorganic support- Mesoporous silica
	1.3	Mesoporous silica with organically modified surface
	1.4	Polymer brushes on silica surface
	1.5	Silica-supported dendrimer
	1.6	Polypeptide brushes on silica
	1.7	Silica- supported metal complexes
	1.8	Organically functionalized silica materials as catalyst
	1.9	Scope of the present study
	1.10	Main objectives of the work
	1.11	Analysis and Characterization

Solid catalysts, especially, those based on micelle-templated silica with high surface area are beginning to play a significant role in organic synthetic chemistry. A wide variety of novel materials can be prepared through the chemical modification of periodic mesoporous silica with organic and inorganic functionalities. They have been increasingly used as catalysts in many organic reactions. A brief introduction on different types of periodic mesoporous silica, their synthesis and organically modified silica through diverse functionalization methods has been described. Recent literature on organic reactions catalyzed by functionalized mesoporous silica is surveyed and the objectives of the present work are described in this chapter. Functionalized mesoporous silica is more environmentally friendly and can be alternative to traditional homogeneous catalysts. They can be used as heterogeneous catalysts in various organic reactions, which constitute the main body of the thesis.

1.1 Introduction

The demand for new, sustainable, and “green” methods in organic chemistry has stimulated the scientific community quite significantly. Catalysis is a good tool to achieve this goal, because catalyzed reactions can be performed more efficiently by reducing the energy consumption and by reducing the waste production. The step towards an ideal synthesis can be achieved by heterogenization of catalyst where it meets the principles of green chemistry.¹ The advantages of heterogeneous catalysts over homogeneous ones are numerous. Heterogeneous catalysts can be recycled after a reaction. They can be used continuously in successive reaction runs. This could improve the environmental, economic and sustainability factors of organic reactions. The separation of the catalyst from the reaction mixture is simplified. The ultimate goal of heterogeneous catalysis must be 100 % product selectivity. This could eliminate the unwanted side products and allow the process to be greener.

1.2 Choice of inorganic support: mesoporous silica

The inert support that is used for heterogenization of catalytically active species should fulfill the following requirements²:

- it should not influence or harm the structure of the catalytically active species
- it should be easy to immobilize the species on the surface of the support
- it should be chemically and mechanically stable under reaction conditions

- it should have a large specific surface area accessible to the reaction media
- it should have a particle size and shape that allows filtration
- it should be non-toxic and cheap to produce and dispose off

Porous silica materials are common supports that satisfy these requirements. Silicon is the second most abundant element in the earth's crust.³ In nature, silicon combines with oxygen and forms a multitude of silicate minerals. Despite the intensive studies on silicon dioxide (silica) over the years, it is still attracting much research interest in different fields.⁴ A great number of natural materials, which possess cavities, cages, or tunnels, such as zeolites are not only of high academic interest, but also of intense practical value, because they exhibit well-defined host-guest chemistry.⁵ Porous materials with high surface area and unique surface chemistry play an important role in the fields of catalysis, adsorption and separation. They offer a unique porous structure, specific reaction and adsorption selectivities. According to IUPAC notation,⁶ three classes of porous materials are

- pore diameter < 2 nm — microporous materials
- 2 nm $<$ pore diameter < 50 nm — mesoporous materials
- pore diameter > 50 nm — macroporous materials

Silica based networks present a great variety of possible structures because of the flexibility of tetra-coordinated Si, and easy control of the sol-gel process (hydrolysis and condensation reactions). Much effort was devoted to creating these zeolite-like materials, and led to the discovery of

the first novel mesoporous silica networks of M41S family, named as MCM-41, which was obtained by Mobil in 1992.^{7,8} These materials superseded zeolite molecular sieves, which were restricted to a pore size of around 15 Å. Like the microporous crystalline zeolites, this class of materials is characterized by large specific surface area, ordered pore systems, and well-defined pore radius distribution. Unlike the zeolites, however, the M41S materials have pore diameters ranging from 2 to 10 nm and exhibit amorphous or crystalline porewalls.⁹ Compared with the dimension of the zeolite micropores (< 2 nm), mesopores (2-50 nm) permit faster migration of guest molecules in the host framework. According to IUPAC, a mesoporous material can be disordered or ordered in a mesostructure.

The discovery of ordered mesoporous materials by the hydrolysis and condensation of inorganic precursors in the presence of surfactant micelles represent a significant breakthrough in porous material synthesis. Soon after the discovery of M41S, significant research effort has been extended to achieve control over physical characteristics of mesoporous silica, including pore size and morphology, by incorporating a broad range of organic and inorganic materials as templates. These templates may be defined as a central structure around which a silica network develops in such a way that removal of the template creates a cavity with morphological features related to those of the template.¹⁰ Hence the pore sizes of these materials can be tailored depending on the synthesis method, ranging from 2 to 30 nm.¹¹⁻¹³ These morphological features could be affected by the association of the template with silica matrix, such as interaction between template and silica matrix, and the relative size of template used to construct the silica matrix.

1.2.2 Periodic mesoporous silica

The work discussed in this thesis will predominantly utilize periodic mesoporous silica, where the mesopores range between 20 and 500 Å. In 1992, a new family of mesoporous inorganic materials named as MCM-41 was originally developed by Mobil scientists through surfactant-temple mechanism which used the hydrolysis of silica sources in water under the presence of surfactant which was self-assembled as micelles in water.^{16,17} MCM-41, one of the members of this family of mesoporous sieves, possesses a hexagonal array of uniform mesopores which can vary from 1.5 nm to 10 nm in size; has surface area above 700 m²/g and hydrocarbon sorption capacity of 0.7 cc/g or greater. Because of the excellent properties of MCM-41, it has attracted significant interest in the fields of catalysis, filtration, separation etc.

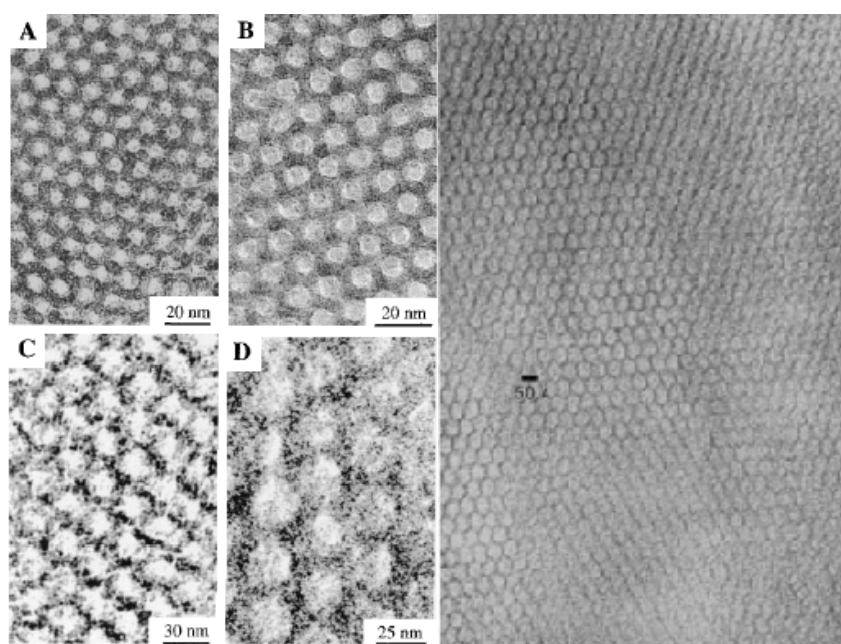


Fig. 1.1 TEM images of SBA-15 mesoporous silica with different pore size & MCM-41^{8,10}

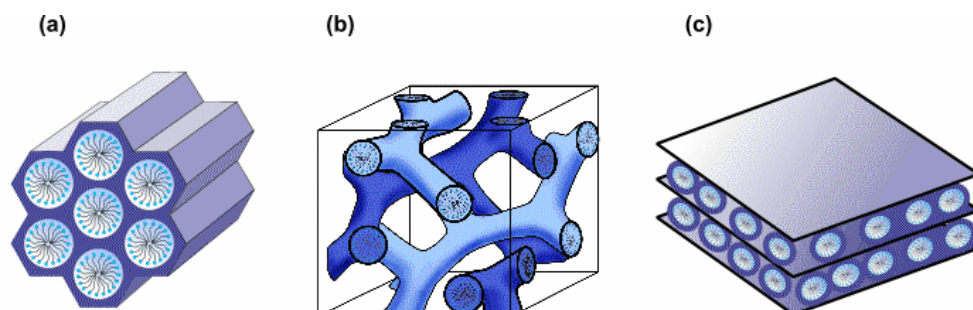


Fig. 1.2 Structure of mesoporous M41S networks: a) hexagonal (MCM-41), b) cubic (MCM-48), and c) lamellar (MCM-50)¹⁸⁻²⁰

Figure 1.1 is the representative TEM image of MCM-41 and SBA-15 which shows the ordered array of hexagonal channels with a diameter of 4-6 nm. This class of periodic mesoporous silica networks is well-known as the M41S phase, including three representatives such as MCM-41, MCM-48 and MCM-50 (Figure 1.2).¹⁸⁻²⁰

After the development of MCM-41, another milestone in the development of mesoporous inorganic solids was SBA-15, which was synthesized by Stucky's group in 1997.^{21,22} Zhao et al.²³ synthesized well-ordered hexagonal mesoporous silica structure named as SBA-15 using an amphiphilic block copolymer of PEO-PPO-PEO to direct the organization of polymerizing silica species. Through choosing the length of block copolymer, reaction condition, the pore sizes can vary from 4.6 to 30 nm, pore volume fractions upto 0.85, and silica wall thickness changes from 3.1 to 6.4 nm.

A common route for the synthesis of periodic mesoporous materials is shown in the Figure 1.3.²³

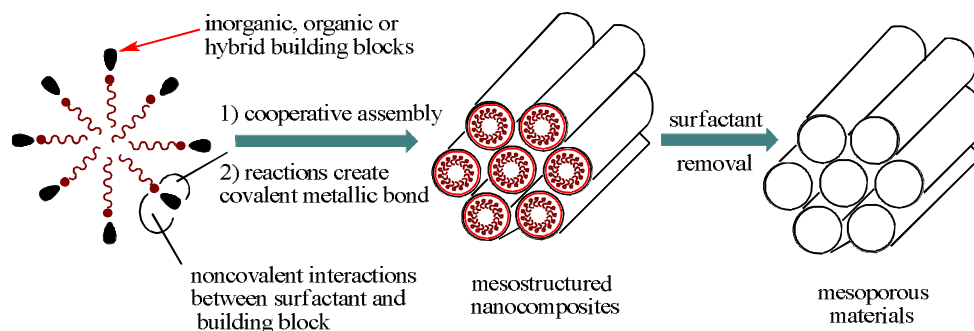


Fig. 1.3 Schematic representation of periodic mesoporous materials

According to the surfactant-templated mechanism, the self-assembly of building block is an essential part.²⁴ In general, self-assembly refers to a spontaneous organization of building blocks driven by non-covalent interactions, such as hydrogen bonding, pi-pi stacking, and electrostatic interactions. The building blocks can range from predesigned molecules (for example, organic molecules, oligomers, and polymers), molecular clusters (for example, inorganic and hybrid organic-inorganic clusters), and low-dimensional objects (for example, nanoparticles, nanorods, and nanowires) to more complicated components. The self-assembly of the building blocks in water can produce well-ordered two dimensional systems or three dimensional systems. The silica species can hydrolyze and polymerize in water and form the mesostructured nanocomposites. After calcination of the surfactant under very high temperature, mesoporous materials are derived. With this surfactant template mechanism, mesoporous silica with different pore sizes, morphologies and pore directions are derived.²⁵⁻²⁸

Another important class of periodic mesoporous material is periodic mesoporous organosilica (PMO). These are the materials in which the organic bridges are integral components of the silica network. The fusion of organic

chemistry and solid-state silica material synthesis allowed the creation of nanomaterials with a uniform distribution of organic spacer and pore size.²⁹ PMOs have several unique features such as high-loading of organic content without significant pore blockage, chemically reactive sites, homogeneously distributed functional groups. The physical and material properties can be easily modified by altering the composition of the bridge-bonded silsesquioxane precursor.³⁰ The synthesis of PMO materials is very similar to the synthesis of either M41S-type materials or SBA type materials. Variety of surfactants can be used and the conditions can be acidic, neutral or basic. The first PMO was synthesized in 1999 by three research groups working independently of one another.³¹⁻³³

The important characteristics of silica materials for the work described here is the ease with which one can tether organic functionalities onto the support material. The silica surface contains silanol (Si-OH) groups onto which organic functional groups can undergo reaction and produce organic/inorganic hybrid materials.³⁴ The silica material can have a mixture of isolated silanols, Figure (1.4A), germinal silanols (1.4B), vicinal silanols (1.4C), and siloxane bridges (1.4D). All of these surface species can be modified to form organic/inorganic hybrid materials.

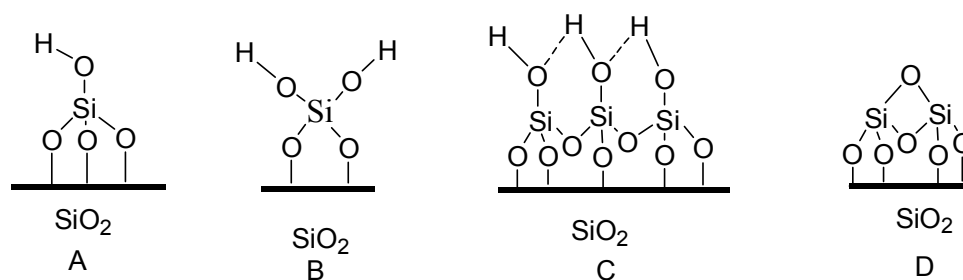
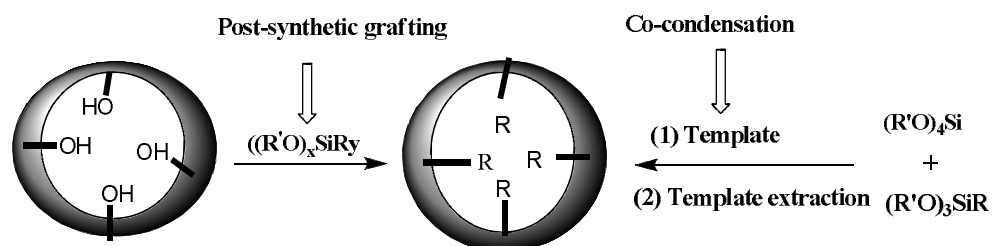


Fig. 1.4 Types of silica surface Si-O species

1.3 Mesoporous silica with organically modified surface

The combination of the properties of organic and inorganic building blocks within a single material is particularly attractive for chemists because of the possibility to combine the enormous functional variation of organic chemistry with the advantages of a thermally stable and robust inorganic substrate.³⁵ The symbiosis of organic and inorganic components can lead to materials whose properties differ considerably from those of their individual, isolated components. This is particularly applicable to heterogeneous catalysis.

Three strategies are available for the synthesis of functionalized silica material via covalent bonding of organic molecules, 1) the subsequent modification of the pore surface of a purely inorganic silica material (“grafting”), 2) the simultaneous condensation of corresponding silica and organosilica precursors (“co-condensation”) (Scheme 1.2) and 3) the incorporation of organic groups as bridging components directly and specifically into the pore walls by the use of bissilylated single-source organosilica precursors (“production of periodic mesoporous organosilicas”).^{34,36-39,32}



Scheme 1.2 Functionalization of silica framework by post-grafting and co-condensation method

1.3.1 Post-synthetic method (“Grafting”)

The grafting process is based on the modification of silica surface with organic groups through silylation reaction occurring on silanol groups using trichloro, trialkoxy organosilane or silylamines as the organic precursors. By varying the organic residue R, variety of functionalized materials can be derived. The main advantage of this method is that mesostructure of the starting silica phase is usually retained, whereas the lining of the walls is accompanied by a reduction in the porosity of the functionalized material. If the organosilanes react preferentially at the pore openings during the initial stages of the synthetic process, the diffusion of further molecules into the center of the pores can be impaired, which can in turn lead to a non homogeneous distribution of the organic groups within the pores and a lower degree of occupation.^{34,36}

1.3.2 Co-condensation (Direct Synthesis)

Direct synthesis refers to the co-condensation of tetraalkoxysilane [Si(OR₁)₄, R₁=Et, Me] and organoalkoxysilane [R-Si(OR₁)₃, R₁=Et, Me] precursors in the presence of Structure Directing Agent (SDA). Organic functionalities are projected into the pores where pore blocking does not occur. This method allows preparation of nanoporous organic-inorganic hybrid materials in a limited time. The advantage of this method include the stability of the inorganic framework even at higher organic loadings, homogeneous distribution of the organic groups in the pore channels as well as the single step preparation procedures. However, the structural ordering was highly dependent on the relative amount of organic precursor used. The organosilane precursor must be chosen carefully to avoid phase

separations and Si-C bond cleavage during the synthesis and surfactant removal process.^{38,39} Care should be taken that the organic group remains intact when the SDA is removed.

Both methods (Scheme 1.2) yielded the organically functionalized silica material and some advantages of post synthesis grafting methods include,

- 1) The structure of the resultant mesoporous material is ordered after the grafting reactions.
- 2) The functional groups can be chosen according to requirements.
- 3) The materials obtained show higher hydrothermal stability.
- 4) The hydrophilic-hydrophobic properties can be better tailored by the judicious choice of the organoalkoxysilane.^{34,40}

1.3.3 Preparation of periodic mesoporous organosilica (PMO)

PMOs which are organic-inorganic hybrid materials can be prepared by hydrolysis and condensation of an organosilica precursor. The general formula of this material is represented as $(R'O)_3\text{-Si-R-Si-(OR)}_3$. In contrast to the hybrid materials synthesized via post-synthetic treatment or co-condensation reactions, the organic functions are directly incorporated into the pore wall network by two covalent bonds. Thus, the distribution of the organic moieties is, in contrast to the materials described above, are completely homogeneous.

The most frequently used surfactants for the synthesis of mesoporous silica and organosilica are long chain alkyltrialkylammonium halides (chloride and bromide), mostly with an octadecyl chain (octadecyltrimethylammonium

chloride/bromide, OTAC/OTAB) or hexadecyl chain (hexadecyltri methylammonium chloride/bromide, HTAC/HTAB) or cetylpyridinium halides (chloride and bromide) (CPB/CPC). Under certain conditions depending on pH value, temperature and solvent concentrations in the presence of a bisilylated organosilica precursor, these surfactants form a lyotropic liquid crystalline phase. Hydrolysis and condensation of the organosilica precursor leads to the periodically ordered mesoporous hybrid material, which exhibits uniform pore diameters after removal of the surfactant (Figure. 1.5).²⁹ In the last few years, some research groups have synthesized PMO materials with a high crystal-like organization of the organic functionalities in the pore walls, in addition to the high ordering of the mesopores.⁴¹⁻⁴³ This means that, the mass centres of the molecules and the inversion centres of the organic bridges show a long-range order. Because of the free rotation of the Si-C bond around the molecular longitudinal axis, the organic bridges have altering orientations in relation to the bordering silica layers. Thus, the organic moieties do not possess any translational symmetry. Structures of some important organosilica precursors that have successfully been applied for the synthesis of PMO materials is given in Figure 1.6.

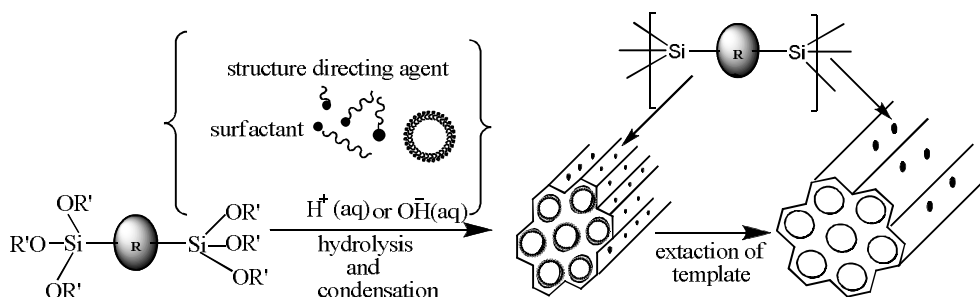


Fig. 1.5 A schematic representation of the synthesis of PMO

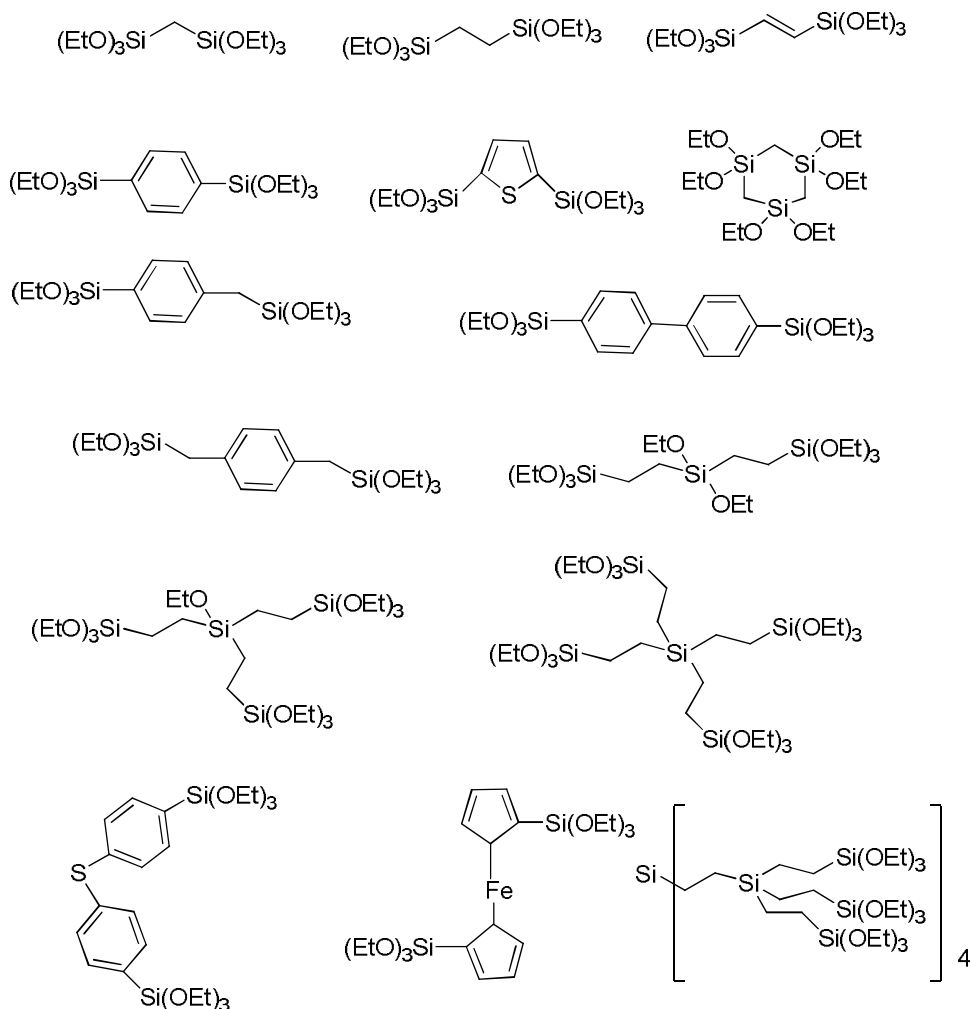


Fig. 1.6 Structures of the organosilica precursors that have successfully been used for the synthesis of PMOs²⁹

First investigation concerning the synthesis of PMOs with a high ordering of organic units in the pore walls were published by Inagaki et al. in 2002.⁴⁴ They have shown that a hierarchically ordered structure with meso- and molecular-scale periodicity is obtained for phenylene and biphenylene-bridged mesoporous systems. The periodicity in the channel

walls is thought to be due to the alternation of arrays of hydrophilic silicate layers and hydrophobic phenylene layers with a periodicity of 7.6 Å along the channel directions. This molecular-scale periodicity in the walls was suggested to arise from the self-organization of the precursor molecules through hydrophobic–hydrophilic or π – π interactions. This novel PMO, with crystal-like walls, are of considerable interest because they may exhibit improved thermal stability, selectivity and activity in catalytic applications. A model of the pore wall structure is presented in Figure 1.7 and Figure 1.8.

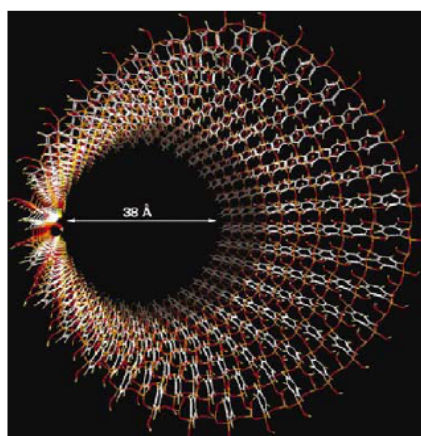


Fig. 1.7 Model of a pore surface. The surface is completely saturated with silanol functions.⁴²

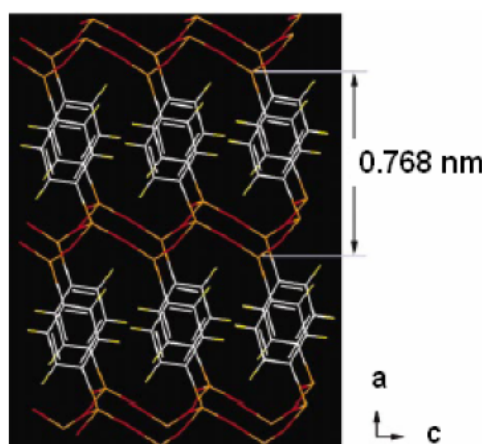
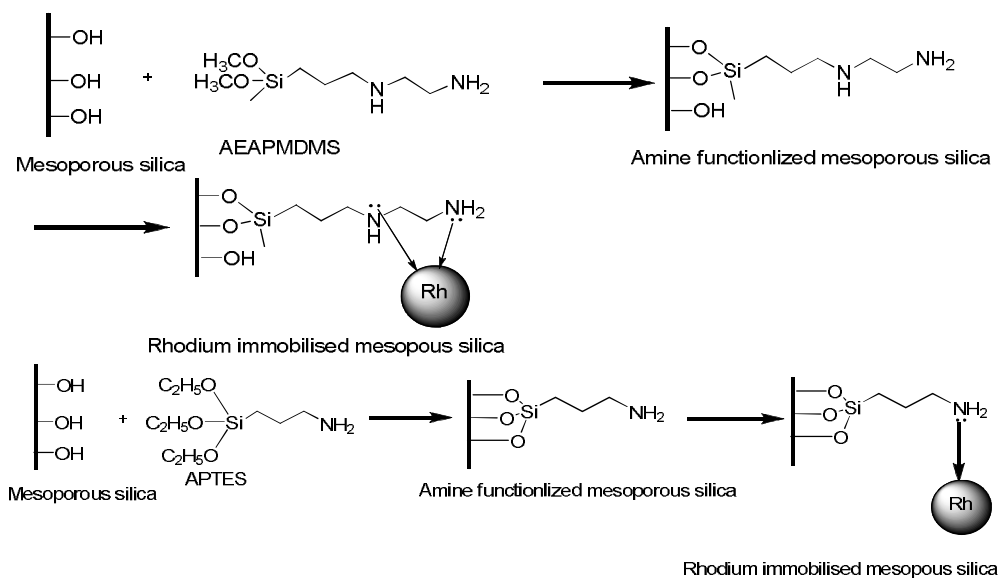


Fig. 1.8 Pore wall section. The aromatic units in the wall show the periodicity of exact one molecule.⁴²

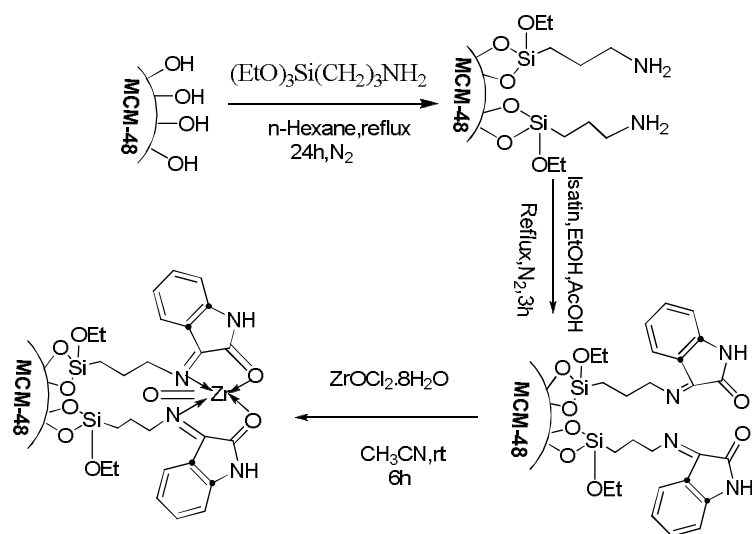
A recent review has comprehensively described the synthesis of PMO materials from simple to complex bridges. All aspects related to the synthesis, morphology and different areas of application have been addressed.⁴⁵

Many spectacular works are progressing in the area of organic functionalization of silica phases through grafting method. Such new frontier

materials have found to have wide application in the field of photochemistry,⁴⁶ thin films,⁴⁷ adsorbents,⁴⁸ drug delivery,⁴⁹ molecular sensors,⁵⁰ optical imaging agent⁵¹ and in heterogeneous catalysis.⁵²⁻⁵⁴ Organically functionalized mesoporous silica phases are in principle suitable candidates for the creation of efficient heterogeneous catalysts. Mhoe et al. prepared N,N dimethyl-3-aminopropyl derived MCM-41 by a post-synthesis method. Higher amount of amino group capacity of 2.22 mol/g could be introduced on MCM-41 and found to be an active catalyst for Michael addition.⁵⁵ 1,5,7-triazabicyclo [4,4,0] dec-5-ene (TBD), a strong base was introduced on MCM-41 through two-step procedure by Subba Rao et al. This material was active for the epoxidation of alkenes with hydrogen peroxide.⁵⁶ Das et al. functionalized MCM-41 and MCM-48 materials post synthetically with propylthiol groups initially, and converted them into propylsulfonic acid groups under mild oxidative conditions with H₂O₂.^{57,58} Corma et al. examined the catalytic properties of cinchonidine- and cinchonine-functionalized MCM-41 phases in the Michael addition of ethyl-2-oxocyclopentane carboxylate with 3-butene-2-ol; although the yields were good, the ee values were only 20–50 %.⁵⁹ Amine-functionalized mesoporous silica with different pore sizes (MCM-41, SBA-15 and amorphous silica) were prepared by using a post-synthesis method using N(beta-aminoethyl)-gamma-aminopropylmethyl dimethoxysilane (AEAPMDMS) and 3-aminopropyl triethoxysilane (APTES) and subsequently, rhodium was immobilized on the aminated mesoporous silica materials (Scheme 1.3).⁶⁰ Recently, a new Schiff base complex of Zr(IV)/isatin-MCM-48 was synthesized via grafting method (Scheme 1.4).⁶¹



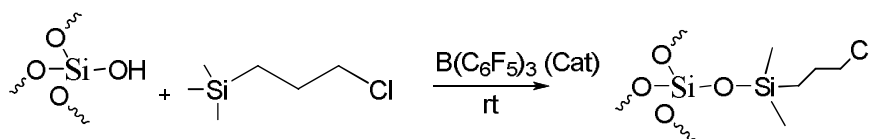
Scheme 1.3 Immobilization of Rh on amine functionalized silica



Scheme 1.4 Zr modified MCM-48

Shimada and Nakanishi introduced a new method for surface modification of silica using hydrosilanes as the modification precursor and tris(pentafluorophenyl) borane ($\text{B}(\text{C}_6\text{F}_5)_3$) as the catalyst (Scheme 1.5).⁶²

Hydrosilanes bearing a range of functional groups, including alcohols and carboxylic acids, have been immobilized by this method. An excellent preservation of delicate functional groups, which are otherwise decomposed in other methods, makes this methodology appealing for versatile applications.



Scheme 1.5 Surface modification of silica using hydrosilanes

The post-synthetic functionalization of mesoporous silica phases is not limited to small organic functional groups. Acosta et al. reported the construction of dendrimer-like structures in the pores of amino-functionalized SBA-15 materials. Melamine-like structures were produced within the pores by means of a stepwise alternating treatment of the substrate with 2,4,6-trichlorotriazine and 4-aminomethylpiperidine (Figure 1.9).⁶³

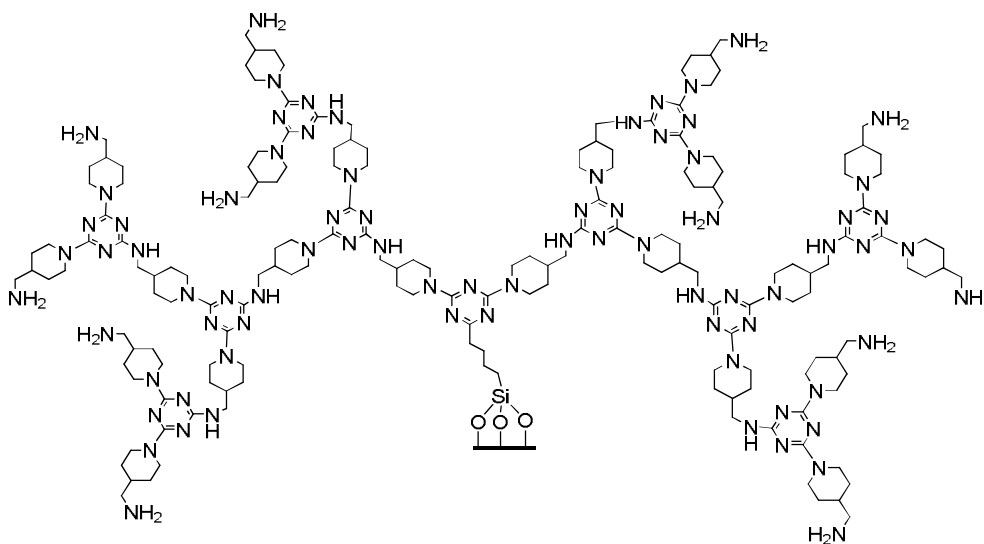
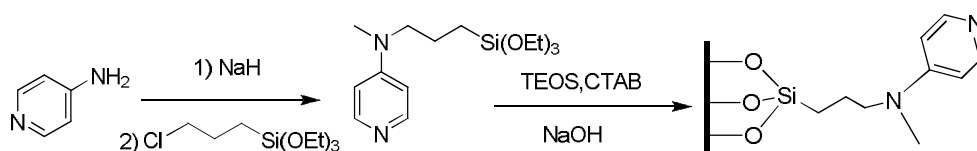


Fig. 1.9 Melamine-like structure within the pores of a mesoporous SBA-15 silica phase constructed by alternating treatment of the substrate with 2,4,6-trichlorotriazine and 4-aminomethylpiperidine.

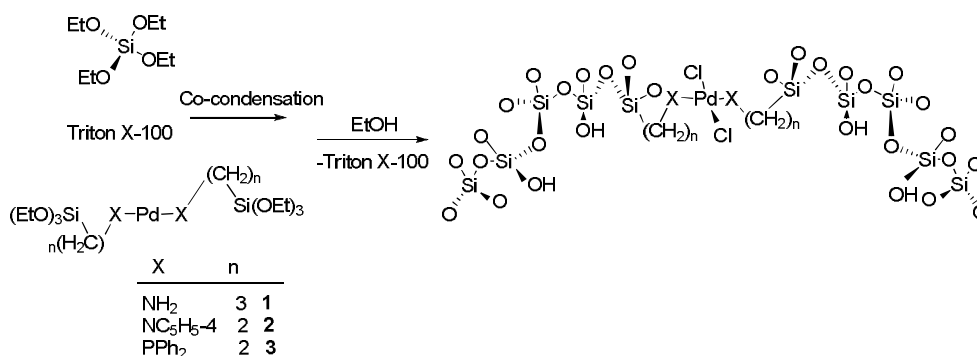
Organically modified silica can be prepared by co-condensation method which involves the use of respective organosilane, organic functionalities such as alkyl,⁶⁴ thiol,⁶⁵ amino,⁶⁶ cyano/isocyano,⁶⁷ vinyl/allyl,⁶⁸ organophosphine,⁶⁹ alkoxy or aromatic groups.⁷⁰ The mesoporous materials obtained by direct synthesis exhibited interesting catalytic^{71,72} and adsorption properties,⁷³ or, by subsequent chemical transformation of the organic groups on the pore surfaces and can act as starting compounds for the synthesis of new organically modified silica phases.⁷⁴ Chen et al. prepared mesoporous silica nanoparticles functionalized with dimethylaminopyridine (DMAP) moieties by direct method (Scheme 1.6). The catalyst contains 1.6 mmol/g of the organic group. The catalyst showed excellent activity for the Baylis-Hillman reaction of aryl aldehyde and various α , β unsaturated aldehydes.⁷⁵



Scheme 1.6 Modification of silica surface with dimethylaminopyridine by co-condensation method

An environmentally benign synthesis of Pd (II) complex incorporated mesoporous silica framework has been achieved by co-condensation using a facile solvent-free one-pot synthesis (Scheme 1.7). The prepared catalyst was found to be efficient for Suzuki-Miyaura reaction under solvent-free conditions. The possibility to work under solvent-free conditions even with solid starting reactants, is a significant step forward in the Suzuki-Miyaura

coupling reaction because of its benefits in terms of cost and impact on the environment.⁷⁶



Scheme 1.7 Pd (II) complex functionalized mesoporous silica synthesized via solvent-free one-pot method

1.4 Polymer brushes on silica surface

Dendrimers are monodisperse, highly branched, three-dimensional macromolecules with a multivalent core, as well as terminal functional units at the periphery (Figure 1.10). After an iterative sequence of reactions, the successive generation of dendrimers is obtained, presenting different sizes, shapes, and terminal units of the branches which can be efficiently controlled.⁷⁷⁻⁷⁹ Because of the well-defined structure as well as a definite number of peripheral groups, dendrimers offer numerous advantages for a variety of applications. For example, their internal cavities can be loaded with guest molecules for drug delivery purposes.⁸⁰⁻⁸² Functionalization of the periphery or the internal backbone with transition metals can result in highly efficient and easily recoverable catalysts.^{83,84} Dendrimers on silica surface can allow production of supported catalysts,^{85,86} chromatographic support,⁸⁷ or porous membrane.⁸⁸

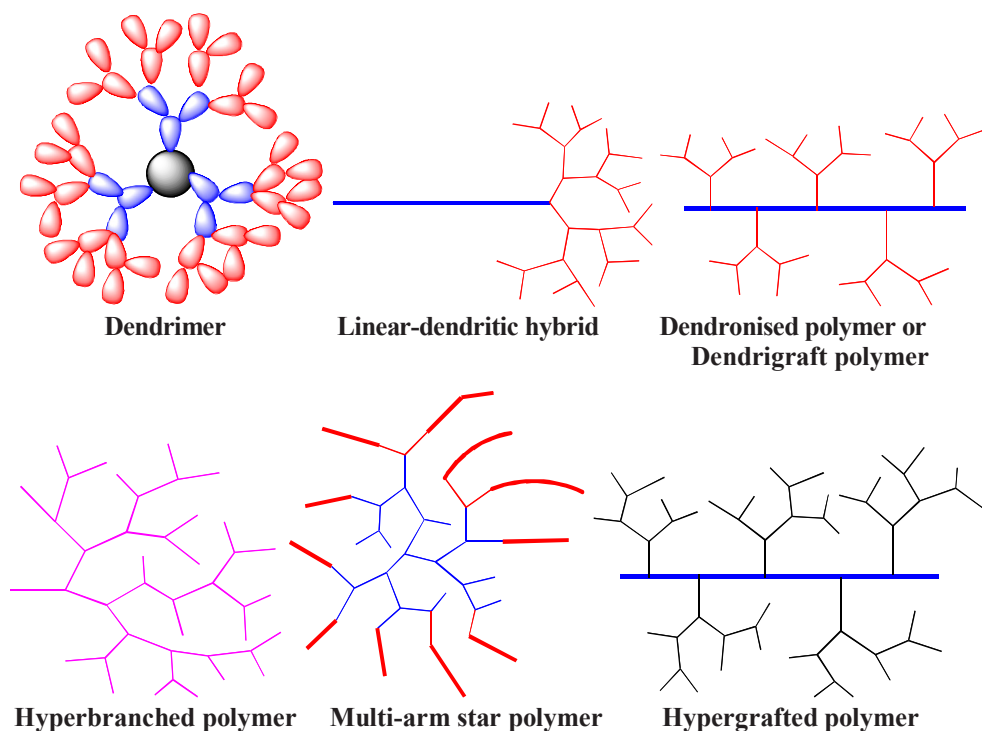


Fig. 1.10 Schematic representation of different types of dendritic polymers

Polymer functionalized inorganic supports exhibited unusual mechanical, electronic, magnetic, and optical properties.⁸⁹⁻⁹¹ The choice of the inorganic support range from reinforcing fillers such as silica, alumina, and carbon black⁹² to metals such as gold⁹³ and silver,⁹⁴ upto semiconductor quantum dots such as cadmium sulfide.⁹⁵ The sizes of the particles range from 1 nm to several mm. These particles find a wide range of applications that include optics, electronics, engineering, biosciences and heterogeneous catalysis.

The surfaces of inorganic materials are functionalized with polymer chains either chemically (through covalent bonding) or physically (by physisorption). Physisorption involves adsorption of block copolymers with

sticky fragments.⁹⁶ The non-covalent adsorption makes the adsorption reversible, especially during processing and it is not a favored technique. Covalent grafting techniques are preferable, where they stabilize an interfacial compatibility between the two phases. Covalent grafting techniques involve either the “grafting to” or “grafting from” methods. In “grafting to” method, pre-formed end-functionalized polymer chains are reacted with a chemically activated substrate (Figure 1.11A). This method usually generates nongrafted chains and prevents attachment of the next chain which leads to get low graft density.⁹⁷ The “grafting from” method involves formation of an initiator layer (I) on the surface of the silica followed by polymerization of monomer (M) (Figure 1.11B). This method is useful to design polymer/mesoporous silica hybrids with covalent interaction between polymer and inorganic support.

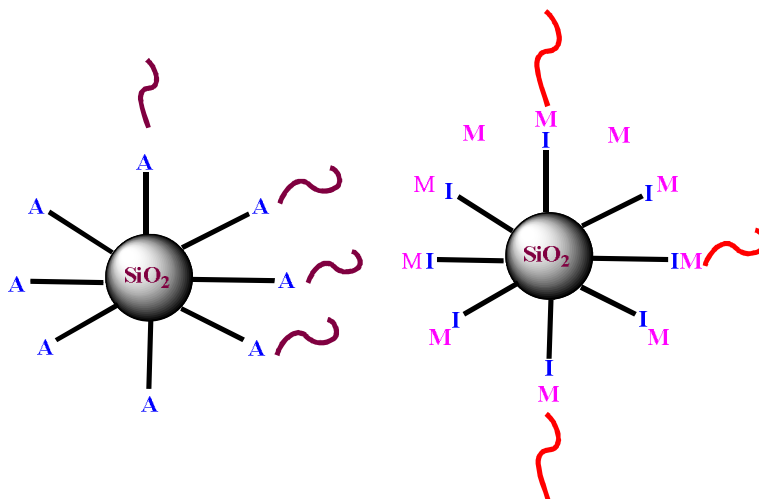


Fig. 1.11 A) Grafting to B) Grafting from

This polymerization technique is also commonly referred to as surface initiated polymerization (SIP).⁹⁸ Preparations of polymer brushes via SIP on

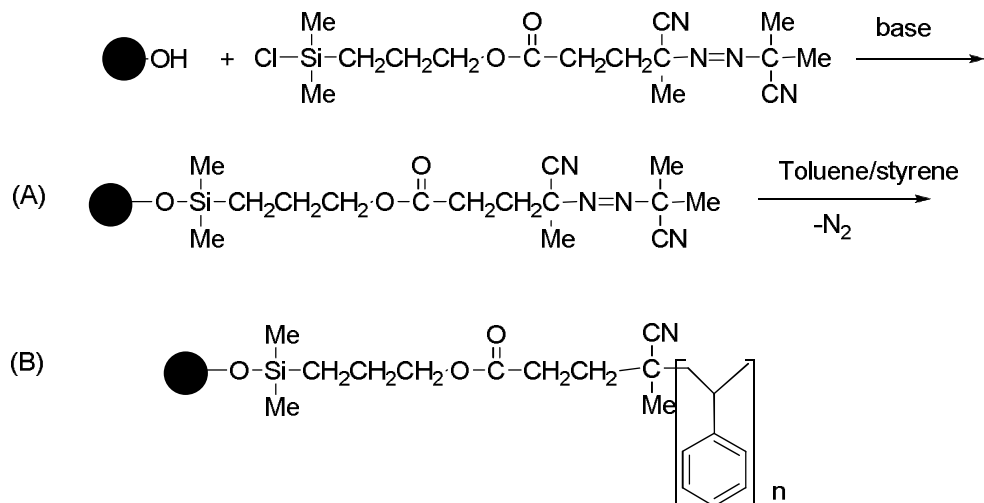
silica can be accomplished by free radical, cationic, anionic, ring opening metathesis, atom transfer radical and reverse addition-fragmentation polymerization techniques.⁹⁹

The hydroxyl groups on the surface of silica particles can be easily tailored with organic compounds or polymers. The procedure reported in the literature involves formation of an initiator layer on the surface of the silica followed by polymerization. Different polymerization techniques can be used to modify the surface of silica. Some of them are reported below.

1.4.1 Conventional radical polymerization

Conventional free radical polymerization is one of the most studied methods. Radical processes are more tolerant of functional groups and impurities and are well suited for polar monomers.¹⁰⁰ The “grafting from” method has been long used for the preparation of covalently attached polymers by free radical techniques. This approach was first reported by Prucker and Ru̇he.¹⁰¹ It consists of grafting an azo initiator onto a particle or flat surface followed by polymerization. A self assembled monolayer (SAM) of the azo initiator is grafted on the surface of silica (Scheme 1.8A) and this is used for the radical chain polymerization of styrene (Scheme 1.8B).

Conventional free radical polymerization is difficult to control and is generally characterized by broad molecular weight distribution, poor control of molecular weight and chain end functionality, and the inability to synthesize well-defined block copolymers. However, many of these drawbacks can be overcome by using controlled free radical polymerization.



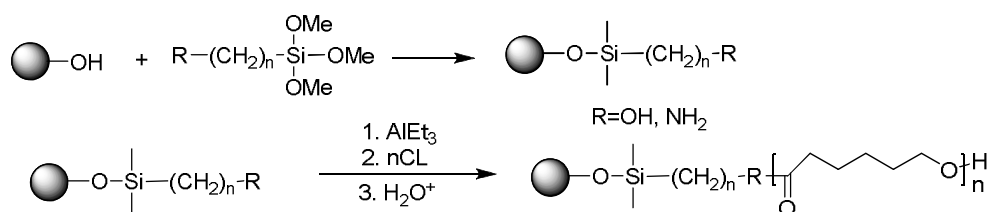
Scheme 1.8 Schematic representation of conventional radical polymerization on silica surface

1.4.2 Controlled radical polymerization

The use of surface initiated controlled/living radical polymerization has proved to be a versatile approach for incorporating different types of organic polymers with varied architecture on the silica surface. By using this technique, one can manipulate the structure of the resultant polymer shell through changes in grafting density, composition and molar mass. In controlled radical polymerization, the life-time of the growing radical can be controlled resulting in the synthesis of predefined molar mass, polymers with low polydispersity, controlled composition, and functionality.¹⁰² In general, controlled/living polymerization can be achieved by stable free radical polymerization, e.g. nitroxide-mediated processes (NMP),¹⁰³ metal catalyzed atom transfer radical polymerization (ATRP)¹⁰⁴ and degenerative transfer, e.g. reversible addition–fragmentation chain transfer (RAFT).¹⁰⁵

1.4.3 Ring opening polymerization

Some vinyl monomers with strong polar functional groups and cyclic monomer can not be initiated through free radical polymerization. Biodegradable polymers like polylactides and polylactones are synthesized by the ring opening polymerization of cyclic monomers catalyzed or initiated by organometallic derivatives. Many of these processes are “living”/controlled methods suitable for the controlled grafting of polymers on surfaces. The surface initiated ring opening polymerization is generally performed after the formation of a self-assembled monolayer (SAM) that contains a polymerization initiator. In the case of aliphatic polyesters, usually a hydroxyl or amine terminated SAM are immobilized on the surface to initiate ring opening polymerization (Scheme 1.9).¹⁰⁶



Scheme 1.9 Schematic representation of ring opening polymerization of cyclic monomer caprolactam (CL) on silica surface

1.4.4 Other methods

Hyperbranched polymers are generally synthesized using AB_x-type monomers via (1) condensation polymerization, (2) self-condensing vinyl polymerization (SCVP), and (3) ring opening multibranch polymerization. The latter two techniques require either vinyl or cyclic monomers that possess an initiating functionality for hyperbranching.¹⁰⁷ Generally, these techniques

produce polymers whose molecular weight and molecular weight distribution (MWD) are difficult to control. Another pathway to hyperbranched polymers, is the ring-opening polymerization of cyclic latent AB_2 -type monomers. In 1998, Suzuki et al. reported polymerization of a cyclic carbamate that may be classified under this third strategy.¹⁰⁸ Suzuki referred to his concept as “multibranching polymerization”. This type of reaction was stated as “*ring opening multibranching polymerization*” (ROMBP) by Frey et al.¹⁰⁹ This synthetic strategy has been little explored so far, but it appears to possess promising potential for the controlled preparation of hyperbranched polymers. A general synthetic scheme of this type of reaction is shown in Figure 1.12, demonstrating the analogy between AB_2 polycondensation and the ROMBP approach.

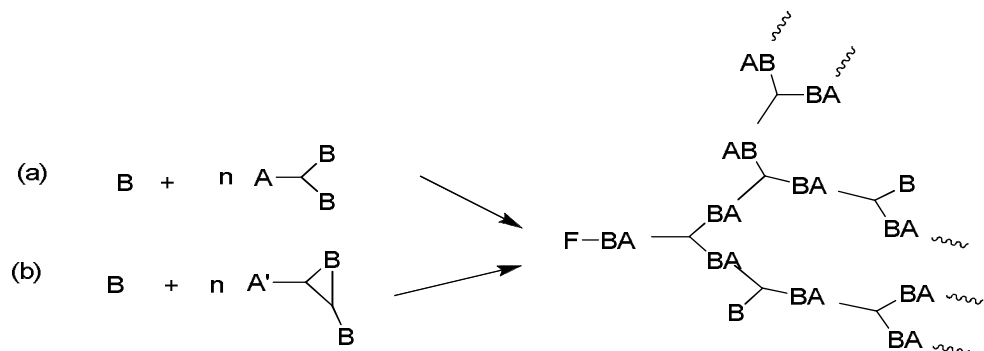


Fig. 1.12 (a) AB_2 polycondensation and (b) ring opening multibranch polymerization

1.5 Silica-supported dendrimer

The most widely studied dendrimer attached to insoluble support is poly(amidoamine) dendrimer. In 1997 Bradley and co-workers introduced the solid phase synthesis of PAMAM dendrimers on organic polymer support.¹¹⁰ Initially, these dendrons were prepared on Tentagel upto the

fourth generation. PAMAM dendrimers were also prepared on silica, as early as 1998, by Tsubokawa et al. and by many other groups.¹¹¹⁻¹¹⁷ Usually, 3-aminopropyl functionalized silica was employed as the parent support. Almost all the attempts to grow PAMAM dendrimers on amorphous silica resulted in defected structures. This can be overcome by generating dendrimer on periodic mesoporous silica support having crystalline wall (Figure 1.13).¹¹⁸

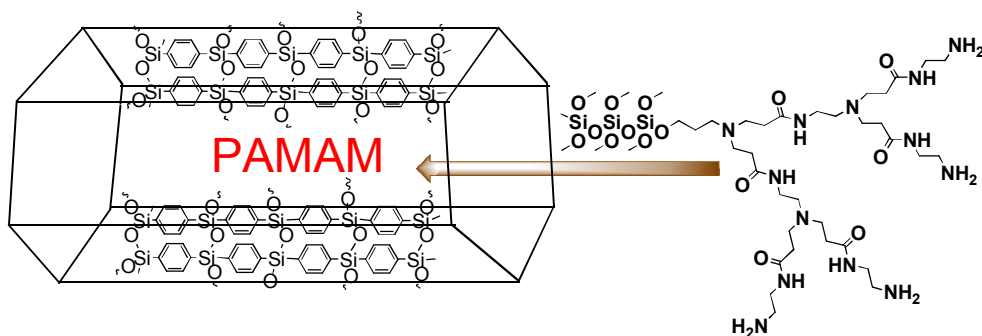
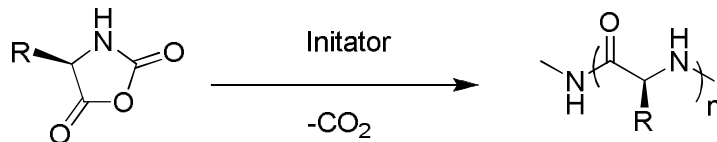


Fig.1.13 Schematic representation of poly(amidoamine) dendrimer on silica having crystalline wall

1.6 Polypeptide brushes on silica

Polypeptides prepared by the ring opening polymerization (ROP) of α -amino acid N-carboxyanhydrides (NCAs) are emerging biomaterials that have received increasing attention due to their various biomedical applications. New synthetic methodologies, mechanistic studies and optimization of polymerization conditions for the preparation of well-defined novel polypeptides are comprehensively reviewed and evaluated by Cheng et al.¹¹⁹ The synthesis and polymerization of NCAs was first reported by Hermann Leuchs in 1906 (Scheme 1.10).¹²⁰



Scheme 1.10 ROP of NCA for the preparation of polypeptides

Polypeptides are responsive to external stimuli (pH, electrolytes, solvent, and temperature) and offer a wide range of side chain chemistries (thiols, amines, carboxylic acids, etc.). So they can be used as suitable organic components in hybrid materials and find application in chiral separations, solid asymmetric catalysis, drug delivery, and sensing. Grafting of polypeptides onto solid support has emerged as a new area in scientific research. Silicon or quartz planar surfaces,¹²¹⁻¹²³ gold supported SAMS^{124,125} and colloidal silica^{126,127} have also been studied as solid supports. There have also been several investigations of polypeptides grafted onto silica/alumina as chiral stationary phases^{128, 129} and on colloidal silica crystals for use as membranes.¹³⁰

1.7 Silica- supported metal complexes

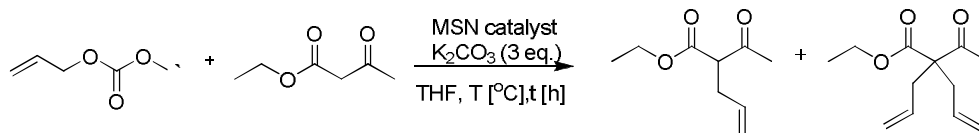
Surface functionalization of mesoporous silica materials by covalent bonding of organic species on preformed silica (grafting) has become the most common approach. At present, many complexes have been heterogenized by this method, and many works are in progress on the catalytic properties of silica materials functionalized with metal salen complexes (e.g., Mn(III),¹³¹ Co(II),¹³² and vanadyl salen,¹³³ H₂salen=N,N'-bis(salicylidene)ethylene diamine). Grafting of pure ligands on the support followed by subsequent reaction with metal yielded the desired catalyst.¹³⁴ Heterogenisation of homogeneous complexes overcomes the main limitations of homogeneous

activity of the supported catalyst towards the Suzuki transformation with a variety of reagents in aqueous media.¹³⁶

1.8 Organically functionalized silica materials as catalyst

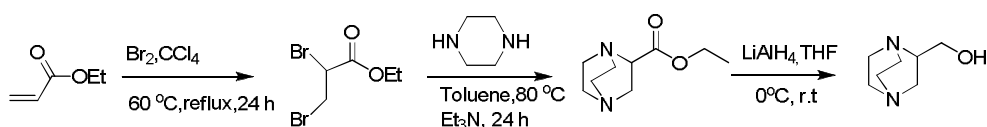
Development of heterogeneous catalysts has become a major area of research in synthetic organic chemistry due to the potential advantages of these materials over homogeneous systems. Easy recovery, reusability, enhanced selectivity and reactivity, easy product isolation and incorporation in continuous reactors and microreactors are some of the advantages of heterogeneous catalysts.¹³⁷⁻¹⁴² During the last two decades, hybrid mesoporous solids have been considered for a wide range of heterogeneous catalysis reactions.¹⁴³⁻¹⁴⁵ Chemically modified mesoporous silica materials are environmentally compatible materials. They have found enormously diverse potential as benign replacements for the many hazardous and environmentally threatening chemicals that we have used as catalysts in chemical manufacturing process. Many groups have extensively applied functionalized silica material as catalyst in numerous organic reactions.¹⁴⁶⁻¹⁴⁸

Armido Studer and coworkers have prepared bifunctional mesoporous silica nanoparticle (MSN) bearing Pd-complexes and additional basic sites and tested their cooperative catalytic activity in the Tsuji–Trost allylation of ethyl acetoacetate (Scheme 1.11). Functionalization of the MSN was realized by post-modification using click chemistry. The selectivity of mono versus double allylation was achieved by the control of reaction temperature and the nature of the catalyst.¹⁴⁹



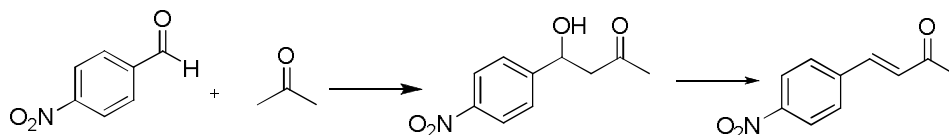
Scheme 1.11 Tsuji–Trost allylation of ethyl acetoacetate by MSN catalyst

Amine-functionalized mesoporous silica-supported copper catalysts were prepared by Yanxing Qi et al. and proved to be efficient and reusable catalyst for homocoupling of terminal alkynes at room temperature with air as the oxidant (Scheme 1.12).¹⁵⁰



Scheme 1.12 Preparation of 1,4-diaza-bicyclo[2.2.2]octan-2-ylmethanol

Jones and coworkers investigated the difference in catalyst performance for the aldol condensation of 4-nitrobenzaldehyde with acetone (Scheme 1.13) using base or acid/base bifunctional silica-based catalytic materials prepared through grafting and co-condensation (Figure 1.15). By using the array of new catalysts they observed differences in reaction rate and concluded that introduction of the carboxylic acid group decreases the rate of reaction relative to the amine functionalized material under the same conditions which suggested that cooperative amine-silanol pairing is more effective than amine-carboxylic acid pairing using the same synthetic and catalytic conditions.¹⁵¹



Scheme 1.13 Aldol condensation of 4-nitrobenzaldehyde with acetone

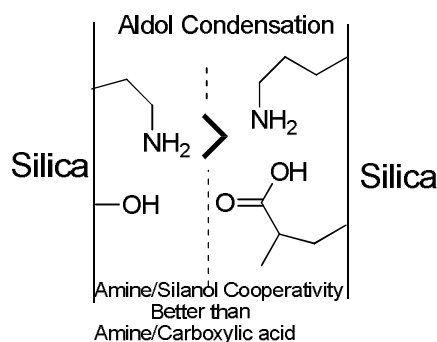
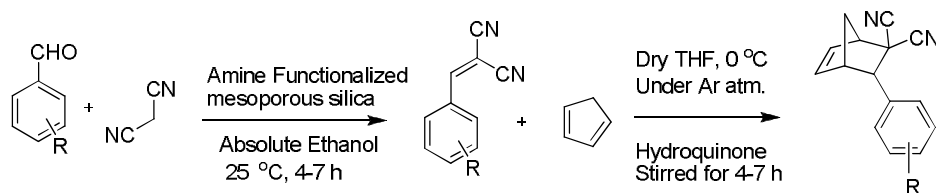


Fig. 1.15 Acid/base bifunctional silica based catalyst

J. Mondal et al. have prepared amino-functionalized mesoporous silica through co- condensation of 3-aminopropyl triethoxysilane (APTES) along with tetraethyl orthosilicate (TEOS) in the presence of a cationic surfactant, CTAB hydrothermally. Authors revealed that amino-functionalized mesoporous silica was found to be efficient base catalyst for the Knoevenagel condensation of different aromatic aldehydes with malononitrile to α,β unsaturated dicyanides under very mild reaction condition and in the presence of ethanol solvent. The isolated α,β unsaturated dicyanides obtained through the condensation reaction further reacted with cyclopentadiene to form a series of Diels–Alder cycloaddition products in excellent yields in the absence of any catalyst (Scheme 1.14).¹⁵²



Scheme 1.14 Reaction pathway for the Knoevenagel condensation reaction over amino functionalized mesoporous silica

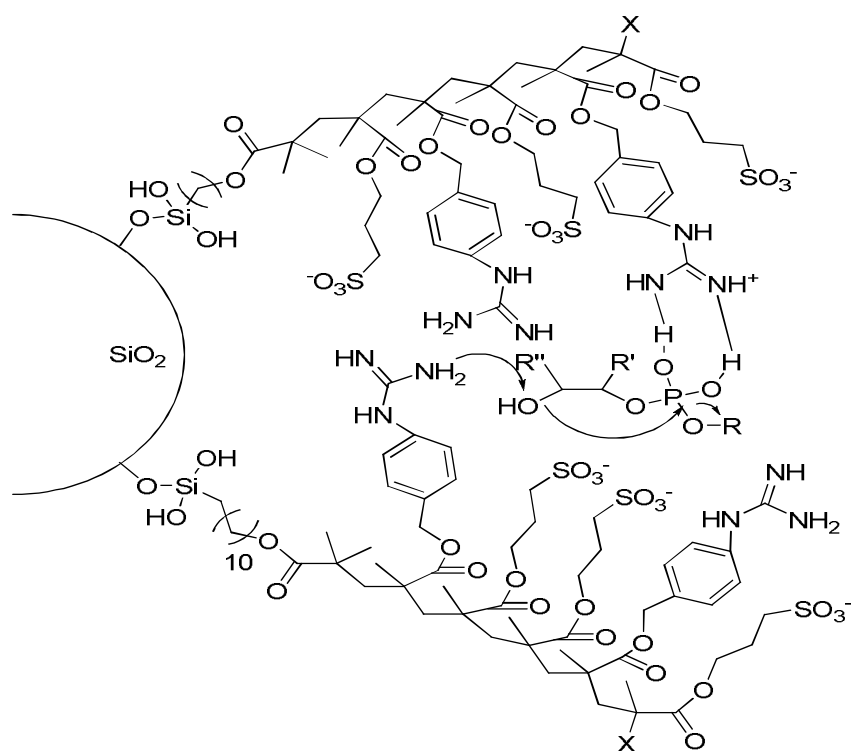
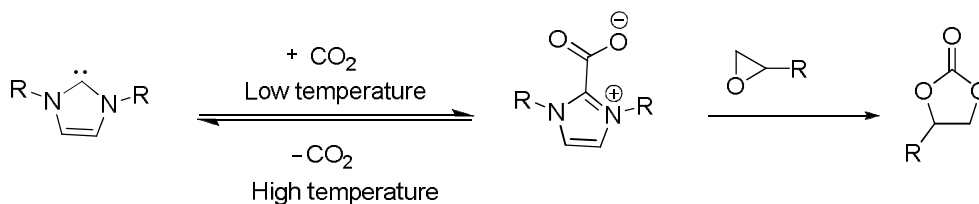


Fig. 1.16 Schematic representation of the suggested mechanism of the HPNP/diribonucleoside cleavage catalyzed by hybrid silica nanoparticles covered with guanidine-based polymer brushes

Recently, another interesting catalyzed reaction was reported by Salvio et al. using polymer brush-silica nanoparticle catalyst.¹⁵³ Guanidine functionalized polymer brushes grafted to the surface of silica nanoparticles

were fabricated by atom-transfer radical polymerization (ATRP) and investigated as catalysts in the cleavage of phosphodiester (Figure 1.16). The activity of the hybrid nanoparticles was tested in the transesterification of the RNA model compound, 2-hydroxypropyl paranitrophenylphosphate (HPNP) and diribonucleoside monophosphates. High catalytic efficiency and selectivity was observed.

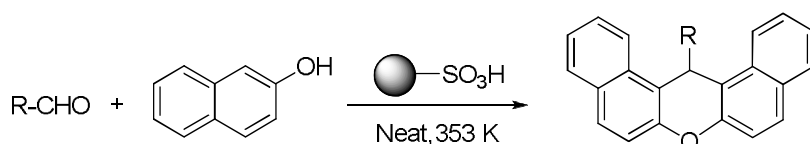
Bing Lu and coworkers found that *N*-Heterocyclic carbene functionalized MCM-41 could act as efficient catalyst for chemical fixation of carbon dioxide. MCM-41-NHC-CO₂ adduct was proved to be an efficient heterogeneous catalyst for the cycloaddition of CO₂ to epoxides or aziridines with excellent regioselectivity under mild conditions. Authors found that NHC could effectively activate CO₂ as a protective group by stabilizing NHC-MCM-41 and catalyzed the coupling reaction of CO₂ with epoxides to give the corresponding cyclic carbonates in excellent yields (Scheme 1.15). Moreover, the catalyst could be recovered easily through a simple filtration process and reused multiple times without obvious loss in activity.¹⁵⁴



Scheme 1.15 Activation of CO₂ and chemical conversion by the coupling with epoxides catalyzed by *N*-heterocyclic carbene

J. Mondal et al. have prepared 2D-hexagonal mesoporous silica materials SBA-15 and MCM-41, functionalized with carboxylic acid (COOH) and sulphonic acid (SO₃H) group by post-synthesis method.¹⁵⁵ The

prepared catalyst was found to be highly efficient and recyclable heterogeneous organocatalysts. The -COOH functionalized material was obtained via schiff-base condensation of 3-aminopropyl grafted SBA-15 with 4-formylbenzoic acid, whereas -SO₃H functionalized material was prepared via partial oxidation of 3-mercaptopropyl grafted MCM-41 with dilute aqueous H₂O₂. These acid functionalized materials have been used as heterogeneous catalysts for the condensation of aromatic aldehydes with 2-naphthol under mild conditions in the presence or absence of a solvent and afforded valuable xanthenes with high yield (Scheme 1.16).



Scheme 1.16 General procedure for synthesis of Xanthene over SO₃H functionalized MCM-41

Alper and co-workers synthesized silica-supported PAMAM-Pd complexes (Figure 1.17), and the prepared catalyst showed good selectivity and activity in the hydrogenation of cyclic and acyclic dienes to monoolefins under very mild conditions. They revealed that the activity and selectivity of this reaction is sensitive to the dendrimer structure. These dendritic complexes displayed excellent recyclability and retaining activity upto eighth recycles.¹⁵⁶

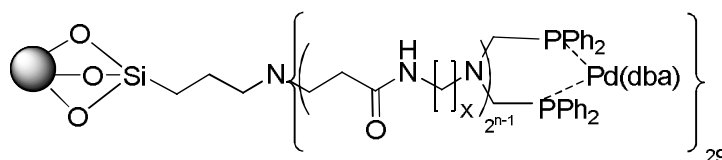
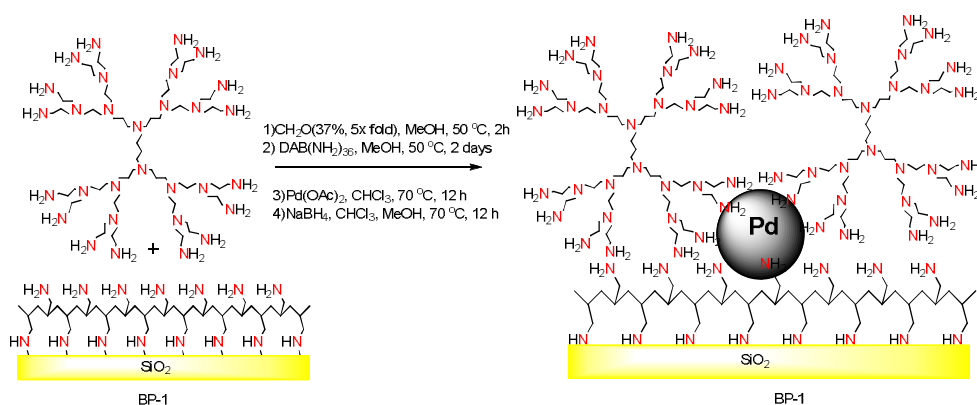


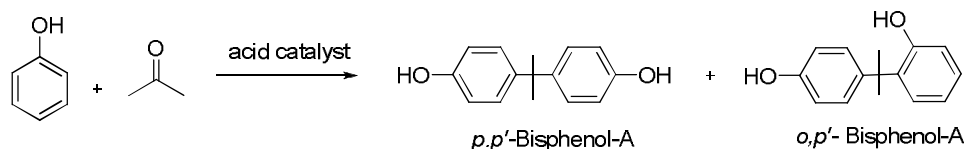
Fig. 1.17 Silica-supported PAMAM-Pd complexes

Polypropyleneimine (PPI) dendrimers upto third generation was successfully generated on silica surface which was previously modified with polyallylamine (PAA). Such dendronised silica was further complexed with $\text{Pd}(\text{OAc})_2$ to generate dendronised Pd nanoparticle silica conjugates (Scheme 1.17).¹⁵⁷ The synthesized catalyst was found to be effective for selective hydrogenation of dienes to monoenes and phenyl acetylene to styrene with higher turnover number than those for related Pd nanoparticle catalyst. The synthesized catalyst can be reused without any loss of activity.



Scheme 1.17 Grafting to silica and incorporation of Pd nanoparticle into PPI dendrimer.¹⁵⁷

Sulfonic acid functionalized MCM-41 silica was found to be an efficient catalyst for the Bisphenol-A synthesis.¹⁵⁸ The catalyst exhibited high selectivity towards *p,p'* Bisphenol-A (Scheme 1.18). The product obtained is an important raw material for polymer and resin production, and it is produced industrially using ion-exchange resins such as Amberlyst.1



Scheme 1.18 Synthesis of Bisphenol-A by sulfonic acid functionalized MCM-41

Mobaraki et al. showed that periodic mesoporous organosilica functionalized sulfonic acids were highly efficient and recyclable catalysts in biodiesel production.¹⁵⁹ Novel water tolerant sulfonic acid based Periodic Mesoporous Organosilica (PMO) having either phenylene or ethyl as bridge and methylpropyl sulfonic acid as functional group have been developed (Figure 1.18). It was revealed that catalyst bearing an ethyl bridging group was a more reactive catalytic system in biodiesel production.

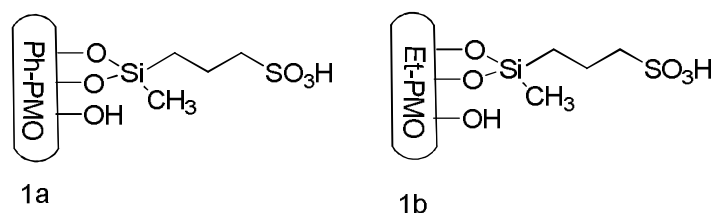
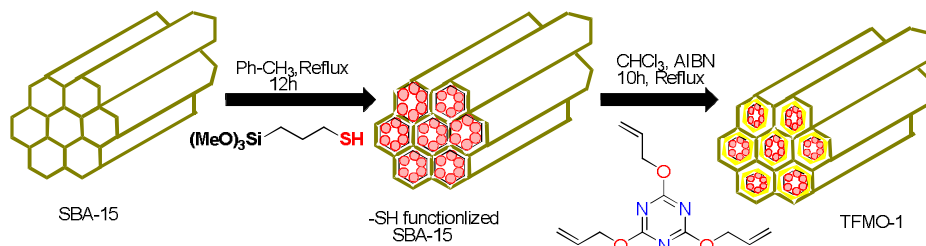
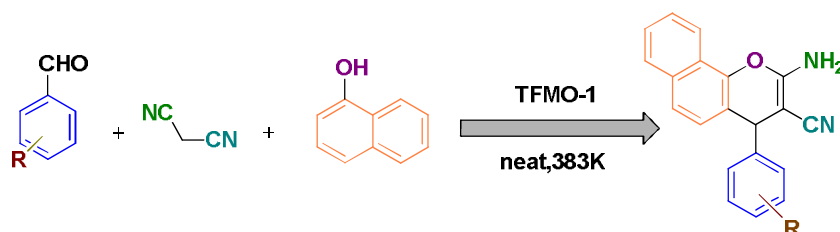


Fig. 1.18 Sulfonic acid based PMOs having either phenylene or ethyl group

Recently, Bhaumik et al. have prepared a highly ordered 2D-hexagonal mesoporous material functionalized with a triazine moiety via post-synthetic modification of mesoporous SBA-15 with thiol followed by a thiol-ene click reaction using 2,4,6-triallyloxy-1,3,5-triazine (Scheme 1.19).¹⁶⁰ This novel mesoporous metal-free support was used as heterogeneous organocatalyst in one-pot three-component condensation reaction of aromatic aldehyde, malononitrile and activated phenols for the synthesis of a diverse range of 2-amino-4*H*-chromenes (Scheme 1.20). The catalysts showed good activity under solvent-free reaction conditions.

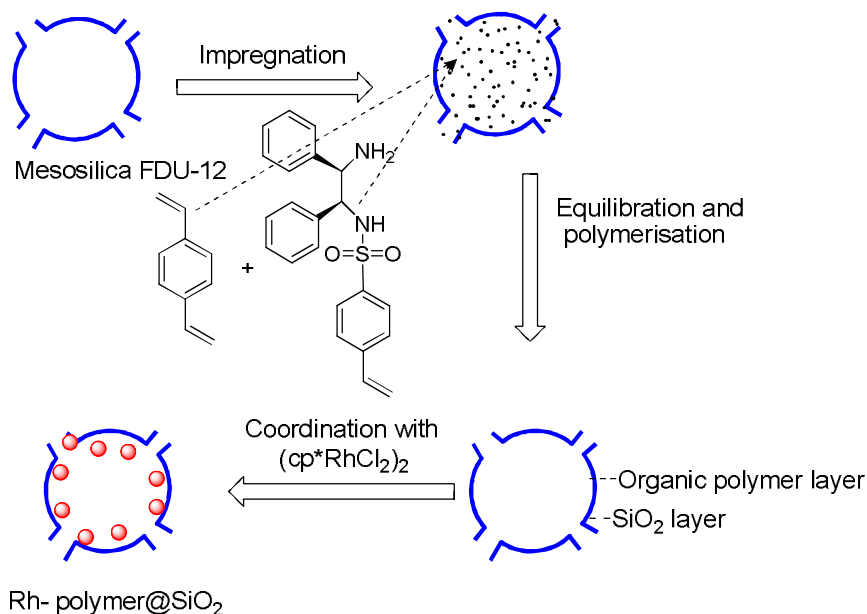


Scheme 1.19 Synthesis of triazine functionalized mesoporous organocatalyst via thiol-ene click reaction.



Scheme 1.20 General procedure for the synthesis of 2-aminochromenes

A highly efficient chiral solid catalyst was developed by Yang et al. through in situ polymerization of a chiral monomer together with divinylbenzene (DVB) in the nanocages of mesoporous silica (FDU-12) followed by coordination with a metal precursor, $[\text{Cp}^*\text{RhCl}_2]_2$ (Cp^* = pentamethylcyclopentadiene) (Scheme 1.21). The authors clearly showed that such solid chiral catalyst exhibited hydrophilic outer and hydrophobic inner surface properties. So it could be well dispersed in aqueous solution and facilitated the adsorption of hydrophobic ketones in it. It is observed that such material efficiently catalyzed the asymmetric transfer hydrogenation (ATH) of ketones with 94 % ee in aqueous medium and showed higher TOF than those for related homogeneous catalyst.¹⁶¹



Scheme 1.21 Schematic illustration for the preparation of the solid composite catalyst Rh-polymer@silica¹⁶¹

Khosropour et al. explored the catalytic properties of copper immobilized on triazine dendrimer functionalized nanosilica. Wide range of 1,4-disubstituted 1,2,3-triazoles was synthesized with excellent yield. It was achieved via a one-pot three-component reaction of alkynes and sodium azide with organic halides or α -bromo ketones in sodium ascorbate solution at room temperature. This catalytic system (Figure 1.19) also showed excellent activity in the synthesis of bis and tris-1,4-substituted 1,2,3-triazoles. Moreover, the catalyst could be recycled and reused for seven cycles without any loss in its catalytic activity.¹⁶²

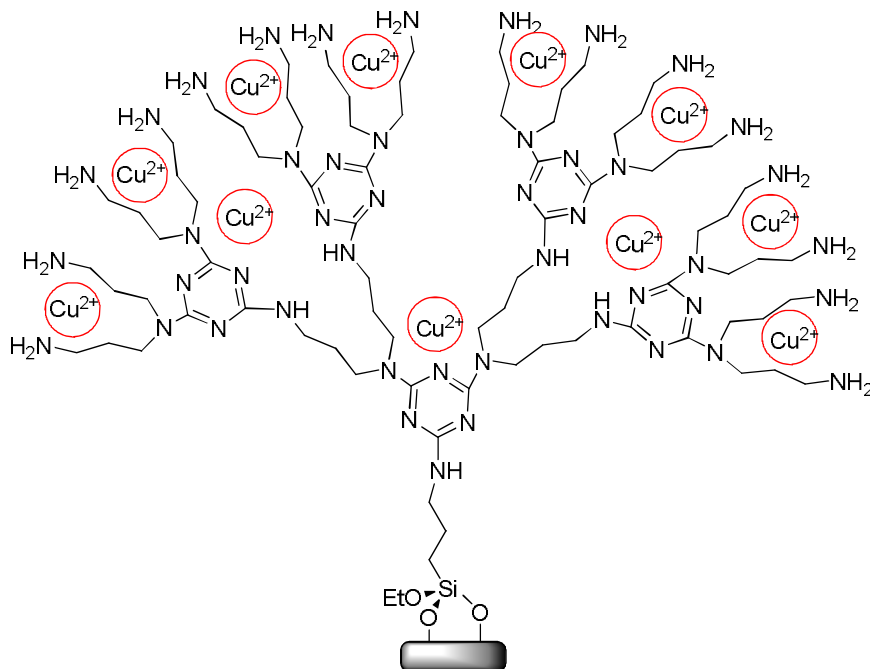
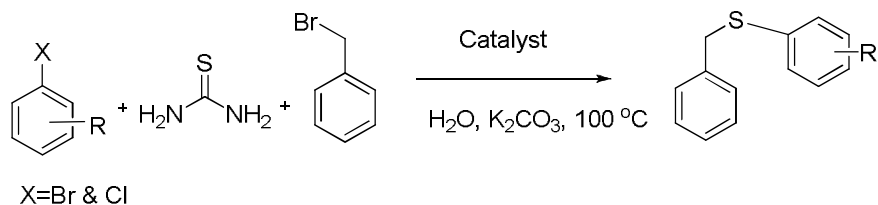


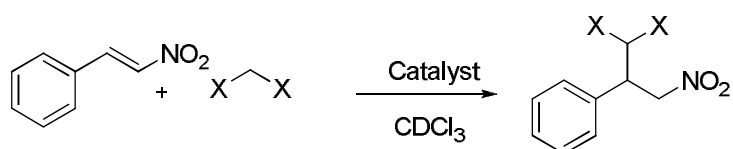
Fig. 1.19 Structure of copper immobilized on nanosilica triazine dendrimer

A highly ordered 2D hexagonal Cu-grafted mesoporous SBA-15 was developed by Bhaumik et al. through post synthetic method. The prepared catalyst exhibited excellent activity in a one-pot three-component C–S coupling reaction for a diverse range of aryl halides (bromide and chloride) with thiourea and benzyl bromide in aqueous medium which produced aryl alkyl thioether in very good yield (Scheme 1.22). Author established the strong binding ability of the imine–N and phenolic–OH functional groups present in the phloroglucinol diimine moiety of the framework. The anchored Cu(II) could not leach out from the surface of the mesoporous catalyst during the course of reaction, and it has been observed that six repetitive reaction cycles could not cause any appreciable loss in the catalytic activity of this material.¹⁶³



Scheme 1.22 One-Pot Three-Component C–S Coupling reaction

S Das et al. reported bifunctional silica catalysts comprising of tertiary amine and silanol (weak acid) groups for Michael addition reaction.¹⁶⁴ The catalysts were synthesized by grafting of tertiary amine containing organosilane into the mesoporous silica in polar-protic and nonpolar-aprotic solvents. They conducted Michael addition reaction over bifunctionalized mesoporous silica catalyst (Scheme 1.23), and proposed dual activation mechanism for the reaction (Fig.1.20). The material grafted in polar solvent, exhibited higher catalytic activity than the corresponding material that was grafted in toluene and that contained less optimized proportions of amine and silanol groups. This acid-base mesoporous silica catalyst showed good recyclability even after four consecutive reaction cycles.



Scheme 1.23 Michael addition reaction over bifunctionalized mesoporous silica

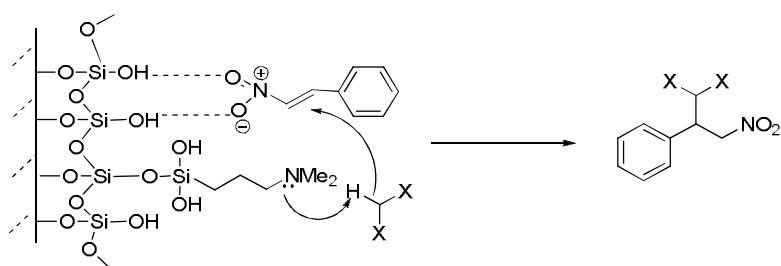


Fig. 1.20 Proposed mechanism of dual activation involving H-bonding by acid/base bifunctional mesoporous catalysts in the Michael addition reaction

1.9 Scope of the present study`

The underlying motivation of this research involved the synthesis and design of novel polyamine (Lewis base) and Lewis acid functionalized silica as well as tuning this organic/inorganic hybrid material for application in heterogeneous catalysis. Traditional routes to synthesize functionalized silica materials resulted in low amount of organic functionality. So our aim was to develop catalysts with high density of active sites on an inorganic solid support (mesoporous material). In the present work, we have integrated the advantages of mesoporous silica, using the advantages of post-synthesis grafting method and surface initiated polymerization method. Exploring the merits of heterogeneous catalysis, some functionalized mesoporous silica with high density of active sites based catalytic systems were designed and their catalytic activity was explored in various multicomponent reactions and C-C bond forming reactions.

1.10 Main objectives of the work

- To synthesize periodic mesoporous silica with different pore size ranges. Eg., (MS-2.8 nm), (MS I-6 nm), (BS-4 nm, a periodic mesoporous organosilica).
- To synthesize and characterize N,N-dialkylated polyamine mesoporous silica as Lewis base catalyst in Strecker amino acid synthesis
- To prepare Ti-grafted poly(amidoamine) dendritic silica hybrid catalyst. Characterization and application of the catalyst in Biginelli reaction and pyranopyrazole synthesis.

- To synthesize and characterize functionalized mesoporous silica (MS I) catalyst and evaluate its catalytic activity in Flavanone synthesis and in asymmetric Mannich reaction.
- To synthesize silica-supported NHC-Pd complex, its characterization and examine its catalytic performance in aromatic coupling reactions.
- To develop polypeptide functionalized mesoporous silica catalyst, the physico-chemical characterization of the catalyst and application of this catalyst in the aminolysis of epoxides.

1.11 Analysis and characterization

Powder XRD patterns of all the samples were collected using Rigaku (D. Max. C) X-ray diffractometer having CuK α ($\lambda=1.5405\text{\AA}$) radiation. (Department of Physics, CUSAT).

Infrared Spectra were recorded using JASCO FTIR Spectrometer as KBr pellets in the range 400-4000 cm^{-1} . Most silica samples were prepared as KBR pellets.

X-ray photoelectron spectroscopy (XPS) analysis was carried out on a Kratos Axis Ultra X-ray photoelectron spectroscope (UK) with Al K α radiation of 1486.6 eV. The base pressure in the analyzing chamber was maintained at 1×10^{-10} mbar. Charging of the samples was corrected by setting the binding energy of the adventitious carbon (C 1s) at 284.6 eV(AIMS, KOCHI).

TG analysis was performed on Perkin Elmer Pyris Diamond 6 thermogravimetric/differential thermal analyzer by heating the sample at the

rate of 10 °C/min from 40 °C to 730 °C in N₂ atmosphere (SAIF-STIC, CUSAT).

The diffuse reflectance UV-Vis spectra of the solid samples were recorded using UV-Vis-NIR Ocean Optics Spectrophotometer SD 2000 model equipped with a diffuse reflectance accessory.

TEM analysis was carried out with JEM 2100 HRTEM from SAIF-STIC, CUSAT. Samples for the TEM measurement were suspended in ethanol and one drop of the dispersion was placed on a graphite foil on a copper grid and allowed to dry, leaving the crystallites in random orientation on the foil.

Melting points were determined in open capillary tubes on a Büchi Melting Point B-540 apparatus and are uncorrected.

GC analysis was carried out on a 1200 L Single Quadrupole, Varian Gas Chromatograph. LC-MS was taken on LC-Waters e 2695 with mass detector-waters 3100.

The SEM characterization was carried out using the JEOL Model Scanning Electron Micrograph with an attached energy-dispersive X-ray detector. Scanning was done at the 1–20 µm range and images were taken at a magnification of 15–20 kV. Data were obtained using INCA software. The standardization of the data analysis is an integral part of the SEM-EDX instrument employed (SAIF-STIC, CUSAT).

Adsorption and desorption isotherms for nitrogen were obtained at 77K using a Micromeritics Gemini 2360 V5.01 Surface Area Analyzer. The sample

was degassed for 16 h at 90 °C in degas port to remove moisture and gaseous impurities present. The isothermal N₂ gas adsorption and desorption were carried out in analysis port at 77 K using liquid nitrogen enclosure. The sample was carefully weighed before degassing, after degassing and after surface area analysis to determine the accuracy of measurement. The specific surface area values were obtained using the BET (Brunauer-Emmett-Teller) equation. The pore size distribution data were obtained using the BJH (Barrett-Joyner-Halenda) method.

Average molecular weights of polymers were determined by gel permeation chromatography (GPC) with Waters 2690 separation module with HR 4, 3 and 1 THF columns equipped with Waters 910 refractive index detector. Polystyrene standards were used for the calibration and tetrahydrofuran was used as solvent (SCTMIST, Trivandrum).

¹³C cross-polarized magic angle-spinning (CP-MAS) NMR spectra were recorded on a Bruker 300 MHz instrument and obtained from IIT, New Delhi. ²⁹Si cross-polarized magic angle-spinning (CP-MAS) NMR spectra were recorded on a Bruker 300 MHz instrument and obtained from NCL, Pune.

Solution ¹H and ¹³C NMR Spectra were taken on Bruker 400 MHz instrument with TMS as internal standard in CDCl₃ and DMSO-*d*₆ (SAIF-STIC, CUSAT).

MALDI-TOF/MS analysis was performed on Bruker Daltonics UltrafleXtreme model equipped with smart beam solid state laser (337 nm) in reflectron positive ion mode using 19KV acceleration voltage. (NIIST, Trivandrum).

Metal content of the samples were measured by Atomic Absorption Spectroscopy (AAS) using the model Thermo Electron Corporation with M Series AA Spectrometer.

Elemental analysis was performed in SAIF-STIC, CUSAT.

Magnetic susceptibility of the Pd complex was measured by the Gouy balance, using the model Scherwood, Scientific (St. Thomas College, Thrissur).

The enantiomeric purity of the isolated products were determined by HPLC on a Chiralpak IB-3 column eluted with a mixture of hexane/iPrOH (90:10) at a flow rate of 0.5 mL min⁻¹ and detected at 254 nm.

References

- [1] G. Centi and S. Perathoner, *Catal. Today*, 2003, **77**, 287.
- [2] K. Smith and Ellis Horwood (Ed.), *Solid Supports and Catalysis in Organic Synthesis*, PTR Prentice Hall, New York, 1992.
- [3] J. Pinkas, *Ceram.-Silik.*, 2005, **4**, 287.
- [4] T. Uchino, *J. Ceram. Soc. Jpn.*, 2005, **1**, 17.
- [5] G. A. Ozin, *Adv. Mater.*, 1992, **4**, 612.
- [6] D. H. Everett. *Pure and Appl. Chem.*, 1972, **31**, 578.
- [7] B. Hatton, K. Landskron, W. Whitnall, D. Perovic and G. A. Ozin, *Acc. Chem. Res.*, 2005, **38**, 305.
- [8] C. T. Kresge, M. E. Leonowicz, W. J. Roth, J. C. Vartuli and J. S. Beck, *Nature*, 1992, 710.
- [9] Y. Tao, R. Kauoh, L. Abranis, and K. Kaneko, *Chem. Rev.*, 2006, **106**, 896.

- [10] J. S. Beck, J. C. Vartuli, G. J. Kennedy, C. T. Kresge, W. J. Roth and S. F. Schramm, *Chem. Mater.*, 1994, **6**, 1816.
- [11] D. Zhao, J. Feng, Q. Huo, N. Melosh, G. H. Fredrickson, B. F. Chmelka and G. D. Stucky, *Science*, 1998, **279**, 548.
- [12] M. Kruk, M. Jaroniec, and A. Sayari, *J. Phys. Chem. B*, 1997, **101**, 583.
- [13] G. Yanga, Y. Denga, J. Wang, *Ceramics International*, 2014, **40**, 7401.
- [14] A. Corma, *Chem. Rev.*, 1997, **97**, 2373.
- [15] G. Kickelbick, *Prog. Polym. Sci.*, 2003, **28**, 83.
- [16] J. S. Beck, J. C. Vartuli, W. J. Roth, M. E. Leonowicz, C. T. Kresge and K. D. Schmitt, *J. Am. Chem. Soc.*, 1992, **114**, 10834.
- [17] G. S. Attard, J. C. Glyde and C. G. Goltner, *Nature*, 1995, **378**, 366.
- [18] L. T. Zhuravlev, *Colloid Surf. A-Physicochem. Eng. Asp.*, 1993, **74**, 71.
- [19] J. C. Vartuli, K. D. Schmitt, C. T. Kresge, W. J. Roth, M. E. Leonowicz, S. B. McCullen, S. D. Hellring, J. S. Beck, J. L. Schlenker, D. H. Olson, and E. W. Sheppard, *Chem. Mat.*, 1994, **6**, 2317.
- [20] A. Monnier, F. Schüth, Q. Huo, D. Kumar, D. Margolese, R. S. Maxwell, G. Stucky, M. Krishnamurty, P. Petroff, A. Firouzi, M. Janicke and B. Chmelka, *Science*, 1993, **261**, 1299.
- [21] Q. S. Huo, D. Y. Zhao, J. L. Feng, W. Kenneth, S. K. Buratto, G. D. Stucky, S. Schacht and F. Schuth, *Adv. Mater.*, 1997, **9**, 974.
- [22] J. F. Wang, J. P. Zhao, B. Y. Asoo and G. D. Stucky, *J. Am. Chem. Soc.*, 2003, **125**, 13966.
- [23] D. Zhao, Q. Huo, J. Feng and B. F. Chemlka, *J. Am. Chem. Soc.*, 1998, **120**, 6024.
- [24] Y. Lu, *Angew. Chem. Int. Ed. Engl.*, 2006, **45**, 7664.
- [25] H. Yang, N. Goombs and G. A. Ozin, *Nature*, 1997, **386**, 692.

- [26] Q. S. Huo, D. I. Margolese, and G. D. Stucky. *Chem. Mat.*, 1996, **8**, 1147.
- [27] M. Widenmeyer and R. Anwander, *Chem. Mater.*, 2002, **14**, 1827.
- [28] H. P. Lin, C. Y. Mou, *Acc. Chem. Res.*, 2002, **35**, 927.
- [29] N. Mizoshita, T. Taniab and S. Inagaki, *Chem. Soc. Rev.*, 2011, **40**, 789.
- [30] W. J. Hunks and G. A. Ozin, *J. Mater. Chem.*, 2005, **15**, 3716.
- [31] S. Inagaki, S. Guan, Y. Fukushima, T. Ohsuna and O. Terasaki, *J. Am. Chem. Soc.*, 1999, **121**, 9611.
- [32] B. J. Melde, B. T. Holland, C. F. Blanford and A. Stein, *Chem. Mater.*, 1999, **11**, 3302.
- [33] T. Asefa, M. J. MacLachlan, N. Coombs and G. A. Ozin, *Nature*, 1999, **402**, 867.
- [34] A. Stein, B. J. Melde and R. C. Schrodén, *Adv Mater.*, 2000, **12**, 1403.
- [35] F. Hoffmann, M. Cornelius, J. Morell and M. Froba, *Angew. Chem. Int. Ed.*, 2006, **45**, 3216.
- [36] J. H. Clark and D. J. Macquarrie, *Chem. Commun.*, 1998, **8**, 853.
- [37] R. Anwander, I. Nagl, M. Widenmeyer, G. Engelhardt, O. Groeger, C. Palm and T. Roser, *J. Phys. Chem. B*, 2000, **104**, 3532.
- [38] S. L. Burkett, S. D. Sims and S. Mann, *Chem. Commun.*, 1996, 1367.
- [39] D. J. Macquarrie, *Chem. Commun.*, 1996, 1961.
- [40] X. S. Zhao and G. Q. Lu, *J. Phys. Chem.*, 1998, **102**, 1556.
- [41] J. Liu, H. Q. Yang, F. Kleitz, Z. G. Chen, T. Yang, E. Strounina and S. Z. Qiao, *Adv. Funct. Mater.*, 2012, **22**, 59.
- [42] N. Ma, Y. Deng, W. Liu, S. Li, J. Xu, Y. Qu, K. Gan, X. Sun and J. Yang, *Chem. Commun.*, 2016, **52**, 3544.
- [43] J. G. Croissant, X. Cattoën, M. W. C. Man, J. -O. Durand and N. M. Khashab, *Nanoscale*, 2015, **7**, 20318.

- [44] S. Inagaki, S. Guan, T. Ohsuna and O. Terasaki, *Nature*, 2002, **416**, 304.
- [45] P. V. Voort, D. Esquivel, E. D. Canck, F. Goethals, I. V. Driesscheb and F. J. R. Salguero, *Chem. Soc. Rev.*, 2013, **42**, 3913.
- [46] N. Hao, H. Yang, L. Li, L. Lia and F. Tang, *New J. Chem.*, 2014, **38**, 4258.
- [47] N. Liu, R. A. Assink and C. J. Brinker, *Chem. Commun.*, 2003, 370.
- [48] A. S. Timin, S. Yu. Khashirova, A. Zhansitov and E. V. Rummyantsev, *Colloid Polym. Sci.*, 2015, **293**, 1667.
- [49] F. Tang, L. Li and D. Chen, *Adv. Mater.*, 2012, **24**, 1504.
- [50] X. Wang, P. Wang, Z. Dong, Z. Dong, Z. Ma, J. Jiang, R. Li and J. Ma, *Nanoscale Res. Lett.*, 2010, **5**, 1468.
- [51] J. M. Rosenholm, T. G. Sarfraz, V. Mamaeva, R. Niemi, E. Özliseli, D. Desai, D. Antfolk, E. von Haartman, D. Lindberg, N. Prabhakar, T. Näreoja and C. Sahlgren, *Small*, 2016, **12**, 1578.
- [52] S. Sisodiya, A. Lazar, S. Shylesh, L. Wang, W. R. Thiel and A. P. Singh, *Catal. Commun.*, 2012, **25**, 22.
- [53] J. P. Mathew and M. Srinivasan, *Polym. Int.*, 1992, **29**, 179.
- [54] W. Long, N. A. Brunelli, S.A. Didas, E. W. Ping, and C. W. Jones, *ACS Catal.*, 2013, **3**, 1700.
- [55] J. E. Mhoe, J. H. Clark and D. J. Mcquirrie, *Synlett*, 1998, 625.
- [56] Y. V. S. Rao, D. E. De vos and P. A. Jacobs, *Angew. Chem. Int. Ed. Engl.*, 1997, **36**, 2661.
- [57] D. Das, J. F. Lee and S. Cheng, *Chem. Commun.*, 2001, 2178.
- [58] D. Das, J. F. Lee and S. Cheng, *J. Catal.*, 2004, **223**, 152.
- [59] A. Corma, S. Iborra, I. RodrWguez, M. Iglesias and F. Snchez, *Catal. Lett.*, 2002, **82**, 237.

- [60] J. A. Bae, K. C. Song, J. K. Jeon, Y. S. Ko, Y. K. Park and J. H. Yim, *Microporous Mesoporous Mater.*, 2009, **123**, 289.
- [61] M. Hajjami and Z. Yousofv, *Catal. Lett.*, 2015, **145**, 1733.
- [62] N. Moitra, S. Ichii, T. Kamei, K. Kanamori, Y. Zhu, K. Takeda, K. Nakanishi and T. Shimada, *J. Am. Chem. Soc.*, 2014, **136**, 11570.
- [63] E. J. Acosta, C. S. Carr, E. E. Simanek and D. F. Shantz, *Adv. Mater.*, 2004, **16**, 985.
- [64] L. Mercier and T. J. Pinnavaia, *Chem. Mater.*, 2000, **12**, 188.
- [65] A. Walcarius and C. Delac, *Chem. Mater.*, 2003, **15**, 4181.
- [66] A. S. M. Chong, X. S. Zhao and *J. Phys. Chem. B*, 2003, **107**, 12650.
- [67] S. Huh, J. W. Wiench, J. C. Yoo, M. Pruski and V. S. Y. Lin, *Chem. Mater.*, 2003, **15**, 4247.
- [68] F. Cagnol, D. Grosso and C. Sanchez, *Chem. Commun.*, 2004, 1742.
- [69] Y. Wang, B. Zibrowius, C. M. Yang, B. Spliethoff and F. SchEh, *Chem. Commun.*, 2004, 46.
- [70] R. J. P. Corriu, C. Hoarau, A. Mehdi and C. ReyL, *Chem. Commun.*, 2000, 71.
- [71] R. J. P. Corriu, L. Datas, Y. Guari, A. Mehdi, C. ReyL and C. Thieuleux, *Chem. Commun.*, 2001, 763.
- [72] A. Modak, J. Mondal and A. Bhaumik, *Green Chem.*, 2012, **14**, 2840.
- [73] A. Bibby and L. Mercier, *Chem. Mater.*, 2002, **14**, 1591.
- [74] M. H. Lim, C. F. Blanford and A. Stein, *J. Am. Chem. Soc.*, 1997, **119**, 4090.
- [75] H. T. Chen, S. Huh, J. W. Wench, M. Pruski and V. Y. Len, *J. Am. Chem. Soc.*, 2005, **127**, 13305.
- [76] N. Linares, A. E. S. Iveda, M. C. Pacheco, J. R. Berenguer, E. Lalinde, C. N. Jerac and J. G. Martinez, *New J. Chem.*, 2011, **35**, 225.

- [77] M. Fisher and F. Vogtle, *Angew. Chem. Int. Ed. Engl.*, 1999, **38**, 884.
- [78] A. K. Patri, I. J. Majoros and J. R. Baker, *Curr. Opin. Chem. Biol.*, 2002, **6**, 466.
- [79] G. R. Newkome, E. He and C. N. Moorefield, *Chem. Rev.*, 1999, **99**, 1689.
- [80] F. Vögtle, *Top. Curr. Chem.*, 1998 **197**, 7.
- [81] J. H. G. Jansen, E. W. Meijer and E. M. Brabander-vander Berg, *J. Am. Chem. Soc.*, 1995, **117**, 4417.
- [82] S. C. Zimmerman, Y. Wang and J. Moore, *J. Chem. Soc.*, 1998, **120**, 2172.
- [83] R. van Heerbeek, P. C. J. Kamer, P. W. N. M. van Leeuwen and J. N. H. Reek, *Chem. Rev.*, 2002, **102**, 3717.
- [84] J. W. J. Knapen, A. W. van der Made, J. C. de Wilde, P. W. N. M. van Leeuwen, P. Wijkens, D. M. Grove and G. van Koten, *Nature*, 1994, **372**, 659.
- [85] G. R. Krishnan and K. Sreekumar, *Tetrahedron Lett.*, 2014, **55**, 2352.
- [86] G. Smitha and K. Sreekumar, *RSC Adv.*, 2016, **6**, 18141.
- [87] E. Linder, M. Kemmler, H. A. Mayer and P. J. Wegner, *J. Am. Chem. Soc.*, 1994, **116**, 348.
- [88] U. Schubert, N. Husing and A. Lorenz, *Chem. Mater.*, 1995, **7**, 2010.
- [89] A. Halperin, M. Tirrell and T. P. Lodge, *Adv. Polym. Sci.*, 1992, **100**, 31.
- [90] M. Alexandre and P. Dubois, *Mater. Sci. Eng.*, 2000, **28**, 1.
- [91] E. P. Giannelis, R. Krishnamoorti and E. Manias, *Adv. Polym. Sci.*, 1999, **138**, 108.
- [92] F. Bauer, H. Ernst, U. Decker, M. Findeisen, H. Glaeser, H. Langguth, E. Hartmann, R. Mehnert and C. Peuker, *Macromol. Chem. Phys.*, 2000, **201**, 2654.
- [93] T. K. Mandal, M. S. Fleming and D. R. Walt, *Nanoletters*, 2002, **2**, 3.

- [94] L. Quaroni and G. Chumanov, *J. Am. Chem. Soc.*, 1999, **121**, 10642.
- [95] G. Carrot, S. M. Scholz, J. G. Plummer and J. G. Hilborn, *Chem. Mater.*, 1999, **11**, 3571.
- [96] B. Zhao and W. J. Brittain, *Prog. Polym. Sci.*, 2000, **25**, 677.
- [97] P. Mansky, Y. Liu, E. Huang, T. P. Russell and C. Hawker, *Science*, 1997, **275**, 1458.
- [98] S. Edmondson, V. L. Osborne and W. T. S. Huck, *Chem. Soc. Rev.*, 2004, **33**, 14.
- [99] B. Radhakrishnan, R. Ranjan and W. J. Brittain, *Soft Mater.*, 2006, **2**, 386.
- [100] K. Matyjaszewski and J. Xia, *Chem. Rev.*, 2001, **101**, 2921.
- [101] O. Prucker and J. Rühle, *Macromolecules*, 1998, **31**, 592.
- [102] K. Matyjaszewski, *Controlled Radical Polymerization*, ACS Symp. Ser., Washington DC, 1998, 685.
- [103] M. Georges, R. Veregin, P. Kazamaier and G. G. Hamer, *Macromolecules*, 1993, **26**, 2987.
- [104] J. S. Wang and K. Matyjaszewski, *J. Am. Chem. Soc.*, 1995, **117**, 5614.
- [105] J. Moraes, K. Ohno, T. Maschmeyer and S. Perrier, *Chem. Commun.*, 2013, **49**, 9077.
- [106] G. Carrot, D. Rutot-Houze, A. Pottier, P. Degee, J. Hilborn and P. Dubois, *Macromolecules*, 2002, **35**, 8400.
- [107] A. Sunder, H. Turk, R. Haag and H. Frey, *Macromolecules*, 2000, **33**, 7682.
- [108] M. Suzuki, S. Yoshida, K. Shivaga and T. Saegusa, *Macromolecules*, 1998, **31**, 1716.
- [109] A. Sunder, R. Hanselmann, H. Frey and M. Rolf, *Macromolecules*, 1999, **32**, 4240.

- [110] V. Swali, N. I. Wells, G. I. Langley and M. I. Bradley, *J. Org. Chem.*, 1997, **62**, 4902.
- [111] N. Tsubokawa, H. Ichioka, T. Satoh, S. Hayashi and K. Fujiki, *React. Funct. Polym.*, 1998, **37**, 75.
- [112] N. Tsubokawa, K. Kotama, H. Saitoh and T. Nishikubo, *Compos. Interfaces*, 2003, **10**, 609.
- [113] Y. Taniguchi, K. Shirai, H. Saitoh, T. Yamauchi and N. Tsubokawa, *Polymer*, 2005, **46**, 2541.
- [114] C. Wang, G. Zhu, X. Cai, J. Li, Y. Wei, D. Zhang and S. Qiu, *Chem. Eur. J.*, 2005, **11**, 4975.
- [115] S. C. Bourque, H. I. Alper, L. E. Manzer and P. I. Arya, *J. Am. Chem. Soc.*, 2000, **122**, 956.
- [116] I. P. K. Reynhardt and H. I. Alper, *J. Org. Chem.*, 2003, **68**, 8353.
- [117] P. P. Zweni and H. Alper, *Adv. Synth. Catal.*, 2004, **346**, 849.
- [118] M. P. Kapoor, Y. Kasama, T. Yokoyama, M. Yanagi and S. Inagaki, *J. Mater. Chem.*, 2006, **16**, 4714.
- [119] H. Lu, J. Wang, Z. Song, L. Yin, Y. Zhang, H. Tang, C. Tu, Y. Lin and J. Cheng, *Chem. Commun.*, 2014, **50**, 139.
- [120] (a) H. Leuchs, *Chem. Ber.*, 1906, **39**, 857; (b) H. Leuchs and W. Manasse, *Chem. Ber.*, 1907, **40**, 3235; (c) H. Leuchs and W. Geiger, *Chem. Ber.*, 1908, **41**, 1721.
- [121] Y. C. Chang and C. W. Frank, *Langmuir*, 1998, **14**, 326.
- [122] A. Heise, H. Menzel, H. Yim, M. D. Foster, R. H. Wieringa, A. J. Schouten, V. Erb and M. Stamm, *Langmuir*, 1997, **13**, 723.
- [123] Y. Wang and Y. C. Chang, *Macromolecules*, 2003, **36**, 6503.
- [124] T. Jaworek, D. Neher, G. Wegner, R. H. Wieringa and A. J. Schouten, *Science*, 1998, **279**, 57.

- [125] J. K. Whitesell and H. K. Chang, *Science*, 1993, **261**, 73.
- [126] B. Fong and P. S. Russo, *Langmuir*, 1999, **15**, 4421.
- [127] B. Fong, S. Turksen, P. S. Russo and W. Stryjewski, *Langmuir*, 2004, **20**, 266.
- [128] M. Czaun, M. M. Rahman, M. Takafuji and H. Ihara, *Polymer*, 2008, **49**, 5410.
- [129] A. Shundo, T. Sakurai, M. Takafuji, S. Nagaoka and H. Ihara, *J. Chromatogr. A*, 2005, **1073**, 169174.
- [130] A. E. Abelow and I. Zharov, *Soft Mater.*, 2009, **5**, 457.
- [131] X. M. Zheng, Y. X. Qi, X. M. Zhang and J. S. Suo, *Chin. Chem. Lett.*, 2004, **15**, 655.
- [132] G. J. Kim and J. H. Shin, *Catal. Lett.*, 1999, **63**, 205.
- [133] C. Baleiz, B. Gigante, D. Das, M. Alvaro, H. Garcia and A. Corma, *Chem. Commun.*, 2003, 1860.
- [134] K. Sarkar, M. Nandi, M. Islam, M. Mubarak and A. Bhaumik, *Appl. Catal. A*, 2009, **352**, 81.
- [135] J. S. Kingsbury, S.B. Garber, J. M. Giftos, B. L. Gray, M. M. Okamoto, R. A. Farrer, J. T. Fourkas and A. H. Hoveyda, *Angew. Chem. Int. Ed.*, 2001, **40**, 4251.
- [136] Y. Zhao, Y. Zhou, D. Ma, J. Liu, L. Li, Y. Z. Tony and H. Zhang, *Org. Biomol. Chem.*, 2003, **1**, 1643.
- [137] A. J. Fatiadi, *Synthesis*, 1987, 85.
- [138] R. K. Sharma, S. Sharma, S. Dutta, R. Zborilb and M. B. Gawande, *Green Chem.*, 2015, **17**, 3207.
- [139] D. Choudhary, S. Paul, R. Gupta and J. H. Clark, *Green Chem.*, 2006, **8**, 479.
- [140] A. Ghorbani-choghamarani and S. Sardari, *J. Sulfur Chem.*, 2011, **32**, 63.
- [141] G. Sharma, R. Kumar and A. K. Chakraborti, *Tetrahedron Lett.*, 2008, **49**, 4272.

- [142] B. Karimi and M. Khalkhali, *J. Mol. Catal. A: Chem.*, 2005, **232**, 113.
- [143] E. Canck, I. D. Rodríguez, E. M. Gaigneaux and P. V. Der Voort, *Materials*, 2013, **6**, 3556.
- [144] A. Dastan, A. Kulkarnia and B. Torok, *Green Chem.*, 2012, **14**, 17.
- [145] N. Salam, P. Mondal, J. Mondal, A. S. Roy, A. Bhaumik and S. M. Islam, *RSC Adv.*, 2012, **2**, 6464.
- [146] Y. Kubota, H. Yamaguchi, T. Yamada, S. Inagaki, Y. Sugi and T. Tatsumi, *Top. Catal.*, 2010, **3**, 492.
- [147] S. Verma, M. Nandi, A. Modak, S. L. Jain and A. Bhaumik, *Adv. Synth. Catal.*, 2011, **353**, 1897.
- [148] J. Mondal, A. Modak, A. Dutta and A. Bhaumik, *Dalton Trans.*, 2011, **40**, 5228.
- [149] A. T. Dickschat, F. Behrends, S. Surmiak, M. Weiß, H. t Eckert and A. Studer, *Chem. Commun.*, 2013, **49**, 2195.
- [150] H. Li, M. Yang, X. Zhang, L. Yan, J. Li and Y. Qi, *New J. Chem.*, 2013, **37**, 1343.
- [151] N. A. Brunelli, K. Venkatasubbaiah, and C. W. Jones, *Chem. Mater.*, 2012, **24**, 2433.
- [152] J. Mondal, A. Modak, A. Bhaumik, *J. Mol. Catal. A: Chem.*, 2011, **335**, 236.
- [153] C. Savelli and R. Salvio, *Chem. Eur. J.*, 2015, **21**, 5856.
- [154] H. Zhou, Y. M. Wang, W. Z. Zhang, J. P. Qu and X. B. Lu, *Green Chem.*, 2011, **13**, 644.
- [155] J. Mondal, A. Modak and A. Bhaumik, *J. Mol. Catal. A: Chem.*, 2012, **363**, 254.
- [156] P. P. Zweni and H. Alper, *Adv. Synth. Catal.*, 2006, **348**, 725.
- [157] E. Karakhanov, A. Maximov, Y. Kardasheva, V. Semernina, A. Zolotukhina, A. Ivanov, G. Abbott, E. Rosenberg and V. Vinokurov, *Appl. Mater. Interfaces*, 2014, **6**, 8807.

- [158] D. Das, J. F. Lee and S. Cheng, *Chem. Commun.*, 2001, 2178.
- [159] B. Karimi, H. M. Mirzaei and A. Mobaraki, *Catal. Sci. Technol.*, 2012, **2**, 828.
- [160] J. Mondal, A. Modak, M. Nandi, H. Uyamab and A. Bhaumik, *RSC Adv.*, 2012, **2**, 11306.
- [161] X. Zhang, Y. Zhao, J. Peng and Q. Yang, *Green Chem.*, 2015, **17**, 1899.
- [162] M. N. Esfahani, I. M. Baltork, A. R. Khosropour, M. Moghadam, V. Mirkhani, S. Tangestaninejad and H. A. Rudbari, *J. Org. Chem.*, 2014, **79**, 1437.
- [163] J. Mondal, P. Borah, A. Modak, Y. Zhao, and A. Bhaumik, *Org. Process Res. Dev.*, 2014, **18**, 257.
- [164] S. Das, A. Goswami, N. Murali and T. Asefa, *Chem. Cat. Chem.*, 2013, **5**, 910.

Chapter 2

MESOPOROUS SILICA SUPPORTED N, N-DIALKYLATED POLYAMINE AS CATALYST IN STRECKER AMINO ACID SYNTHESIS

Contents	2.1	Introduction
	2.2	Results and Discussion
	2.3	Conclusion
	2.4	Experimental

The synthetic route to mesoporous silica supported polymer materials offers remarkable flexibility in the design of solid catalysts. The present chapter focuses on the synthesis of polymer functionality on mesoporous silica (MS) through surface initiated polymerization (SIP), and explores their heterogeneous Lewis base activity for the synthesis of α -amino nitriles. Simple, clean and eco-friendly approach for the preparation of α -amino nitriles is discussed in this chapter. Hyperbranched polyamine and N,N-dialkylated polyamine were developed on MS and thiol functionalized MS respectively. The physico-chemical characterization of the catalyst was done. Amine capacity of these materials was measured. Studies demonstrated the synthesis of α -amino nitriles by N,N-dialkylated catalyst which gave high TOFs compared to polyamine functionalized MS hybrid catalyst.

2.1 Introduction

The grafting of polymers to periodic mesoporous silica (PMS) has become a major route to develop a new class of fascinating functional materials (also called inorganic–organic hybrid materials). Such surface functionalization by polymers offers some value-added properties for new emerging applications such as electronic/optoelectronic devices, biomolecule, drug release and catalysis.¹⁻⁷ Recently, many different strategies have been reported for grafting of polymers to PMS.⁸⁻¹⁰ Among this, surface initiated polymerization (SIP), e.g., polymerization performed using initiator sites previously immobilized on mineral surfaces (using the so-called “graft-from” technique), appears to be a promising and versatile method.¹¹ This method ensures the formation of polymer brushes and a tighter control over polymer molecular weight and architecture. Another clear advantage of this process is that the polymer chains are covalently attached to the surface. By grafting from method, the polymers successfully grafted on the PMS included poly(lactic acid), polystyrene, poly(methyl methacrylate) and poly(N-isopropyl acrylamide).¹²⁻¹⁴ A large variety of initiating mechanisms, including atom transfer radical polymerization (ATRP), free radical and ring opening polymerizations (ROP) have been reported.¹⁵⁻¹⁷

The functionalization of PMS with molecular, supramolecular or polymer moieties, provides materials with great versatility in heterogeneous catalysis, tissue engineering, drug delivery system etc. Herein, we describe a significant step in expanding hyperbranched polyamine functionalized mesoporous material as base catalyst via ring opening polymerization technique to create polyamine –mesoporous silica hybrids with high density

of tertiary amino groups. Many groups have successfully developed hyperbranched polyamine via ring opening polymerization of epichlorohydrin with glycerol and pentaerythritol as initial core.¹⁸⁻²⁰ In this perspective, we have attempted to synthesize hyperbranched polyamine on silica surface (where silanols act as initial core, PA@MS). But studies revealed that the molecular mass of grafted polymer chain was less. With this background, we have functionalized the silica surface with thiol moiety. Since -SH groups are more nucleophilic than -OH, this increases the degree of polymerization on the silica surface to a great extent. Recently, Merrifield resin supported polymer having glycerol and pentaerythritol core was also reported from our lab.²¹ The reported strategy adopted for the synthesis involved many steps. In this chapter, we have tried to develop high amine capacity on solid support even in a single step. So far, no report has appeared on the synthesis of hyperbranched polyamine on thiol functionalized silica.

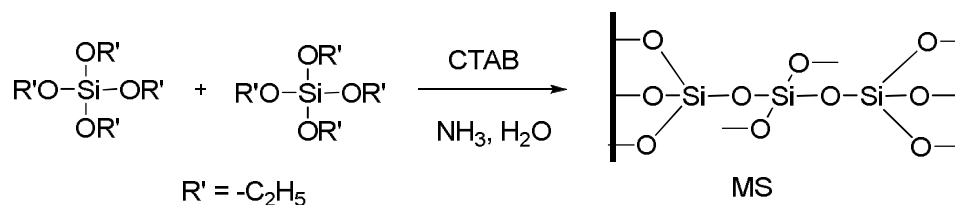
In the present work, we take advantage of the activity of N,N-dialkylated polyamine and mesoporous silica to prepare new hybrid materials and explore their catalytic properties. This chapter describes the synthesis, characterization, and catalytic activity study of N,N-dialkylated polyamine@MS as heterogeneous catalyst in Strecker amino acid synthesis in water.

2.2 Results and Discussion

2.2.1 Synthesis of mesoporous silica (MS) and N,N-dialkylated polyamine@MS

Under basic condition, an ordered mesoporous silica material with uniform pore diameter was synthesized successfully using TEOS as the silica precursor and CTAB (Cetyltrimethylammonium bromide) as the

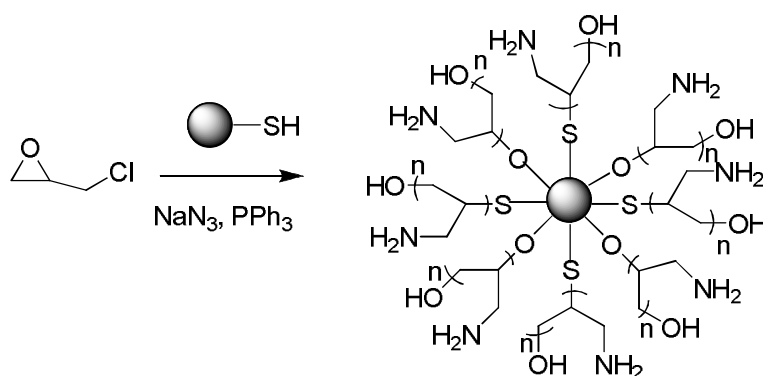
surfactant in aqueous NH_3 (Scheme 2.1). A hexagonal surfactant silicate mesophase was formed from positively charged surfactant molecules and silicate oligomers carrying multiple negative charges. This negative charge has stabilized ammonium ions. Partial stabilization of silicate species facilitated the approach and condensation between the template-silicate agglomerates to form a well ordered surfactant silicate mesophase. Removal of the surfactant by calcination and further condensation between adjacent silicate species has led to highly ordered mesoporous silica.^{22,23}



Scheme 2.1 Synthetic procedure for mesoporous silica (MS)

A thiol moiety was introduced into silica framework by post-grafting method. It is now understood that hybrid materials synthesized from post-grafting method are more catalytically active than their directly prepared analogues because of the higher accessibility of active sites.²⁴ Since thiol group in mercaptotriethoxysilane is more nucleophilic than -OH group in silica, the best choice of anchoring group as initiator is thiol. A single monomer methodology (SMM) was adopted here, in which hyperbranched polymers are grafted to the silica surface by self-condensing ring opening polymerization (SCROP) of epichlorohydrin.²⁵ Subsequent ring opening of epoxides under different conditions has led to PECH polymer with different functionalities and structures depending on the reactants. Azide polymer functionalized silica was prepared by simultaneous mixing of hot solutions of

sodium azide with epichlorohydrin and tetrabutylammonium bromide (PTC) in DMSO.²⁶ An excess of NaN₃ present in the reaction medium helps the conversion of chloromethyl group to azidomethyl group. The polymer containing the azidomethyl side chain was converted to a polymer containing aminomethyl side chain by the reduction of the azide group to amino group. The search for a suitable reducing agent to reduce the azide group to amino group ended in the choice of triphenylphosphine. The efficiency of PPh₃ in the reduction of azide groups is well known.²⁷ The backbone of polymeric chain is depicted in Scheme 2.2.



Scheme 2.2 Ring opening polymerization of epichlorohydrin by MS-SH

Finally, the polyamine was refluxed with excess dimethyl sulphate, which acts as a protective group in organic transformations. The free silanol and hydroxyl group of the polymer on MS may also be protected by dimethyl sulphate at this stage. The stepwise preparation of polymeric mesoporous silica hybrid is shown in Scheme 2.3. This scheme shows the synthesis of PA@MS where silanol function initiates the polymerization of epichlorohydrin.

Amine capacity of the functionalized silica was measured by titration method and this shows good agreement with the result obtained from UV-Visible spectrophotometric analysis.²⁸ The results are given in Table 2.2.

Table 2.2 Amine content of functionalized silica

Sample	NH ₂ content mmol/g ^a	NH ₂ content mmol/g ^b
PA@MS	0.9	1.03
PA@MS-SH	13.1	12.7

^aTitration, ^b UV-Visible spectrophotometry

2.2.2 Characterization of MS and N,N-dialkylated polyamine@MS

2.2.2.1 X-ray diffraction studies

PXRD analysis was carried out to study the structural ordering of the samples. PXRD diagram of synthesized MS (Figure 2.1) showed a distinct peak at low angle region, $2\theta = 2-5$ which confirmed the presence of hexagonal mesophase. The thiol functionalization of MS and further polymerization of epichlorohydrin resulted in a decrease in the intensity of diffraction peak suggesting the successful grafting of functionality and that the mesostructure of the material was maintained. But in alkylated polymeric silica material, intensity of the peak was diminished. The overall decrease in intensity may be because, the polymerization may have interrupted the periodic arrangement of the silica framework.

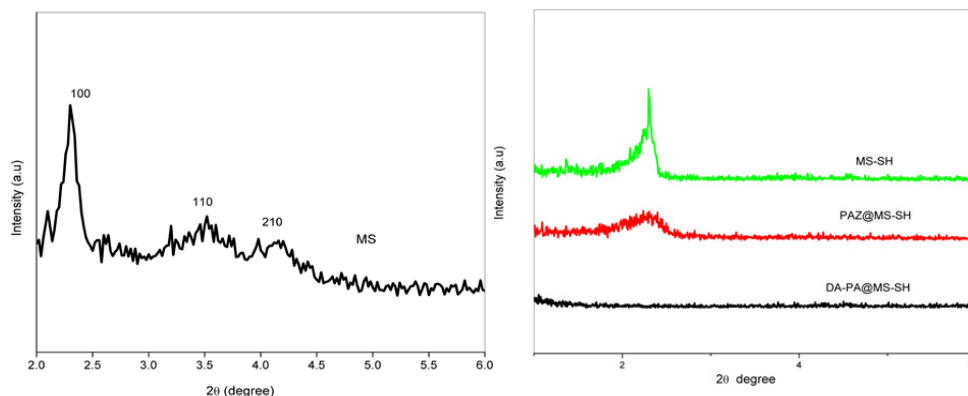


Fig. 2.1 XRD of MS, MS-SH, PAZ@MS-SH and DA-PA@MS-SH

2.2.2.2 TEM analysis

The morphology of the mesoporous silica (MS) and functionalized silica catalyst was examined by transmission electron microscopy analysis. TEM image of MS showed parallel porous channels characteristic of ordered mesoporous materials.²⁹ Polymerized silica material (DA-PA@MS-SH) exhibited disordered surface morphology and also showed a blackish zone of polymer suggesting that polymer chain was successfully grafted on the silica surface (Figure 2.2).

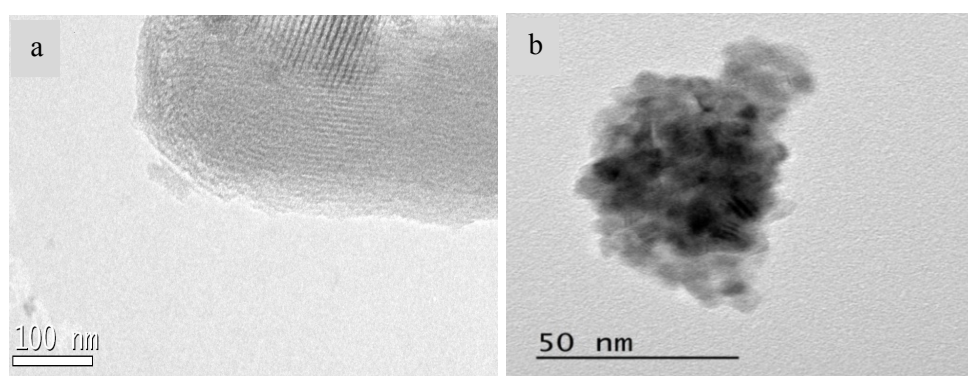


Fig. 2.2 TEM images of (a) MS and (b) DA-PA@MS-SH

2.2.2.3 IR spectral studies

FTIR spectroscopy was used to verify the presence of organic functional groups present in the samples. Immobilization of functional groups into silica framework was tracked by IR spectroscopy in every step (Figure 2.3).

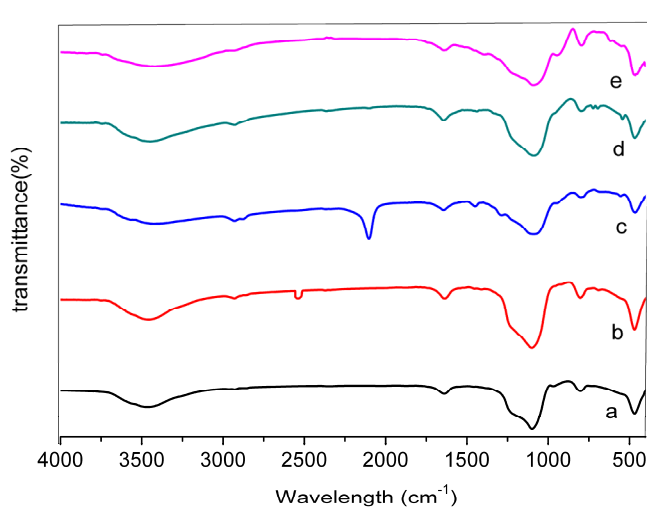


Fig. 2.3 IR spectra of (a) MS, (b) MS-SH, (c) PAZ@ MS-SH, (d) PA@ MS-SH and (e) DA-PA@ MS-SH

The -OH bond stretching bands of the silanol groups and Si-O-Si bands of MS were observed at 3443 cm^{-1} and 1082 cm^{-1} , respectively. After immobilization of the thiol functionality, the intensity of the -OH stretching band of silanol groups of MS was decreased and a weak S-H stretching peak was seen at 2532 cm^{-1} for thiol functionalized silica (MS-SH). Besides the characteristic Si-O stretching and C-H bending vibrations at 1101 and 1640 cm^{-1} , a new band at 2108 cm^{-1} ascribed to azide group was observed in silylazide polymer (PAZ@MS-SH). After reduction with triphenylphosphine, it disappeared (PA@MS-SH).

2.2.2.4 Surface area analysis

N₂ adsorption/desorption isotherms for MS, MS-SH and polymeric MS showed type IV adsorption isotherms with H1 hysteresis loop as defined by IUPAC³⁰ (Figure 2.4). The physical properties of MS and MS-SH and DA-PA@MS, such as surface area, pore size, pore volume, are listed in Table 2.3.

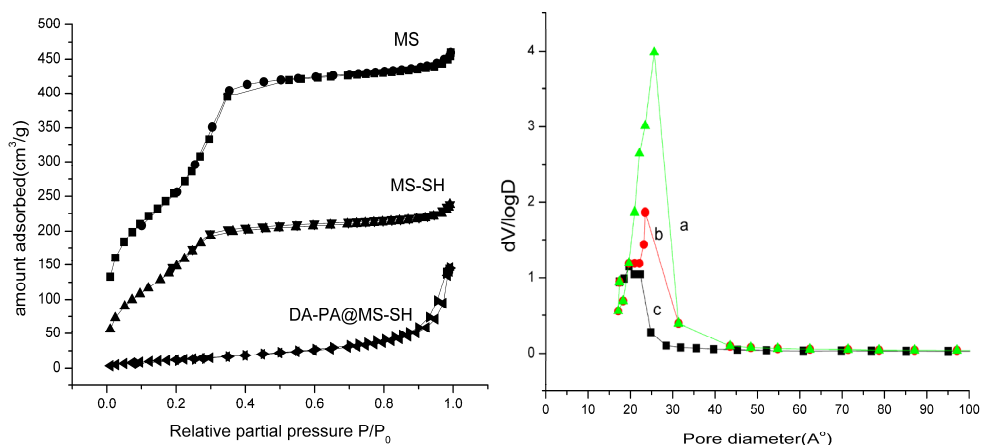


Fig. 2.4 N₂ adsorption/desorption isotherms and pore size distribution of (a) MS, (b) MS-SH and (c) DA-PA@ MS-SH

The surface area was decreased after each step of functionalization. The sharpness of the adsorption branches is indicative of a narrow mesopore size distribution. The position of capillary condensation steps shifted to low pressure values, suggesting a reduction in the mesopore size, because the capillary condensation is an increasing function of the pore diameter. This was also confirmed by changes in the pore size calculated from the adsorption branch of the nitrogen adsorption/desorption isotherm using the Barrett-Joyner-Halenda formula.³¹ The surface area, pore diameter,

and pore volume of MS decreased as a result of the grafting of the organic functional group. The overall shape of the adsorption/desorption isotherms remained unchanged. The pronounced steps of capillary condensation in primary mesopores were evident, indicating that ordering of the MS support was not affected by the modification upto the polymerization step.

Table 2.3 Physical properties of functionalized mesoporous silica

Sample ID	S_{BET} (m ² /g)	V_{meso}	d_p (BJH) [nm]
MS	1039	0.75	2.8
MS-SH	655	0.36	2.5
DA-PA@MS-SH	155	0.22	2.0

V_{meso} =Pore volume, d_p =Pore diameter

2.2.2.5 TG-DTG analysis

Thermogravimetric analysis (TGA/DTG) was conducted to measure the thermal stability of the functionalized MS samples. The TG curves of silica are displayed in (Figure 2.5). A weight loss at 70°C was observed in bare silica (MS) which was due to the removal of physisorbed water. There was no appreciable weight loss at this temperature in the case of functionalized sample, indicating that the surface of silica has become more hydrophobic by functionalization. Polyamine functionalized silica (PA@MS) exhibited weight loss of about 15 % between 220 °C-650 °C (Figure 2.5a). TG curve of MS-SH silica showed nearly 11.6 % of weight loss between 250-380 °C. It was assigned to decomposition of thiol group on silica surface,³² and it was further confirmed by elemental analysis (Table 2.2). Polymerized silica material showed two distinct weight losses at 220 °C and

330 °C respectively. It was about 48 % suggesting that percentage weight loss was significantly enhanced in thiol functionalized polymerized silica (Figure 2.5b).

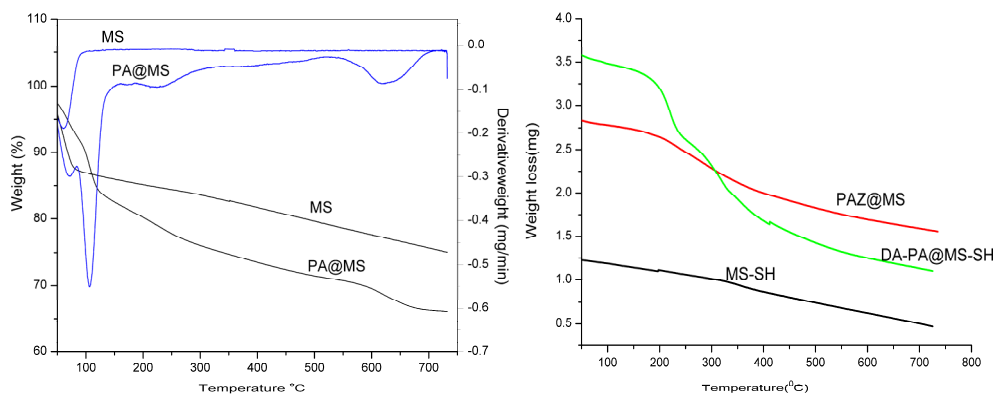


Fig. 2.5 (a) TG-DTG plots of MS and PA@MS and (b) TG plots of MS-SH, PAZ@MS-SH and DA-PA@MS-SH

2.2.2.6 Mass spectrometry

It is quite useful in determining molecular weight distribution of low molecular weight homopolymers. The grafted polymer was cleaved from the silica surface according to the procedure described in literature.³³ MALDI-TOF-MS of the cleaved dialkylated polyamine from MS is shown in Figure 2.6. The highest molecular weight of the polymer was found to be 2353.39 with a base peak at 1227.45. The polymer cleaved had fluorinated silane end group and from the highest molecular weight, it was assumed that 26 repeating units were incorporated in polymeric chain.

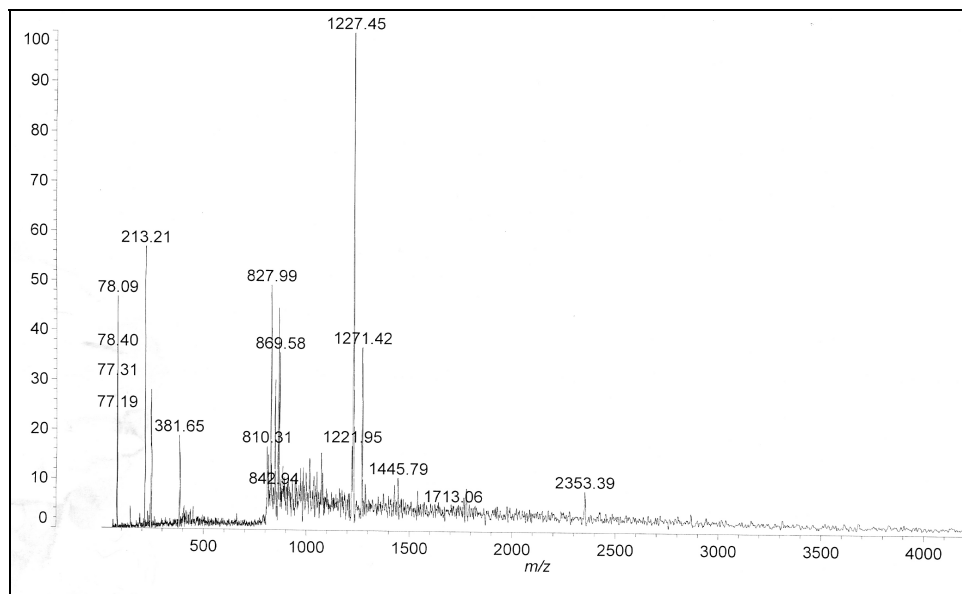


Fig. 2.6 MALDI-TOF-MS of the DA-PA cleaved from MS

2.2.2.7 Solid state ^{13}C CP-MAS NMR spectroscopy

The incorporation of functional groups into the silica surface was further confirmed by solid-state ^{13}C CP-MAS NMR spectroscopy. The ^{13}C CP-MAS NMR spectrum of DA-PA@MS-SH is shown in Figure 2.7. The peaks between 20-30 ppm are the characteristic peaks of aliphatic side chain carbon atoms of mercaptosilane group. The characteristic peaks of *N,N* dialkylated carbon atom of polymeric chain was observed at 71-72 ppm. The peak at 65 ppm corresponds to methylene carbons attached to amine moiety. The other strong peaks at 74 and 88.5 ppm correspond to the methyl and methylene carbons of polymeric chain which is attached to the electronegative oxygen atom. The peaks for the tertiary carbon atom on the surface appeared at 103 and 105 ppm which is a strong evidence for the ring opening of epichlorohydrin.

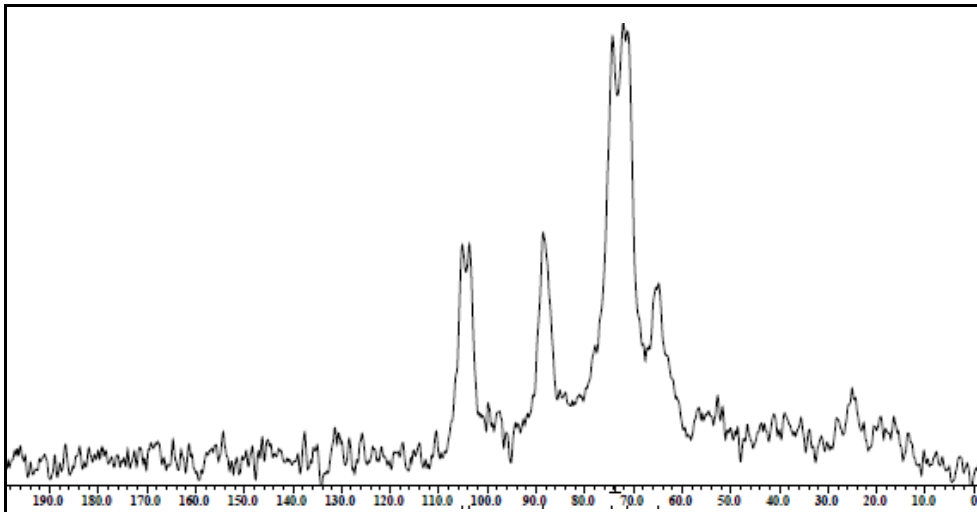


Fig. 2.7 ^{13}C CP-MAS NMR spectrum of DA-PA@MS-SH

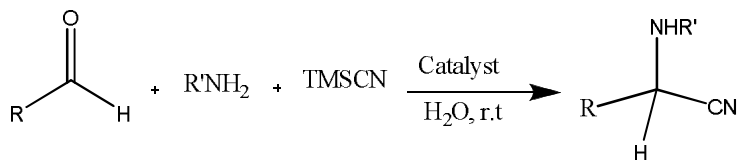
2.2.3 Evaluation of catalytic performance

2.2.3.1 Strecker amino acid synthesis (synthesis of α -amino nitriles)

Synthesis of α -amino nitriles (precursor to α -amino acids) by condensation of an aldehyde, NH_3 , and KCN , was first reported by Strecker in 1850.³⁴ The so-called Strecker reaction, which is a multicomponent reaction (MCR), has received great interest as the oldest and most viable multicomponent reaction (MCR) in organic synthesis due to the C-C bond formation and rich chemistry of the nitrile functional group.³⁵⁻³⁷ For example, they serve as efficient precursors, for the synthesis of natural and unnatural α -amino acids, different nitrogen containing heterocycles like imidazoles, thiadiazoles,^{38,39} bioactive molecules like clopidogrel, prasugrel, saframycin A,⁴⁰ and short-acting opioid analgesics.⁴¹

α -amino nitriles are generally prepared by the nucleophilic addition of the cyanide anion to an imine formed in situ (classical Strecker reaction)³⁴ or preformed imine (modified Strecker reaction).^{42,43} The commonly used cyanide sources are HCN,⁴⁴ KCN,⁴⁵ (EtO)₂P(O)CN,⁴⁶ Et₂AlCN,⁴⁷ Bu₃SnCN,⁴⁸ acetyl cyanide⁴⁹ and TMSCN.^{50,51} Among these, trimethylsilylcyanide (TMSCN) is relatively easy to handle and highly soluble in organic solvents. Classical reaction required long reaction times, harsh reaction conditions and unsatisfactory yields. Many of the reported methods involve the use of expensive reagents, hazardous solvents, and tedious workup procedure. This problem has led to the development of many strategies that could overcome the problems of classical reaction. Since the first report of the catalytic version by the group of Lipton in 1996, many efficient catalysts have been successfully developed to obtain various α -amino nitriles with excellent yields and enantioselectivity.⁵²⁻⁵⁴ Recent literature include both homogeneous and heterogeneous catalysts for the preparation of α -amino nitriles. Among different Lewis bases, stable N-heterocyclic carbenes (NHCs), quaternary ammonium halides, tertiary amines, N,N-dimethylcyclohexylamine, tetrabutylammonium phthalimide- N-oxides (TBAPINO) have been used as catalysts in S-3CR.^{49,55-58} To the best of our knowledge, this is the first reported solid base catalyzed S-3CR.

Acosta et al. reported Lewis base catalyzed S-3CR in water.⁴⁹ According to their hypothesis, the advantages of S-3CR in water are the following: (1) intermediates (imines) are expected to form strong and better H-bonds than their parent carbonyl compounds; (2) H-bond interactions and lewis basic sites on the catalyst favour carbonyl activation.



Scheme 2.4 Strecker reaction of carbonyl compounds and amines with TMSCN catalyzed by polyamine silica catalyst

The use of DA-PA@MS-SH in the three-component Strecker-type reaction of benzaldehyde (1 mmol), aniline (1 mmol) and TMSCN (1.2 mmol) was carried out in water (Scheme 2.4). To identify the best condition, reaction was performed in various solvents and also by using different amounts of the catalyst at room temperature. The results are shown in Table 2.4 & 2.5. It is noted that the reaction hardly proceeded in the absence of a catalyst and took 24 h in the presence of polyamine@MS catalyst, and the product was obtained in trace amount (nearly 30 %).

Under homogeneous condition, N,N-dimethylcyclohexylamine as catalyst afforded the desired α -amino nitriles in 65 % yield, whereas dialkylated polyamine tethered mesoporous silica (MS) afforded the desired product in almost 100 % yield. The yield was increased with increasing amount of catalyst, the use of 1.5 mol% was sufficient to obtain the best result. Effect of solvent was studied by selecting different solvents, and water was found to be the effective solvent.

As we go through the literature, it is noticed that most of the catalyzed processes for the preparation of α -amino nitriles required high amount of catalyst loading, organic solvents and toxic cyanide sources. In the present work, we could successfully generate the desired products under mild conditions ie, low catalyst loading, room temperature, and eco-friendly

solvent. Encouraged with this procedure, we applied the optimized conditions into various aldehydes and amines (summarized in Table 2.6). As shown in Table 2.6, the nature of substituents on benzaldehyde has a great effect on the required reaction time for completion. In general, aldehydes bearing electron-withdrawing groups react faster than those with electron-donating groups. Aromatic primary amine and heterocyclic amine could effectively undergo Strecker reaction with aldehydes and TMSCN to give the corresponding products in excellent yields (94-97 %). For amines such as benzyl amine and piperidine, relatively low yield was observed. Among ketones, acetone and cyclohexanone gave high yield within a short period of time, whereas, acetophenone required longer time.

Table 2.4 Effect of catalyst amount

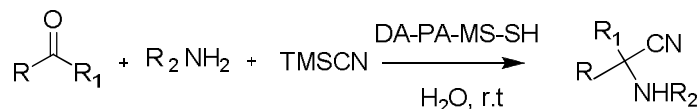
Catalyst (mol%)	0.5	1	1.5	2
Yield (%)	80	89	100	90

Reaction conditions: C₆H₅CHO (5 mmol), C₆H₅NH₂ (5 mmol), TMSCN (5.2 mmol), r.t, 0.5 h, H₂O

Table 2.5 Effect of various solvents

Entry	Solvent	Yield (%)
1	THF	82
2	CH ₂ Cl ₂	80
3	DMF	82
4	CH ₃ CN	86
5	Ethanol	92
6	Water	100

Reaction conditions: C₆H₅CHO (5 mmol), C₆H₅NH₂ (5 mmol), TMSCN (5.2 mmol), 1.5 mol% catalyst, r.t, 0.5 h

Table 2.6 Synthesis of α -amino nitriles by DA-PA@MS-SH in aqueous medium

Entry	R	R ₁	R ₂	Yield % ^{a,b}	Time (min)
1	C ₆ H ₅	H	C ₆ H ₅	100	30
2	4-OCH ₃ -C ₆ H ₄ -	H	C ₆ H ₅	98	45
3	C ₆ H ₅ -CH=CH	H	C ₆ H ₅	75	90
4	4-OCH ₃ -C ₆ H ₄ -	H	C ₆ H ₅ CH ₂	90	90
5	C ₆ H ₅	H	C ₆ H ₅ CH ₂	88	90
6	C ₅ H ₄ S	H	C ₆ H ₅ CH ₂	90	60
7	C ₅ H ₄ S	H	C ₆ H ₅	100	45
8	CH ₃	CH ₃	C ₆ H ₅	100	45
9	C ₆ H ₁₁	H	C ₆ H ₅	95	60
10	3-Br-C ₆ H ₄	H	C ₆ H ₅	80	75
11	-C ₆ H ₅	CH ₃	C ₆ H ₅ CH ₂	70	255
12	4-OCH ₃ -C ₆ H ₄ -	CH ₃	C ₆ H ₅	75	200
13	-C ₆ H ₅	CH ₃	C ₆ H ₅	78	200
14	C ₆ H ₅	CH ₃	2-Cl-C ₆ H ₄	85	120
15	C ₆ H ₅	H	piperidine	75	120
16	C ₂ H ₅	C ₂ H ₅	C ₆ H ₅	65	150

^a Reaction conditions: carbonyl compounds (5 mmol), amines (5 mmol), TMSCN (5.2 mmol), 1.5 mol% catalyst, r.t, aqueous medium, ^b isolated yield

Turn over frequency of the reaction was calculated with the same amount of different catalysts (Figure 2.9). It is noticed that DA-PA@MS-SH gave larger TOFs compared to PA@MS and PA@MS-SH. The observation of such enhanced turn over frequency may be due to the presence of high Lewis basicity of $-(\text{CH}_3)_2\text{N}$ functionality of DA-PA@MS-SH catalyst. The $-\text{NH}_2$ functionality of PA@MS and PA@MS-SH would compete with amines, one of the substrates in the reaction and may retard the reaction.

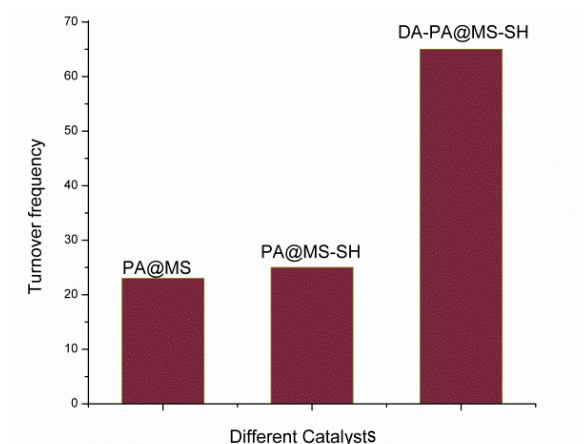
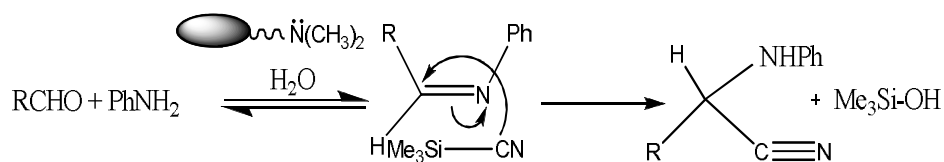


Fig. 2.9 Turn over frequency of the reaction using different catalysts under identical reaction conditions

2.2.3.1.1 Proposed mechanism

A possible mechanism is proposed for the solid base catalyzed reaction and is shown in Scheme 2.5. Lewis basicity of the catalyst enhances nucleophilicity of carbonyl group. The carbonyl compound reacts with primary amine to form the imine by dehydration and this step was activated by Lewis base part on the silica surface and this step is considered to be rate-determining. This equilibrium process is driven by excess water, shifting the carbonyl-imine equilibrium towards the imine side by operating a “dry” organic chemistry in water.⁴⁹ In the next step, the imine is attacked by cyanide ion to give the α -amino nitrile.



Scheme 2.5 Possible mechanism for the Strecker α -amino nitrile synthesis

2.2.3.1.2 Recycling study of catalyst

After the reaction, catalyst was washed with methanol repeatedly, and dried at 60 °C under vacuum for 4 h and reused. The DA-PA@MS catalyst has been proved to be very robust and stable through recycling study. After the fifth run the catalyst preserved 70 % of its original activity (Figure 2.10) and the catalyst can be readily reused without loss of activity.

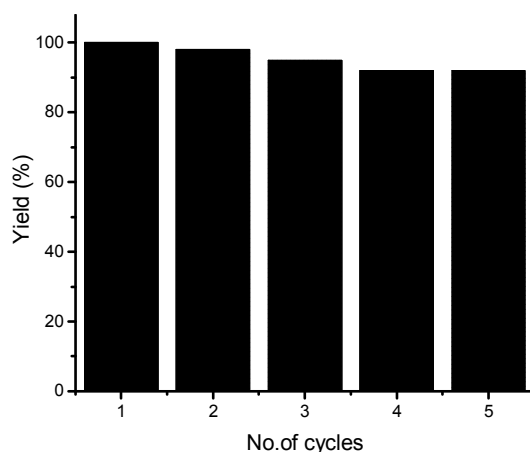


Fig. 2.10 Recyclability of DA-PA@MS in α -amino nitrile synthesis
Reaction conditions: C_6H_5CHO (5 mmol), $C_6H_5NH_2$ (5 mmol),
TMSCN (5.2 mmol), 1.5 mol% catalyst, r.t, 0.5 h, aqueous
medium

2.3 Conclusion

We have developed silica supported dialkylated polyamine hybrid material by ring opening polymerization of epichlorohydrin with thiol grafted silica. A high density of tertiary amine can be developed on the silica surface through surface initiated polymerization. The polyamine functionalized silica material exhibited high catalytic activity in the S-3CR in water using TMSCN as cyanide source, where the use of water promoted an ecofriendly approach in

the synthesis. A variety of carbonyl compounds, and amines have shown to undergo reaction under mild experimental condition. The merit of this catalyst is high accessibility of Lewis base active site, low amount of catalyst loading, easy separation of catalyst by filtration, and could be recycled without loss of significant activity after 4 cycles. The proposed solid catalyst provides a prominent solution for boosting the activity of supported catalyst in many base catalyzed reactions.

2.4 Experimental

2.4.1 Materials

All the solvents were purified according to the standard procedures. All reagents used in the preparation and modification of mesoporous silica were used as received. Tetraethyl orthosilicate (TEOS, 98 %), 3-mercaptopropyl trimetoxysilane (MPTMS, 95 %) and cetyltrimethylammonium bromide (CTAB, 98 %) were received from Aldrich.

2.4.2 Synthesis of mesoporous silica particles (MS)

Mesoporous silica particles were synthesized according to the method reported by Grun et al.⁵⁹ Cetyltrimethylammonium bromide (2.2 g) was dissolved in deionized water (120 mL). 9.5 g aq. ammonia (25 wt%, 0.14 mol) was added to the solution. While stirring, tetraethyl orthosilicate (10 g, 0.05 mol) was added slowly to the surfactant solution over a period of 15 minutes. The mixture was stirred for 1 h. The white precipitate was filtered and washed with 100 mL of deionized water. After drying at 363 K for 12 h, the sample was heated to 773 K in air and kept at this temperature for 5 h to remove the template. The prepared silica was designated as MS.

Yield 75 %, White powder; IR (KBr): $\bar{\nu}$ 3443, 1635, 1082, 820 cm^{-1} .

2.4.3 Preparation of thiol functionalized mesoporous silica (MS-SH)

A 2 g quantity of MS was dried under vacuum at 110 °C, and refluxed with 3-mercaptopropyl trimethoxysilane (3.62 mL, 1.07 mmol) in 50 mL of dry toluene for 24 h. After filtration, the solid material was washed with toluene followed by ethanol. Any residual organosilane was removed by soxhlet extraction over ethanol for 24 h.

Yield 2.12 g; White powder; IR (KBr): $\bar{\nu}$ 3443, 2944, 2532, 1635, 1082, 820 cm^{-1} ; CHNS analysis: C (6.74 %), H (1.37 %), S (4.64 %).

2.4.4 Preparation of silylazide polymer (PAZ@MS-SH)

A mixture of tetrabutylammonium bromide (0.5 g, 1.55 mmol), epichlorohydrin (8.47 mL, 0.11 mmol), DMSO (25 mL) and MS-SH silica (2 g) was introduced into 250mL two-necked round bottom flask and heated at 40 °C with stirring. By controlling the temperature within this range, NaN_3 (10 g, 0.15 mol) was gradually added to the reaction mixture with stirring. The temperature was allowed to rise to 90 °C and stirring was continued at this temperature for about 20 h. The reaction mixture was allowed to cool. After cooling silica residue was washed with hot water (60 °C, 50 mL \times 3 times) to remove NaN_3 and NaCl, and thoroughly washed with methanol and dichloromethane. Finally, polymerized MS material was dried at 50 °C for 10 h. The polyazide silica was designated as PAZ@MS-SH.

Yield 2.5 g; Yellow powder; IR (KBr): $\bar{\nu}$ 3443, 2942, 2108, 1635, 1082, 820 cm^{-1} ; CHNS analysis: C (22.8 %), N (19.7 %), H (4.1 %), S (4.61 %).

2.4.5 Preparation of silylamine polymer (PA@MS-SH)

The polyazide silica (1 g) was treated with THF (25 mL), PPh₃ (3.85 g, 14.7 mmol) and water (1 mL), the reaction mixture was stirred at room temperature for 24 h. The resulting material was filtered and washed thoroughly with hexane in order to remove unreacted PPh₃ (removed as triphenylphosphine oxide) and finally washed with dichloromethane /methanol (1:1v/v, 20 mL) mixture and dried in vacuum. The product was designated as PA@MS-SH. Same synthetic strategy was followed in the preparation of PA@MS.

Yield 1.05 g; pale yellow powder; IR (KBr): $\bar{\nu}$ 3425, 2922, 1645, 1082, 820 cm⁻¹; Amine capacity: 12.9 mmol/g.

2.4.6 Protection of PA@MS-SH with dimethyl sulphate

The product (1 g), 18-crown-6 (0.02 g), Dimethyl sulphate (2 mL, 20 mmol) and dry toluene (25 mL) were added to 100 mL two-necked round bottom flask. The reaction mixture was refluxed at 80 °C for 24 h. After cooling, silica particles were washed with distilled water, dichloromethane and methanol respectively. The product was dried under vacuum for 5 h at 60 °C. Schematic representation of the development of N,N-dialkylated polyamine@MS (DA-PA@MS-SH) is shown in Scheme 2.2.

Yield 1.48 g; Light brown powder; IR (KBr): $\bar{\nu}$ 3435, 2924, 1645, 1082, 820 cm⁻¹; CHNS analysis: C (26.5 %), N (13.5 %), H (7.35 %), S (4.62 %); Solid state ¹³C CP-MAS NMR (100 MHz): 25.5, 64.8, 71.2, 74.3, 88.5, 103.7, 105.3 ppm.

2.4.7 Cleaving of grafted polymer from silica

Dialkylated polyamine from the silica surface was cleaved by dissolving 50 mg of silica in 10 mL of 1:1 solution of 48 wt % aqueous HF and THF respectively. The mixture was stirred for 24 h and evaporated to dryness in a Teflon petridish. The residue was decanted with THF and subjected to spectral analysis.

MALDI MS: 2353.9; ^1H NMR (CDCl_3 , 400 MHz): δ 0.99 (t, CH_2 proton), 1.15 (m, CH_2 proton), 2.25 (s, $-\text{N}(\text{CH}_3)_2$ proton), 2.68 (m, CH_2 proton), 2.71 (s, CH_2 proton), 3.3 (s, $-\text{OCH}_3$ proton), 3.5 (m, CH proton), 3.9 (d, CH_2 proton).

2.4.8 Estimation of $-\text{NH}_2$ group capacity

The amine content of functionalized MS was estimated via aqueous HCl consumption using the acid–base titration method. Typically, 100 mg of functionalized MS was suspended in 30 mL of 0.1 M HCl solution and stirred at ambient temperature for 24 h. The filtrate was titrated with NaOH solution (0.1 M). The $-\text{NH}_2$ group capacity was further verified using UV-Visible spectrophotometric analysis.²⁸

2.4.9 Estimation of $-\text{NH}_2$ group capacity by UV-Visible spectrophotometry

The amine-functionalized mesoporous silica (50 mg) was immersed in anhydrous ethanol (40 mL) containing 4-nitrobenzaldehyde (75 mg) and acetic acid (0.05 mL) and the mixture was heated to 50 °C for 5 h. After the condensation, the silica particle was washed with ethanol and sonicated in ethanol for 2 min and dried under vacuum. The imine formed on silica was immersed in water (40 mL) containing acetic acid (0.05 mL), and the aqueous solution was heated at 30 °C for 5 h. The solution was sonicated for

10 min. Absorbance of 4-nitrobenzaldehyde produced by hydrolysis can be measured at this stage. From the absorbance, its concentration was determined.

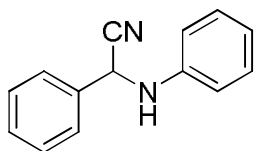
2.4.10 Typical procedure for the synthesis of α -amino nitriles

A 25 ml round bottom flask was charged with the catalyst (1.5 mol%), aniline (5 mmol), benzaldehyde (5 mmol) and TMSCN (5.2 mmol) in water (5 mL). The resulting mixture was stirred at room temperature and the progress of the reaction was monitored by TLC. After completion of the reaction, diethyl ether was added and the solution was filtered, washed with brine and water. It was dried over anhydrous sodium sulphate and filtered. A short column of silica gel was used to purify the product α -amino nitrile in 90-100 % yield.

Spectral characterization of the products

2-(Anilino)-2-phenylacetonitrile (Table 2.6, Entry 1):

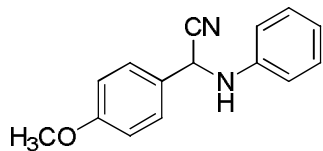
White crystal, m.p 76-78 °C



LCMS (M+1) m/z 209; IR (KBr): $\bar{\nu}$ 3338, 3029, 2940, 2237, 1600, 1515, 1497, 1283, 1243, 1114, 924, 753, 693 cm^{-1} ; ^1H NMR (400 MHz, CDCl_3): δ 4.02 (d, $J = 8.4$ Hz, 1H), 5.43 (d, $J = 8.4$ Hz, 1H), 6.77 (d, $J = 8.8$ Hz, 2H), 6.92 (t, $J = 8.4$ Hz, 1H), 7.2-7.3 (m, 2H), 7.4-7.5 (m, 3H), 7.5-7.6 (m, 2H).

2-(Anilino)-2-(4-methoxyphenyl) acetonitrile (Table 2.6, Entry 2):

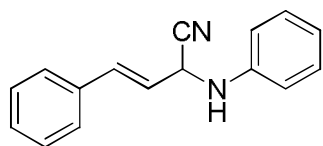
White solid, m.p 95-96 °C



LCMS (M+1) m/z 239; IR (KBr): $\bar{\nu}$ 3330, 3011, 2934, 2229, 1602, 1507, 1436, 1242, 1178, 1022, 929, 827, 758 cm^{-1} ; ^1H NMR (400 MHz, CDCl_3): δ 3.9 (s, 3H), 4.1 (d, $J = 8.4$ Hz, 1H), 5.3 (d, $J = 8$ Hz, 1H), 6.7 (d, $J = 8$ Hz, 2H), 6.8-6.9 (m, 3H), 7.2-7.3 (m, 3H), 7.5 (d, $J = 8.6$ Hz, 2H).

2-(Anilino)-2-(3-phenylpropene) acetonitrile (Table 2.6, Entry 3):

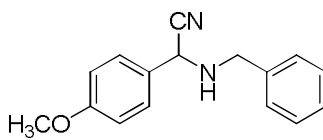
Light yellow solid, m.p 120-122°C



LCMS (M+1) m/z 235; IR (KBr): $\bar{\nu}$ 3354, 2925, 2240, 1601, 1508, 1468, 1338, 1279, 1030, 980, 898, 750 cm^{-1} ; ^1H NMR (400 MHz, CDCl_3): δ 4.0 (d, $J = 8.8$ Hz, 1H), 5.2 (bs, 1H), 6.6 (dd, $J = 5.8$ Hz, 10.9, 1H), 6.7-7.0 (m, 4H), 7.2-7.4 (m, 7H).

2-(Benzylamino)-2-(4-methoxyphenyl) acetonitrile (Table 2.6, Entry 4):

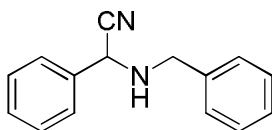
Yellow oil



LCMS (M+1) m/z 252; IR (neat): $\bar{\nu}$ 3332, 2930, 2221, 1600, 1503, 1431, 1240, 1018, 930, 784 cm^{-1} ; ^1H NMR (CDCl_3 , 400 MHz): δ 1.8 (s, 1H), 3.83 (s, 3H), 4.01 (q, $J = 13.2$ Hz, 2H), 4.72 (s, 1H), 6.92-6.96 (m, 2H), 7.49-7.28 (m, 7H).

2-(Benzylamino)-2-phenylacetonitrile (Table 2.6, Entry 5):

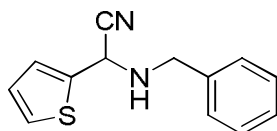
Colorless oil



LCMS (M+1) m/z 222; IR (neat): $\bar{\nu}$ 3320, 2929, 2229, 1650, 1548, 1408, 1260, 1109, 1030, 980, 919, 830, 760 cm^{-1} ; ^1H NMR (400 MHz, CDCl_3): δ 1.8 (s, 1H), 4.02 (q, $J = 13.8$ Hz, 2H), 4.7 (s, 1H), 7.2-7.5 (m, 10H).

2-(Benzylamino)-2-thiophenylacetonitrile (Table 2.6, Entry 6):

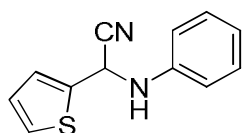
Colorless oil



LCMS (M+1) m/z 228.1; IR (neat): $\bar{\nu}$ 3348, 3100, 2245, 1650, 1578, 1489, 1260, 1109, 1278, 1167, 1063, 923, 845 cm^{-1} ; ^1H NMR (400 MHz, CDCl_3): δ 2.1 (s, 1H), 4.12 (q, $J = 13.8$ Hz, 2H), 4.9 (s, 1H), 6.9-7.3 (m, 5H), 7.5-7.7 (m, 3H).

2-(Anilino)-2-thiophenylacetonitrile (Table 2.6, Entry 7):

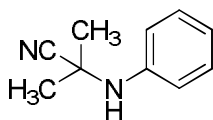
White solid, m.p 100-101 °C



LCMS (M+1) m/z 215; IR (KBr): $\bar{\nu}$ 3357, 3100, 2237, 1599, 1500, 1436, 1348, 1252, 1149, 1063, 884, 833, 751 cm^{-1} ; ^1H NMR (400 MHz, CDCl_3): δ 4.26 (d, $J = 9.8$ Hz, 1H), 5.66 (d, $J = 9.2$ Hz, 1H), 6.7-7.0 (m, 5H), 7.3-7.4 (m, 3H).

2-Methyl-2-(phenylamino) propanenitrile (Table 2.6, Entry 8):

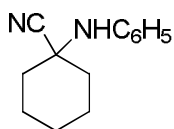
Off-white solid, m.p-68-70°C



LCMS (M+1) m/z 161.2; IR (KBr): $\bar{\nu}$ 3348, 3100, 2245, 1650, 1578, 1489, 1260, 1109, 1278, 1167, 1063, 923, 845 cm^{-1} ; ^1H NMR (400 MHz, CDCl_3): δ 1.76 (s, 6H), 5.32 (s, 1H), 7.0-7.2 (m, 3H), 7.4 (d, $J = 8.6$ Hz, 2H).

1-(Anilino) cyclohexanecarbonitrile (Table 2.6, Entry 9):

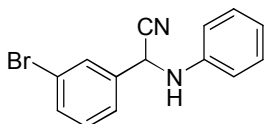
Off-white crystal, m.p 69-71°C



LCMS (M+1) m/z 200.9; IR (KBr): $\bar{\nu}$ 3020, 2929, 2876, 2546, 1650, 1548, 1408, 1260, 1109, 919, 820, 710 cm^{-1} ; ^1H NMR (400 MHz, CDCl_3): δ 1.5-2.3 (m, 8H), 4.72 (s, 1H), 6.7-7.2 (m, 5H).

2-(Anilino)-2-(3-bromophenyl) acetonitrile (Table 2.6, Entry 10):

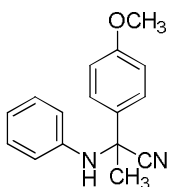
Light brown oil



LCMS (M+1) m/z 287.2; IR (neat): $\bar{\nu}$ 3321, 3090, 2937, 2285, 1600, 1515, 1497, 1243, 1114, 924, 857, 765, 693 cm^{-1} ; ^1H NMR (400 MHz, CDCl_3): δ 4.02 (d, $J = 8.4$ Hz, 1H), 5.43 (d, $J = 8.4$ Hz, 1H), 7.31 (s, 1H), 7.68 (d, $J = 8.5$ Hz, 1H), 7.42-7.45 (m, 2H).

2-(Anilino)-2-(4-methoxyphenyl)propanenitrile (Table 2.6, Entry 11):

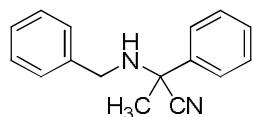
White solid, m.p 142-144°C



LCMS (M+1) m/z 252.2; IR (KBr): $\bar{\nu}$ 3390, 2923, 2234, 1605, 1506, 1440, 1293, 1242, 1193, 1078, 933, 812, 755 cm⁻¹; ¹H NMR (400 MHz, CDCl₃): δ 1.91 (s, 3H), 2.9 (s, 3H), 4.1 (s, 1H), 6.7-6.9 (m, 3H), 7.2-7.3 (m, 4H), 7.5 (m, 2H).

2-Benzylamino-2-phenylpropanenitrile (Table 2.6, Entry 12):

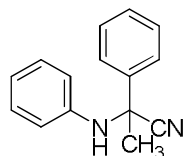
Colorless oil



LCMS (M+1) m/z 236; IR (neat): $\bar{\nu}$ 3320, 3030, 2849, 2223, 1958, 1897, 1811, 1603, 1494, 1372, 1214, 1152, 1075, 1037, 863, 765 cm⁻¹; ¹H NMR (400 MHz, CDCl₃): δ 1.83 (s, 3H), 3.82 (q, *J* = 13.0 Hz, 2H), 7.28-7.68 (m, 10H).

2-(Anilino)-2-(phenyl)propanenitrile (Table 2.6, Entry 13):

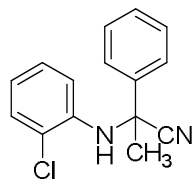
White crystal, m.p 141-143°C



LCMS (M+1) 222.3 m/z; IR (KBr): $\bar{\nu}$ 3382, 3068, 2942, 2246, 1923, 1691, 1604, 1515, 1346, 1264, 1177, 1099, 852, 743 cm⁻¹; ¹H NMR (400 MHz, CDCl₃): δ 2.1 (s, 3H), 4.48 (s, 1H), 6.50 (d, 8.5 Hz, 2H), 6.81 (t, *J* = 7.4 Hz, 1H), 7.01 (t, *J* = 7.5 Hz, 2H), 7.75 (d, *J* = 8.8 Hz, 2H), 7.99 (d, *J* = 8.8 Hz, 2H).

2-(2-Chlorophenylamino)-2-phenylpropanenitrile (Table 2.6, Entry 14):

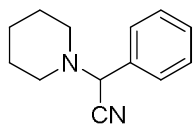
Light yellow oil



LCMS (M+1) m/z 256.1; IR (neat): $\bar{\nu}$ 3395, 2929, 2228, 1630, 1508, 1460, 1260, 1138, 1052, 792 cm⁻¹; ¹H NMR (400 MHz, CDCl₃): δ 2.60 (s, 3H), 4.0 (s, 1H), 6.37-7.95 (m, 9H).

2-Phenyl-2-(piperidin-1-yl) acetonitrile (Table 2.6, Entry 15):

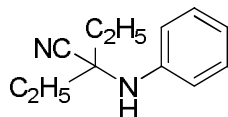
Off-white solid, m.p 62-63 °C



LCMS (M+1) m/z: 200.05; IR (KBr): $\bar{\nu}$ 3382, 3068, 2942, 2876, 2246, 1923, 1691, 1293, 1247, 1193, 1078, 903, 812 cm^{-1} ; ^1H NMR (400 MHz, CDCl_3): δ 1.24-1.38 (m, 6H), 2.33 (t, 4H), 4.76 (s, 1H) 7.1-7.4 (m, 5H).

2-(Anilino)-2-ethyl butanenitrile (Table 2.6, Entry 16):

Colorless oil



LCMS(M+1) m/z: 188.1; IR (neat): $\bar{\nu}$ 3321, 3090, 2937, 2546, 2235, 1643, 1545, 1445, 1213, 1114, 924, 765 cm^{-1} ; ^1H NMR (400 MHz, CDCl_3): δ 1.06 (t, 6H), 1.55 (q, 4H) 5.12 (s, 1H), 7.0-7.2 (m, 3H), 7.4 (d, $J = 8.6$ Hz, 2H).

References

- [1] A. P. Wight and M. E. Davis, *Chem. Rev.*, 2002, **102**, 3589.
- [2] J. Evans, A. B. Zaki, M. Y. El-Sheikh and S. A. El-Safty, *J. Phys. Chem. B*, 2000, **104**, 10271.
- [3] J. Kramer, A. R. Garcia, W. L. Driessen and J. Reedijk, *Chem. Commun.*, 2001, 2420.
- [4] A. Walcarius, M. Etienne and J. Bessiere, *Chem. Mater.*, 2002, **14**, 2757.
- [5] R. Voss, A. Thomas, M. Antonietti and G. A. Ozin, *J. Mater. Chem.*, 2005, **15**, 4010.
- [6] S. Yoo, J. D. Lunn, S. Gonzalez, J. A. Ristich, E. E. Simanek and D. F. Shantz, *Chem. Mater.*, 2006, **18**, 2935.
- [7] M. E. Davis, A. Katz and W. R. Ahman, *Chem. Mater.*, 1996, **8**, 1820.

- [8] C. M. Hui, J. Pietrasik, M. Schmitt, C. Mahoney and J. Choi, *Chem. Mater.*, 2014, **26**, 745.
- [9] M. Kruk, B. Dufour, E. B. Celer, T. Kowalewski, M. Jaroniec and K. Matyjaszewski, *Macromolecules*, 2008, **41**, 8584.
- [10] D. R. Radu, C.Y. Lai, J. W. Wiench, M. Pruski and V. S. Y. Lin, *J. Am. Chem. Soc.*, 2004, **126**, 1640.
- [11] C. Y. Hong, X. Li and C.Y. Pan, *Eur. Polym. J.*, 2007, **43**, 4114.
- [12] F. Audouin, H. Blas, P. Pasetto, P. Beaunier, M. Save and B. Charleux, *Macromol. Rapid. Commun.*, 2008, **29**, 914.
- [13] Q. Zhou, S. Wang, X. Fan, R. Advincula and J. Mays, *Langmuir*, 2002, **18**, 3324.
- [14] P. Quirck and R.T. Mathers, *Polym. Bull. (Berlin)*, 2001, **45**, 471.
- [15] P. W. Chung, R. Kumar, M. Pruski and V. S. Y. Lin, *Adv. Funct. Mater.*, 2008, **18**, 1390.
- [16] J. Moraes, K. Ohno, T. Maschmeyer and S. Perrier, *Chem. Commun.*, 2013, **49**, 9077.
- [17] T. von Werne and T. E. Patten, *J. Am. Chem. Soc.*, 1999, **121**, 7409.
- [18] K. Ito, N. Usami and Y. Yamashita, *J. Polym. Sci., Part A: Polym. Chem.*, 1979, **11**, 171.
- [19] T. Urbanski, *Chemistry and Technology of Explosives*, Vol. IV, Pergamon Press, New York, 1984.
- [20] M. B. Frenkel, E. F. Witucki and D.O. Wooley, *US Patent* 4 379 894, 1983.
- [21] Smitha George, Ph. D Thesis, 2015, Cochin University of Science and Technology, Cochin, India.
- [22] A. Firouzi, D. Kumar, L. M. Bull, T. Besier, P. Sieger, Q. Huo, S. A. Walker, J. A. Zasadzinski, C. Glinka, J. Nicol, D. Margolese, G. D. Stucky, and B. F. Chmelka, *Science*, 1995, **267**, 1138.

- [23] J. S. Beck, J. C. Vartuli, W. J. Roth, M. E. Leonowicz, C. T. Kresge, K. D. Schmitt, C. T. W. Chu, D. H. Olson and E. W. Sheppard, *J. Am. Chem. Soc.*, 1992, **114**, 10834.
- [24] M. P. Kapoor, Y. Kasama, T. Yokoyama, M. Yanagi and S. Inagaki, *J. Mater. Chem.*, 2006, **16**, 4714.
- [25] M. Suzuki, A. Li and T. Saegus, *Macromolecules*, 1992, **25**, 7071.
- [26] (a) G. Ampleman, *US patent 5 256 804*, 1990, **5**, 256; (b) M. B. Frankel, I. R. Grant, J. E. Flanagan, *J. Prop. Power*, 1992, **8**, 560.
- [27] R. Inoubli, S. Dagr eou, A. Lapp, L. Billon and J. Peyrelasse, *Langmuir*, 2006, **22**, 6683.
- [28] (a) J. H. Moon, J. W. Shin and J. W. Pa, *Mol. Cryst. Liq. Cryst.*, 1997, **295**, 185; (b) C. O. Kim, *J. Colloid Interface Sci.*, 2003, **24**, 374.
- [29] J. S. Beck, J. C. Vartuli, W. J. Roth, G. J. Kennedy, C. T. Kresge and F. Schramm, *Chem. Mater.*, 1994, **6**, 1816.
- [30] K. S. W. Sing, D. H. Everett, R. A. W. Haul, L. Moscou, R. A. Pierotti, J. Rouquerol, and T. Siemieniewska. *Pure and Appl. Chem.*, 1985, **57**, 603.
- [31] E. P. Barrett, L. G. Joyner, and P. P. Halenda, *J. Am. Chem. Soc.*, 1951, **73**, 373.
- [32] P. Jayhyun, H. Kim, and J. Park, *IJESD*, 2012, **3**, 81.
- [33] Yu. Li and B. C. Benicewicz, *Macromolecules*, 2008, **41**, 21.
- [34] A. Strecker, *Ann. Chem. Pharm.*, 1850, **75**, 27.
- [35] M. B. Smith and J. March, *Advanced Organic Chemistry: Reactions, Mechanisms, and Structure*, 5th ed.; Wiley-Interscience: New York, 2001, 1240.
- [36] K. Matsumoto, J. C. Kim, H. Iida, H. Hamana, K. Kumamoto, H. Kotsuki and G. Jenner, *Helv. Chim. Acta*, 2005, **88**, 1734.
- [37] L. Yet, *Angew. Chem. Int. Ed.*, 2001, **40**, 875.

- [38] L. M. Weinstok, P. Davis, B. Handelsman and R. Tull, *J. Org. Chem.*, 1967, **32**, 2823.
- [39] W. L. Matier, D. A. Owens, W. T. Comer, D. Deitchman, H. C. Ferguson, R. J. Seidehamel and J. R. Young, *J. Med. Chem.*, 1973, **16**, 901.
- [40] R. O. Duthaler, *Tetrahedron*, 1994, **50**, 1539.
- [41] P. L. Feldman, M. K. James, M. F. Brackeen, J. M. Bilotta, S. V. Schuster, A. P.M. W. Lahey Lutz, M. R. Johnson and H. J. Leighton, *J. Med. Chem.*, 1991, **34**, 2202.
- [42] X. Huang, J. Huang, Y. Wen and X. Feng, *Adv. Synth. Catal.*, 2006, **348**, 2579.
- [43] Z. Jiao, X. Feng, B. Liu, F. Chen, G. Zhang and Y. Jiang, *Eur. J. Org. Chem.*, 2003, **68**, 3818.
- [44] D. Enders and J. P. Shilvock, *Chem. Soc. Rev.*, 2000, **29**, 359.
- [45] S. Kobayashi and H. Ishitani, *Chem. Rev.*, 1999, **99**, 1069.
- [46] J. P. Abell and H. Yamamoto, *J. Am. Chem. Soc.*, 2009, **131**, 15118.
- [47] S. Harusawa, Y. Hamada and T. Shioiri, *Tetrahedron Lett.*, 1979, **20**, 4664.
- [48] S. J. Zuend, M. P. Coughlin, M. P. Lalonde and E. N. Jacobsen, *Nature*, 2009, **461**, 968.
- [49] F.C. Acosta, A. S. Exposito, P. Armas and F. G. Tellado, *Chem. Commun.*, 2009, 6839.
- [50] D. Bandyopadhyay, J. M. Velazquez and B. K. Banik, *Org Med Chem Lett.*, 2011, **1**, 11.
- [51] K. Iwanami, H. Seo, J. Choi, T. Sakakura and H. Yasuda, *Tetrahedron*, 2010, **66**, 1898.
- [52] M. S. Iyer, K. M. Gigstad, N. D. Namdev and M. Lipton, *J. Am. Chem. Soc.*, 1996, **118**, 4910.

- [53] N. H. Khan, S. Agrawal, R. I. Kureshy, S. H. R. Abdi, S. Singh, E. Sureshand R. V. Jasra, *Tetrahedron Lett.*, 2008, **49**, 640.
- [54] M. Brandon, N. K. Fetterly and J. G. Verkade, *Tetrahedron*, 2006, **62**, 440.
- [55] M. G. Dekamin and Z. Mokhtari, *Tetrahedron*, 2012, **68**, 922.
- [56] J. Wang, X. Liu and X. Feng, *Chem. Rev.*, 2011, **111**, 6947.
- [57] P. Merino, E. M. Lopez, T. P. Tejero, R. Herrera, *Tetrahedron Lett.*, 2009, **65**, 1219.
- [58] J. Jarusiewicz, Y. Choe, K. S. Yoo, C. P. Park, and K. W. Jung , *J. Org. Chem.*, 2009, **74**, 2873.
- [59] M. Grun, K. K. Unger, A. Matsumoto and K. Tsutsumi, *Microporous Mesoporous Mater.*, 1999, **27**, 207.

Chapter 3

Ti-GRAFTED POLYAMIDOAMINE DENDRITIC SILICA HYBRID CATALYST IN BIGINELLI REACTION AND PYRANOPYRAZOLE SYNTHESIS

Contents	3.1 Introduction
	3.2 Results and Discussion
	3.3 Conclusion
	3.4 Experimental

Designing organic reactions in aqueous media and under solvent-free conditions have gained popularity in recent years. A simple, highly efficient and eco-friendly approach for the preparation of biologically potent pyranopyrazoles and 3,4-dihydropyrimidin-2(1H)-ones are discussed in this chapter. Ti-grafted polyamidoamine dendritic silica hybrid catalyst was successfully synthesized and physicochemical characterization was done by various techniques like FT-IR, TG-DTG, BET, UV-Vis DRS and XPS. Studies demonstrate that the crystalline pore wall structure of dendritic silica hybrid catalyst makes easy adsorption of reactants. Combining the property of Lewis acidic and Lewis basic property of the silica surface facilitates and accelerates the synthesis of the desired products in high yields. The key advantages of this method are excellent yield of the products, use of small amount of catalyst, shorter reaction time, facile work-up, purification of products by non-chromatographic method and the reusability of the catalyst. This protocol also combines the synergistic effect of green chemistry with mesoporous silica hybrid materials.

3.1 Introduction

Periodic mesoporous organosilica (PMO) represents an exciting new class of organic-inorganic hybrid materials targeted for a broad range of applications such as catalysis and sensing, separation, and microelectronics. Recent progress regarding the design and synthesis of heterogeneous mesoporous silica catalysts, particularly, PMO catalysts, is quite impressive.¹⁻³ Several PMO materials have been successfully prepared for catalytic applications. Dendrimers are a new class of polymeric materials. They are highly branched, monodisperse macromolecules. Several groups have promoted the synthesis and characterization of metal encapsulated dendrimers on inorganic and organic supports.^{4,5} Alper et al. have carried out extensive work on Rh- and Pd-complexed dendrimers anchored on amorphous silica with an average pore size of 6 nm.^{6,7} Later, Alper and coworkers⁸ synthesized generation G(4) dendrimers using a MCM-41 mesoporous material with much larger pores (10.6 nm), whose pores were enlarged via post-synthesis treatment. Acosta et al. prepared upto generation G(4) triazine-diamine dendrimers inside the support channels.⁹ However, the structural ordering and stability were rather poor, which would limit their application in the field of catalysis, as ion-exchanger or as adsorbent. The synthesis of periodic mesoporous dendrisilicas (PMD) was reported using PAMAM building blocks generated on PMO by Kapoor et al. and they found them active as effective base catalysts in organic elimination reaction.¹⁰ The high surface area of the PMO materials together with strong covalent attachment of catalytically active metal centers at the mesopore surface can make them promising candidates for

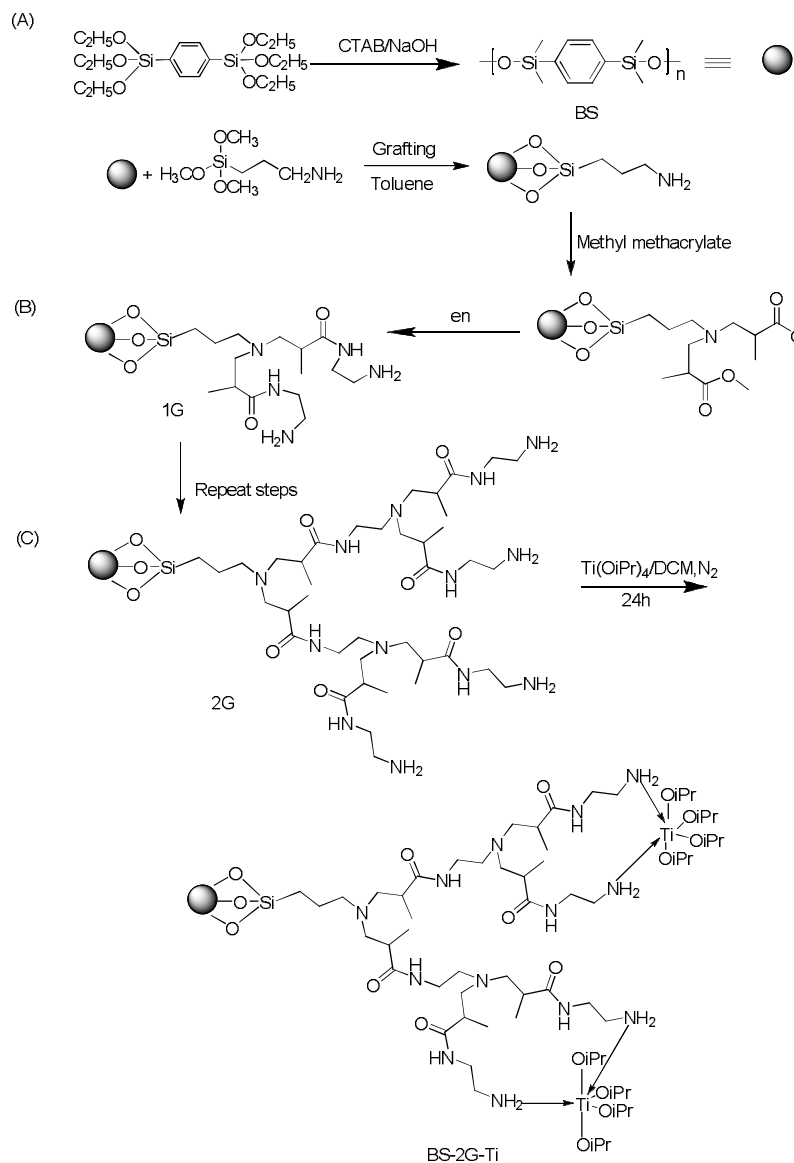
heterogeneous catalysis together with good reusability and a minimum possibility for leaching of the grafted metals. Hence, utility of these catalysts is gaining significant attention and becomes a more potential thrust area for the synthesis of highly functionalized pharmaceutically significant heterocyclic compounds.¹¹⁻¹³

In this chapter, a periodic mesoporous organo-silica has been synthesized via polycondensation of 1,4-bis(triethoxysilyl)benzene. A novel polyamidoamine dendrimer was generated on the silica framework by successively following Michael addition of methyl methacrylate and reaction with ethylene diamine. The functionalized 2G dendrimer was complexed with titanium (IV) and its catalytic efficiency was studied in two important multicomponent reactions such as Biginelli reaction and pyranopyrazole synthesis.

3.2 Results and Discussion

3.2.1 Synthesis of mesoporous benzene silica and Ti-grafted polyamidoamine dendritic silica hybrid catalyst

Mesoporous benzene silica was synthesized using cetyltrimethylammonium bromide (CTAB) as surfactant under basic condition. The precursor used for the synthesis of mesoporous benzene silica was 1,4-bis(triethoxysilyl)benzene (BTEB). Mesoporous silica was prepared by the hydrolysis and condensation of the precursors in the presence of surfactant under basic condition, the sample was designated as BS.



Scheme 3.1 (A) Synthesis of periodic mesoporous benzene silica, (B) Generation of PAMAM dendrimer on benzene silica and (C) preparation of Ti-grafted silica

BS silica was functionalized with 3-aminopropyl trimethoxysilane. The product was designated as BS-NH₂. The propylamine group grafted onto the mesoporous silica can easily undergo a Michael addition with methyl

methacrylate to yield an aminopropionate ester which in turn on amidation with ethylene diamine under nitrogen atmosphere resulted in the formation of the first generation mesoporous silica dendrimer (BS-1G). Repetition of the two reactions produced the desired generation of the mesoporous silica dendrimers (BS-2G). It was complexed with Titanium (IV) isopropoxide in dichloromethane under nitrogen atmosphere, represented as (BS-2G-Ti). Schematic representation of the preparation of hybrid catalyst is shown in Scheme 3.1.

3.2.2 Characterization of mesoporous benzene silica and periodic mesoporous dendritic silica hybrids

3.2.2.1 ^{29}Si CP MAS NMR spectrum

^{29}Si CP MAS NMR spectrum of BS silica (Figure. 3.1) showed characteristic signals attributed to $(\text{HO})\text{Si}(\text{OSi})_3$ (Q^3 $\delta \sim 102$ ppm), which clearly indicated that a proportion of the Si-C bonds have been cleaved, as well as a strong signal at -80 ppm showed the presence of the organic moieties attributed to $\text{CSi}(\text{OSi})_3$ T^3 state.

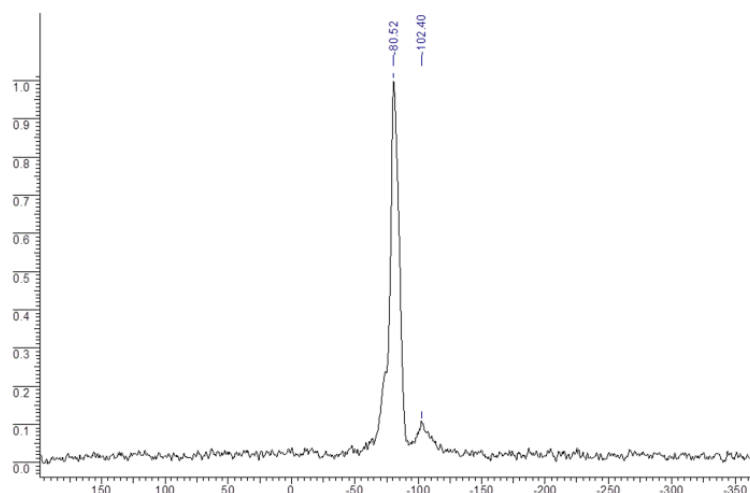


Fig. 3.1 ^{29}Si CP MAS NMR spectrum of periodic mesoporous benzene silica

3.2.2.2 X-ray diffraction studies

The structural order of the samples was studied by PXRD. Diffraction in the low angle region confirms the presence of mesophase in the synthesized sample. Diffraction patterns in small angle region are typical of ordered mesoporous materials. Well-defined first order (100), second order (110) and (200) signals are observed, which can be assigned to a 2D-hexagonal mesostructure. After functionalization, this meso-scale periodicity was diminished (Figure 3.2).

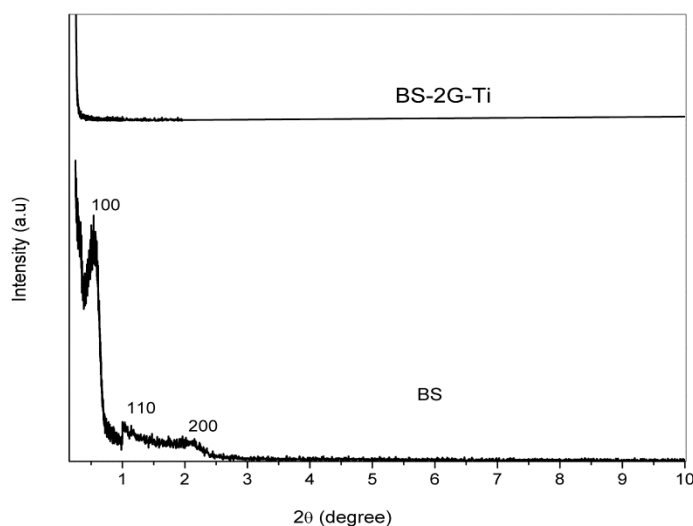


Fig. 3.2 Low angle XRD of BS and BS-2G-Ti

Wide angle X-ray diffraction analysis was performed in order to investigate the texture properties of mesoporous silica. Strong peaks were observed between $10 < 2\theta < 50$ angles, indicating the crystalline nature and molecular-scale periodicity of the synthesized materials. After functionalization, there was no considerable decrease in intensity which

showed that the crystalline nature and molecular-scale periodicity was maintained (Figure 3.3).

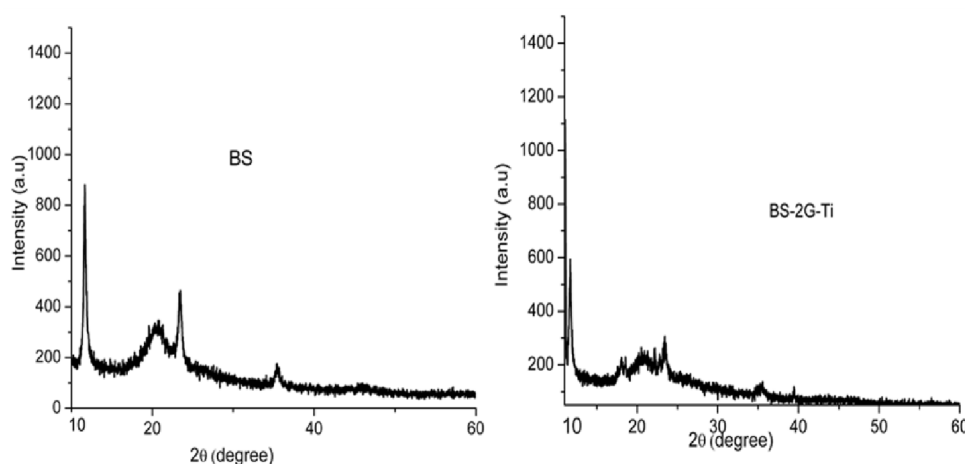


Fig. 3.3 Wide angle XRD pattern of BS and BS-2G-Ti

3.2.2.3 Surface area analysis

Nitrogen sorption measurements were performed to examine the porosity of the different materials (Figure 3.4). A summary of the textural properties of these materials is shown in Table 3.1.

Table 3.1 Structural properties of the BS and functionalized BS silica materials

Sample	S_{BET} (m^2/g)	V_p (cm^3/g)	PD (nm)
BS	580	0.77	4.0
BS-NH ₂	478	0.68	3.8
BS-1G	321	0.29	3.6
BS-2G-Ti	185	0.19	2.0

PD=pore diameter, V_p =pore volume

The materials exhibited high specific surface area (S_{BET}) ranging from 580 to 185 m^2/g . Bare BS silica has a large total pore volume of around 0.77 cm^3/g . The S_{BET} , pore volume and pore diameter decreases when the

material is functionalized from lower generation to higher generation. This is due to pore filling at relatively low pressure range, thus indicating the formation of dendritic species inside the mesopores resulting in a significant reduction in the pore size.

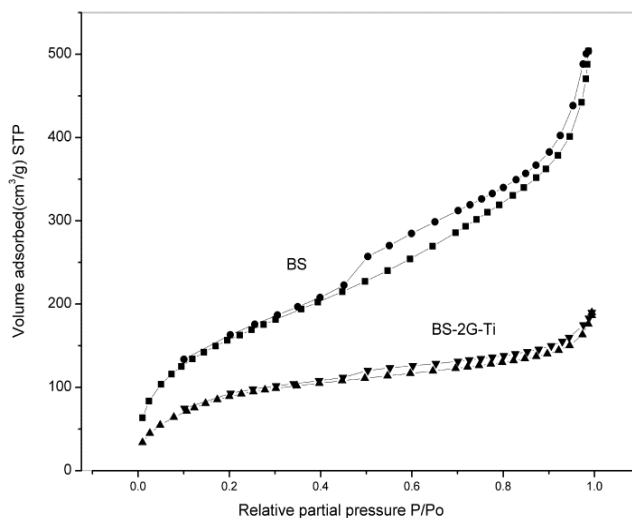


Fig. 3.4 Nitrogen adsorption-desorption plot of BS and BS-2G-Ti

3.2.2.4 IR spectral studies

The dendritic functionalization was monitored using Infrared spectroscopy (IR) at each step of preparation. The results are given in Figure 3.5. The C-H stretching vibrations observed in the $2950\text{-}2900\text{ cm}^{-1}$ region confirmed the grafting of aminopropyl groups on to the mesoporous silica. The N-H stretching vibrations occur as two weak absorption bands in the $3500\text{-}3400\text{ cm}^{-1}$ region. Here the bands are masked by the bands of silanol groups. The N-H bending vibrations of primary amines are observed in the $1650\text{-}1580\text{ cm}^{-1}$ region. After Michael addition with methyl methacrylate group, the material yielded an aminopropionate ester, which showed a

strong vibration at 1742 cm^{-1} attributed to the CO stretching of the ester group (BS-0.5G and BS-1.5G). In BS-1G and BS-2G, a band in the region of $1650\text{--}1515\text{ cm}^{-1}$ is caused by N-H bending of secondary amide which is a strong evidence for amidation with ethylene diamine. The C=O stretching vibration at 1640 cm^{-1} and the N-H stretching vibration at $3500\text{--}3400\text{ cm}^{-1}$ are observed in the secondary amide. Further, the IR spectral results confirmed the presence of the designed functional groups with higher intensity in the second-generation dendritic mesoporous silica hybrids prepared by the repetition of a set of the aforementioned reactions.

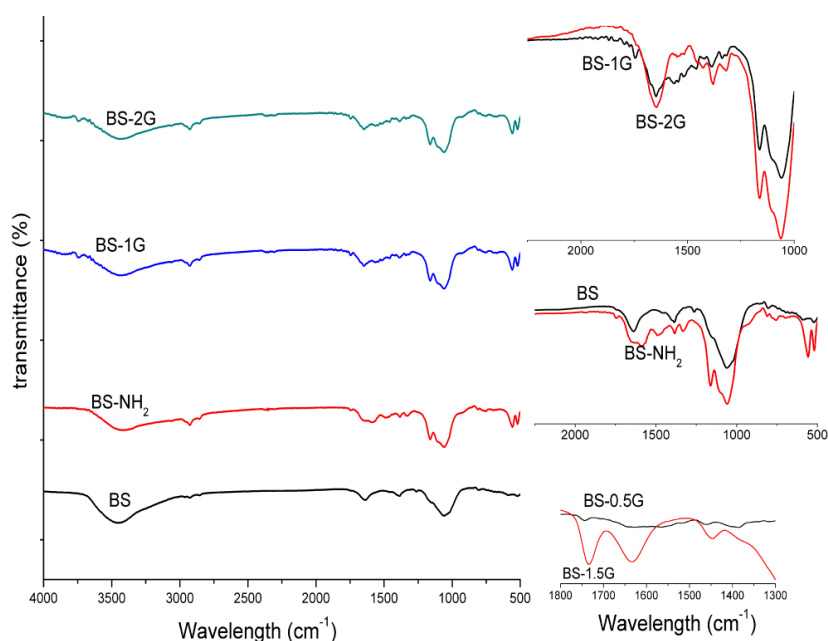


Fig. 3.5 IR spectra of functionalized BS silica

The FT-IR bands due to the primary amino groups get shifted from 3441 to 3389 cm^{-1} after complexation with Titanium isopropoxide as shown in Figure 3.6.

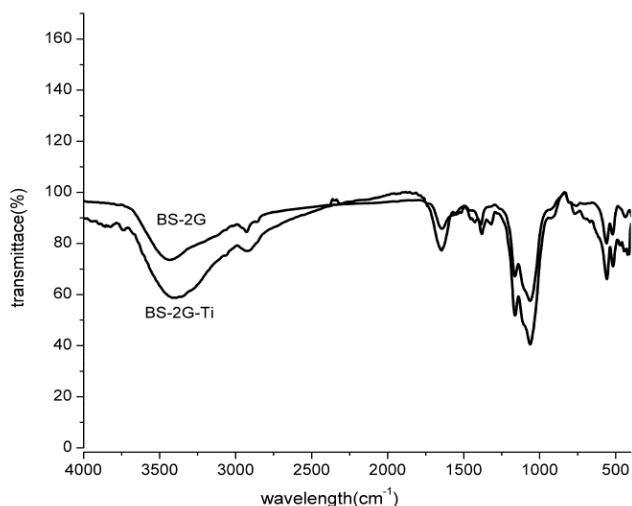


Fig. 3.6 IR spectra of BS-2G & BS-2G-Ti

This shows that the complexation was taking place with primary amino groups of the dendrimers. The carbonyl-stretching band of the amide groups remained unaltered at 1654 cm^{-1} which proved that the amide group was not involved in the complex formation.

3.2.2.5 Electronic spectral studies (UV-Vis DRS)

UV-Vis spectroscopy is used to find out the stereochemistry of metal complexes. The ligands after complexation with transition metal ions showed considerable changes in electronic properties. This may be due to the splitting of d orbitals in different environments and charge transfer spectra from metal to ligand ($M \rightarrow L$) or ligand to metal ($L \rightarrow M$). Another evidence of complexation of dendrimer was obtained from DRS-UV-Vis spectrum (Figure 3.7).

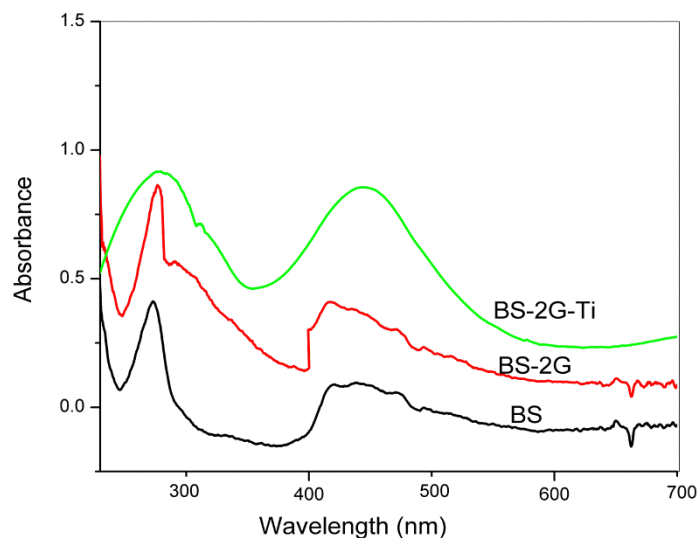


Fig. 3.7 UV-Vis-DRS spectra of BS-2G & BS-2G-Ti

The DRS-UV-Vis spectroscopic analysis is a tool to evaluate the coordination state of Ti(IV) (species in tetrahedral coordination at 220–260 nm and species in octahedral coordination at 260–290 nm) as well as the degree of isolation of Ti(IV) species in the silica matrix.¹⁴ BS-2G does not show any characteristic absorption band other than the original band at 273 nm caused by benzene bridging group in PMO pore walls. BS-2G-Ti showed an intense broad absorption band centered at 278 nm and a new band at 450 nm. This indicated that successful incorporation of Ti(iOPr)₄ and broadness of the band may be due to the overlapping of the existing band of BS silica. Oxana et al. reported that peak at 270–290 nm indicated the presence of hexa-coordinated Ti species in the supported matrix.¹⁵ They noted that UV-Vis-DRS spectrum of the sample with high Ti surface concentration (0.60–1.0 Ti/nm²) revealed the characteristic broad band in the range of 270–290 nm. Based on the above reports, we have assumed that Titanium is

hexa-coordinated onto the silica frame work. And the peak at 450 nm may be due to the charge transfer transition from ligand to metal.

3.2.2.6 TG-DTG analysis

The thermal stability of dendritic silica system was studied by thermogravimetric analysis. TG plots of the hybrid material (Figure 3.8) showed a weight loss below 100 °C due to loss of physically adsorbed water.

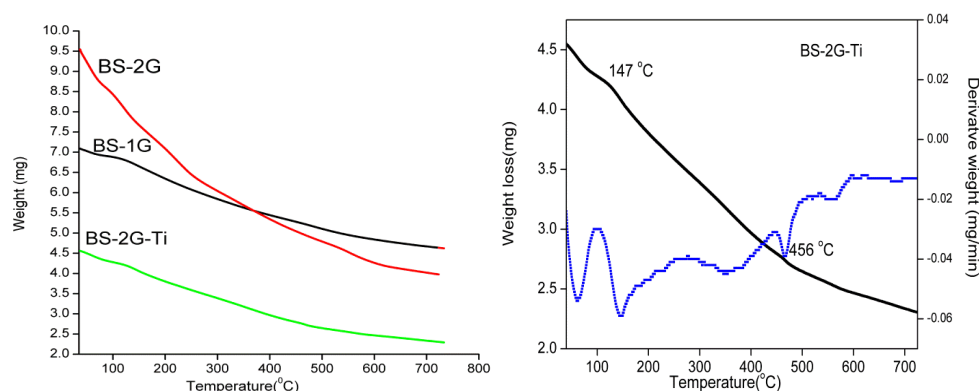


Fig. 3.8 TG and DTG plots of functionalized silica hybrids

Weight loss of 3.1 % in BS-1G, 6.2 % in BS-2G and 2.1 % in BS-2G-Ti was observed between 100 and 150 °C which may be due to the elimination of amine moiety. In addition, a weight loss at 560 °C can be observed in all hybrid materials which suggested the decomposition of benzene fragment from the pore walls.¹⁶ In BS-2G-Ti, a weight loss at 456 °C corresponding to the decomposition of titanium fragment and the residue may correspond to the formation of TiO₂. A continuous weight loss may be due to the oxidation of dendritic functionality from the silica framework. These results revealed the incorporation and integrity of designed functional groups in the

mesoporous silica hybrids. The amine capacity of hybrid material was measured by titration method and UV-Visible spectrophotometric analysis.¹⁷ The capacity of -NH_2 group was further verified using thermogravimetric analysis (TGA/DTG). The amine group capacity of functionalized materials is listed in Table 3.2.

Table 3.2 Amine capacity of functionalized BS silica

Sample	NH ₂ content (mmol/g) ^a	NH ₂ content (mmol/g) ^b	NH ₂ content (mmol/g) ^c
BS-NH ₂	0.774	0.763	0.789
BS-1G	1.820	1.890	1.800
BS-2G	3.050	3.680	3.450
BS-2G-Ti	1.260	1.310	1.210

^a Titration method, ^b UV-Vis spectrophotometric method, ^c TG/DTA

3.2.2.7 X-ray photoelectron spectroscopy

Elemental composition on the silica surface was studied using X-ray photoelectron spectroscopy (Figure 3.9). In high resolution spectra Ti shows a Ti ($2p_{3/2}$) and Ti ($2p_{1/2}$) doublet with a separation of 5.72 eV (Figure. 3.10). The lower binding energy values of $2p_{3/2}$ and $2p_{1/2}$ from the acceptable value reveals that titanium exist as Ti^{4+} and also has coordinated to amine moiety on the silica framework which confirms the incorporation of titanium species. Based on the results from XPS and UV-DRS, it was clear that titanium is hexa-coordinated onto the silica frame work. The Ti content from XPS measurement (0.54 mmol/g) agreed with the result obtained from AAS measurement (0.58 mmol/g).

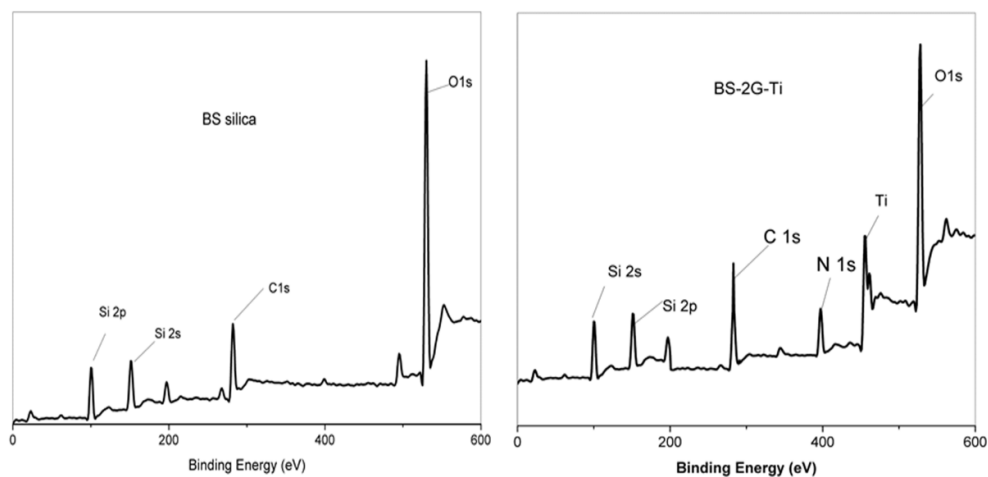


Fig. 3.9 XPS spectra of BS & BS-2G-Ti

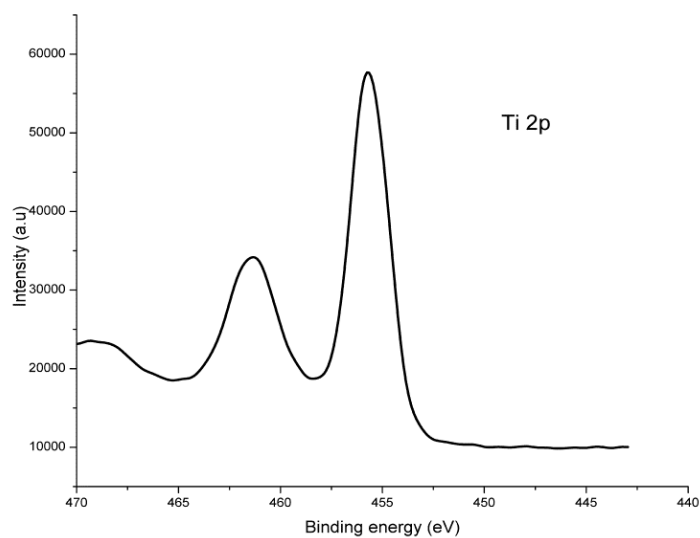


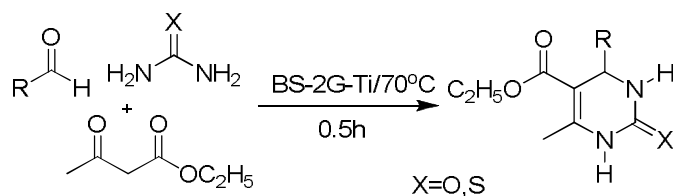
Fig. 3.10 High resolution spectrum of Ti⁴⁺

3.2.3 Catalytic performance

Here, we have investigated the catalytic activity of the prepared catalysts in two important multicomponent reactions such as pyranopyrazole

synthesis and Biginelli reaction. MCRs fascinate chemists because, they combine three or more starting reactants in a one-pot and one-step process to generate single product. Pyranopyrazoles and 3,4-dihydropyrimidin-2(1*H*)-ones are important classes of heterocyclic compounds, and they find application in pharmaceutical and agricultural field. Their derivatives possess significant biological activities such as anti-inflammatory, molluscicidal, insecticidal, antitumor, and anticancer properties.¹⁸⁻²¹ Classical Biginelli reaction required long reaction times, harsh reaction conditions and unsatisfactory yields.²²⁻²⁴ This problem has led to the development of many strategies that overcome the problems of classical reaction.²⁵⁻⁴² Pyranopyrazoles and their derivatives have attracted much attention in recent years because of the possibility of diversity generation which can lead to new libraries of bioactive compounds. Thus, several improved catalytic systems have been reported recently using ionic liquids, ammonium acetate, piperidine, L-proline, MgO, β -cyclodextrin, alumina, Meglumine and also solvent free condition.⁴³⁻⁵⁰ These methods are effective in terms of high yield; but suffer from several short comings, such as use of toxic base, organic solvents, longer reaction time, and non recoverable catalyst. With these considerations, development of facile, commercially and environmentally benign synthetic strategies for these heterocycles is highly desirable. Several synthetic methods using the cooperative combination of Lewis base with Lewis acid have been reported and have proved to yield the desired products in more efficient C-C bond forming reactions.⁵¹⁻⁵⁵ We have successfully synthesized the desired products with excellent yield under green chemical approach.

3.2.3.1 Biginelli reaction



Scheme 3.2 BS-2G-Ti catalyzed Biginelli reaction

Here, we have attempted to synthesize 3,4-dihydropyrimidin-2(1H)-one under solvent free condition, since the use of organic solvents decreased the catalytic activity and selectivity. Firstly, no desirable product could be detected in the absence of catalyst, indicating that a catalyst must be needed for the Biginelli reaction. Conversion of reactant was increased with increasing amount of catalyst upto 10 mg (0.1 mol%). The results are shown in Table 3.3a. Effect of solvent was studied by selecting different solvents at 70 °C, good result was obtained in water. Under solvent free conditions, the corresponding product was obtained in high-to-quantitative yield with high purity (Table 3.3b). Reaction was also carried out at 30 °C giving the desired product with low yield and required more time. The optimized condition was applied to various aldehydes, it was noticed that all the employed aldehydes reacted very well under the solvent free condition (Table 3.3c).

Table 3.3a Effect of amount catalyst

Catalyst amount (mg)	7	10	13
Yield (%)	85	96	95

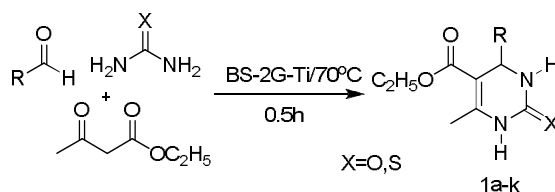
Reaction conditions: C₆H₅CHO (25.0 mmol), CH₃COCH₂COOC₂H₅ (25.0 mmol), urea (37.5 mmol), 70 °C, 0.5 h, No solvent

Table 3.3b Effect of solvent

Entry	Solvent	Yield (%)
1	Ethanol	82
2	CH ₃ CN	86
3	DMF	86
4	Water	90
5	No solvent	96

Reaction conditions: C₆H₅CHO (25.0 mmol), CH₃COCH₂COOC₂H₅ (25.0 mmol), urea (37.5 mmol), 70 °C, 0.5 h

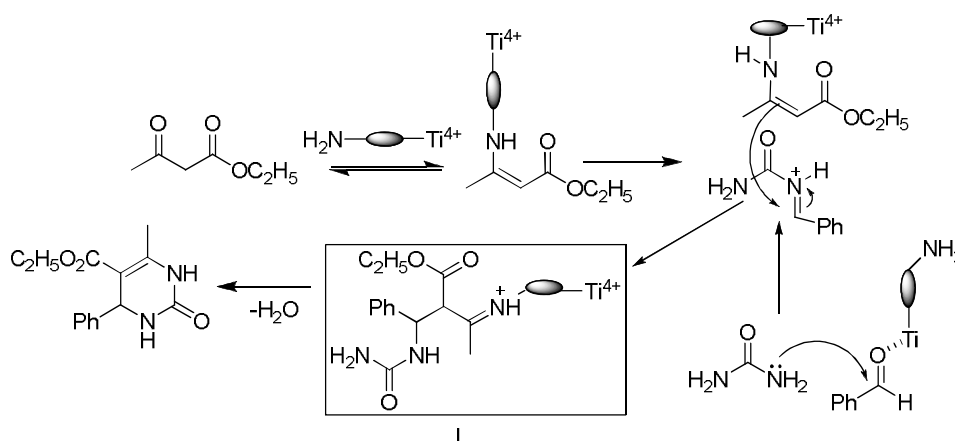
Table 3.3c BS-2G-Ti catalyzed synthesis of DHPMS



Entry	R	X	product	Yield %
1	Ph	O	1a	96
2	2-OH-C ₆ H ₄ -	O	1b	92
3	4-OCH ₃ -C ₆ H ₄ -	O	1c	95
4	4-OCH ₃ -C ₆ H ₄ -	S	1d	90
5	- C ₁₀ H ₁₁ -	O	1e	85
6	4-Cl- C ₆ H ₄ -	O	1f	85
7	4-Cl- C ₆ H ₄ -	S	1g	80
8	Ph	S	1h	86
9	4-Br-C ₆ H ₄ -	O	1i	85
10	4-NO ₂ -C ₆ H ₄ -	O	1j	85
11	Ph-CH=CH	O	1k	96

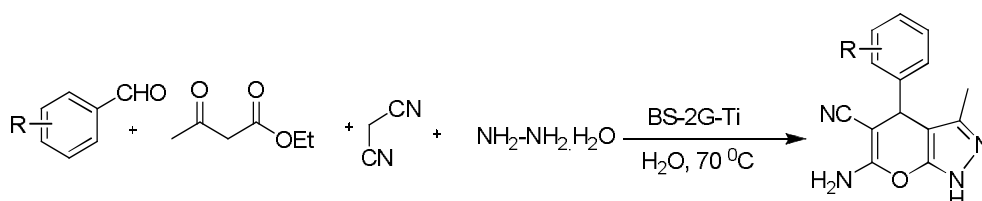
Reaction conditions: C₆H₅CHO (25.0 mmol), CH₃COCH₂COOC₂H₅ (25.0 mmol), urea/thiourea (37.5 mmol), 70 °C, No solvent, 0.5 h

A dual activation mechanism is shown in Scheme 3.3. The primary amino group on the side chain of the catalyst activates ethyl acetoacetate through the formation of an enamine. The imine formed between benzaldehyde and urea is attacked by Ti activated enamine complex to form intermediate I, which, after hydrolysis, intramolecular cyclization, and dehydration reaction, yielded the desired product.



Scheme 3.3 Dual activation mechanism of Biginelli reaction

3.2.3.2 Pyranopyrazole synthesis



Scheme 3.4 BS-2G-Ti catalyzed pyranopyrazole synthesis

The reaction between hydrazine hydrate, ethyl acetoacetate (EAA), malononitrile, and benzaldehyde, in water was chosen as a model condensation reaction for optimization. Initially, the reaction was conducted without catalyst, no product was obtained. By adding 1 mol% of BS-2G-Ti

catalyst, the reaction proceeded slowly at room temperature and took more than 15 h for completion. To enhance the rate of the reaction, the temperature was raised to 70 °C, so the reaction was completed within 1 h. Further increase of temperature did not affect the yield.

In order to quantify the amount of catalyst, reaction was carried out by adding different amounts of catalyst. When catalyst amount was increased from 5 mg to 15 mg, yield of the desired product was increased. It was found that 13 mg (2 mol%) of the catalyst was sufficient for the reaction.

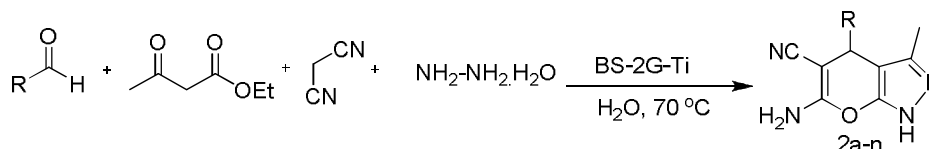
To examine the influence of solvent, the reaction was conducted in protic and aprotic solvents such as ethanol, water and acetonitrile. The reaction in protic solvent showed satisfying performance, but in the aprotic solvent (acetonitrile), efficiency was poor (Table 3.4a). This suggests that the solvent polarity also contributed a significant role to the synthesis of pyranopyrazoles and better result was obtained in water.

To evaluate the scope of the reaction, it was performed with various substrates under the optimized condition and the corresponding results are given in Table 3.4b. Almost all the employed aldehydes resulted in good to-excellent yield of the corresponding products without any side products. Aldehydes having electron-withdrawing substituents reacted faster and gave high yield as compared to the aldehydes having electron-donating substituents. The reaction proceeded satisfactorily with aliphatic aldehyde and cyclic ketone.

Table 3.4a Effect of solvent

Entry	Solvent	Yield (%)	Temp (°C)
1	Ethanol	65	70
2	Acetonitrile	45	70
3	DMF	60	70
4	Water	95	reflux
5	Water	96	70

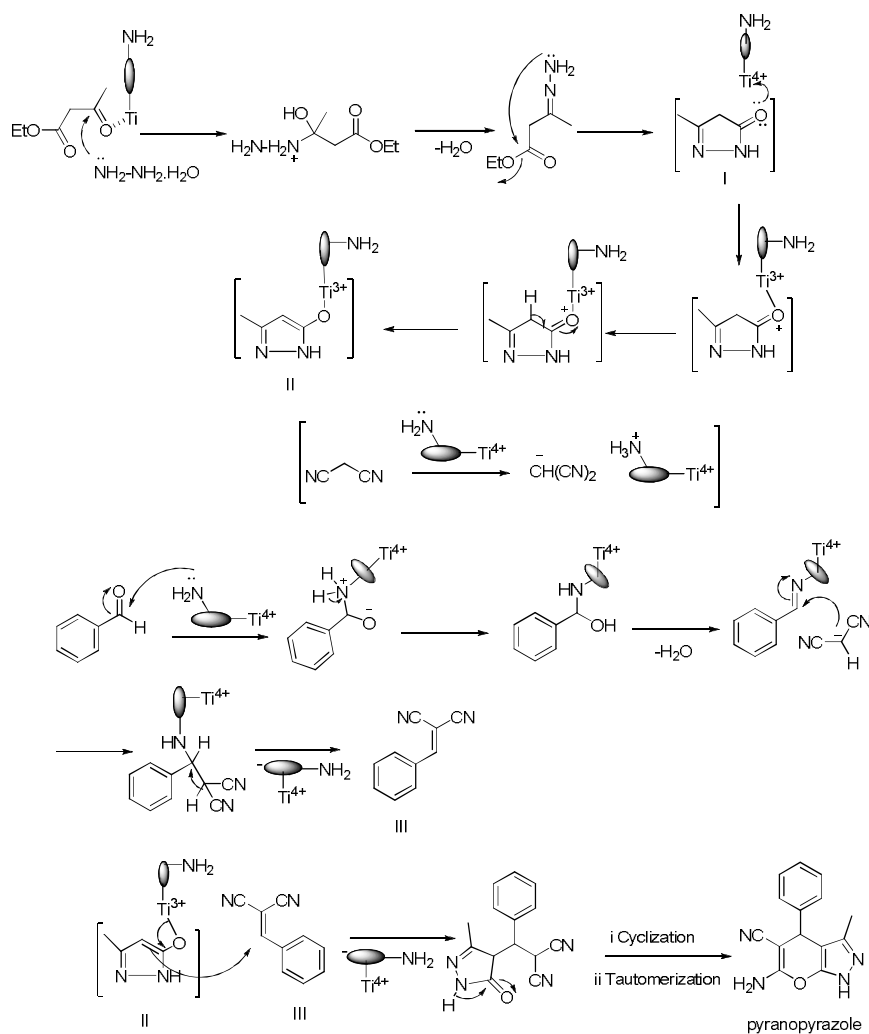
Reaction was tried on benzaldehyde (1 mmol), EAA (1 mmol), malononitrile (1 mmol), hydrazine hydrate (1.5 mmol) in aqueous medium

Table 3.4b Synthesis of substituted pyranopyrazole using BS-2G-Ti in aqueous medium

Entry	Carbonyl compounds	Product	Yield (%)	Time (min)
1	Ph	2a	94	60
2	4-OCH ₃ -C ₆ H ₄ -	2b	91	70
3	3-NO ₂ -C ₆ H ₄	2c	85	90
4	-CH=CH-Ph	2d	94	60
5	4-Cl-C ₆ H ₄ -	2e	95	60
6	2-OH-C ₆ H ₄ -	2f	90	90
7	4-Br-C ₆ H ₄ -	2g	95	70
8	4-NO ₂ -C ₆ H ₄ -	2h	96	90
9	4-OH-C ₆ H ₄ -	2i	94	70
10	2-NO ₂ -C ₆ H ₄ -	2j	96	90
11	2-Thiophenyl	2k	75	60
12	CH ₃ -CHO	2l	45	100
13	4-methyl acetophenone	2m	50	90
14	cyclohexanone	2n	56	90

Reaction was tried on benzaldehyde (1mmol), EAA (1 mmol), malononitrile (1 mmol), hydrazine hydrate (1.5 mmol) in aqueous medium at 70 °C

The possible mechanism for BS-2G-Ti catalyzed synthesis of pyranopyrazoles is shown in Scheme 3.5.



Scheme 3.5 Dual activation mechanism of pyranopyrazole synthesis

Initially, ethyl acetoacetate was activated by lewis acid part on the catalyst and hydrazine attacks the carbonyl group of the activated ethyl acetoacetate. Loss of H₂O, and intramolecular nucleophilic attack by NH₂ group of hydrazine to the next carbonyl group of ethyl acetoacetate affords

5-methyl-2,4-dihydropyrazol-3-one (intermediate I) and removes EtOH. Simultaneously, there is formation of arylidene malononitrile (III) by the Knoevenagel condensation between aldehyde and malononitrile. This step is activated by free amino groups on the catalyst. Michael addition of pyrazolone (I) to arylidene malononitrile (III), followed by cyclization and then tautomerization, afforded the pyranopyrazole.

To examine the catalytic efficiency of BS-2G-Ti, both reactions were also performed in the presence of BS-2G under identical reaction conditions. It was found that this dendritic functionalized catalyst also exhibited high catalytic activity, but took more time for the completion of reaction and the product yield was lower compared to BS-2G-Ti. The results are given in Table 3.5.

Table 3.5 BS-2G catalyzed reactions

Catalyst	Reaction	Time (h)	Yield (%)
BS-2G (10 mg)	Biginelli reaction ^a	2	85
BS-2G (13 mg)	Pyranopyrazole synthesis ^b	4	88

^a Reaction conditions: C₆H₅CHO (25.0 mmol), CH₃COCH₂COOC₂H₅ (25.0 mmol), urea (37.5 mmol), No solvent, 70 °C; ^b Reaction conditions: C₆H₅CHO (1 mmol), malononitrile (1 mmol), CH₃COCH₂COOC₂H₅ (1 mmol), hydrazine hydrate (1.5 mmol), H₂O, 70 °C

We have also investigated Biginelli reaction and pyranopyrazole synthesis with Ti activated on amorphous silica. The metal intake capacity was found to be 0.49 mmol of Ti in one gram silica from AAS measurement. Catalytic activity of Ti-SiO₂ was performed in Biginelli reaction and pyranopyrazole synthesis under identical reaction conditions. The targeted

products were obtained with 80 and 85 % yield respectively with prolonged reaction time. Ti-SiO₂ catalyst showed significant metal leaching after reaction, whereas, BS-2G-Ti showed high stability and negligible metal leaching and can be reused with same activity.

3.2.3.3 Recycling of catalyst

It was found that the catalyst could be efficiently recycled and reused for 3 repeating cycles without much loss of efficiency (Figure 3.11). This indicated that Ti-grafted amine functionalized mesoporous silica was an efficient catalyst for both the reactions. For the recycling study, catalyst was washed with methanol (3 times), dried at 50 °C and subjected to recycling.

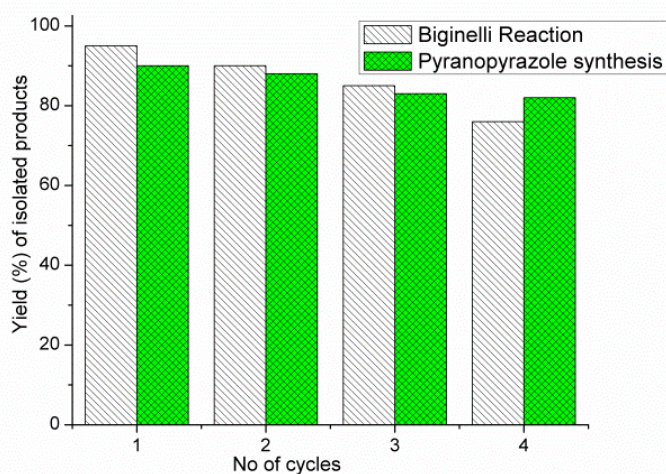


Fig. 3.11 Recycling study of BS-2G-Ti in Biginelli reaction and pyranopyrazole synthesis

Reaction conditions: Biginelli reaction :- C₆H₅CHO (25.0 mmol), CH₃COCH₂COOC₂H₅(25.0 mmol), urea (37.5 mmol), 70 °C, 0.5 h, Pyranopyrazole synthesis:- C₆H₅CHO (1mmol), malononitrile (1mmol), CH₃COCH₂COOC₂H₅ (1mmol), hydrazine hydrate (1.5 mmol), H₂O, 70 °C

3.3 Conclusion

In summary, Ti-grafted polyamidoamine dendritic silica hybrid catalyst was synthesized and characterized by various techniques. It was found that this dendritic silica hybrid catalyst exhibited high catalytic activity in the synthesis of 3,4-dihydropyrimidin-2-one under solvent free condition and pyranopyrazoles in aqueous medium. Dual nature of the hybrid catalyst played a vital role in the mechanism of both the reactions by activating the formation of intermediates resulting in the desired products in excellent yield within a short period of time.

3.4 Experimental

3.4.1 Materials and methods

All the solvents were purified according to the standard procedures. All reagents and solvents used in the preparation and modification of mesoporous silica were used as received. 1,4-bis(triethoxysilyl)benzene, cetyltrimethylammonium bromide (CTAB), 3-aminopropyl trimethoxysilane and Titanium (IV) isopropoxide (98 %) were received from Aldrich. Amorphous silica was purchased from Loba Chemie Pvt. Ltd., India. TLC was done on silica coated alumina plates (Merck, 60F254).

3.4.2 Synthesis of benzene mesoporous silica and polyamidoamine dendrimer (2G) on silica

The periodic mesoporous benzene-silica with crystal-like pore walls (BS) was prepared using the 1,4-bis(triethoxysilane)benzene monomer precursor and CTAB using the similar procedure described earlier.⁵⁶ CTAB (4.7 mmol) was dissolved in a mixture of ion exchanged water (50 mL) and

6M aq.NaOH solution at 50-60 °C. BTEB (4.96 mmol) was added to the CTAB solution under vigorous stirring at room temperature. The mixture was treated ultrasonically for 20 minutes to disperse the hydrophobic BTEB in the aqueous solution and stirred for 20 h at room temperature. The solution was kept at 95 °C for 20 h under static condition. The resulting white precipitate was recovered by filtration and dried to yield as made mesoporous benzene silica material. Surfactant was removed by stirring 1g of as synthesized material in 250 mL of ethanol with 3N aq.HCl at 70 °C for 8 h to yield mesoporous benzene silica.

Yield 70 %; White powder; IR (KBr): $\bar{\nu}$ 3458, 1633, 1391, 1056 cm^{-1} ; ^{29}Si CP MAS NMR (75 MHz): -80.5, -102.4 ppm.

Polyamidoamine upto second generation was developed on benzene silica according to a similar procedure described in literature.⁷

3.4.3 Synthesis of amine-functionalized mesoporous silica (BS-NH₂)

Mesoporous benzene silica (BS 4 g) was suspended in 40 mL of toluene and 3-aminopropyl trimethoxysilane (4 g) in methanol (4 mL) was slowly added to avoid gel formation under nitrogen atmosphere. The mixture was refluxed with continuous stirring for 20 h followed by extraction with methanol at 60 °C for 8 h. After filtration and washing with methanol, the recovered powder was dried at 100 °C for 12 h.

Yield 4.07; White powder; IR (cm^{-1}): 2930 (C-H stretching), 1700-1400 (C-H bending), 1650-1580 (N-H bending); CHN analysis: C (4.92 %), N (1.25 %), H (1.85 %); Amine capacity: 0.775 mmol/g.

3.4.4 Synthesis of first-generation dendritic mesoporous silica (BS-1G)

The propylamine group grafted onto the mesoporous silica (BS-NH₂) can easily undergo Michael addition with methyl methacrylate to yield an aminopropionate ester which in turn on amidation with ethylene diamine resulted in the formation of the first generation of mesoporous silica. In a closed vessel under nitrogen, aminopropyl-functionalized mesoporous silica (3 g) was suspended in methyl methacrylate solution (6 g, 60 mmol) in methanol and the mixture was heated at 55 °C and stirred for 60 h. After filtration, the powder was repeatedly washed with methanol and dried under vacuum. The aminopropionate derivative of mesoporous silica was designated as BS-0.5G. BS-0.5G (3 g) was further suspended in ethylene diamine solution (30 mL) in methanol (30 mL) in a closed vessel under nitrogen atmosphere and stirred at ambient conditions for 4 days. After filtration and subsequent washing with ethanol and dichloromethane the resulting material was vacuum dried and kept in desiccator. The obtained mesoporous silica hybrid material was designated as BS-1G.

BS-0.5G (White powder); IR (cm⁻¹): 1742 (CO stretching of ester)

BS-1G (Light yellow powder); Yield 3.20 g; IR (cm⁻¹): 1515 (N-H bending of amide), 1640 (CO stretching of amide), 3500-3400 (N-H stretching of amine); Amine capacity: 1.83 mmol/g.

3.4.5 Synthesis of second generation dendritic mesoporous silica (BS-2G)

Under nitrogen atmosphere BS-1G (3 g) was stirred with methyl methacrylate solution (6 g, 60 mmol) in methanol (60 mL) at 55 °C for 4 consecutive days followed by filtration and washing with methanol. The

recovered vacuum dried material was designated as BS-1.5G. It was (3 g) further suspended in ethylene diamine solution (100 mL) in methanol (50 mL) and stirred at ambient conditions for 6 days to yield the corresponding second generation mesoporous silica designated as BS-2G.

BS-1.5G (Yellow powder); IR (cm^{-1}): 1742 (CO stretching of ester), 1515 (N-H bending of secondary amide),

BS-2G (Yellow powder); Yield 3.38 g; IR (cm^{-1}): 1515 (N-H bending of secondary amide), 1640 (CO stretching of secondary amide), 3500-3400 (N-H stretching of secondary amine); Amine capacity: 3.39 mmol/g.

3.4.6 Preparation of Ti-grafted polyamidoamine dendritic silica hybrid catalyst

The periodic mesoporous dendritic silica hybrid (2 g) was suspended in CH_2Cl_2 (40 mL). To this $\text{Ti}(\text{OiPr})_4$ (1.2 mL, 4 mmol) was added. The mixture was stirred for 24 h under N_2 atmosphere. After the reaction, the product was filtered and washed with isopropanol (30 mL \times 3 times) and dry ether (30 mL \times 3 times) and dried at 50 °C.

BS-2G-Ti (Pale yellow powder); Yield 3.35 g; IR (KBr): $\bar{\nu}$ 3389, 1650, 1515, 1391, 1056 cm^{-1} ; Ti content (AAS): 0.58 mmol/g; Amine capacity: 1.26 mmol/g.

3.4.7 Preparation of Ti incorporated SiO_2

Ti activated on amorphous silica (Ti-SiO_2) was prepared by stirring an isopropanol solution of $\text{Ti}(\text{iOPr})_4$ (2 mmol, 0.6 mL) with 1 g SiO_2 for 12 h. It was filtered, and washed with ethanol in Soxhlet extractor and dried under

vacuum. The metal intake capacity was found to be 0.49 mmol of Ti per gram silica.

3.4.8 Estimation of -NH₂ group capacity

The amine content of functionalized BS silica materials was estimated *via* dil. HCl consumption using the acid–base titration method. Typically, 100 mg of functionalized BS silica material was suspended in 30 mL of 0.1 M HCl solution and stirred at ambient temperature for 24 h. The filtrate was titrated with NaOH solution (0.1 M).

3.4.9 Procedure for Biginelli reaction and Pyranopyrazole synthesis

3.4.9.1 Biginelli reaction

Aldehyde (25.0 mmol), β -dicarbonyl compound (25.0 mmol), urea (37.5 mmol) and BS-2G-Ti (0.15 mol%) were successively charged into a 50 mL round bottomed flask with a magnetic stirring bar. The reaction proceeded at 70 °C for 30 min during which time a solid product was gradually formed. After the reaction, the resulting solid product with pale yellow color was crushed and washed with ethyl acetate, filtered and extracted with water; organic layer was collected and dried under vacuum to afford the primary product. The pure product was obtained by further recrystallization of the primary product with ethyl acetate.

3.4.9.2 Synthesis of pyranopyrazoles

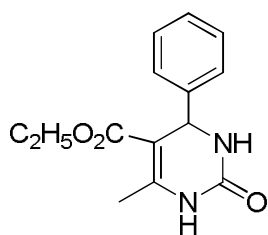
To a magnetically stirred aqueous solution of ethyl acetoacetate (1 mmol) and hydrazine hydrate (1.5 mmol), aldehyde (1 mmol), malononitrile (1 mmol), and a catalytic amount of BS-2G-Ti (2 mol%) were successively

added. The resulting suspension was stirred and heated at 70 °C for appropriate reaction time as specified in (Table 4a). The progress of the reaction was monitored by TLC (3:7, ethyl acetate: hexane). After completion, the reaction mixture was cooled to room temperature, and acetonitrile was added and shaken well for 5 min, filtered and poured over crushed ice, stirred for 10 min, precipitated product was filtered, washed with water, dried and recrystallized from methanol.

Spectral characterization data of compounds 1a-1k

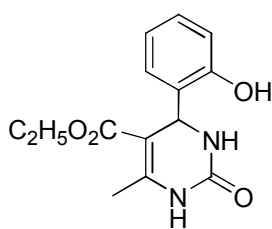
5-Ethoxycarbonyl-6-methyl-4-phenyl-3,4-dihydropyrimidin-2(1H)-one

(Table 3.3c, 1a): White solid, m. p 202-204 °C



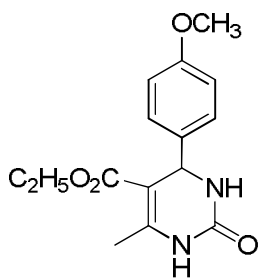
LCMS (M+1) m/z 261; IR (KBr): $\bar{\nu}$ 3240, 2945, 1610, 678 cm^{-1} ; ^1H NMR (400 MHz, CDCl_3): δ 8.20 (s, 1H), 7.16 (s, 1H), 6.86 (s, 5H), 5.14 (s, 1H), 3.97 (q, $J = 6.4$ Hz, 2H), 2.23 (s, 3H), 1.10 (t, $J = 6.4$ Hz, 3H); ^{13}C NMR (100 MHz, CDCl_3): 167.4, 154.2, 149.8, 146.2, 129.6, 127.9, 128.5, 99.3, 59.9, 56.0, 18.5, 15.1.

5-Ethoxycarbonyl-6-methyl-4-(2-hydroxyphenyl)-3,4-dihydropyrimidin-2(1H)-one (Table 3.3c 1b): White solid, m. p 200-202 °C



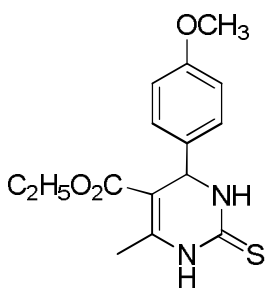
LCMS (M+1) m/z 276.1; IR (KBr): $\bar{\nu}$ 1705, 1748, 2926, 3084, 3224 cm^{-1} ; ^1H NMR (400 MHz, CDCl_3): δ = 7.3 (s, 1H), 8.14 (s, 1H), 7.87 (s, 1H), 7.46-6.95 (m, 4H), 5.24 (s, 1H), 3.92 (q, $J = 7.1$ Hz, 2H), 2.23 (s, 3H), 1.08 (t, $J = 7.1$ Hz, 3H); ^{13}C NMR (100 MHz, CDCl_3): 175.7, 168.3, 160.2, 143.1, 135.4, 130.2, 127.3, 126.7, 125.8, 105.6, 63.2, 58.2, 20.1, 19.8, 15.5.

5-(Ethoxycarbonyl)-6-methyl-4-(4-methoxyphenyl)-3,4-dihydropyrimidin-2(1H)-one (Table 3.3c, 1c): White solid, m. p 198-200 °C



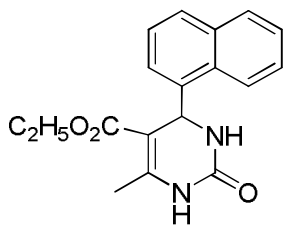
LCMS (M+1) m/z 290.1; IR (KBr): $\bar{\nu}$ 3242, 2956, 1704, 1681, 1504 cm^{-1} ; ^1H NMR (400 MHz, CDCl_3): δ 9.1 (s, 1H), 7.7 (s, 1H), 7.1 (d, $J = 8.2$ Hz, 2H), 6.9 (d, $J = 8.2$ Hz, 2H), 5.1 (d, $J = 2.6$ Hz, 1H), 3.9 (q, $J = 7.0$ Hz, 2H), 3.7 (s, 3H), 2.2 (s, 3H), 1.1 (t, $J = 7.2$ Hz, 3H); ^{13}C NMR (100 MHz, $\text{DMSO}-d_6$): 198.4, 160.5, 155.1, 149.8, 138.4, 130.7, 118.9, 113.6, 58.1, 56.3, 32.2, 22.8.

5-(Ethoxycarbonyl)-6-methyl-4-(4-methoxyphenyl)-3,4-dihydropyrimidin-2(1H)-thione (Table 3.3c, 1d): White solid, m. p 145-146 °C



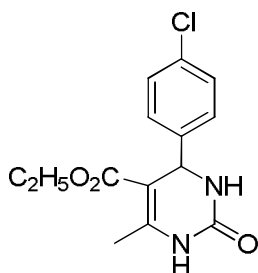
LCMS (M+1) m/z 307; IR (KBr): $\bar{\nu}$ 3256, 1659, 1595, 1569 cm^{-1} ; ^1H NMR (400 MHz, $\text{DMSO}-d_6$): δ 9.89 (s, 1H), 9.3 (s, 1H), 7.2 (d, $J = 8.1$ Hz, 2H), 6.7 (d, $J = 8.1$ Hz, 2H), 5.2 (s, 1H), 4.1 (q, $J = 7.2$ Hz, 2H), 2.3 (s, 3H), 1.2 (t, $J = 7.2$ Hz, 3H); ^{13}C NMR (100 MHz, $\text{DMSO}-d_6$): 173.9, 174.3, 165.9, 126.8, 158.5, 145.2, 135.9, 128.0, 114.0, 101.5, 59.8, 55.3, 53.6, 17.4, 14.3.

5-(Ethoxycarbonyl)-6-methyl-4-(2-naphthyl)-3,4-dihydropyrimidin-2(1H)-one (Table 3.3c, 1e): Yellow Solid, m. p 247-249 °C



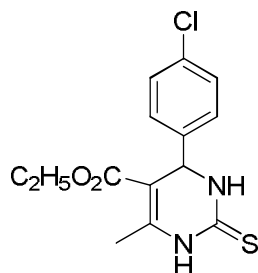
LCMS (M+1) m/z 310.5; IR (KBr): $\bar{\nu}$ 3245, 3118, 2977, 1698, 1647, 1431, 1231, 1088, 790 cm^{-1} ; ^1H NMR (400 MHz, $\text{DMSO}-d_6$): δ 9.01 (s, 1H), 8.28 (d, $J = 8.2$ Hz, 1 H), 7.80 (d, $J = 8.2$ Hz, 1 H), 7.75 (t, $J = 8.1$ Hz, 1 H), 7.40-7.55 (m, 5H), 6.10 (s, 1 H), 3.75 (q, $J = 7.1$ Hz, 2 H), 2.32 (s, 3 H), 0.90 (t, $J = 7.1$ Hz, 3H); ^{13}C NMR (100 MHz, CDCl_3): 165.1, 152.3, 147.3, 148.2, 135.3, 134.5, 128.0, 126.6, 122.5, 98.5, 61.4, 53.5, 18.2, 15.5.

5-(Ethoxycarbonyl)-6-methyl-4-(4-chlorophenyl)-3,4-dihydropyrimidin-2(1H)-one (Table 3.3c, 1f): White solid, m. p 209-211 °C



LCMS (M+1) m/z 294; IR (KBr): $\bar{\nu}$ 3233, 3093, 2976, 2933, 1701, 1643 670 cm^{-1} ; ^1H NMR (400 MHz, CDCl_3) δ : 9.3 (s, 1H), 7.8 (s, 1H), 7.40–7.30 (m, 4H), 5.1 (s, 1H), 3.9 (q, $J = 7.2$ Hz, 2H), 2.3 (s, 3H), 1.0 (t, $J = 7.2$ Hz, 3H); ^{13}C NMR (100 MHz, CDCl_3): 165.0, 151.4, 148.9, 141.2, 131.7, 129.2, 128.7, 98.2, 58.9, 51.9, 17.9.

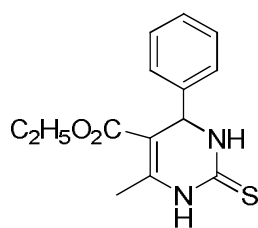
5-(Ethoxycarbonyl)-6-methyl-4-(4-chlorophenyl)-3,4-dihydropyrimidin-2(1H)-thione (Table 3.3c, 1g): White solid, m. p 192-194 °C



LCMS (M+1) m/z 310.8; IR (KBr): $\bar{\nu}$ 3255, 1657, 1560 cm^{-1} ; ^1H NMR (400 MHz, CDCl_3): δ 10.0 (s, 1H), 9.30 (s, 1H), 7.15 (m, 4 H), 5.25 (s, 1 H), 4.10 (q, $J = 7.1$ Hz, 2 H), 2.41 (s, 3 H), 1.13 (t, $J = 7.1$ Hz, 3H); ^{13}C NMR (100 MHz, $\text{DMSO}-d_6$): 178.3, 169.0, 150.3, 148.4, 137.3, 133.6, 135.4, 105.4, 64.7, 55.5, 19.2, 17.0.

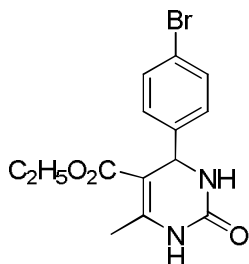
5-(Ethoxycarbonyl)-6-methyl-4-phenyl-3,4-dihydropyrimidin-2(1H)-thione (Table 3.3c, 1h):

White solid, m.p 207-209 °C



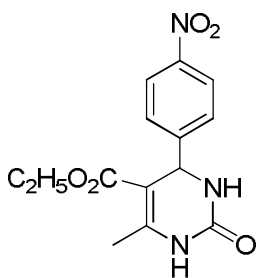
LCMS (M+1) m/z 276; IR (KBr): $\bar{\nu}$ 3282, 1615, 1575, 1268 cm^{-1} ; ^1H NMR (400 MHz, CDCl_3): δ 7.40 (s, 1 H), 7.15 (m, 5 H), 5.8 (s, 1 H), 4.57 (s, 1H), 3.85 (q, $J = 7.1$ Hz, 2H), 2.15 (s, 3 H), 0.95 (t, $J = 7.1$ Hz, 3 H); ^{13}C NMR (100 MHz, CDCl_3): 179.4, 164.2, 159.8, 146.2, 129.6, 127.9, 128.5, 99.3, 62.3, 59.9, 18.5, 15.5.

5-(Ethoxycarbonyl)-6-methyl-4-(4-bromophenyl)-3,4-dihydropyrimidin-2(1H)-one (Table 3.3c, 1i): White solid; m. p 218-220 °C



LCMS (M+1) m/z 339; IR (KBr): $\bar{\nu}$ 3233, 3093, 2976, 2933, 1701, 1643 cm^{-1} ; ^1H NMR (400 MHz, CDCl_3): δ 9.2 (s, 1H), 7.5 (s, 1H), 7.40–7.30 (m, 4H), 4.9 (s, 1H), 3.3 (q, $J=7.0$ Hz, 2H), 2.0 (s, 3H), 0.89 (t, $J=7.0$ Hz, 3H); ^{13}C NMR (100 MHz, CDCl_3): 164.0, 149.4, 146, 137.2, 128.7, 125.2, 123.7, 97.2, 56.9, 47.9, 15.9.

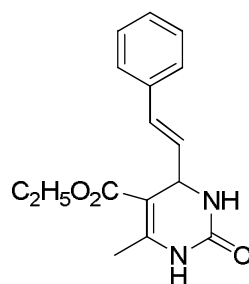
5-(Ethoxycarbonyl)-6-methyl-4-(4-nitrophenyl)-3,4-dihydropyrimidin-2(1H)-one (Table 3.3c, 1j): White solid, m. p 206-208 °C



LCMS (M+1) m/z 305; IR (KBr): $\bar{\nu}$ 3233, 3000, 1710, 1675, 1630, 1613, 1560, 1524, 1309 cm^{-1} ; ^1H NMR (400 MHz, CDCl_3): δ 9.30(s, 1H), 8.25 (d, $J=8.4$ Hz 2H), 7.90 (s, 1H), 7.50 (d, $J=8.4$ Hz 2H), 5.15 (d, 1H), 3.90 (q, $J=7.1$ Hz, 2H), 2.34 (s, 3H), 1.10 (t, $J=7.1$ Hz, 3H); ^{13}C NMR (100 MHz, $\text{DMSO-}d_6$): 164.7, 151.3, 149.3, 146.4, 126.8, 123.7, 59.3, 52.8, 17.8, 13.7.

5-(Ethoxycarbonyl)-6-methyl-(4-styryl)-3,4-dihydropyrimidin-2(1H)-one (Table 3.3c, 1k):

Colorless crystals, m. p 230-231 °C



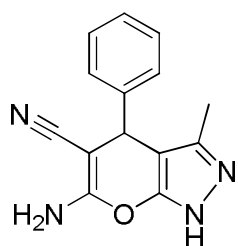
LCMS (M+1) m/z 286; IR (KBr): $\bar{\nu}$ 3241, 1704, 1650 cm^{-1} ; ^1H NMR (400 MHz, CDCl_3): δ 8.5 (s, 1H), 7.80 (s, 1 H), 7.15 (m, 5 H), 6.35 (d, $J=4.0$ Hz, 1 H), 6.08 (dd, 14.5, 4.0 Hz, 1 H), 5.24 (d, $J=4.0$ Hz, 1H), 3.9 (q, $J=7.1$ Hz, 2 H), 2.19 (s, 3 H), 1.08 (t, $J=7.1$ Hz, 3H); ^{13}C NMR (100 MHz, CDCl_3): 168.1, 159.6, 152.5, 140.2, 135.0, 131.6, 132.1, 130.5, 128.2, 99.8, 61.2, 53.8, 18.7, 15.2.

Spectral characterization data of compounds 2a-2n

6-Amino-2,4-dihydro-3-methyl-4-phenylpyrano-[2,3-c]pyrazole-5-carbonitrile

(Table 3.4b, 2a):

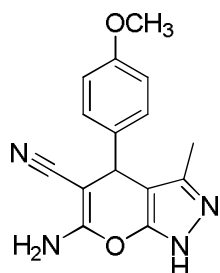
White solid, m. p 246-248 °C



GC-MS (M^+): 252; IR (KBr): $\bar{\nu}$ 3410, 3356, 3167, 2990, 1646, 1596, 1399, 1276 cm^{-1} ; ^1H NMR (400 MHz, CDCl_3): δ 1.77 (s, 3H), 4.80 (s, 1H), 6.89 (s, 2H), 7.05-7.35 (m, 5H), 12.05 (s, 1H); ^{13}C NMR (100 MHz, CDCl_3): 146.5, 136.5, 128.7, 127.9, 126.9, 121.0, 58.1, 36.8, 10.1.

6-Amino-2,4-dihydro-3-methyl-4-(4-methoxyphenyl)pyrano-[2,3-c]pyrazole-5-carbonitrile (Table 3.4b, 2b):

White solid, m. p 209-211 °C



GC-MS (M^+): 282; IR (KBr): $\bar{\nu}$ 3485, 3258, 2185, 1608, 1442 cm^{-1} ; ^1H NMR (400 MHz, CDCl_3): δ 1.75 (s, 3H), 3.80 (s, 3H), 4.58 (s, 1H), 6.88 (d, $J = 8.1$ Hz, 2H), 6.88 (d, $J = 8.1$ Hz, 2H), 7.09 (s, 2H), 12.10 (s, 1H); ^{13}C NMR (100 MHz, CDCl_3): 160.5, 156.3, 155.8, 144.2, 136.8, 118.5, 114.2, 111.5, 107.4, 57.9, 55.1, 36.2, 9.89.

6-Amino-2,4-dihydro-3-methyl-4-(3-nitrophenyl)pyrano-[2,3-c]pyrazole-5-carbonitrile (Table 3.4b, 2c):

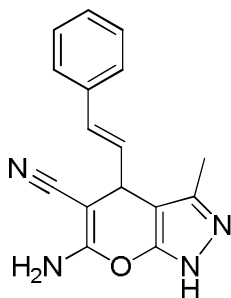
Brown solid, m.p 243-245 °C



GC-MS (M^+): 297; IR (KBr): $\bar{\nu}$ 3385, 3278, 2189, 1622, 1456 cm^{-1} ; ^1H NMR (400 MHz, CDCl_3): δ 1.80 (s, 3H), 4.92 (s, 1H), 6.90 (s, 2H), 7.81 (s, 1H), 7.78 (d, $J = 8.5$ Hz, 1H), 7.42-7.45 (m, 2H), 12.12 (s, 1H); ^{13}C NMR (100 MHz, CDCl_3): 175.9, 148.8, 146.2, 141.8, 135.3, 134.1, 130.0, 127.6, 124.7, 121.4, 120.2, 59.6, 32.5, 10.7.

6-Amino-2,4-dihydro-3-methyl-4-(4-styryl)pyrano-[2,3-c]pyrazole-5-carbonitrile (Table 3.4b, 2d):

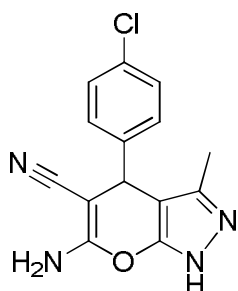
Colorless crystal, m.p 235-238 °C



GC-MS (M^+): 278; IR (KBr): $\bar{\nu}$ 3485, 33241, 2856, 1704, 1650, 1325 cm^{-1} ; ^1H NMR (400 MHz, CDCl_3): δ 1.89 (s, 3H), 4.88 (s, 1H), 6.38(d, $J=14.2$ Hz, 1H), 6.18 (dd, $J=14.2, 4.0$ Hz, 1 H), 5.24 (d, $J=4.0$ Hz, 1H), 7.05-7.16 (m, 5H), 7.8 (s, 2H), 12.1 (s, 1H); ^{13}C NMR (100 MHz, CDCl_3): 167.5, 159.3, 158.8, 149.2, 136.8, 134.5, 128.5, 127.1, 114.4, 58.9, 57.1, 38.2, 10.8.

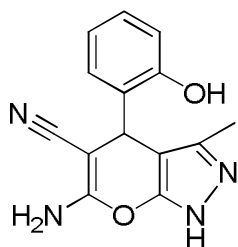
6-Amino-2,4-dihydro-3-methyl-4-(4-chlorophenyl)pyrano-[2,3-c]pyrazole-5-carbonitrile (Table 3.4b, 2e):

White solid, m.p 234-236 °C



GC-MS (M^+): 286; IR (KBr): $\bar{\nu}$ 3485, 3258, 2185, 1608, 1442, 755 cm^{-1} ; ^1H NMR (400 MHz, CDCl_3): δ 1.79 (s, 3H), 3.92 (s, 3H), 4.88 (s, 1H), 7.22 (d, $J=8.2$ Hz, 2H), 7.22 (d, $J=8.2$ Hz, 2H), 7.2 (s, 2H), 12.15 (s, 1H); ^{13}C NMR (100 MHz, CDCl_3): 165.5, 162.3, 160.8, 148.2, 142.8, 126.3, 122.2, 120.4, 115.4, 62.9, 38.2, 13.0.

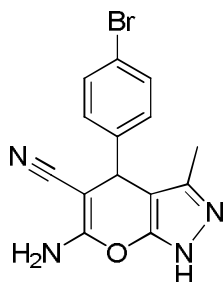
6-Amino-2,4-dihydro-3-methyl-4-(2-hydroxyphenyl)pyrano-[2,3-c]pyrazole-5-carbonitrile (Table 3.4b, 2f): White solid, m. p 210-212 °C



GC-MS (M^+): 268; IR (KBr): $\bar{\nu}$ 3485, 3258, 2185, 1608, 1442 cm^{-1} ; ^1H NMR (CDCl_3 , 400 MHz): δ 1.82 (s, 3H), 4.54 (s, 1H), 5.32 (s, 1H), 6.98-7.25 (m, 4H), 6.87 (s, 2H), 12.01 (s, 1H); ^{13}C NMR (100 M Hz, CDCl_3): 167.5, 148.8, 136.7, 131.8, 126.2, 117.5, 114.4, 110.8, 105.1, 49.7, 19.3, 15.5.

6-Amino-2,4-dihydro-3-methyl-4-(4-bromophenyl)pyrano-[2,3-c]pyrazole-5-carbonitrile (Table 3.4b, 2g):

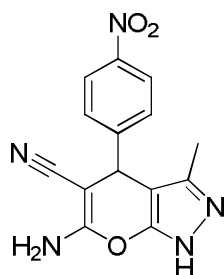
White solid, m. p183-185 °C



GC-MS (M^+): 330; IR (KBr): $\bar{\nu}$ 3485, 3258, 2185, 1618, 1442, 755 cm^{-1} ; ^1H NMR (400 MHz, CDCl_3): δ 1.70 (s, 3H), 3.72 (s, 3H), 4.68 (s, 1H), 6.79 (d, $J=8.1$ Hz, 2H), 6.79 (d, $J=8.0$ Hz, 2H), 6.98 (s, 2H), 12.03 (s, 1H); ^{13}C NMR (100 MHz, CDCl_3): 160.5, 156.3, 155.8, 144.2, 136.8, 118.5, 114.2, 113.4, 107.4, 57.9, 34.2, 12.0.

6-Amino-2,4-dihydro-3-methyl-4-(4-nitrophenyl)pyrano-[2,3-c]pyrazole-5-carbonitrile (Table 3.4b, 2h):

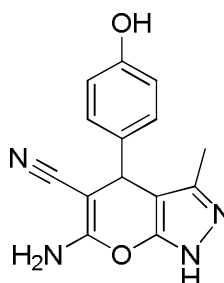
White solid, m.p 250-252 °C



GC-MS (M^+): 296; IR (KBr): $\bar{\nu}$ 3385, 3278, 2189, 1622, 1456 cm^{-1} ; ^1H NMR (400 MHz, CDCl_3): δ 1.72 (s, 3H), 3.79 (s, 3H), 4.89 (s, 1H), 7.29 (d, $J=8.5$ Hz, 2H), 7.27 (d, $J=8.5$ Hz, 2H), 7.01 (s, 2H), 12.13 (s, 1H); ^{13}C NMR (100 MHz, CDCl_3): 172.5, 168.3, 165.8, 149.2, 140.8, 127.5, 124.2, 121.4, 115.4, 60.1, 20.2, 14.9.

6-Amino-2,4-dihydro-3-methyl-4-(4-hydroxyphenyl)pyrano-[2,3-c]pyrazole-5-carbonitrile (Table 3.4b, 2i):

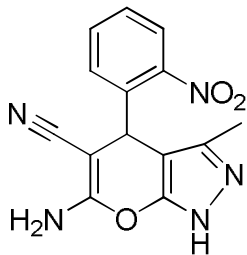
White solid, m.p 222-224 °C



GC-MS (M^+): 268; IR (KBr): $\bar{\nu}$ 3485, 3258, 2185, 1608, 1442 cm^{-1} ; ^1H NMR (400 MHz, CDCl_3): δ 1.75 (s, 3H), 4.14 (s, 1H) 5.38 (s, 1H), 7.01 (d, $J=8.2$ Hz, 2H), 7.13 (d, $J=8.2$ Hz, 2H), 6.87 (s, 2H), 11.8 (s, 1H); ^{13}C NMR (100 MHz, CDCl_3): 165.1, 159.0, 157.8, 146.2, 138.8, 124.1, 117.2, 116.5, 113.4, 59.9, 37.2, 12.8.

6-Amino-2,4-dihydro-3-methyl -4-(2-nitrophenyl) pyrano-[2,3-c]pyrazole-5-carbonitrile (Table 3.4b, 2j):

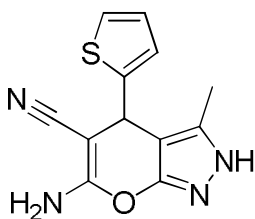
White solid m. p 221-223 °C



GC-MS (M^+): 297; IR (KBr): $\bar{\nu}$ 3375, 3258, 2169, 1602, 1454 cm^{-1} ; ^1H NMR (400 MHz, CDCl_3): δ 1.82 (s, 3H), 5.16 (s, 1H), 7.12 (s, 2H), 7.35-7.59 (m, 4H), 12.4 (s, 1H); ^{13}C NMR (100 MHz, CDCl_3): 170, 152, 140, 138.4, 128.2, 120.1, 118.4, 115.2, 110.1, 56.7, 22.3, 19.5.

6-Amino-2,4-dihydro-3-methyl -4-(thiophen-2-yl)pyrano-[2,3-c]pyrazole-5-carbonitrile (Table 3.4b, 2k):

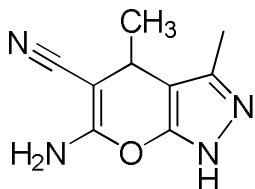
White solid, m. p 242-246 °C



GC-MS (M^+): 258; IR (KBr): $\bar{\nu}$ 3368, 3148, 2890, 2569, 1602, 1454 cm^{-1} ; ^1H NMR (400 MHz, $\text{DMSO}-d_6$): δ 1.95 (s, 3H), 5.03 (s, 1H), 6.96-6.99 (m, 3H), 7.04 (d, $J = 8.0$ Hz, 1H), 7.41 (d, $J = 8.4$ Hz, 1H), 12.2 (s, 1H, NH).

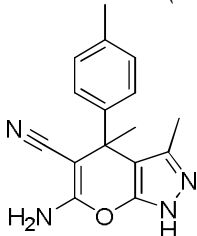
6-Amino-2,4-dihydro-3-methyl-4-(methyl)pyrano-[2,3-c]pyrazole-5-carbonitrile (Table 3.4b, 2l):

White solid, m. p 156-158 °C



GC-MS (M^+): 190; IR (KBr): $\bar{\nu}$ 3485, 3232, 2187, 1641 cm^{-1} ; ^1H NMR (400 MHz, CDCl_3): δ 1.42 (s, 3H), 1.9 (s, 3H), 3.86 (q, $J = 7.2$ Hz, 1H), 7.09 (s, 2H), 12.4 (s, 1H).

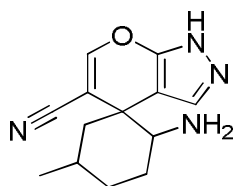
6-Amino-1,4-dihydro-3,4-dimethyl-4-p-tolyl-pyrano[2,3-c]pyrazole-5-carbonitrile (Table 3.4b, 2m): White solid, 182-184 °C



GC-MS (M^+): 266; IR (KBr): $\bar{\nu}$ 3439, 2980, 2185, 1645, 1516, 1349, 1026, 763 cm^{-1} ; ^1H NMR (400 MHz, CDCl_3): δ 1.62 (s, 3H), 1.8 (s, 3H), 2.66 (s, 3H), 6.92 (s, 2H) 7.09-7.18 (m, 5H), 2.09 (s, 1H).

6-amino-3-methyl-1H-spiro(cyclohexane)-1,4-pyrano[2,3-c]pyrazole-5-carbonitrile (Table 3.4b 2n):

White solid, m.p 150-152 °C



GC-MS (M^+): 244; IR (KBr): $\bar{\nu}$ 3244, 2179, 1629, 1491, 1406, 1053, 717 cm^{-1} ; ^1H NMR (400 MHz, CDCl_3): δ 1.62-1.85 (m, 4H), 1.9 (s, 3H), 7.12 (s, 2H), 12.09 (s, 1H); ^{13}C NMR (100 MHz, $\text{DMSO}-d_6$): 162.1, 154.8, 134.6, 124.6, 103.8, 60.8, 33.2, 32.8, 31.7, 30.7, 12.0.

References

- [1] C.Y. Ishii, T. Asefa, N. Coombs, M. J. MacLachlan and G.A. Ozin, *Chem. Commun.*, 1999, 2539.
- [2] F. Hoffmann, M. Cornelius, J. Morell and M. Froba, *Angew. Chem. Int. Ed.*, 2006, **45**, 3216.
- [3] W. J. Hunks and G.A. Ozin, *J. Mater. Chem.*, 2005, **15**, 3716.
- [4] J. P. K. Reynhardt, Y. Yang, A. Sayari and H. Alper, *Chem. Mater.*, 2004, **16**, 4095.
- [5] J. Bu, Z. M. A. Judeh and C. B. Ching, *Catal. Lett.*, 2003, **85**, 183.
- [6] J. P. K. Reynhardt, Y. Yang, A. Sayari and H. Alper, *Adv. Synth. Catal.*, 2005, **347**, 137.

- [7] S. Antebi, P. Arya, L. E. Manzer and H. Alper, *J. Org. Chem.*, 2002, **67**, 6623.
- [8] J. P. K. Reynhardt, Y. Yang, A. Sayari and H. Alper, *Adv. Funct. Mater.*, 2005, **15**, 1641.
- [9] E. J. Acosta, C. S. Carr, E. E. Simanek and D. F. Shantz, *Adv. Mater.*, 2004, **16**, 985.
- [10] M. P. Kapoor, Y. Kasama, T. Yokoyama, M. Yanagi and S. Inagaki, *J. Mater. Chem.*, 2006, **16**, 4714.
- [11] S. B Sapkal, K. F. Shelke, B. B. Shingate and M. S. Shingare, *Tetrahedron Lett.*, 2009, **50**, 1754.
- [12] K. Yamamoto, Y. G. Chen and F. G. Buono, *Org. Lett.*, 2005, **7**, 4673.
- [13] S.S. Kim, B. S. Choi, J. H. Lee, K. K. Lee, T. H. Lee, Y. H. Kim and S. Hyunik, *Synlett.*, 2009, 599.
- [14] M. Guidotti, E. Gavrilova, A. Galarneau, B. Coq, R. Psaroa and N. Ravasio, *Green Chem.*, 2011, **13**, 1806.
- [15] A. K. Oxana, I.D. Ivanchikova, M. Guidotti, C. Pirovano, N. Ravasio, M.V. Barmatova and Y.A. Chesalova, *Adv. Synth. Catal.*, 2009, **351**, 1877.
- [16] N. Bion, P. Ferreira, A. Valente, I.S. Goncalvesa and J. Rocha, *J. Mater. Chem.*, 2003, **13**, 1910.
- [17] C.O. Kim, *J. Colloid Interface Sci.*, 2003, **24**, 374.
- [18] H. Wamhoff, E. Kroth and K. Strauch, *Synthesis*, 1993, **11**, 1129.
- [19] G. Tacconi, G. Gatti and D. T. Prakt, *Chem. Commun.*, 1980, **322**, 831.
- [20] C. O. Kappe, *Acc. Chem. Res.*, 2000, **33**, 879.
- [21] S. S. Panda, P. Khanna and L. Khanna, *Curr. Org. Chem.*, 2012 **16**, 507.
- [22] P. Biginelli, *Gazz. Chim. Ital.*, 1893, **23**, 360.
- [23] K. S. Atwal, G. C. Rovnyak, B. C. O'Reilly and J. Schwartz, *J. Org. Chem.*, **54**, 1989, 5898.

- [24] J. Barluenga, M. Tomas, A. Ballesteros and L. A. Lopez, *Tetrahedron Lett.*, 1989, **30**, 4573.
- [25] Y. Ma, C. Qian, L. Wang and M. Yang, *J. Org. Chem.*, 2000, **65**, 3864.
- [26] J. S. Yadav, B. V. Subba Reddy, P. Sridhar, J. S. S. Reddy, K. Nagaiah, N. Lingaiah and P. S. Saiprasad, *Eur. J. Org. Chem.*, 2004, 552.
- [27] Li. Q. Kang, D. Y. Jin and Y. Q. Cai, *Synth. Commun.*, 2013, **43**, 1896.
- [28] G. Aridoss and Y. T. Jeong, *Bull. Korean Chem. Soc.*, 2010, **31**, 863.
- [29] Ch. V. Reddy, M. Mahesh, P. V. K. Raju, T. R. Babu and V. V.N. Reddy, *Tetrahedron Lett.*, 2002, **43**, 2657.
- [30] S. Paraskar, G. K. Dewkar and A. Sudalai, *Tetrahedron Lett.*, 2003, **44**, 3305.
- [31] A. Shaabani and F. Bazgir, *Tetrahedron Lett.*, 2003, **44**, 857.
- [32] J. Peng and Y. Deng, *Tetrahedron Lett.*, 2001, **42**, 5917.
- [33] J. Lu, H. Ma and W. C. Li, *J. Org. Chem.*, 2000, **20**, 815.
- [34] S. L. Jain, S. Singhal and B. Sain, *Green Chem.*, 2007, **9**, 740.
- [35] D. Rodriguez, O. Bemardi and G. Kirsch, *Tetrahedron Lett.*, 2007, **48**, 5777.
- [36] S. R. Narahari, B. R. Reguri, O. Gudaparthi and K. Mukkanti, *Tetrahedron Lett.*, 2012, **53**, 1543.
- [37] P. K. Sahu and D. D. Agarwal, *RSC Adv.*, 2013, **3**, 9854.
- [38] X. Shi, H. Yang, M. Tao and W. Zhang, *RSC Adv.*, 2013, **3**, 3939.
- [39] Y. Wang, J. Yu, H. Yang, Z. M. Miao and R. Chen, *Lett. Org. Chem.*, 2011, **8**, 264.
- [40] S. Gore, S. Baskaran and B. Koenig, *Green Chem.*, 2011, **13**, 1009.
- [41] Y. Ren, C. Cai and R. Yang, *RSC Adv.*, 2013, **3**, 7182.
- [42] H. G. O. Alvim, T. B. Lima, A. L. deOliveira, H. C. B. deOliveira, F. M. Silva, F. C. Gozzo and A. D. N. Brenno, *J. Org. Chem.*, 2014, **79**, 3383.

- [43] H. V. Chavan, S. B. Babar, R.U. Hoval and B.P.Bandgar, *Bull. Korean Chem. Soc.*, 2011, **32**, 3963.
- [44] G. Vasuki and K. Kumaravel, *Tetrahedron Lett.*, 2008, **49**, 5636.
- [45] N. M. H. Elnagdi and N. S. Al-Hokbany, *Molecules*, 2012, **17**, 4300.
- [46] M. Babaie and H. Sheibani, *Arabian J. Chem.*, 2011, **4**, 159.
- [47] H. Mecadon, M. R.Rohman, I. Kharbangar, B. M. Laloo, I. Kharkongor, M. Rajbangshi and B. Myrboh, *Tetrahedron Lett.*, 2011, **52**, 3228.
- [48] H. Mecadon, M. R. Rohman, M. Rajbangshi, B. Myrboh, *Tetrahedron Lett.*, 2011, **52**, 2523.
- [49] G. R. Yun, Z. M. An, L. P. Mo, S. T. Yang, H. X. Liu, S. X. Wang and Z. H. Zhang, *Tetrahedron*, 2013, **69**, 9931.
- [50] M. A. Zolfigol, M. Tavasoli, A. R. Moosavi, P. M. Zare, H. G. Kruger, M. Shirid and V. Khakyzadeha, *RSC Adv.*, 2013, **3**, 25681.
- [51] M. A. E. Aleem and A. A. El-Remaily, *Tetrahedron*, 2014, **70**, 2971.
- [52] Y. F. Cai, H. M. Yang, L. Li, K. Z. Jiang, G. Q. Lai, J. X. Jiang and L. W. Xu, *Eur. J. Org Chem.*, 2010, **26**, 4986.
- [53] B. Boumoud, I. Mennanaa and T. Boumoud, *Lett. Org. Chem.*, 2013, **10**, 8.
- [54] N. A. Brunelli, K. Venkatasubbaiah and C. W. Jones, *Chem. Mater.*, 2012, **24**, 2433.
- [55] J. B. Gujar, M. A. Chaudhari, D. S. Kawade and M. S. Shingare, *Tetrahedron Lett.*, 2014, **55**, 6030.
- [56] S. Inagaki, S. Guan, T. Ohsuna and O. Terasaki, *Nature*, 2002, **416**, 304.

Chapter 4

FUNCTIONALIZED MESOPOROUS SILICA CATALYSTS IN FLAVANONE SYNTHESIS AND ASYMMETRIC MANNICH REACTION

Contents	4.1 Introduction
	4.2 Results and Discussion
	4.3 Conclusion
	4.4 Experimental

Novel polyamine functionalized mesoporous silica catalyst was synthesized via radical polymerization of vinyl monomer such as α -methyl styrene and methyl acrylate within silica framework followed by post-functionalization. The presented strategies have led to the development of well ordered mesoporous material with high amine capacity. XRD, BET, TG-DTG, FT-IR and solid state NMR spectroscopic analysis were used to study the physical and chemical characteristics of the material. The resultant polyamine functionalized mesoporous material was used as solid Lewis base catalyst in flavanone synthesis and asymmetric Mannich reaction.

4.1 Introduction

Inorganic-organic hybrid materials have attracted much interest in catalysis because, these materials combine the properties of high surface area, high dispersion, high amount of active surface and high thermal stability.^{1,2} Mesoporous silica is considered as one of the best inorganic supports, since it is thermally and mechanically stable, and provides large number of silanol functionalities that allow bonding of organic molecules.³⁻⁸ Surface functionalization of silica with polymer is very important in

catalysis. This combines the properties of high surface area, structural and thermal stability, porous nature, high amount of active sites and the reusability without loss of activity. Thus mesoporous silica is an environmentally benign catalyst in heterogeneous catalysis.

The polymerization inside the nano-channels of the mesoporous materials was first reported by Aida et al.⁹ Several studies were reported on the encapsulation of organic polymers within the channels of mesoporous silica materials.¹⁰⁻¹⁴ In 1998, Moller et al. reported poly(methyl methacrylate) (PMMA)/mesoporous silica composites synthesized by adsorption of MMA into the pores followed by polymerization initiated with benzoyl peroxide.¹⁵ Zhang et al. synthesized PMMA-mesocellular foam silica nanocomposite via batch emulsion polymerization.¹⁶ Covalent graft of polyaniline onto the pore walls of SBA-15 was done by Sasidharan et al.¹⁷ A hybrid structure based on vinyl-functionalized MCM-48 and PS was prepared through *in situ* polymerization of styrene monomer.¹⁸ An alternative synthesis route to mesoporous/polymer nanocomposites through controlled radical polymerization of vinyl monomers on SBA-15 was developed by Choi et al.¹⁹

Using the right system and technique, one can control the functionality, density and molecular weight of the polymer chain. Preparation of polymer chain on silica can be accomplished by conventional free radical, controlled free radical, cationic, anionic and ring opening metathesis polymerization techniques.²⁰ Among these techniques, controlled free radical polymerization is a versatile method to engineer the silica particle surface. Controlled free radical polymerization can produce polymers with controlled molecular weight, composition and functionality.

The present chapter discusses the development of amine functionalized polystyrene based silica and chiral amine functionalized poly(methyl acrylate) based silica framework by radical polymerization of α -methyl styrene (AMS) and methyl acrylate in the presence of crosslinking agent, divinyl benzene (DVB) on periodic mesoporous silica (MS I). The selection of MS I type silica material is based on the following reasons. Studies demonstrated that MS I material was accompanied with complementary pores having disordered micropore/small mesopores in the pore walls, providing various degrees of interconnectivity between adjacent large pore channels.²¹⁻²³ Such complementary pores would stabilize the polymer layer onto silica framework. The polymer chains, interpenetrating with the silica framework through the complementary pores, would form a physically inseparable polymer. This increases significantly the stability of the entire polymeric system.²⁴⁻²⁶

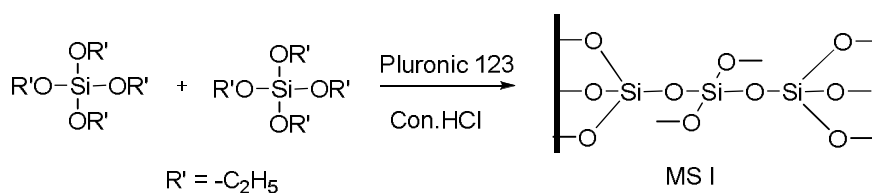
4.1.1 Aim of this study

The efforts to synthesize highly functionalized silica have always received great interest in heterogeneous catalysis. The synthesis strategy using vinyl monomer deposition followed by thermal polymerization have resulted in materials with highly stable C-C bond rather than hydrolysis-susceptible siloxane bonds.²⁵ Due to facile functionalization and attractive textural properties, the present approach would be useful for the development of high performance systems for applications, such as adsorption, separation, sensing, host-guest complexes, and catalysis, in addition to the conventional method to functionalize mesoporous silica using organosilanes.¹⁹ This chapter focuses on the synthesis and characterization of alkylated polyamine and

chiral amine functionalized silica and the use of these materials as good candidates for solid base catalyzed organic transformations. Catalytic performance was studied in flavanone synthesis under solvent free condition and also in asymmetric Mannich reaction.

4.2 Results and Discussion

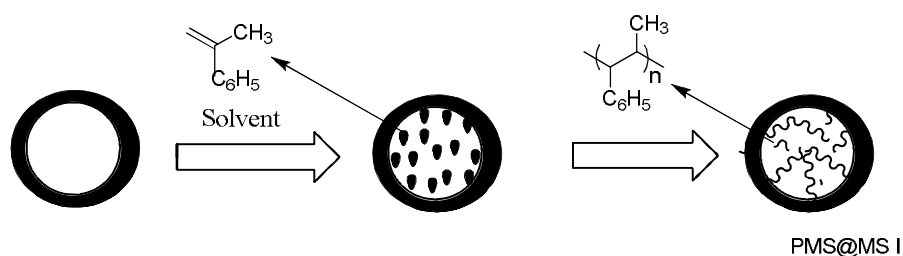
Periodic mesoporous silica with complementary pores (MS I) was successfully synthesized using tetraethyl orthosilicate (TEOS, $\text{Si}(\text{OEt})_4$) and non-ionic triblock copolymer (Pluronic 123), which serves as a structure directing agent under acidic conditions.^{27,28} Here, the triblock copolymer forms micelles in an acidic aqueous ethanol solution. After dispersion of the micelles, TEOS was added as the silica source, and it was polymerized around the micelles to form the inorganic framework. Subsequently, the copolymer was removed from the support material by calcination in air and left behind unidirectional, hexagonally aligned mesoporous silica material (Scheme 4.1). The triblock copolymer directs the silica source to form pore channels according to the shape and size of the micelles, allowing for control of the pore size in the silica product.



Scheme 4.1 Synthetic procedure for mesoporous silica (MS I)

Poly(α -methyl styrene) (PMS), functionalized material was synthesized on MS I silica by copolymerization of α -methyl styrene (80 mol%) and DVB (20 mol%). A schematic representation of polymerization of α -methyl styrene

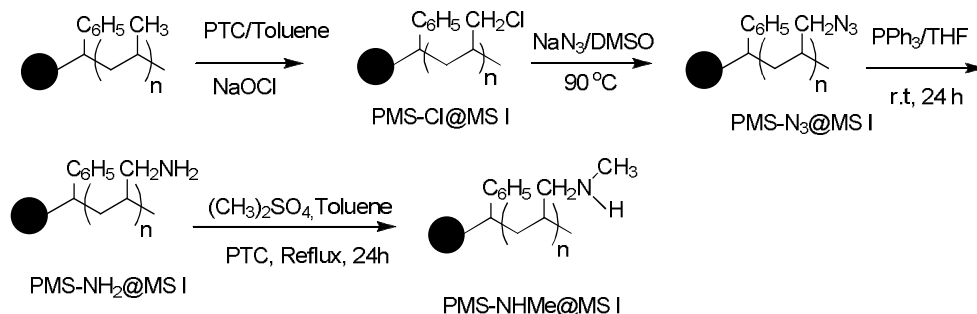
on silica is shown in Scheme 4.2. The monomer loading amounted to 30 wt% of the silica weight. The monomer such as methyl acrylate (80 mol%), DVB (20 mol%) are employed for another set of polymerization. The product obtained was designated as PMA@MS I. The interlocked polymer was cleaved from the silica surface using HF/THF and subjected to GPC analysis. From GPC, the molecular weights of PMS and PMA were found to be 1037 with polydispersity index of 1.27 and 957 with polydispersity index of 1.17 respectively.



Scheme 4.2 Polymerization of α -methyl styrene on silica

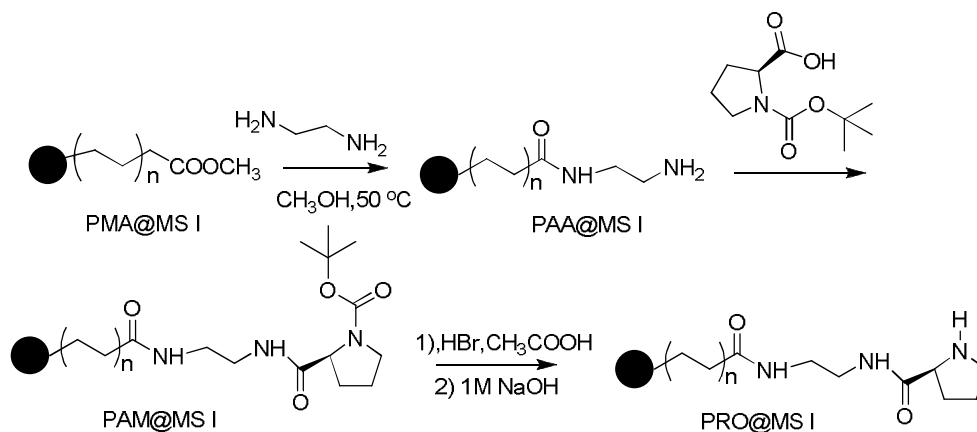
4.2.1 Post-functionalization of the polymer-MS I silica material

Various functional groups can be introduced into silica framework through different organic reactions by post-functionalization methods which are currently available to prepare solid catalysts and ion-exchange materials.^{29,30} The PMS@MS I can be functionalized through chlorination with sodium hypochlorite.³¹ The resultant material undergoes nucleophilic displacement with sodium azide. An excess of NaN_3 present in the reaction medium helps the conversion of chloromethyl group to azidomethyl group. The polymer containing the azidomethyl side chain was converted to a polymer containing aminomethyl side chain by the reduction of the azide group to amino group. Finally, the polyamine was refluxed with dimethyl sulphate under controlled reaction condition (Scheme 4.3).



Scheme 4.3 Synthesis of methylated polyamine functionalized MS I

The poly(methyl acrylate) functionalized silica material undergoes amidation with ethylene diamine under nitrogen atmosphere which resulted in the formation of polyamidoamine silica. Chiral modification of polymerized silica was done using BOC-L-proline followed by deprotection with HBr in acetic acid. Synthetic procedure for the development of chiral amine functionality on silica is shown in Scheme 4.4.



Scheme 4.4 Synthesis of proline functionalized MS I

Estimation of chlorine capacity and amine capacity of functionalized silica confirmed that high amount of chlorine and amine was present

in functionalized material. It was measured by titration method and UV-Visible spectrophotometry.³² The results are given in Table 4.1.

Table 4.1 Amine and chlorine capacity of functionalized silica materials

Sample	Cl content (mmol/g)	NH ₂ content (mmol/g) ^a	NH ₂ content (mmol/g) ^b
PMS-Cl@MS I	14.5	-	-
PMS-NH ₂ @MS I	-	12.2	12.1
PMS-NH-Me@MS I	-	12.3	-
PMA-NH ₂ @MS I	-	11.6	11.1
PRO@MS I	-	10.9	-

^atitration method, ^bUV-Visible spectrophotometry

4.2.2 Physicochemical characterization of MS I and polymer functionalized MS I material

4.2.2.1 TEM analysis

The surface morphology of the synthesized silica was analyzed by TEM. The calcined MS I material exhibited ordered mesoporous nature similar to that in the literature.³³ In Figure 4.1, the hexagonal-packed ordering of the nano channels is clearly demonstrated (the incident electron beam parallel to the direction of the nano channels during TEM analysis).

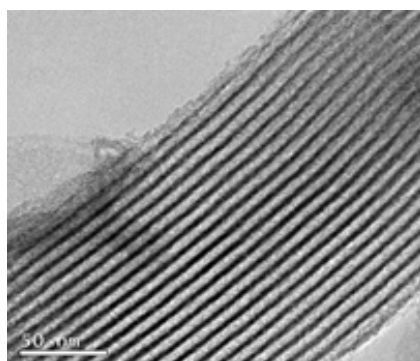


Fig. 4.1 TEM image of calcined MS I

4.2.2.2 X-ray diffraction studies

X-ray diffraction patterns were recorded for the bare silica and the functionalized MS I. The XRD patterns are shown in Figure 4.2. The calcined MS I material showed three well resolved peaks that correspond to the (100), (110) and (200) reflections. It corresponds to a well-defined 2D hexagonal meso structure (p6mm). After polymerization, the intensity was decreased in functionalized MS I material which suggested random deposition of polymers into the mesopores and exhibited crystallinity by maintaining diffraction peak.

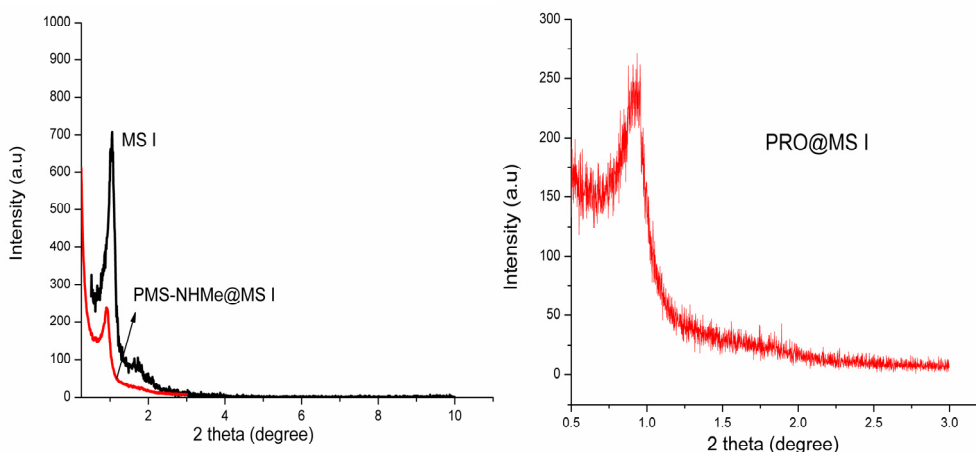


Fig. 4.2 XRD pattern of MS I, PMS-NHMe@MS I and PRO@MS I

4.2.2.3 Surface area analysis

The pore diameter and surface area of the silica material was analyzed in each step by BET analysis. N₂ adsorption isotherms for MS I and functionalized MS I showed type IV adsorption isotherms with H1 hysteresis loop as defined by IUPAC³⁴ (Figure 4.3). The calcined MS I gave BET surface area of 625 m²/g and a pore diameter of 65 Å determined from the BJH

adsorption curve (Figure 4.3 (d)). The sharpness of the adsorption branches is indicative of a narrow mesopore size distribution. The broadening of the hysteresis loop in the N₂ adsorption isotherm clearly indicates random polymerization taking place in the inside of mesopores of silica material. The position of capillary condensation steps was shifted to lower pressure values, after the polymerization step. This suggests that, due to polymer immobilization, a reduction in the mesopore size was observed. Structural properties of the materials are displayed in Table 4.2.

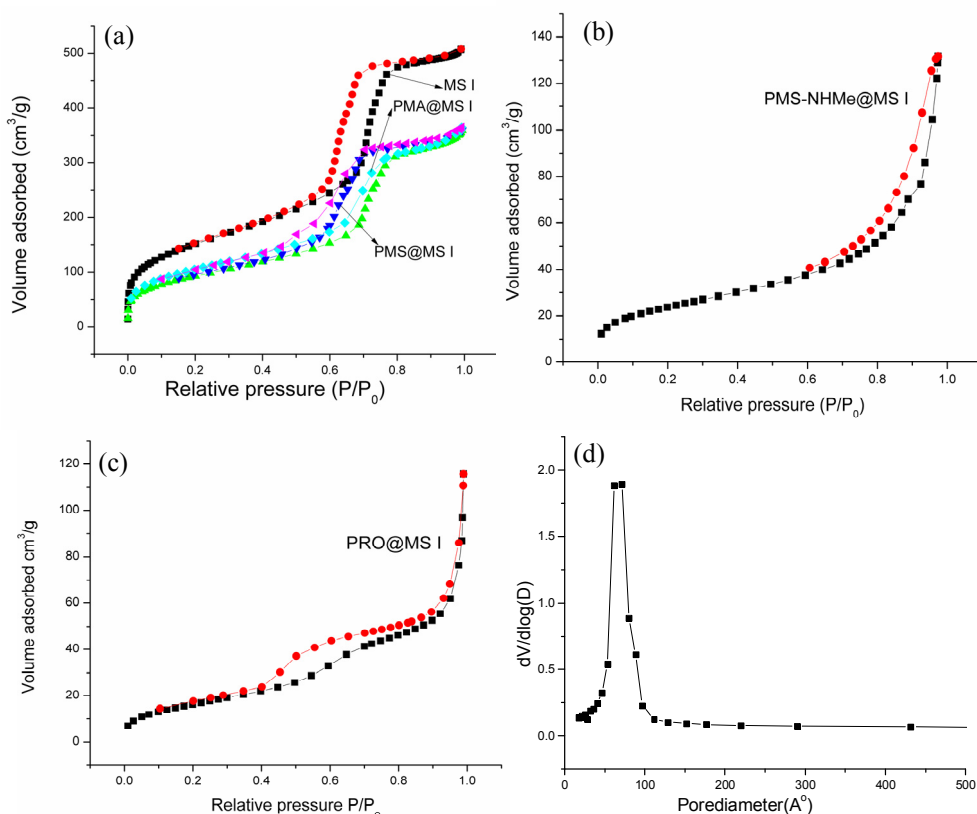


Fig. 4.3 N₂ adsorption/desorption isotherms of a) MS I, PMA@MS I, PMS@MS I, b) PMS-NHMe@MS I, c) PRO@MS I and d) pore size distribution of MS I

Table 4.2 Structural properties of the silica material

Samples	S_{BET} (m^2/g)	Pore diameter (nm)	Pore volume (cm^3/g)
MS I	625	6.7	0.87
PMS@MS I	367	6.0	0.72
PMA@MS I	377	5.9	0.56
PMS-NHMe@MS I	85	4.5	0.20
PRO@MS I	70	4.1	0.17

4.2.2.4 IR spectral studies

Immobilization of functional groups into silica framework was examined by IR spectroscopy in every step (Figure 4.4). The silanol (Si-OH) and Si-O-Si bands from the parent silica materials are observed at 3454 cm^{-1} (broad) and 1088 cm^{-1} , respectively. In polymerized material (PMS@MS I), a band at 2353 cm^{-1} may correspond to the C-H stretching vibration of methyl group. A sharp absorption band at 740 cm^{-1} may be due to the stretching vibration of C-Cl group which resulted from chlorination of polymerized material with hypohalite (PMS-Cl@MS I). A new absorption band at 2100 cm^{-1} corresponds to the azide group, formed by reaction with polychlorinated silica material and sodium azide (PMS-N₃@MS I). After reduction with PPh₃, azide peak was disappeared (PMS-NH₂@MS I).

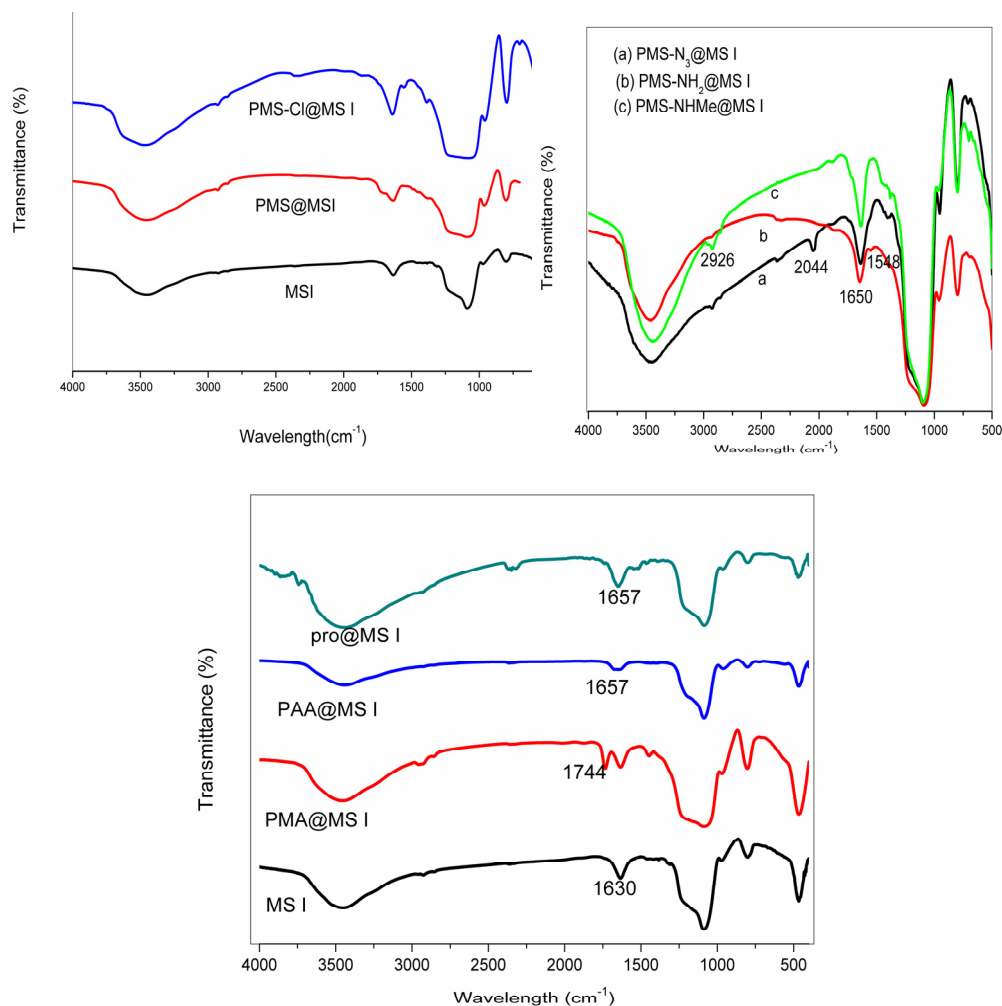


Fig. 4.4 IR spectra of functionalized MS I

A strong absorption band at 1728 cm^{-1} in PMA@MS I due to the CO stretching frequency of ester confirms the effective grafting of poly(methyl acrylate) group. In PRO@MS I, a band in the region of $1650\text{--}1515\text{ cm}^{-1}$ is caused by N-H bending of secondary amide which is a strong evidence for amidation with ethylene diamine. The intensity of this region was increased

after coupling with BOC-L-proline, which confirmed the successful coupling of amine moiety with chiral amino acid.

4.2.2.5 NMR studies

^{13}C CP-MAS NMR spectra of the functionalized materials are shown in Figure 4.5 and Figure 4.7. The peak at 25 ppm is assigned to the characteristic peak of methyl carbon atom. The peaks at 40 ppm and 50.8 ppm in PMS@MS I are assigned to the backbone methylene and methine carbons of polymeric chain respectively. The peak at 128 ppm belongs to the aromatic carbons. The peak at 147 ppm is assigned to the ipso carbon of the aromatic ring.

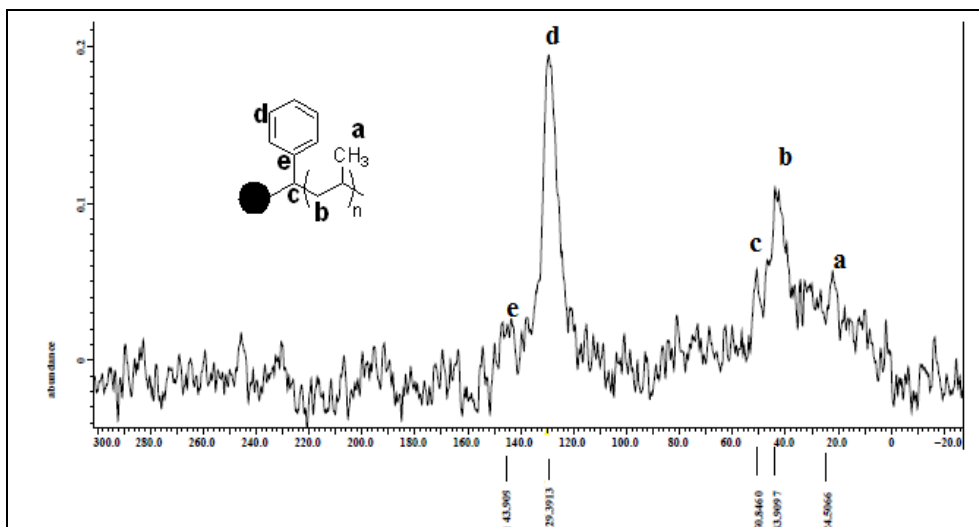


Fig. 4.5 ^{13}C CP-MAS NMR spectrum of PMS@MS I

The ^1H NMR spectrum (Figure 4.6) of N-alkylated polyamine cleaved from the surface of silica clearly showed a broad singlet at 3.5 ppm ascribed

to secondary amine proton. It is a strong evidence for monoalkylation. The signal at 0.76 ppm corresponds to the residual methyl protons in the backbone of poly(α -methyl styrene).

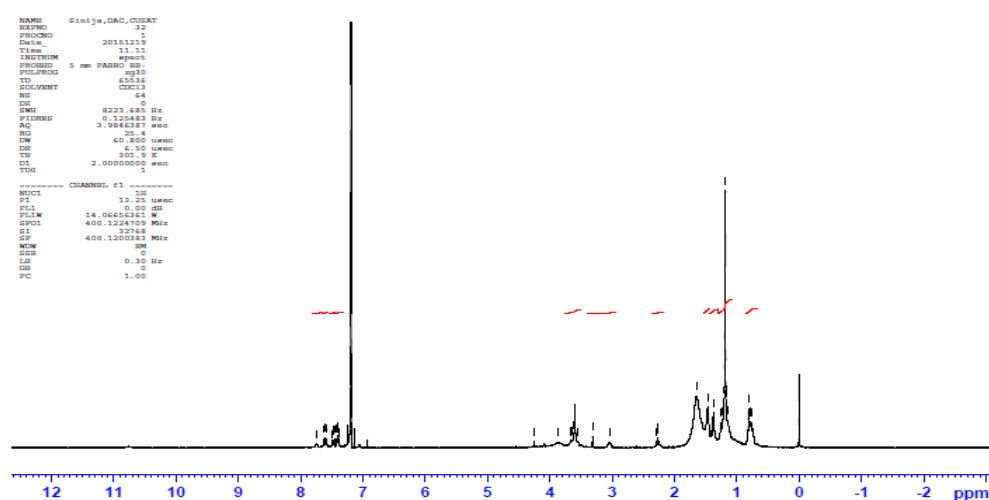


Fig. 4.6 ^1H NMR spectrum of N-alkylated polyamine

The signals between 1.6-1.8 ppm correspond to the CH_2 protons of the polymeric chain. The signals in the region of 3.0-3.3 ppm are attributed to methyl and methylene protons which are attached to the nitrogen atom. The signals at 7.3-7.7 ppm are ascribed to aromatic protons.

The ^{13}C CP-MAS NMR spectrum of L-proline functionalized MS I (Figure 4.7) exhibits a sharp signal at 164 ppm assigned to the characteristic peak of carbonyl group in amide, and the other peaks ranging from 18 ppm to 60 ppm are attributed to the acyclic and cyclic carbon structures in different chemical environment.

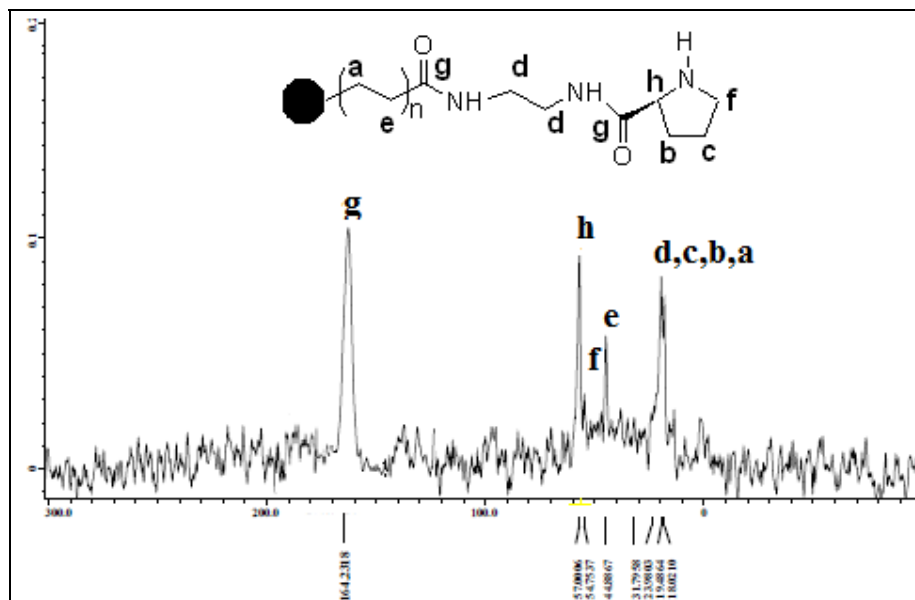


Fig. 4.7 ^{13}C CP-MAS NMR spectrum of PRO@MS I material

4.2.2.6 TG-DTG analysis

TG-DTG analysis was performed to determine the thermal stability and degree of organic functionalization of the functionalized MS I samples. The samples were subjected to temperature scan from 35 °C to 800 °C at a rate of 20 °C /min. The results are illustrated in Figure 4.8 & Figure 4.9. TG plot of PMS@MS I showed 15 % of weight loss between 100-550 °C. PMS-NHMe@MS I material showed weight loss of 24.3 % between 150-300 °C which suggested the decomposition of methylamine fragment.³⁵ Another decomposition above 300 °C was probably due to the decomposition of polymeric chain.

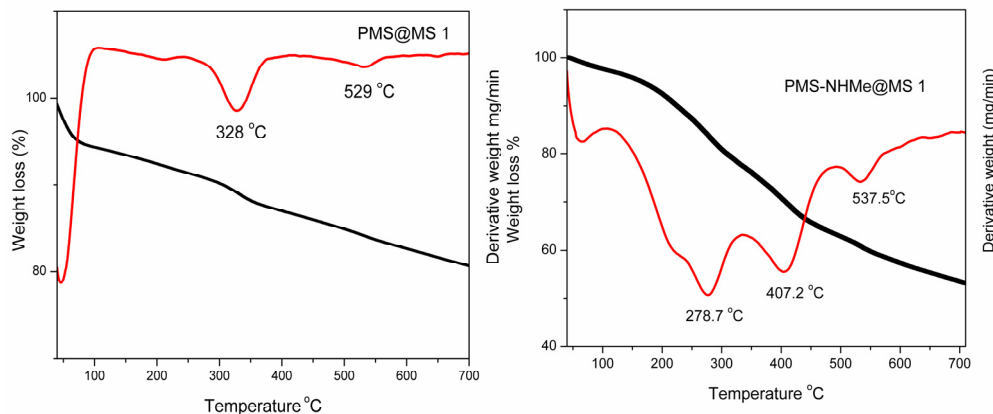


Fig. 4.8 TG-DTG plots of PMS@MS 1 & PMS-NHMe@MS I

PMA-NH₂@MS I showed first step degradation at 60 °C corresponding to the removal of moisture. Another weight loss of 19 % was observed at 231 °C which was attributed to the decomposition of amine fragment and it corresponded to 11.8 mmol NH₂/g silica. PRO@MS I exhibited weight loss of 23 % at 356 °C which was ascribed to the decomposition of chiral amine fragment³⁶ and further weight loss at 559 °C revealed the decomposition of polymeric methyl acrylate chains.

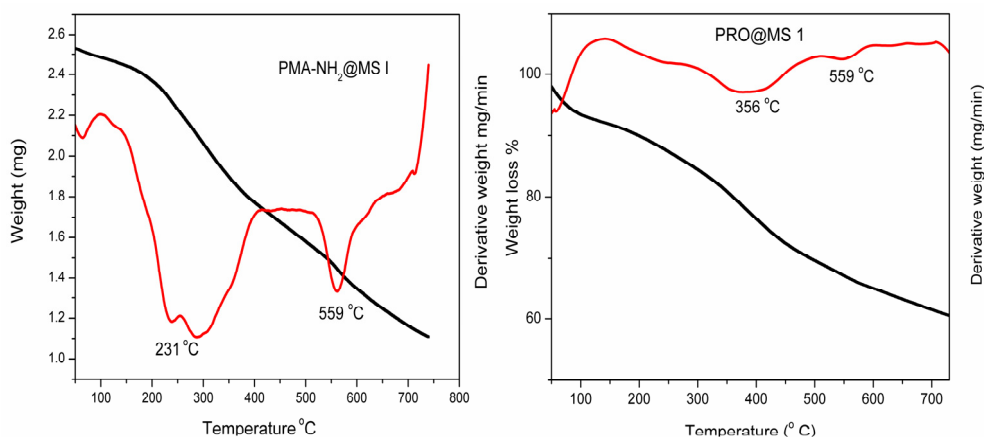


Fig. 4.9 TG-DTG plots of PMA-NH₂@MS I & PRO@MS I

4.2.3 Catalytic performance

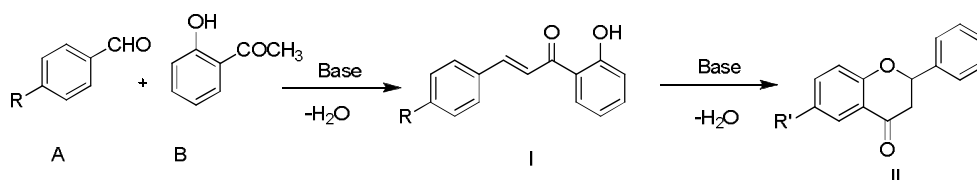
4.2.3.1 Flavanone synthesis

Flavanoids are naturally occurring oxygen containing heterocyclic compounds and they are classified into flavanone, flavones, isoflavones, flavonols and anthocyanin. Flavanone is a key intermediate for the synthesis of flavones or isoflavones and flavonols.³⁷ Flavanones and their derivatives are important classes of flavanoid family. In addition to the general features of flavanoids, flavanones possess a chiral center at C2 position. This usually distinguishes them from other classes of flavanoids. They have attracted increasing attention due to numerous pharmacological applications.^{38,39} They exhibited excellent biological profiles including anticancer, anti inflammatory, antitumor, antibacterial and antioxidant properties.⁴⁰⁻⁴² Moreover, these kinds of compounds are important intermediates in the synthesis of flavanone glycosides and 2-aryl chromans.⁴³ Despite these impressive contributions, more efficient and practical catalytic systems for the synthesis of flavanones are still in high demand.

A common route to flavanone is the Claisen-Schmidt condensation of benzaldehyde and 2-hydroxyacetophenone to form 2-hydroxychalcone and the subsequent isomerization of this intermediate to flavanone. Both reactions are catalyzed by acids or bases in homogeneous media, and also through electrochemical transformation, photochemical cyclization, thermal isomerization, and using ionic liquids.⁴⁴⁻⁴⁹ However, most of the methods required expensive and toxic solvents, high temperature, and low conversion of reactants with byproducts. The main goal of heterogeneous catalytic systems is

to eliminate the use of volatile solvents. Many solvent free methods are reported for Knoevenagel condensation and Michael addition reaction using amine-functionalized silica.^{50,51} Mesoporous silica functionalized with amino groups is active for flavanone synthesis.^{35,52}

Here, alkylated polyamine PMS-NHMe@MS I catalyst was used to test the Claisen–Schmidt condensation of 2-hydroxyacetophenones and benzaldehyde derivatives and subsequent intramolecular Michael addition in the absence of solvent. The reaction studied is shown in Scheme 4.5, in which benzaldehyde (A) is taken as model substrate and heated with 2-hydroxyacetophenone (B) in the presence of dried catalyst (catalyst should be free from moisture) under N₂ atmosphere. The liquid products were separated from the reaction mixture at appropriate reaction intervals and subjected to GC-MS analysis.



Scheme 4.5 Synthesis of flavanone by PMS-NHMe@MS I catalyst

The reaction was optimized using different amounts of the catalyst, different solvents, varying time and temperature. Reaction was carried out by mixing 2-hydroxyacetophenone and benzaldehyde at 80 °C without catalyst and no reaction was observed. When the reaction mixture was charged with the prepared catalyst, conversion of A was slightly increased and it was found that 32.5 mg (3 mol%) of the catalyst was sufficient for the

reaction. Low amount of catalyst provides low base active sites which will retard the conversion rate. A high density of amino groups on the surface may provide large amounts of base to catalyze the Claisen-Schmidt condensation of benzaldehyde and 2-hydroxyacetophenone to form 2-hydroxychalcone I. The optimized reaction temperature was found to be 90 °C. Further increase of temperature did not affect the conversion of reactants.

4.2.3.1.1 Effect of solvent

Solvent effect was studied with various solvents and the results are illustrated in Table 4.3. It is found that solvent has significant role. However, there is no obvious correlation between the solvent polarity and the conversion or the flavanone selectivity. The catalyst has much higher conversion of I and selectivity to flavanone under the solvent-free condition.

Table 4.3 Effect of solvent on Flavanone synthesis

Entry	Solvent	Conversion of B ^{a,b}	Selectivity to I	Selectivity to II
1	DMSO	50	32	68
2	Toluene	40	37	63
3	DMF	30	52	48
4	No solvent	95	31	69

^a Reaction conditions: aldehyde (10 mmol), 2-hydroxyacetophenone (10 mmol), 90 °C, 10 h, No solvent, ^b GC-MS

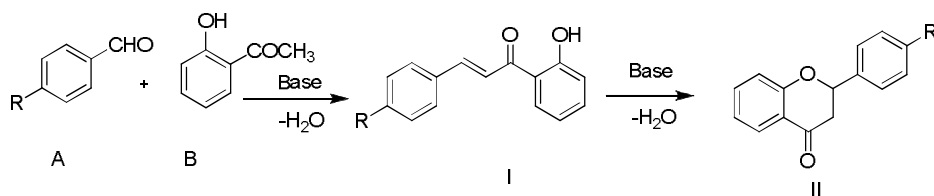
4.2.3.1.2 Effect of reaction temperature and time

The effect of temperature on the reaction was studied between 80-120 °C. When the temperature increases, conversion and selectivity to flavanone

gradually increases, and high conversion was obtained at 90 °C. With increase of temperature, the conversion and selectivity remained almost unchanged and kept around 95 % and 69 %, respectively. The leveling off of percentage conversion is probably due to the blockage of catalytic centers by the high concentration of the products.

The catalytic performance of the material as a function of the reaction time was studied under solvent-free condition at 90 °C. The catalytic activity was found to increase rapidly with the reaction time upto 10 h and then remained unchanged. The selectivity to flavanone also increased gradually with time upto 10 h, and then it was kept around 69 % as the reaction time was prolonged to 16 h.

The PMS-NH₂@MS I catalyst gave conversion of 50 % of 2-hydroxyacetophenone whereas, alkylated polyamine@MS I gave conversion of about 90 % with higher selectivity to flavanone than PMS-NH₂@MS I. The high catalytic activity should be due to the presence of methyl groups on aminated mesoporous materials which enhanced the basic strength of the catalyst. The basicity of primary amines is weaker than that of secondary amines, resulting in an increment of the catalytic activity with secondary amine catalyst. The results of optimized conditions are applied into various substituents. The substituent groups in the aromatic ring have great influence on the conversion and selectivity.

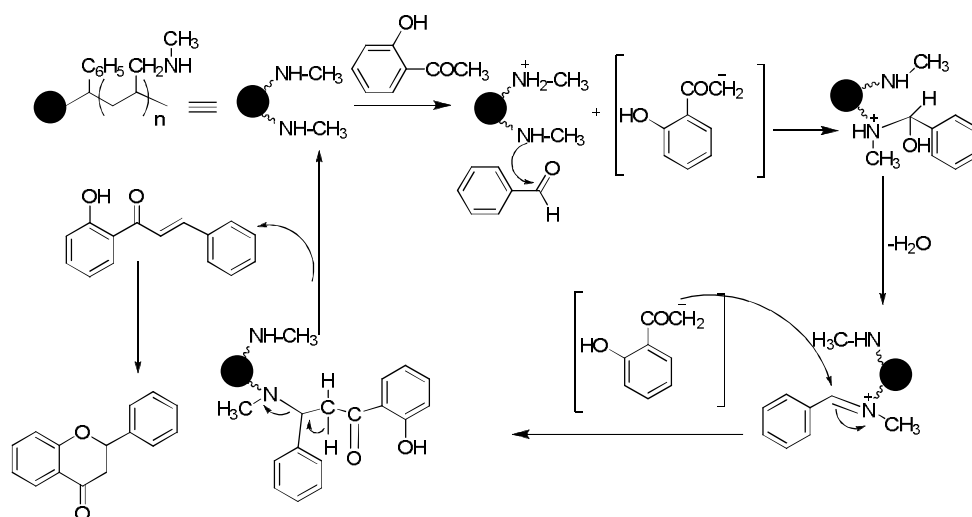
Table 4.5 Flavanone synthesis with diverse aldehydes

Entry	Catalyst	R	Conversion of B ^{a,b}	Selectivity to I	Selectivity to II
1	PMSN ₂ @MS I	H	50	32	68
2	PMSNHMe@MS I	H	95	31	69
3	PMSNHMe@MS I	-OCH ₃	87	39	61
4	PMSNHMe@MS I	-OH	72	40	60
5	PMSNHMe@MS I	-Br	30	28	72
6	PMSNHMe@MS I	-Cl	23	26	74
7	PMSNHMe@MS I	-NO ₂	35	15	85

^a Reaction conditions: aldehyde (10 mmol), 2-hydroxyacetophenone (10 mmol), 90 °C, 10 h, No solvent, ^b GC-MS

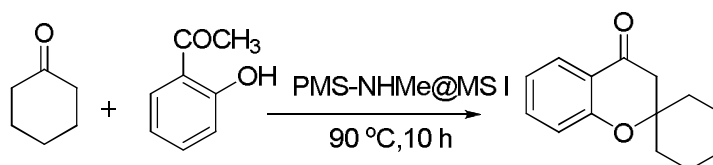
The electron donating group at the para-position of benzaldehyde increases the percentage conversion, but decreases the selectivity to flavanones, while the electron withdrawing groups decrease the conversion but increases the selectivity to flavanones. These trends in conversion are opposite to that of reported Claisen-Schmidt condensation mechanisms.⁵³ Sartori et al. studied adsorption of benzaldehyde on the aminopropyl xerogels.⁵⁴ They showed that the C=N imine species were formed as the main component and on the basis of imine formation, a reaction mechanism for the nitroaldol condensation was proposed. Based on this, a similar reaction pathway is suggested here for the Claisen-Schmidt condensation over amine-functionalized mesoporous silica. The imine species is proposed to be one of the intermediates and the attack of imine by the anion of 2-hydroxyl

acetophenone produces the corresponding adducts. The first step of the imine formation is the attack by the nucleophilic amine on the carbonyl. A rapid proton transfer results in an unstable carbinolamine. The carbinolamine then reacts to form imine by the loss of water (Scheme 4.6).⁵⁵ An electron withdrawing group on benzaldehyde would favor the formation of carbinolamine intermediate, but hinder the dehydration process and the formation of imine. As a result, the conversion of the reactants decreases.



Scheme 4.6 Mechanism of solid base catalyzed flavanone synthesis

Cyclohexanone was also used as partner in the flavanone synthesis. This reaction is important for the synthesis of spiroflavanone, Scheme 4.7.



Scheme 4.7 Synthesis of spiroflavanone

4.2.3.1.3 Recycling study

After completion of the reaction, catalyst was filtered and treated with CH_2Cl_2 (20 mL), subjected to sonication for half an hour, filtered, again washed with CH_2Cl_2 , dried at 80 °C for 3 h and reused. Results are summarized in Table 4.6. It was found that the catalyst could be efficiently recycled and reused for 5 repeating cycles without much loss of efficiency.

Table 4.6 Recycling study

No. of cycles	Conversion of B ^{a,b}
1	95
2	88
3	85
4	81
5	78

^a Reaction conditions: benzaldehyde (10 mmol), 2-hydroxyacetophenone (10 mmol), 90 °C, 10 h, No solvent, ^b GC-MS

Polyamine-functionalized mesoporous silica was found to be an efficient base catalyst for the synthesis of flavanones under solvent free condition. The ordered pore structure and large pore volume of the catalyst would facilitate the diffusion of the reactant and product molecules in the pore channels. The use of solvents markedly decreased both the catalytic activity and selectivity to flavanone.

4.2.3.2 Asymmetric Mannich reaction

Asymmetric organocatalysis is a branch of catalysis that uses small chiral molecules in sub-stoichiometric ratios and allowed to obtain chiral organic products in enantio enriched form.⁵⁶ Major advantages of organocatalysts are: highly stable, easy handling, readily available and

inexpensive raw materials. Representative examples of organocatalysts are given in Figure 4.10. They are alkaloids or amino acids and their derivatives have great economic interest e.g. cinchonidine (1), L-proline (2), and MacMillan-type catalysts (3).⁵⁷ For most organocatalysts, there are no concerns with regard to moisture sensitivity, which can be a serious issue for chiral metal complexes.⁵⁶

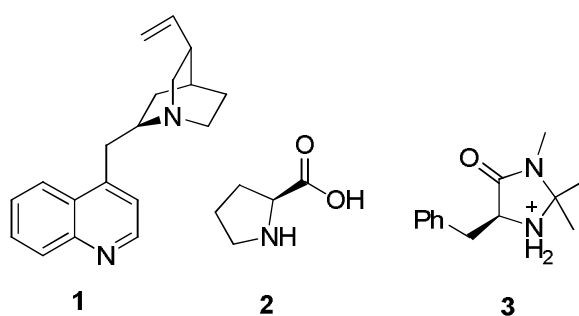


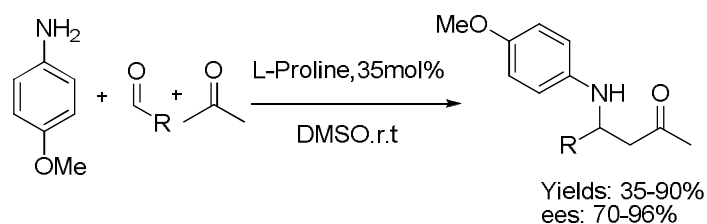
Fig. 4.10 Examples of organocatalysts

Supported chiral organic catalysts have become an emerging area in heterogeneous catalysis.⁵⁸⁻⁶⁹ The supported organocatalysts are easily recoverable and reusable many times with unchanged reactivity and selectivity. The interest in proline arises because, it is active organocatalyst for many useful transformations and they are good “probes” for the preparation of new catalytic materials. The first example of proline covalently attached to silica for the aldol reaction was reported in 2003.⁷⁰ Here, we would like to focus our attention on proline immobilization on functionalized polyamine MS I silica, and to extend its application as organocatalyst in asymmetric Mannich reaction.

The Mannich reaction is a classic example of a three component condensation (A3 coupling). In general, an aldehyde, an amine and an active hydrogen compound such as an enolizable ketone or terminal alkyne,

react affording the corresponding β -aminoketone or β -aminoalkyne. β -aminocarbonyl compounds are important building blocks for the synthesis of biologically active nitrogen containing compounds such as β -amino alcohols, β -amino acids and β -lactams and pharmaceuticals.^{71,72}

The first reported Mannich reaction was the condensation of formaldehyde with ammonia to form the corresponding iminium ion and a subsequent addition of a carbon nucleophile.⁷³ The product was a β -amino carbonyl compound and named as Mannich base (Scheme 4.8). In this three component reaction, the catalyst forms a nucleophilic enamine combining with acetone, which reacts with an electrophilic imine preformed in situ. Chiral nitrogen-containing compounds are widely distributed in nature and contained in many biologically important molecules. The nitrogen-containing units also play important roles in bioactivities. The use of imines as electrophiles is one of the most promising and convenient routes for the synthesis of these chiral nitrogen-containing building blocks.⁷⁴



Scheme 4.8 L-Proline catalyzed Mannich reaction⁷³

In a survey of catalytic activity, chiral amine supported silica catalyst (PRO@MS I) was used in asymmetric Mannich reaction. Initially, the reaction was conducted with cyclohexanone, benzaldehyde, aniline and using L-proline (10 mol%) as catalyst in ethanol at room temperature. Reaction was completed within 24 h. It was found that the desired product

was obtained in 60 % yield with 65 % ee for the syn and dr of 8:2 (syn:anti). No product was formed in the absence of catalyst. Reaction was repeated with PRO@MS I catalyst, in ethanol. The corresponding Mannich product was obtained within 5 h, with 65 % yield and 68 % ee. The aldol addition and condensation products were observed as side products in all the cases.

To establish the generality, the effects of various reaction parameters, such as type of solvent, reaction temperature, catalyst concentration, etc., were evaluated in the model reaction.

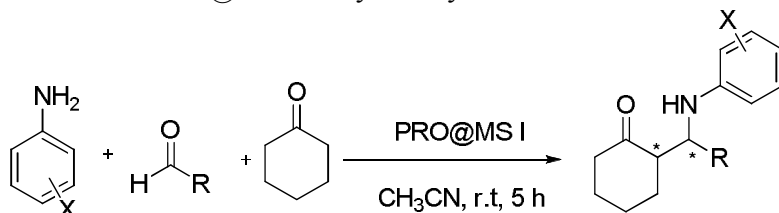
The time for the reaction was set as 5 h, further increase of time did not affect the yield and maximum yield was obtained with 3 mol% of catalyst. Various solvents were used in the model reaction with 3 mol% catalyst. Better stereoselectivity and high yield was obtained in acetonitrile. In methanol, percentage conversion was low and reaction took more time for completion. In the case of water, many side products were obtained. So acetonitrile was selected as the solvent for further studies. The results are given in Table 4.7. To check the reliability, the reaction was carried out with various substrates and the results are shown in Table 4.8.

Table 4.7 Effect of various solvents

Entry	Solvent	Yield ^{a,b}	dr	ee (%) ^c
1	Ethanol	65	8:2	68
2	Methanol	65	8:2	65
3	Water	60	6:4	60
4	Acetonitrile	68	8:2	68
5	DMSO	55	8:2	65

^a Reaction conditions: benzaldehyde (3 mmol), aniline (3.1 mmol), cyclohexanone (5 mmol), r.t, 5 h, Catalyst (PRO@MS I-3 mol%),

^b isolated yield, ^c determined by HPLC with chiral OJ-Hcolumns

Table 4.8 PRO@MSI catalyzed asymmetric Mannich reaction

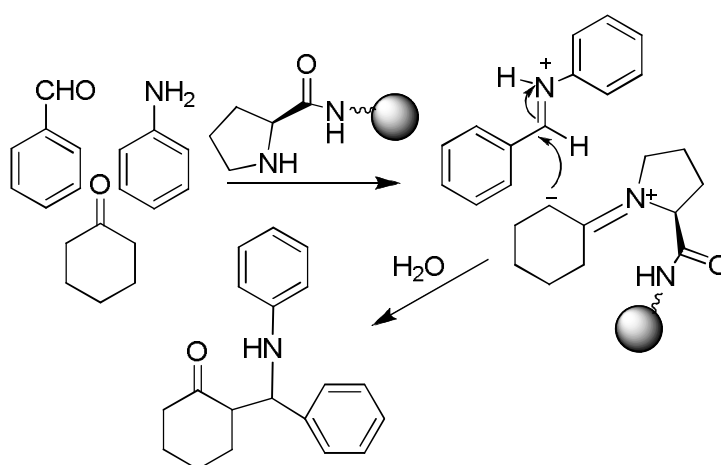
Entry	R	X	Ketone	Yield (%) ^{a,b}	dr ^c	ee (%) ^d
1	C ₆ H ₅ -	H	Cyclohexanone	68	8:2	68
2	4-OCH ₃ -C ₆ H ₄	H	Cyclohexanone	72	6:4	65
3	4-Cl-C ₆ H ₄ -	H	Cyclohexanone	63	7.2:2.8	73
4	4-CH ₃ -C ₆ H ₄ -	H	Cyclohexanone	68	9:1	56
5	2-OH-C ₆ H ₄ -	H	Cyclohexanone	70	7:3	15
6	4-OH-C ₆ H ₄ -	H	Cyclohexanone	72	9:1	66
7	4-Br-C ₆ H ₄ -	H	Cyclohexanone	65	7:3	74
8	3-Br-C ₆ H ₄ -	H	Cyclohexanone	61	9:1	61
9	C ₆ H ₅ -	4-OCH ₃ -	Cyclohexanone	70	9:1	90
10	C ₆ H ₅ -	2-CH ₃ -	Cyclohexanone	71	5:5	81
11	4-NO ₂ -C ₆ H ₅ -	H	Cyclohexanone	68	6:4	80
12	4-NO ₂ -C ₆ H ₄ -	4-CH ₃ -	Cyclohexanone	72	9:1	89
13	C ₆ H ₅ CHO	2-OCH ₃ -4-NO ₂ -	Cyclohexanone	69	9:1	91
14	4-NO ₂ -C ₆ H ₄ -	4-OCH ₃ -	Cyclohexanone	65	9:1	90
15	2-Thiophenyl	H	Cyclohexanone	58	8:2	rm
16	4-NO ₂ -C ₆ H ₄ -	3-Br-	Cyclohexanone	50	7:3	39
17	C ₆ H ₅ -	3-Cl-	Cyclohexanone	45	7.5:2.5	18

^a Reaction conditions: benzaldehyde (3 mmol), aniline (3.1 mmol), cyclohexanone (5 mmol), r.t, 5 h, Catalyst (PRO@MS I-3 mol%), ^b isolated yield, ^{c, d} determined by HPLC with chiral OJ-Hcolumns

Aldehydes bearing electron withdrawing substituents and amines having electron donating substituents gave high yield and better stereoselectivity. In almost all cases, the aldol reaction products were observed as side products. Also, reaction showed different degrees of enantioselectivity for syn-isomers, but low or no enantioselectivity for anti-isomers, indicating that PRO@MS I catalyst has a specific selectivity for the Mannich reaction.

4.2.3.2.1 Reaction mechanism

In general, the reaction proceeded in a *syn* selective fashion, as observed from NMR spectral data. A possible mechanism of the reaction can be predicted to explain the stereoselective nature of the reaction. (Scheme 4.9).



Scheme 4.9 Possible mechanism of three component Mannich reaction catalyzed by PRO@MS I catalyst

Chiral amine on the silica reacted with Mannich donor ketone to form chiral enamine which then reacted with Mannich acceptor (imine) formed from aldehyde and primary amine in situ. The imine formed is supposed to be an *E*-aldimine, which is important for the explanation of the preferred diastereo- and enantioselectivities of this Mannich reaction.^{75,76} The imine is attacked by the enamine to form new stereocenters in iminium product, followed by hydrolysis to give Mannich product stereoselectively and release the catalyst for the next cycle of reaction.

4.2.3.2.2 Recycling study

After completion of the reaction, catalyst was filtered and washed with methanol and dried at 60 °C for 2 h and reused. Results are summarized in Table 4.9.

Table 4.9 Recycling studies of the PRO@MSI catalyst

No. of cycles	% yield ^{a,b}
1	68
2	65
3	60

^a Reaction conditions: benzaldehyde (3 mmol), aniline(3.1 mmol), cyclohexanone (5 mmol), r.t, 5 h, ^b isolated yield

4.3 Conclusion

Monoalkylated polyamine and chiral amine functionalized mesoporous silica with high degree of functionality were synthesized and characterized by various physicochemical techniques. The prepared catalysts were found to be very efficient in flavanone synthesis and asymmetric Mannich reaction respectively. The high density of amino groups on the surface of catalyst provided large amount of basic sites to catalyze the reaction. In flavanone synthesis, better selectivity and higher conversion was obtained under solvent free condition. Enantiomeric excess of the isolated product was found to be 60-90 % in asymmetric Mannich reaction. It was found that the catalysts can be efficiently recycled and reused for further reaction without much loss of efficiency. Also, it is a benign protocol avoiding hazardous metal-based catalysts and solvents.

4.4 Experimental

4.4.1 Materials

Styrene (Acros, 99 %), DVB (Aldrich, 99 %), ethylene diamine and all solvents were distilled by standard procedures prior to use. Tetraethoxysilane (TEOS, Aldrich, > 99 %), Pluronic P123 (poly(ethylene oxide)-*b*-poly(propylene oxide)-*b*-poly(ethylene oxide) triblock copolymer, $\bar{M}_n \approx 5800$, Aldrich) were used as received. All other reagents were purchased from local chemical suppliers and were used as received.

4.4.2 Synthesis of mesoporous silica (MS I)

Mesoporous silica (MS I) was synthesized according to the method reported by Zhao et al.² Pluronic P123 (3.46 g) was dissolved in distilled water (63 mL) and conc. HCl (2 g, 35 %). To this, TEOS (5.58 g) was added at once under stirring at 35 °C. Stirring was continued for 24 h and subsequently heated for 24 h at 100 °C under static conditions. The solid product was filtered and dried at 100 °C. To remove the template, the solid was stirred in ethanol/HCl mixture, filtered, dried, and finally calcined in air flow at 550 °C.

Yield 85 %; White powder; IR (KBr): $\bar{\nu}$ 3454, 1630, 1220, 1088, 745 cm^{-1} .

4.4.3 Polymerization inside the mesoporous silica

In a typical synthesis (30 wt% loading), MS I (2 g) was impregnated with 0.207 mL of α -methyl styrene (80 mol %) and dissolved with 0.055 mL of DVB (20 mol%) and 0.064 g (3 % relative to total vinyl group) of azoisobutyronitrile (AIBN) in 20 mL of dichloromethane. After impregnating, the silica sample was dried at 40 °C for 2 h to remove dichloromethane and

was heated for polymerization. The temperature scheme for the polymerization was 60 °C, 4 h or 100 °C, 1 h and finally at 120 °C for 1 h. The resultant sample was extensively washed with chloroform and ethanol, followed by drying at 80 °C for 5 h. The product obtained was designated as PMS@MS I.

Yield 2.20 g; Light yellow powder; IR (KBr): $\bar{\nu}$ 3456, 2910, 1630, 1220, 108, 735 cm^{-1} ; \bar{M}_n (GPC): 1037, Polydispersity: 1.26; Solid State ^{13}C NMR (100 MHz): 24.5, 43.9, 50.8, 129.3, 143.7 ppm.

Other composition of monomers such as methyl acrylate (80 mol%), DVB (20 mol%) were tried and same synthetic condition was applied without any modification, designated as PMA@MS I.

Yield 2.22 g; White powder; IR (KBr): $\bar{\nu}$ 3456, 2935, 1728, 1645, 1223, 1085, 725 cm^{-1} ; \bar{M}_n (GPC): 957, Polydispersity: 1.17.

4.4.4 Conversion of methyl group into chloromethyl group

PMS@MS I (1.5 g) was dispersed in a mixture of toluene (20 mL) and sodium hypochlorite (8 mL, 15 wt% aqueous solution). To this, 18-crown-6 (0.03 g) was added as the phase transfer catalyst. The solution was heated under stirring at 80 °C for 15 h, The resulting product was filtered and washed thoroughly with distilled water until the filtrate gave no white precipitate with AgNO_3 . The resultant sample was dried at 50 °C. The product obtained was designated as PMS-Cl@MS I. The chlorine capacity of the material was determined by Volhard's method.

Yield 1.80 g; IR (KBr): $\bar{\nu}$ 3456, 2920, 1645, 1120, 740 cm^{-1} ; Chlorine Capacity: 14.5 mmol/g.

4.4.5 Estimation of chlorine capacity (Volhard's method)

Silica sample (PMS-Cl@MS I, 100 mg) was refluxed in pyridine (5 mL) for 1 h, CH₃COOH (5 mL) and H₂O (5 mL) were added to the reaction mixture. The Cl⁻ ions were displaced by the addition of conc. HNO₃ (5 mL) and precipitated with excess AgNO₃ solution. The AgCl formed was coated with toluene (5 mL). The excess of AgNO₃ was back titrated with standardized ammonium thiocyanate solution using ferric alum as indicator (1 mL, 40 % freshly prepared solution of ferric alum). A red color due to the formation of Fe(SCN)₃ indicated the end point. The amount of chloro group per gram of the silica was calculated from the titre value.

4.4.6 Preparation of silylazide and polyamine functionalized mesoporous silica

A mixture of tetrabutylammonium bromide (1.55 mmol), DMSO (25 mL) and PMS-Cl@MS I (1 g, 14.5 mmol of Cl content) was taken in a 250 mL round bottom flask. Sodium azide (10 g, 0.15 mol) was gradually added to the reaction mixture with stirring. The temperature was allowed to rise to 90 °C and stirring was continued at this temperature for about 20 h. The reaction mixture was allowed to cool. The silica residue was washed with hot water (60 °C, 50 mL x 3) to remove NaN₃ and NaCl. Finally, the product was washed with methanol and dichloromethane and dried at 60 °C for 5 h. (PMS-N₃@MS I).

Yield 1.45 g; yellow powder; IR (KBr): $\bar{\nu}$ 3456, 2920, 1645, 1120, 2100, 728 cm⁻¹; CHN analysis: C (28.6 %), N (22.5 %), H (7.1 %).

The product obtained above (1 g) was treated with THF (10 mL), PPh₃ (3.85 g, 14.7 mmol) and water (1 mL), the reaction mixture was stirred at room temperature for 24 h. The resulting material was filtered and washed thoroughly with hexane in order to remove unreacted PPh₃ (removed as triphenylphosphine oxide) and finally washed with dichloromethane/methanol (v/v, 20 mL, 1:1) mixture and dried under vacuum for 5 h. The product obtained was designated as PMS-NH₂@MS I. Amine capacity of the obtained silica was determined by titration method.

Yield 1.05 g; Light brown powder; IR (KBr): $\bar{\nu}$ 3456, 2920, 1645, 1556, 1120, 728 cm⁻¹; CHN analysis: C (28.2 %), N (18.2 %), H (8.1 %); Amine Capacity: 12.1 mmols/g.

4.4.7 Alkylation of polyamine with dimethyl sulphate (PMS-NHMe@MS I)

The PMS-NH₂@MS I (1 g) was dispersed in dry toluene (25 mL). To this, 18-crown-6 (0.06 g) and dimethyl sulphate (8 mL) were added and vigorously stirred with refluxing for 24 h. After cooling to room temperature, silica particles were washed with distilled water followed by methanol and dried under vacuum for 5 h at 60 °C.

Yield 1.40 g; brown powder; IR (KBr): $\bar{\nu}$ 3456, 2980, 1645, 1120, 728 cm⁻¹; Amine Capacity: 12.3 mmol/g; After cleavage with HF: ¹H NMR (400 MHz, CDCl₃): δ 0.76 (CH₃ proton), 1.6-1.8 (m, CH₂ proton), 2.2 (t, CH proton), 3.04 (s, CH₃-N proton), 3.31(d, CH₂-N proton), 3.55-3.66 (NH proton, m), 7.3-7.7 (aromatic proton).

4.4.8 Synthesis of polyamidoamine silica (PAA@MS I)

Poly(methyl acrylate) functionalized silica (PMA@MS I, 2 g) was suspended in ethylene diamine solution (30 mL) in methanol (30 mL) in a closed vessel under nitrogen atmosphere and stirred at ambient conditions for 3 days. After filtration and subsequent washing with ethanol and dichloromethane, the resulting material was vacuum dried and kept in desiccator. The mesoporous silica obtained was designated as PAA@MS I.

Yield 2.2 g; yellow powder; IR (KBr): $\bar{\nu}$ 3456, 2920, 1650, 1515, 1120, 728 cm^{-1} .

CHN analysis: C (22.6 %), N (16.8 %), H (7.2 %).

4.4.9 Synthesis of proline functionalized MS I

Active ester of amino acid was prepared by adding 5 meq of HOBt (3.28 g) and 5 meq of DCC (5.21 g) to a solution of BOC-L Proline (5.23 g) in NMP. This was stirred for 10 min. DCU formed during the reaction was filtered off before the addition of HOBt ester of amino acid to the amino silica (1 g). The mixture was stirred for 24 h. DMSO was added to the mixture and shaken for 15 min. At the end of 15 min. DIEA was added. The unreacted reagents and byproducts were filtered off. The product was washed with $\text{CH}_2\text{Cl}_2:\text{CH}_3\text{OH}$ (66:33 v/v), CH_2Cl_2 , NMP and dried under vacuum at 50 °C for 5 h.

4.4.10 Deprotection of BOC group

The BOC-protected proline functionalized silica was deprotected using 33 wt% solution of HBr in acetic acid. The silica material (1 g) was

stirred for 1 h in 10 mL of HBr solution. The material was filtered and rinsed several times with toluene and acetone. The sample was neutralized by stirring in 1 M NaOH solution (30 mL) overnight and filtered and rinsed with water and methanol.

Yield 0.95 g; yellow powder; IR (KBr): $\bar{\nu}$ 3456, 2920, 1650, 1515, 1120, 728 cm^{-1} .

Solid state ^{13}C NMR (100 MHz,): 18.1, 19.4, 23.9, 31.7, 44.2, 54.8, 57, 164.2 ppm; Amine Capacity: 10.4 mmol g^{-1} .

4.4.11 Estimation of -NH₂ group capacity

The amine content of proline functionalized silica was estimated via aqueous HCl consumption using the acid–base titration method. Typically, 100 mg of functionalized MS was suspended in 30 mL of 0.1 M HCl solution and stirred at ambient temperature for 24h. The filtrate was titrated with NaOH solution (0.1 M). The -NH₂ group capacity was further verified using UV-Visible spectrophotometry.

4.4.12 General procedure for the synthesis of flavanone

A 25 mL two-necked round bottom flask was charged with benzaldehyde (10 mmol), and 2-hydroxyacetophenone (10 mmol). The catalyst (25 mg) was added to it and the mixture was heated at 90 °C for 10 h under N₂ atmosphere. After the reaction, the catalyst was separated by filtration and the products were analyzed by GC-MS. Product was isolated from a short column using silica gel with petroleum ether: CHCl₃ (3:1 v/v) as eluents. The products were characterized by FT-IR and ^1H NMR.

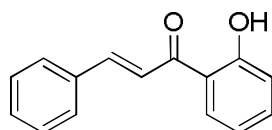
4.4.13`General procedure for Mannich reaction

A mixture of an aromatic aldehyde (3 mmol), aniline (3.1 mmol) and cyclohexanone (5 mmol) in acetonitrile (5 mL) and PRO@MS I (20 mg) was stirred at room temperature and the reaction was monitored by thin-layer chromatography (TLC). After completion, the mixture was filtered, and extracted with ethyl acetate. Pure product was obtained from column chromatography using silica gel with hexane:ethyl acetate as eluent (25:1). The products were characterized by ^1H NMR and ^{13}C NMR. The enantiomeric excess was determined by HPLC (Daicel Chiralpak AD-H, hexane/isopropanol = 90:10, flow rate 1.0 mL/min, $\lambda = 254$ nm). The *syn/anti* and ee ratio was determined from the relative areas of the peaks obtained in HPLC diagram. The peaks with major and minor area are considered to be *syn* and *anti* diastereomer respectively.

Spectral characterization data of representative products

1-(2-hydroxy phenyl)-3-phenyl prop-2-en-1-one (Table 4.5, Entry 1):

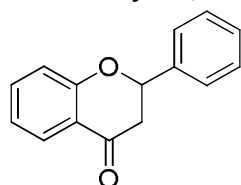
Light yellow crystal



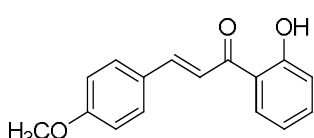
GC-MS (M^+): 224; IR (KBr): $\bar{\nu}$ 3312, 2318, 1645, 1593, 1451 cm^{-1} ; ^1H NMR (400 MHz, CDCl_3): δ 9.31 (s, 1H), 7.31-7.69 (m, 10H), 7.79 (d, $J = 13.2$ Hz, 1H), 7.01 (d, $J = 13.2$ Hz, 1H).

2-phenylchroman-4-one (Table 4.5, Entry 1):

Yellow crystal, m. p 79-81 $^\circ\text{C}$;



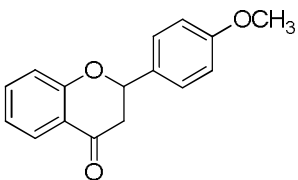
GC-MS (M^+): 224; IR (KBr): $\bar{\nu}$ 3132, 2818, 1665, 1323, 1151 cm^{-1} ; ^1H NMR (400 MHz, CDCl_3): δ 7.31-7.25 (m, 5H), 7.09- 7.12 (m, 5H), 4.67 (t, 1H), 3.09-3.12 (m, 2H).

1-(2-hydroxyphenyl)-3-(4-methoxyphenyl) prop-2-en-1-one (Table 4.5, Entry 3):

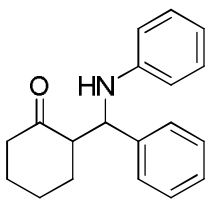
Light yellow crystal, GC-MS (M^+): 254; IR (KBr): $\bar{\nu}$ 3322, 2410, 1655, 1593, 1332, 1451 cm^{-1} ; ^1H NMR (400 MHz, CDCl_3): δ 9.48 (s, 1H) 7.35-7.46 (m, 5H), 7.59-7.65 (m, 10H), 7.89 (d, $J = 13.2$ Hz, 1H), 7.31(d, $J = 13.2$ Hz, 1H), 3.6 (s, 3H).

2-(4-methoxyphenyl) chroman-4-one (Table 4.5, Entry 3):

Yellow crystal; m. p 96-98 $^\circ\text{C}$

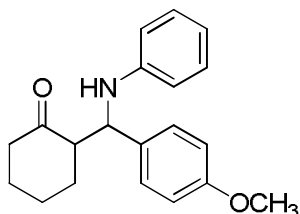


GC-MS (M^+): 254; IR KBr): $\bar{\nu}$ 3032, 2818, 1675, 1316, 1154 cm^{-1} ; ^1H NMR (400 MHz, CDCl_3): δ 7.30-7.22 (m, 5H), 6.89-7.12 (m, 5H), 4.65 (t, 1H), 3.09-3.11 (m, 2H), 3.5 (s, 3H).

Characterization of Mannich products**2-[phenyl(phenylamino)methyl] cyclohexanone (Table 4.8, Entry 1):**

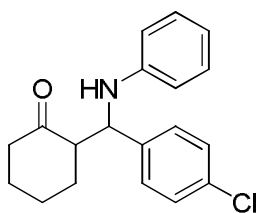
LCMS ($M+1$) m/z 279; ^1H NMR (400 MHz, CDCl_3): δ 7.35-7.19 (m, 5H), 7.09-7.04 (m, 2H), 6.66-6.53 (m, 3H), 4.80-4.56 (m, 2H), 2.78-2.76 (m, 1H), 2.43-2.23 (m, 2H), 2.03-1.88 (m, 3H), 1.67-1.57 (m, 3H); ^{13}C NMR (100 MHz, CDCl_3): 211.3, 147.4, 141.5, 129.0, 128.3, 127.5, 117.6, 114.0, 57.2, 56.6, 42.4, 28.6, 27.0, 24.8; HPLC (*syn*-diastereomer): $t_R = 8.265$ min (minor), 10.080 min (major).

2-[4-methoxyphenyl(phenylamino)methyl] cyclohexanone (Table 4.8, Entry 2):



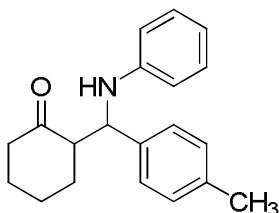
LCMS (M+1) m/z 309; ^1H NMR (400 MHz, CDCl_3): δ 7.22-7.20 (m, 2H), 7.12-7.04 (m, 4H), 6.68-6.60 (m, 1H), 6.53-6.50 (m, 2H), 4.74-4.51 (m, 2H), 2.76-2.75 (m, 1H), 2.42-2.39 (m, 2H), 3.26 (s, 3H), 2.04-1.89 (m, 3H), 1.66-1.58 (m, 3H); ^{13}C NMR (100 MHz, CDCl_3): 210.5, 145.5, 137.4, 135.5, 127.0, 127.0, 125.4, 114.5, 110.0, 54.9, 55.6, 40.4, 26.7, 25.0, 22.8, 19.8; HPLC (*syn*-diastereomer): tR = 12.603 min (minor), 9.640 min (major).

2-[4-chlorophenyl(phenylamino)methyl] cyclohexanone (Table 4.8, Entry 3):

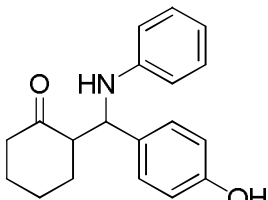


LCMS (M+1) m/z 311; ^1H NMR (400 MHz, CDCl_3): δ 7.31-7.23 (m, 4H), 7.10-7.05 (m, 2H), 6.68-6.63 (m, 1H), 6.52-6.50 (m, 2H), 4.72-4.55 (m, 2H), 2.77-2.39 (m, 3H), 2.33-1.89 (m, 3H), 1.61-1.55 (m, 3H); ^{13}C NMR (100 MHz, CDCl_3): 211.2, 147.1, 140.0, 132.6, 129.0, 129.0, 128.5, 117.9, 114.0, 56.9, 56.3, 42.4, 28.9, 27.0, 24.8; HPLC (*syn*-diastereomer): tR = 13.139 min (minor), 16.600 min (major).

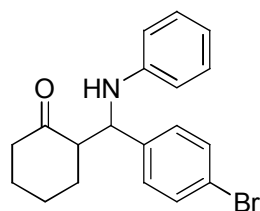
2-[4-methylphenyl(phenylamino)methyl] cyclohexanone (Table 4.8, Entry 4):



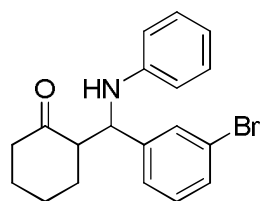
LCMS (M+1) m/z 291; ^1H NMR (400 MHz, CDCl_3): δ 7.24-7.21 (m, 2H), 7.15-7.04 (m, 4H), 6.69-6.61 (m, 1H), 6.56-6.53 (m, 2H), 4.76-4.51 (m, 2H), 2.78-2.75 (m, 1H), 2.42-2.39 (m, 2H), 2.29 (s, 3H), 2.04-1.89 (m, 3H), 1.68-1.58 (m, 3H); ^{13}C NMR (100 MHz, CDCl_3): 211.5, 147.5, 138.4, 136.5, 129.0, 129.0, 127.4, 117.5, 114.0, 56.9, 56.6, 42.4, 28.7, 27.0, 24.8, 21.0; HPLC (*syn*-diastereomer): tR = 15.603 min (minor), 10.640 min (major).

2-[4-hydroxyphenyl(phenylamino)methyl] cyclohexanone (Table 4.8, Entry 6):

LCMS (M+1) m/z 295; ^1H NMR (400 MHz, CDCl_3): δ 7.44-7.42 (m, 2H), 7.17-7.4 (m, 2H), 6.11-7.05 (m, 2H), 6.70-6.65 (m, 1H), 6.51-6.48 (m, 2H), 4.86-4.59 (m, 2H), 2.86-2.83 (m, 1H), 2.46-2.27 (m, 2H), 2.06-1.93 (m, 3H), 1.72-1.57 (m, 3H); ^{13}C NMR (100 MHz, CDCl_3): 210.6, 149.6, 147.0, 146.6, 129.1, 128.6, 123.6, 118.3, 114.0, 57.1, 56.2, 42.4, 29.0, 27.0, 24.9; HPLC (*syn*-diastereomer): tR = 15.550 min (minor), 18.850 min (major).

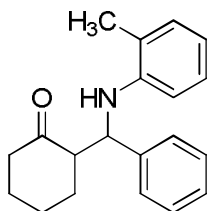
2-[4-bromophenyl(phenylamino)methyl] cyclohexanone (Table 4.8, Entry 7):

LCMS (M+1) m/z 356; ^1H NMR (400 MHz, CDCl_3): δ 7.41-7.39 (m, 2H), 7.25-7.22 (m, 2H), 7.10-7.05 (m, 2H), 6.68-6.63 (m, 1H), 6.52-6.49 (m, 2H), 4.71-4.55 (m, 2H), 2.76-2.39 (m, 2H), 2.32-2.24 (m, 1H), 2.02-1.89 (m, 3H), 1.60-1.54 (m, 3H); ^{13}C NMR (100 MHz, CDCl_3): 211.1, 147.1, 140.5, 131.4, 129.4, 129.0, 120.8, 117.9, 114.0, 56.9, 56.3, 42.4, 28.8, 27.0, 24.8; HPLC (*syn*-diastereomer): tR = 15.856 min (minor), 19.884 min (major).

2-[3-bromophenyl(phenylamino)methyl] cyclohexanone (Table 4.8, Entry 8):

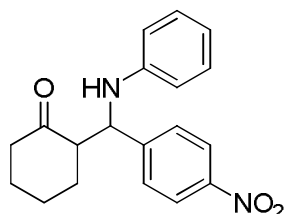
LCMS (M+1) m/z 356; ^1H NMR (400 MHz, CDCl_3): δ 1.65 (2H, m), 1.82-1.93 (4H, m), 2.33-2.44 (2H, m), 2.73-2.77 (1H, m), 4.61-4.65 (1H, d, $J = 7.09$ Hz), 6.53-6.56 (2H, d, $J = 7.90$ Hz), 6.63-6.65 (1H, m), 7.03-7.07 (2H, m), 7.22-7.27 (1H, m), 7.30-7.34 (2H, m), 7.38-7.40 (2H, m), 7.41-7.44 (2H, d, $J = 7.9$ Hz); ^{13}C NMR (100 MHz, CDCl_3): 210.1, 148.1, 141.5, 133.4, 129.4, 129.2, 120.8, 118.2, 117.9, 114.0, 56.9, 56.3, 42.4, 28.8, 27.0, 24.8; HPLC (*syn*-diastereomer): tR = 16.856 min (minor), 20.884 min (major).

2-[phenyl(2-methylphenylamino)methyl] cyclohexanone (Table 4.8, Entry 10):



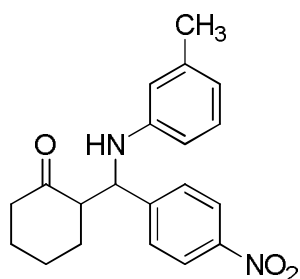
LCMS (M+1) m/z 291; ^1H NMR (400 MHz; CDCl_3): δ 1.70-1.79 (m, 3H,), 1.83-1.94 (m, 3H), 2.27 (m, 2H), 2.35 (s, 3H), 2.79-2.88 (m, 1H), 4.0 (bs, 1H), 4.1 (q, 2H), 6.39 (d, $J = 8.0$ Hz, 1H), 6.6-6.7(m, 1H), 6.9-7.1 (m, 2H), 7.2-7.4 (m, 5H); HPLC (*syn*-diastereomer): tR = 16.603 min (minor), 10.640 min (major).

2-[4-nitrophenyl(phenylamino)methyl] cyclohexanone (Table 4.8, Entry 11):

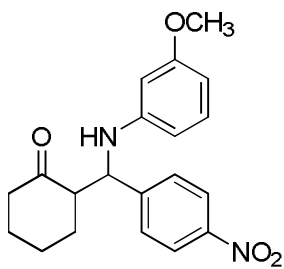


LCMS (M+1) m/z 322; ^1H NMR (400 MHz, CDCl_3): δ 8.16-8.13 (m, 2H), 7.57-7.54 (m, 2H), 7.11-7.05 (m, 2H), 6.70-6.65 (m, 1H), 6.51-6.48 (m, 2H), 4.86-4.59 (m, 2H), 2.86-2.83 (m, 1H), 2.46-2.27 (m, 2H), 2.06-1.93 (m, 3H), 1.72-1.57 (m, 3H); ^{13}C NMR (100 MHz, CDCl_3): 210.6, 149.6, 147.0, 146.6, 129.1, 128.6, 123.6, 118.3, 114.0, 57.1, 56.2, 42.4, 29.0, 27.0, 24.9; HPLC (*syn*-diastereomer): tR = 12.550 min (minor), 15.850 min (major).

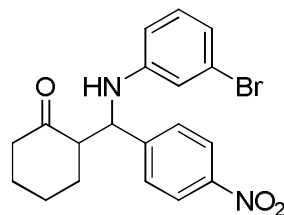
2-[4-methylphenylamino(4-nitrophenyl)methyl] cyclohexanone (Table 4.8, Entry 12):



LCMS (M+1) m/z 336; ^1H NMR (300 MHz, CDCl_3): δ 8.14-8.11 (m, 2H), 7.55-7.52 (m, 2H), 6.90-6.87 (m, 2H), 6.43-6.40 (m, 2H), 4.83-4.42 (m, 2H), 2.85-2.81 (m, 1H), 2.46-2.29 (m, 2H), 2.17 (s, 3H), 2.05-1.92 (m, 3H), 1.68-1.56 (m, 3H); ^{13}C NMR (100 MHz, CDCl_3): 210.7, 149.8, 147.0, 129.6, 128.6, 127.6, 123.6, 113.6, 57.4, 57.0, 42.4, 29.0, 27.1, 24.9, 20.3; HPLC (*syn*-diastereomer): tR = 20.458 min (minor), 21.325 min (major).

2-[4-methoxyphenylamino(4-nitrophenyl)methyl] cyclohexanone (Table 4.8, Entry 14):

LCMS (M+1) m/z 354; ^1H NMR (400 MHz, CDCl_3): δ 8.15-8.12 (m, 2H), 7.55-7.52 (m, 2H), 6.68-6.65 (m, 2H), 6.47-6.45 (m, 2H), 4.80-4.64 (m, 1H), 4.29 (bs, 1H), 3.67 (s, 3H), 2.82-2.32 (m, 3H), 2.04-1.92 (m, 3H), 1.72-1.61 (m, 3H); ^{13}C NMR (100 MHz, CDCl_3): 210.8, 152.6, 149.9, 147.0, 140.7, 128.5, 123.6, 115.6, 114.6, 58.0, 56.3, 55.6, 42.4, 31.8, 27.1, 24.9; HPLC (*syn*-diastereomer): tR = 35.254 min (minor), 37.339 min (major).

2-[3-bromophenylamino(4-nitrophenyl)methyl] cyclohexanone (Table 4.8, Entry 16):

LCMS (M+1) m/z 402; ^1H NMR (400 MHz, CDCl_3): δ 8.18-8.15 (m, 2H), 7.55-7.52 (m, 2H), 6.95-6.90 (m, 1H), 6.80-6.77 (m, 1H), 6.66-6.65 (m, 1H), 6.41-6.37 (m, 1H), 4.83-4.71 (m, 2H), 2.88-2.82 (m, 1H), 2.47-2.28 (m, 2H), 2.06-1.93 (m, 2H), 1.66-1.55 (m, 4H); ^{13}C NMR (100 MHz, CDCl_3): 210.5, 148.7, 148.3, 147.2, 130.4, 128.5, 123.7, 121.1, 116.7, 112.4, 57.0, 42.3, 32.0, 29.0, 26.9, 24.8; HPLC (*syn*-diastereomer): tR = 23.254 min (minor), 27.339 min (major).

References

- [1] A. P. Wight and M. E. Davis, *Chem. Rev.*, 2002, **102**, 3589.
- [2] D. Zhao, Q. Huo, J. Feng, B.F. Chmelka and G. D. Stucky, *J. Am. Chem. Soc.*, 1998, **120**, 6024.
- [3] S. Inagaki, S. Guan, Y. Fukushima, T. Ohsuna and O. Terasaki, *J. Am. Chem. Soc.*, 1999, **121**, 9611.

- [4] K. Moller and T. Bein, *Chem. Mater.*, 1998, **10**, 2950.
- [5] B. J. Melde, B. T. Holland, C. F. Blanford and A. Stein, *Chem. Mater.*, 1999, **11**, 3302.
- [6] T. Asefa, M. J. MacLachlan, N. Coombs and G. A. Ozin, *Nature*, 1999, **402**, 867.
- [7] M. J. MacLachlan, T. Asefa and G. A. Ozin, *Chem. Eur. J.*, 2000, **6**, 2507.
- [8] J. H. Clark and D. J. Macquarrie, *Chem. Commun.*, 1998, 853.
- [9] K. Kageyama, J. Tamazawa and T. Aida, *Science*, 1999, **285**, 2113.
- [10] X. Ding, J. Zhao, Y. Liu, H. Zhang and Z. Wang, *Mater. Lett.*, 2004, **58**, 3126.
- [11] S. Wei, Z. Guo, H. Gu, J. Guo, Q. He, X. Zhang, Y. Huang and H. A. Colorado, *Ind. Eng. Chem. Res.*, 2013, **52**, 7718.
- [12] W. Cheng, Z. Wang, C. Ren, H. Chen and T. Tang, *Mater. Lett.*, 2007, **61**, 3193.
- [13] Y. L. Liu, C. Y. Hsu and K. Y. Hsu, *Polymer*, 2005, **46**, 1851.
- [14] J. He, Y. Shen, J. Yang, D. Evans, and X. Duan. *Chem. Mater.*, 2003, **15**, 3894.
- [15] K. Moller, T. Bein and R. X. Fischer, *Chem. Mater.*, 1998, **10**, 1841.
- [16] F. A. Zhang, D. K. Lee and T.J. Pinnavaia, *Polymer*, 2009, **50**, 4768.
- [17] M. Sasidharan, N. K. Mal and A. Bhaumik, *J. Mater. Chem.*, 2007, **17**, 278.
- [18] M. Choi, F. Kleitz, D. Liu, H. Y. Lee, W.S. Ahn and R. Ryoo, *J. Am Chem. Soc.*, 2005, **127**, 1924.
- [19] M. Choi, W. Heo, F. Kleitz and R. Ryoo, *Chem. Commun.*, 2003, 1340.
- [20] B. Radhakrishnan, R. Ranjan and W. Brittain, *J. Soft Mater.*, 2006, **2**, 386.
- [21] C. G. Goltner, B. Smarsly, B. Berton and M. Antonietti, *Chem. Mater.*, 2001, **13**, 1617.
- [22] R. Ryoo, C. H. Ko, M. Kruk, V. Antochshuk and M. Jaroniec, *J. Phys. Chem. B*, 2000, **104**, 11465.

- [23] S. Jun, S. H. Joo, R. Ryoo, M. Kruk, M. Jaroniec, Z. Liu, T. Ohsuna and O. Terasaki, *J. Am. Chem. Soc.*, 2000, **122**, 10712.
- [24] B. Smarsly, C. G. Goltner, M. Antonietti, W. Ruland and E. Hoinkis, *J. Phys. Chem. B*, 2001, **105**, 831.
- [25] Z. Liu, O. Terasaki, T. Ohsuna, K. Hiraga, H. J. Shin and R. Ryoo, *Chem. Phys. Chem.*, 2001, 229.
- [26] H. J. Shin, R. Ryoo, M. Kruk and M. Jaroniec, *Chem. Commun.*, 2001, 349.
- [27] A. Galarneau, H. Cambon, F. DiRenzo, R. Ryoo, M. Choi and F. Fajula, *New J. Chem.*, 2003, **27**, 73.
- [28] D. Zhao, J. Feng, Q. Huo, N. Melosh, G. H. Fredrickson, B. F. Chmelka and G. D. Stucky, *Science*, 1998, **279**, 548.
- [29] A. Kirschning, H. Monenschein, R. Wittenberg, *Angew. Chem. Int. Ed.*, 2001, **40**, 650.
- [30] C. A. McNamara, M. J. Dixon and M. Bradley, *Chem. Rev.*, 2002, **102**, 3275.
- [31] (a) S. Mohanraj and W. T. Ford, *US Patent* 4,713,423, 1987; (b) S. Mohanraj and W. T. Ford, *Polym. Prepr.*, 1986, **27**, 5.
- [32] (a) J. H. Moon, J. W. Shin and J. W. Pa, *Mol. Cryst. Liq. Cryst.*, 1997, **295**, 185; (b) C.O. Kim, *J. Colloid Interface Sci.*, 2003, **24**, 374.
- [33] M. Kruk, M. Jaroniec, S. H. Joo and R. Ryoo, *J. Phys. Chem. B*, 2003, **107**, 2205.
- [34] K. S. W. Sing, D. H. Everett, R. A. W. Haul, L. Moscou, R. A. Pierotti, J. Rouquerol, and T. Siemieniewska. *Pure and Appl. Chem.*, 1985, **57**, 603.
- [35] X. Wang, Y. Hung, T. Jerry C. C. Chan and S. Cheng, *Microporous and Mesoporous Mater.*, 2005, **85**, 241.
- [36] Y. Kong, R. Tan, L. Zhaoa and D. Yin, *Green Chem.*, 2013, **15**, 2422.
- [37] J. P. E Spencer, *Chem. Soc. Rev.*, 2009, **38**, 1152.

- [38] L. C. Chang and A. D. Kinghorn, *Bioactive Compounds from Natural Sources: Isolation Characterisation and Biological Properties*, Taylor & Francis, London, 2001.
- [39] Ø. M. Andersen and K. R. Markham, *Flavonoids: Chemistry, Biochemistry and Applications*, Taylor & Francis, London, 2006.
- [40] C. Pouget, C. Fagnere, J. P. Basly, G. Habrioux and A. J. Chulia, *Bioorg. Med. Chem. Lett.*, 2002, **12**, 1059.
- [41] H. K. Hsieh, T. H. Lee, J. P. Wang, J. J. Wang and C. N. Lin, *Pharm. Res.*, 1998, **15**, 39.
- [42] M. D. Ankiwala, *J. Indian Chem. Soc.*, 1990, **67**, 913.
- [43] K. Oyama and T. Kondo, *J. Org. Chem.*, 2004, **69**, 5240.
- [44] M. Besson, M. C. Bonnet, P. Gallezot, I. Tkatchenko and A. Tuel, *Catal. Today*, 1999, **51**, 547.
- [45] M.T. Drexler and M.D. Amiridis, *J. Catal.*, 2003, **214**, 136.
- [46] Z. Sanieanin and I. Tabakovik, *Tetrahedron Lett.*, 1986, **27**, 407.
- [47] Y. Maki, K. Shimada, M. Sako, and R. Hirota, *Tetrahedron*, 1988, **44**, 3187.
- [48] Y. Zhou, W. Huang, X. -S. Chen, Z. -B. Song, D.-J. Tao, *Catal Lett.*, 2015, **145**, 1830.
- [49] C. Pandey, A. Krishna and G. Yumaraswamy, *Tetrahedron Lett.*, 1987, **28**, 4615.
- [50] D. J. Macquarrie and D.B. Jackson, *Chem. Commun.*, 1997, 1781.
- [51] J. E. Mdoe, G. J. H. Clark and D. J. Macquarrie, *Synlett*, 1998, 625.
- [52] S. Y. Chen, C.Y. Huang, T. Yokoi, S. Cheng, *Mater. Chem.*, 2012, **22**, 2233.
- [53] D. N. Dhar, *The Chemistry of Chalcone and Related Compounds*, Cambridge University Press, London, 1973.
- [54] G. Sartori, F. Bigi, R. Maggi, R. Sartorio, D. J. Macquarrie, M. Lenarda, L. Storaro, S. Coluccia and G. Martra, *J. Catal.*, 2004, **222**, 410.

- [55] R. Mosconi, J. P. Ferraz, E. A. Neves, J. O. Tognoli, M. I. El Seoud and do L. Amaral, *J. Org. Chem.*, 1976, **41**, 4093.
- [56] A. Berkessel and H. Gröger, *Asymmetric Organocatalysis: from Biomimetic Concepts to Applications in Asymmetric Synthesis*, Wiley-VCH, Weinheim, 2005.
- [57] P. I. Dalko, *Enantioselective Organocatalysis*, Wiley-VCH, Weinheim, 2007.
- [58] M. Benaglia, G. Celentano and F. Cozzi, *Adv. Synth. Catal.*, 2001, **343**, 171.
- [59] M. Benaglia, M. Cinquini, F. Cozzi, A. Puglisi and G. Celentano, *Adv. Synth. Catal.*, 2002, **344**, 533.
- [60] F. Caldero'n, R. Ferna'ndez, F. Sa'nchez and A. F. Mayoralas, *Adv. Synth. Catal.*, 2005, **347**, 1395.
- [61] T. P. Loh, L. C. Feng, H. Y. Yang and J. Y. Yang, *Tetrahedron Lett.*, 2002, **43**, 8741.
- [62] G. Chouhan, D. Wang and H. Alper, *Chem. Commun.*, 2007, 4809.
- [63] Z. Tang and A. Marx, *Angew. Chem. Int. Ed.*, 2007, **46**, 7297.
- [64] S. Bahmayar, K. N. Houk, H. J. Martin and B. List, *J. Am. Chem. Soc.*, 2003, **125**, 2475.
- [65] D. E. Siyutkin, A. S. Kucherenko, M. I. Struchkova and S. G. Zlotin, *Tetrahedron Lett.*, 2008, **49**, 1212.
- [66] M. Gruttadauria, F. Giacalone and R. Noto, *Chem. Soc. Rev.*, 2008, **37**, 1666.
- [67] J. D. White, P.R. Blakemore, N. J. Green, E. B. Hauser, M. A. Holoboski, L. E. Keown, C. S. N Kolz, B. W. Phillips, *J. Org. Chem.* 2002, **67**, 7750.
- [68] M. Arend, B. Westermann and N. Risch, *Angew. Chem. Int. Ed.*, 1998, **37**, 1044.
- [69] J. Yani and L. Wang, *Chirality*, 2009, **21**, 413.

- [70] D. Dhar, I. Beadham and S. Chandrasekaran, *Proc. Indian Acad. Sci. Chem. Sci.*, 2003, **115**, 365.
- [71] E. F. Kleinmann, *Comprehensive Organic Synthesis*, Pergamon Press, New York, 1991.
- [72] R. Muller, H. Waldmann and H. Goesmann, *Angew. Chem. Int. Ed.*, 1999, **38**, 184.
- [73] C. Mannich and W. Krösche, *Archiv der Pharmazie*, 1912, **250**, 647.
- [74] J. H. Lee and D. Y. Kim, *Adv. Synth. Catal.*, 2009, **351**, 1779.
- [75] B. List, *Tetrahedron*, 2002, **58**, 5573.
- [76] B. List, *J. Am. Chem. Soc.*, 2000, **122**, 9336.

Chapter 5

MESOPOROUS SILICA-SUPPORTED NHC-Pd COMPLEX: SYNTHESIS AND APPLICATION IN AROMATIC COUPLING REACTIONS

Contents	5.1 Introduction
	5.2 Results and Discussion
	5.3 Conclusion
	5.4 Experimental

A novel synthesis of mesoporous silica-supported NHC-Pd complex and its detailed characterization is described in this chapter. This supported catalyst can be efficiently applied in palladium-catalyzed Suzuki coupling and direct arylation reaction. The catalyst showed excellent reusability and activity in aromatic coupling reactions. Good yield of products and no evidence of leaching of Pd from the catalyst during the reaction confirm the true heterogeneous nature of the synthesized catalyst.

5.1 Introduction

N-Heterocyclic carbenes (NHCs), are highly stable, crystalline, air sensitive ligands, which can serve as spectator ligands in transition-metal complexes. They are first discovered by Ofele and Wanzlick in the late 1960s.^{1,2} Their potential was exploited in the field of transition metal complexes. Now, metal complexes of *N*-heterocyclic carbenes have become effective catalysts for various organic reactions.³⁻⁶ This particular class of

ligands is called phosphine mimic and it has several advantages over the closely related phosphine ligands.^{7,8} The primary advantage of these ligands is that they do not easily dissociate from the metal center. As a result, an excess of the ligand is not required, thereby preventing aggregation of the catalyst to yield bulk metal.⁹ They have high thermal and air stability and low toxicity. Such peculiarities make them ideal candidates for catalysis. NHCs derived from imidazolium or 4,5 dihydroimidazolium salts have found wide-spread use in homogeneous catalysis.¹⁰ Some common examples of the NHC ligand that are widely used in catalysis are shown in Figure 5.1.

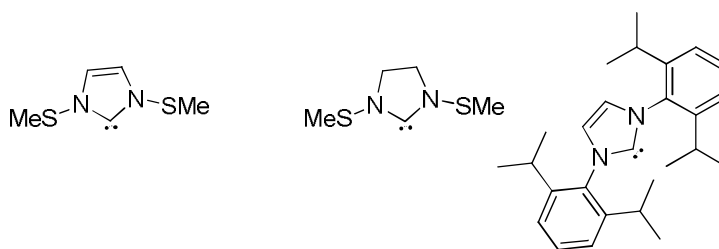


Fig. 5.1 Some examples of the NHC ligand

Synthesis of N-heterocyclic carbenes (NHCs) and their use as ligands has led to a new platform in the development of Pd-catalyzed cross-coupling reactions.¹¹⁻¹³ Palladium is an important transition metal capable of directing a wide range of useful transformations, in particular, C-C and C-heteroatom cross-coupling and carbopalladation reactions.^{14,15} The use of bulky carbene ligands in these transformations have resulted in significant improvements in catalyst performance compared to the more traditional phosphine ligands.¹⁶⁻¹⁸ However, these homogeneous catalyst systems have some basic problems in terms of the separation and recycling of the catalysts. They also induce contamination of the ligand residue in the products. Therefore, the

development of solid-supported N-heterocyclic carbene metal complexes as catalysts has attracted more attention in recent years.¹⁹⁻²² This heterogeneous catalyst system has several advantages, such as fast recovery of the catalyst by filtration and the simple recycling, which in turn prevents the contamination of the ligand and decreases the environmental pollution caused by residual metals in the waste.

5.1.2 Silica supported catalyst for C-C bond forming reactions

Recently, supported palladium catalysts have become promising candidates for the design of true heterogeneous catalysts, where they satisfy the principles such as chemical robustness, recyclability, environmentally benign as well as economic aspects. In this regard, silica fulfils many of the required criteria as suitable solid supports for immobilization of palladium catalysts. The structural diversity together with favourable chemical properties (stability, chemical inertness, accessibility to functional modifications etc.) renders these materials very attractive for catalyst design. The basic critical parameters, overall structure and diameter of the pores can be tuned for this purpose.^{23, 24}

In order to minimize the undesired leaching from the surface, a covalent bond was established between silica support and active metal site. Many synthetic strategies are available towards the preparation of silica supported Pd catalysts. A Pd-NHC complex was immobilized on amorphous silica by Artok and co-workers (Figure 5.2).²⁵ The complex itself was found thermally stable. However, TEM observation, hot filtration, reusability and poisoning tests revealed that the complex acted only as a precursor of active Pd species in the Heck reaction when immobilized. Mubofu et al. prepared a

highly recyclable supported palladium catalyst for Suzuki reaction between phenylboronic acid and bromobenzene. The catalysts were obtained by interaction of aminopropylated silica with pyridine carbaldehyde and subsequent complexation of palladium acetate.²⁶ Tyrrell and co-workers studied the activity of Pd-supported catalysts prepared via two complementary methodologies i.e., by complexation of grafted imidazolium moieties and by immobilization of defined complexes.²⁷ Studies revealed that catalysts prepared by immobilizing the pre-formed palladium complexes is slightly more active in the Suzuki coupling of aryl bromides than that prepared by the reaction of palladium acetate with the tethered imidazolium salt.

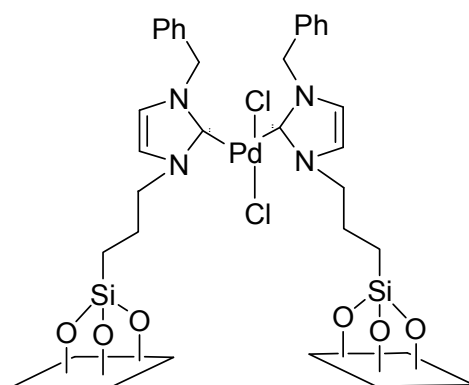


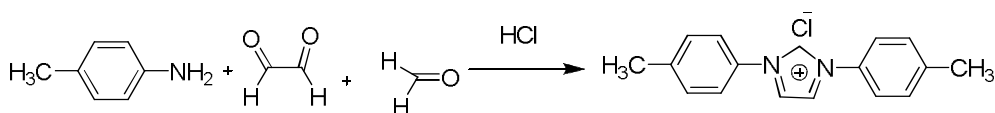
Fig. 5.2 Example of Pd-NHC complex immobilized on silica for utilization in Heck reaction²⁵

The present chapter deals with the synthesis and characterization of mesoporous silica (MS)-supported N-heterocyclic carbene (NHC)-Pd complex. Application of the catalyst in Suzuki coupling and direct arylation reactions is described. The experimental parameters are optimized, scope of substrates, reusability of the catalyst and mechanism are studied.

5.2 Results and Discussion

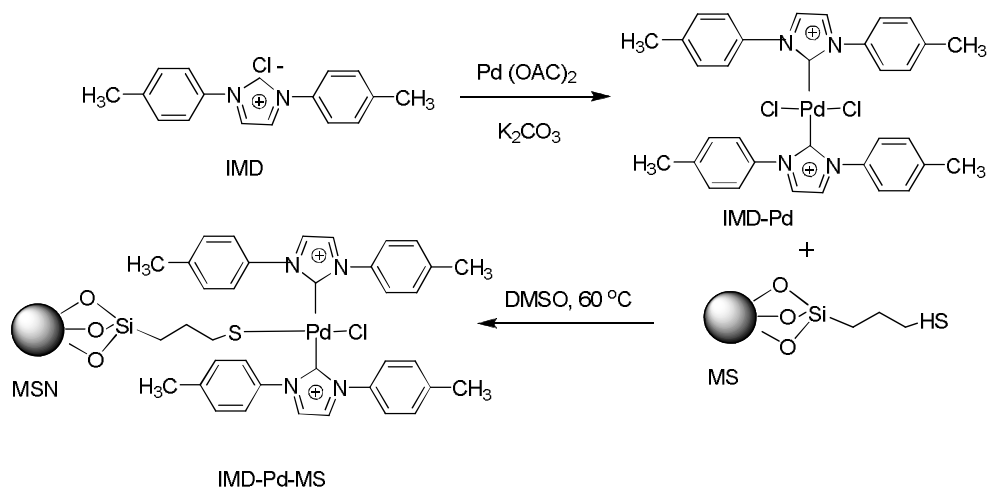
5.2.1 Synthesis of silica-supported NHC-Pd complex

Mesoporous silica (MS), (see section 2.2.1) was selected as silica support for immobilization of the complex. Among the different periodic mesoporous silica, MS showed high surface area which makes it a suitable candidate for immobilization. It is generally believed that high surface area of heterogeneous catalysts results in high catalytic activity. The other silica are also suitable, even though they exhibited lower surface area compared to MS. 1,3-bis(p-tolylimidazolium) chloride (IMD-Cl), the immediate precursor of *N*-Heterocyclic carbene was prepared by the condensation of p-toluidine with formaldehyde and glyoxal in the presence of conc. HCl (Scheme 5.1). The corresponding metal complex was synthesized by deprotonating the acidic protons with suitable base. Two equivalents of imidazolium salt were reacted with one equivalent of palladium acetate in DMSO using K₂CO₃ as base.



Scheme 5.1 Synthesis of 1,3-bis(p-tolylimidazolium) chloride (IMD-Cl)

Immobilization of NHC-Pd complex onto the surface of silica is shown in Scheme 5.2. NHC-Pd complex was treated with thiol functionalized mesoporous silica in DMSO. The sulphur ligands in the mesopores of mesoporous silica were effective for preventing aggregation of Pd species, which in turn resulted in high durability and good recycling characteristics of the prepared supported catalysts.²⁸



Scheme 5.2 Synthesis of silica-supported NHC-Pd complex

5.2.2 Characterization of NHC-Pd complex and silica-supported NHC-Pd complex

The 1,3-bis(p-tolylimidazolium) chloride (IMD-Cl) was characterized by ^1H NMR, ^{13}C NMR and mass spectra. The metal complex was characterized by FT-IR, CHN analysis, conductivity measurement, magnetic susceptibility measurements and thermal analysis. The metal content of the complex was estimated using atomic absorption spectroscopy. The results are shown in Table 5.1. The FTIR spectrum of the metal complex showed a characteristic band of C-Cl stretching vibration at 720 cm^{-1} and absence of ester peak rules out the presence of acetate ion of palladium acetate after complexation. This result suggested that counter ion of imidazolium ligand was coordinated to the metal. Thermal analysis of the complex showed a weight loss of about 10 % between 200-250 °C. This is due to the loss of two chlorine ligand species coordinated to the central metal atom. Another degradation of 15 % occurred at 326 °C which was ascribed to the

elimination of imidazolium ligand. From the above results, the tentative structure of IMD-Pd is shown in Scheme 5.2

Table 5.1 Chemical properties of NHC-Pd complex

CHN analysis	Conductivity measurement	Magnetic susceptibility	Metal (Pd) content (AAS)
C (60.7 %), N (7.2%)	Non-Conductive	Diamagnetic	24.5 %
H (4.01 %)	(3.5 μ S)	(< 1 BM)	

5.2.2.1 X-ray diffraction studies

PXRD analysis was carried out to study the structural ordering of synthesized catalyst. Silica-supported NHC-Pd complex showed a low angle diffraction $d100$ peak at 2θ value 2.35° with low intensity. This is characteristic of mesoporous material which confirmed that the ordered nature of the support was preserved after functionalization (Figure 5.3).

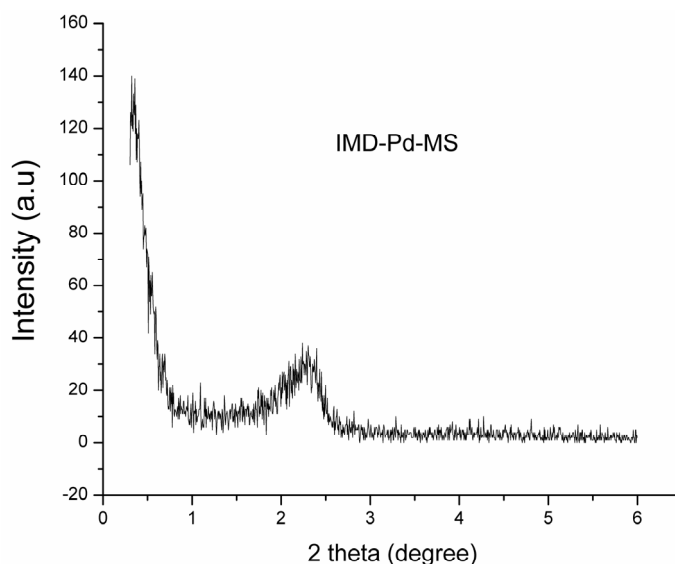


Fig. 5.3 XRD diagram of IMD Pd-MS

5.2.2.2 Surface area analysis

BET plots of the functionalized materials showed a typical type IV isotherm and corresponding hysteresis loop, confirming the nature of mesoporous materials. Surface area, pore diameter and pore volume decreased after each functionalization. Structural properties of the samples are summarized in Table 5.2. The overall shape of the adsorption/ desorption isotherms remained unchanged. The pronounced steps of capillary condensation in primary mesopores were evident, indicating that ordering of the MS support was not affected by the modification (Figure 5.4).

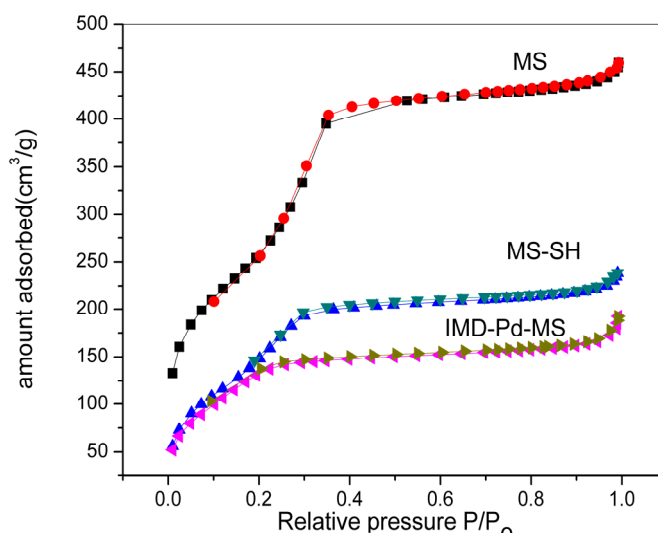


Fig. 5.4 N_2 adsorption/desorption isotherms of functionalized MS

Table 5.2 Structural properties of MS and functionalized MS

Sample	S_{BET} (m^2/g)	Pore volume (cm^3/g)	Pore diameter (nm)
MS	1039	0.75	2.8
MS-SH	655	0.45	2.5
IMD-Pd-MS	455	0.36	2.3

5.2.2.3 IR spectral studies

FTIR spectra of the thiol functionalized silica and supported Pd complex are shown in Figure 5.5. The silanol (Si-OH) and Si-O-Si bands from the parent silica material are observed at 3450 cm^{-1} (broad) and 1080 cm^{-1} , respectively. After immobilization of the thiol functionality, a weak S-H stretching peak was seen at 2530 cm^{-1} for thiol functionalized silica (MS-SH). The stretching frequency of the thiol group got disappeared after complexation with metal complex (IMD-Pd). It revealed that SH group on the silica has participated in the reaction forming coordinate bond with Pd of the complex. It gives an additional proof for the role of sulphur ligand in complexation.

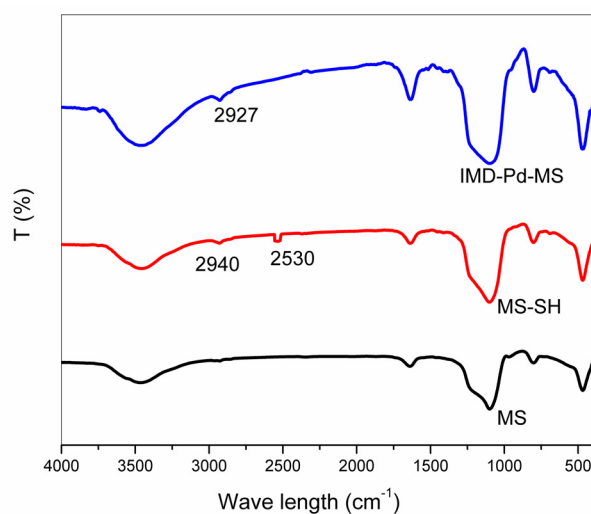


Fig. 5.5 IR spectra of functionalized MS

5.2.2.4 Electronic spectral studies (UV-Vis DRS)

UV-Vis- DRS spectra of the supported-Pd complex showed a peak at 320 nm and another at 425 nm (Figure 5.6). These transitions correspond to the

charge transfer transition from the ligand to metal and overlapping of allowed d-d transitions in palladium after coordination with thiol functionalized silica. The possible structure of the supported-Pd complex may be square planar.

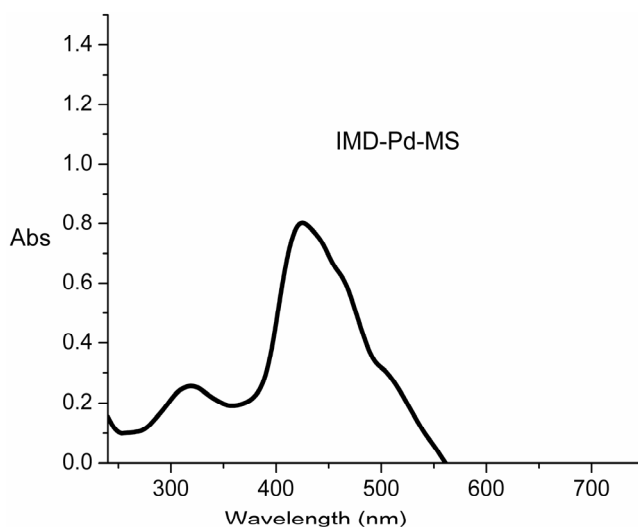


Fig. 5.6 UV-Vis-DRS spectrum of IMD-Pd-MS

5.2.2.5 SEM & energy dispersive X-ray (EDX) analysis

Energy dispersive X-ray spectroscopic analysis gives both qualitative and quantitative information about the elemental composition of the samples. It is an insitu chemical analysis of the bulk, and was carried out focusing multiple regions over the surface of the silica. EDX spectra clearly showed Pd, C, N, S, Si and O as the constituents of the catalyst (Figure 5.7). The morphological changes occurring on the surface of the support after functionalization was examined by employing scanning electron microscopy. SEM analysis of silica supported complex showed that mesoporous nature was maintained even after functionalization. Morphology is regular, composed of independent and sintered hexagonal particles (Figure 5.8).

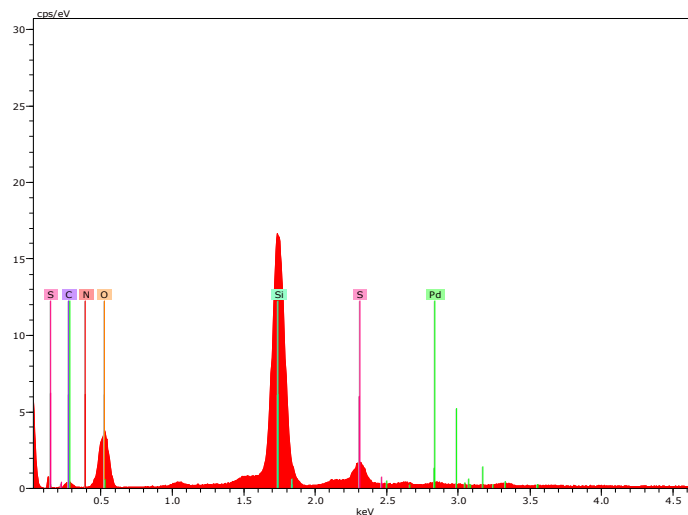


Fig. 5.7 EDX spectrum of IMD-Pd-MS

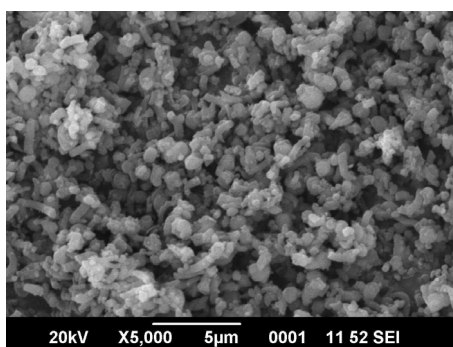


Fig. 5.8 SEM image of IMD-Pd-MS

5.2.2.6 TG-DTG Analysis

TG-DTG analysis was performed to determine the thermal stability and degree of organic functionalization of the sample. Thermal analysis of the silica supported complex showed a small weight loss of about 2 % between 100-150 °C attributed to the loss of non-coordinated water. Another weight loss of 14 % was observed at 360 °C corresponding to the decomposition of complex functionality (Figure 5.9).

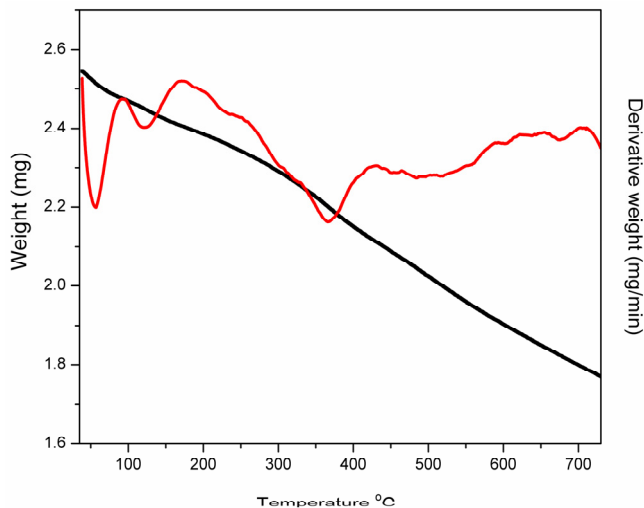


Fig. 5.9 TG-DTG plot of IMD-Pd-MS

5.2.2.7 X-ray photoelectron spectroscopy

In order to study the elemental composition of silica-supported complex, XPS analysis was performed (Figure 5.10). The XPS results indicated that significant amount of IMD-Pd complex was coordinated to the support. Deconvoluted spectra of Pd showed two doublets of $3d_{5/2}$ and $3d_{3/2}$ at 337.4 eV and 342.6 eV respectively with energy difference of 5.2 eV. This value confirmed that Pd existed in the +2 oxidation state and slight shift from the reported value suggested that strong interaction existed between Pd complex and silica support. Deconvoluted spectra of S, Si and Pd are depicted in Figure 5.11 and 5.12. The atom percentage values and mass percentage values derived from XPS data are presented in Table 5.3. The percentage of Pd obtained from XPS measurement was in good agreement with the result obtained from AAS measurement. The results are given in Table 5.4.

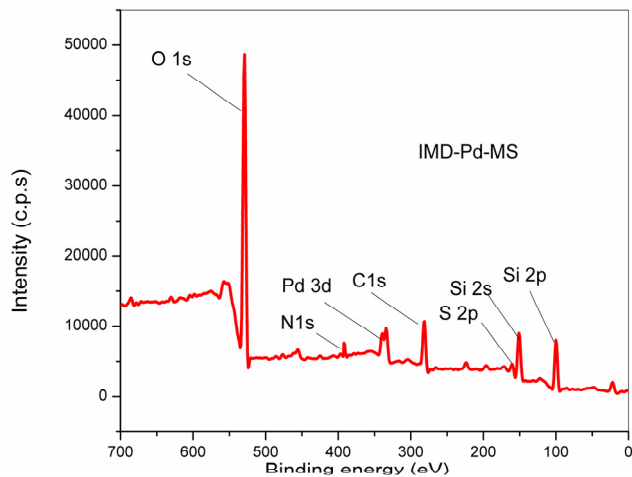


Fig. 5.10 XPS spectra of IMD-Pd-MS

Table 5.3 Elemental composition of IMD-Pd-MS

Element	Atom %	Mass %
C (1s)	19.8	11.4
O (1s)	40.2	30.1
Si (2p)	15.3	21
S (2p)	1.93	3.0
Pd(3d)	1.2	6.4
Si (2s)	17.4	25.1
N(1s)	4.05	3.1

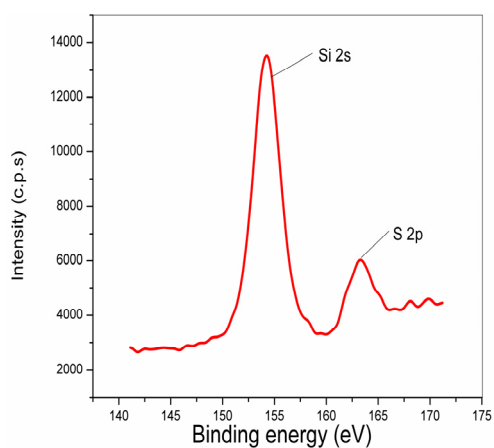


Fig. 5.11 Deconvoluted spectra of Si & S

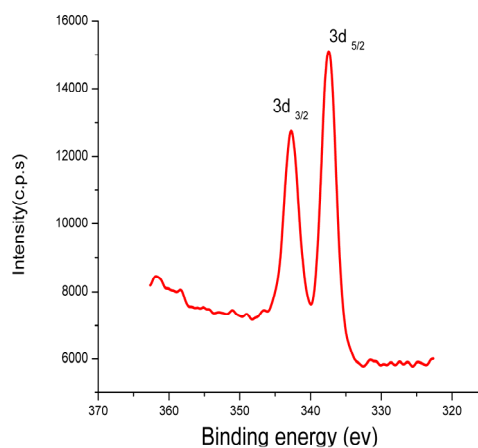


Fig. 5.12 Deconvoluted spectra of Pd

Table 5.4 Pd content on IMD-Pd-MS

XPS	1.64 mmol/g
AAS	1.59 mmol/g

5.2.3 Catalytic performance

The C-C cross-coupling reactions constitute one of the most important and useful reactions in organic synthesis and organometallic chemistry, since a large variety of complex compounds can be synthesized from readily accessible reactants. Biaryls are prevalent structures in many natural products, pharmaceuticals, agrochemicals, conjugated materials and chiral liquid crystals.²⁹⁻³¹ This has led to significant interest in the development of new reactions to efficiently construct Ar-Ar bonds. Here, we have investigated the catalytic activity of the NHC-Pd catalyst in aromatic coupling reactions such as Suzuki coupling and direct arylation reaction. Numerous homogeneous and heterogeneous catalysts were developed for C-C cross-coupling reactions.³²⁻³⁷ But these methods suffered from several drawbacks, such as higher temperatures, longer reaction times, expensive catalyst, toxic solvents, and significant leaching of active metal sites.

5.2.3.1 Suzuki coupling reaction

Among cross-coupling reactions, the Suzuki-Miyaura reaction,³⁸⁻⁴⁰ has emerged as the most practical synthetic method for biaryl compounds. Arylboronic acids are air, moisture tolerant, commercially available reagents and most frequently used nucleophilic partners in Suzuki coupling reaction. The reaction proceeds well in a wide range of solvents, including alcohols

and water and the by-products formed are nontoxic. In order to activate the boron derivative, stoichiometric amount of base is necessary. The reaction is tolerant to wide range of functional groups and applicable to complex reaction partners.

The model reaction between phenylboronic acid and 1-iodobenzene was studied in DMF in the presence of Na_2CO_3 , as the base (Scheme 5.3). Initially, the influence of the concentration of the catalyst on the reaction was studied. Different amounts of the catalyst ranging from 5 mg to 10 mg were tested. The best result was obtained using 7 mg (1 mol%) of the catalyst. No significant improvement in yield was observed by further increasing the quantity of the catalyst in the reaction.



Scheme 5.3 IMD-Pd-MS catalyzed Suzuki coupling reaction

Reaction was also carried out at 30 °C giving the desired product with low yield and required more time. To enhance the rate of reaction, the temperature was raised to 60 °C, so the reaction was completed within 2 h. Further increase of temperature did not affect the yield.

Effect of solvent on reaction was studied with various solvents. The reaction proceeded well in polar solvents like ethanol, dioxane and DMF, but slowly in nonpolar solvents like toluene. Water played a crucial role in Suzuki coupling reaction. When water was used along with a miscible

organic solvent, the yield was increased.³³ The results are given in Table 5.5. It was found that 96 % yield was obtained when volume ratio of water reached upto 1:1. Reaction was carried out with series of bases including NaOH, K₂CO₃, Na₂CO₃ and Et₃N. Better result was obtained with K₂CO₃. The results are summarized in Table 5.5.

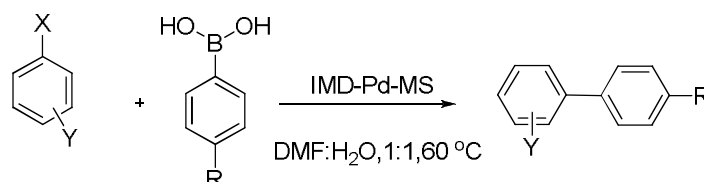
Table 5.5 Influence of solvent and base in Suzuki coupling reaction

Entry	Solvent	Base	Yield (%) ^{a, b}
1	DMF	Na ₂ CO ₃ /K ₂ CO ₃	88/90
2	Ethanol	K ₂ CO ₃	85
3	Toluene	Na ₂ CO ₃	75
4	Dioxane	K ₂ CO ₃	90
5	DMF	NaOH	85
6	DMF-H ₂ O (1:1)	K ₂ CO ₃	96
7	DMF-H ₂ O (2:1)	K ₂ CO ₃	92
8	DMF-H ₂ O (1:1)	Et ₃ N	88

^a Reaction conditions: 1-iodobenzene (1 mmol), phenylboronic acid (1.2 mmol), 60 °C, DMF:H₂O (1:1), 2 h, K₂CO₃ (3 mmol), catalyst (1 mol%), ^b isolated yield

To evaluate the scope of the reaction, reaction was performed with various sets of aryl halides under the optimized condition and the corresponding results are given in Table 5.6.

It was found that aryl iodides reacted faster compared to other aryl halides. Yield of the product was slightly higher for aryl halides having electron donating substituents. It was noticed that, aryl chlorides gave moderate yield within specified time. Thus, electronic factors have only small impact on reaction rate.

Table 5.6 Suzuki coupling reaction of various substrates

Entry	X	Y	R	Yield (%) ^{a, b}
1	I	H	H	96
2	Br	H	H	95
3	I	4-CH ₃	H	98
4	I	4-OCH ₃	H	100
5	Cl	H	H	92
6	I	2-OCH ₃	H	98
7	Br	4-OCH ₃	H	96
8	I	4-NO ₂	H	89
9	Br	4-CH ₃	H	95
10	I	C(CH ₃) ₂	H	98

^a Reaction conditions: aryl halides (1 mmol), phenylboronic acid (1.2 mmol), 60 °C, DMF:H₂O (1:1), 2 h, K₂CO₃ (3 mmol), catalyst (1 mol%), ^b isolated yield

In order to examine the catalytic efficiency of IMD-Pd-MS catalyst we have compared the result with other catalysts. The metal contents of the catalysts are given in Table 5.7.

Table 5.7 Suzuki coupling reaction carried out with various types of catalysts

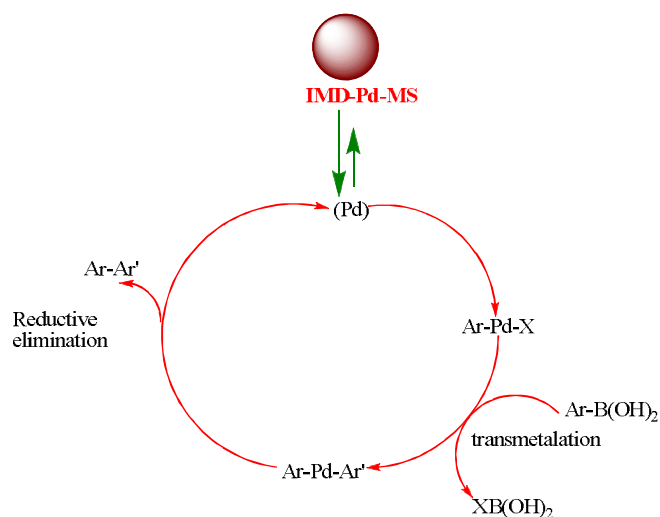
Entry	Types of catalyst	Pd content (mmol/g) ^a	Pd content (mmol/g) ^b	Yield (%) ^{c, d}	Time (h)
1	IMD-Pd-MS	1.59	1.58	96	2
2	Pd-MS I	0.88	0.49	88	5
3	Pd-SiO ₂	0.57	0.20	82	8
4	Pd-C	0.94	0.51	75	24

^a Pd content before reaction ^b Pd content after reaction ^c 1-iodobenzene (1 mmol), phenylboronic acid (1.2 mmol), 60 °C, DMF:H₂O (1:1), K₂CO₃ (3 mmol), catalyst (1 mol%), ^d isolated yield

Catalytic activity of all the catalysts was performed in Suzuki coupling under identical reaction conditions. Pd-MS I & Pd activated on amorphous silica (Pd-SiO₂) gave good yield while Pd activated on charcoal gave poor yield and required longer reaction time. Other catalysts showed significant metal leaching after reaction where as IMD-Pd-MS showed high stability, and negligible metal leaching and can be reused with same activity.

5.2.3.1.1 Reaction mechanism

The general mechanism of Suzuki coupling reaction is shown in Scheme 5.4. It follows the generic three-stage “oxidative addition, transmetalation, reductive elimination” sequence. It differs from other transition metal catalyzed cross-coupling reaction as it required a base for activation to proceed. Mechanism involves a transition metal-catalyzed oxidative addition reaction across the C-X bond of an electrophile. It is followed by transmetalation with a main group organometallic nucleophile, which was followed by a reductive elimination step leading to the carbon-carbon bond formation.³⁸



Scheme 5.4 Mechanism of Suzuki coupling reaction

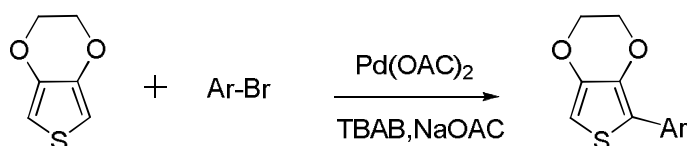
5.2.3.1.2 Direct arylation

Direct arylation is a reaction formally similar to cross-coupling, with the key difference that one of the carbons involved in the process is bound not to a hetero atom, but to hydrogen. This turns the reaction into a very powerful method for synthesis of aryl-aryl bonds, since it allows skipping the introduction of electropositive heteroatom as required in cross-coupling reactions.^{41,42} A potential alternative to traditional metal catalyzed cross-coupling chemistry, would be employment of metal mediated C-H activation chemistry to afford functionalization. This approach addresses some of the challenges associated with traditional cross-coupling reactions. First, this methodology would eliminate the metal salts resultant from the transmetallating reagent. Second, prefunctionalization of each of the coupling partners would no longer be required. However, the challenge of attaining site selective C-H activation in the presence of all C-H bonds within a molecule arises when employing this approach.

5.2.3.3 Direct arylation of 3,4-(ethylenedioxythiophene) using palladium catalyst

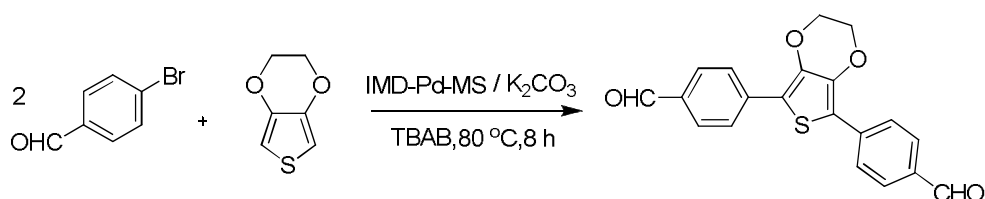
In recent years, oligothiophenes, have received widespread attention as components of molecular electronic and optical devices. 3,4-ethylenedioxythiophene (EDOT) has been used as a building block in several conjugated systems that incorporate unique properties such as electrochromic behavior and in low band gap polymers.⁴³⁻⁴⁶ The functionalization of conducting polymers has powerful application for modification of electrode surfaces and as electronic and optoelectronic devices. The electronic properties of materials are dependent on the planarity of the structure. So, regioselective methods are needed to obtain

a structurally homogeneous head to tail (HT) arrangement in which steric interaction is limited. It can be carried out using methods described by Suzuki,⁴⁷ Kumuda,⁴⁸ Stille⁴⁹ etc. However, these techniques proceed in two steps via an organometallic intermediate and their chemical compatibility is often limited. An alternative method is regioselective direct arylation by Heck method under Jeffery conditions (Scheme 5.5).⁵⁰



Scheme 5.5 Direct arylation of EDOT by Heck method under Jeffery conditions⁵⁰

The present work emphasizes on the synthesis of bis-arylated 3,4-(ethylenedioxythiophene) using solid catalyst. Since most of the arylation reactions are carried out under homogeneous condition, there is a scope for the improvement in the synthetic strategy, by reducing reaction time and by using reusable catalyst. Silica-supported NHC-Pd complex (IMD-Pd-MS) was found to be efficient catalyst for direct arylation reaction. The scheme of the model reaction is shown in Scheme 5.6.



Scheme 5.6 IMD-Pd-MS catalyzed direct arylation reaction

Reaction was carried out under various conditions. Effect of catalyst amount, effect of temperature and effect of various solvents was studied in

the model reaction. To inspect the catalytic efficiency of silica supported NHC-Pd catalyst, the reaction was conducted with another catalyst, $(\text{CH}_3\text{COO})_2\text{Pd}$ in DMSO. The optimized results, comparison of performance and effect of solvents on the reaction are given in Table 5.8 and Table 5.9.

Table 5.8 Optimization studies and comparison of performance in direct arylation reaction

Catalyst	Amount of catalyst	Temperature	Time	Yield (%) ^a
IMD-Pd-MS	4 mol%	80 °C	8 h	50
$(\text{CH}_3\text{COO})_2\text{Pd}$	10 mol%	80 °C	16 h	50

^a 3,4-(ethylenedioxythiophene) (0.17 mmol), 4-bromobenzaldehyde (0.34 mmol), tetrabutylammonium bromide (0.17 mmol), sodium acetate (0.69 mmol), DMSO (10 mL)

Table 5.9 Effect of solvent on direct arylation

Entry	Solvent	Yield (%)
1	DMSO	50
2	DMF	46
3	THF	Trace amount

5.2.3.3 Recycling study of catalyst

After the reactions, the catalyst was washed with ethyl acetate and methanol repeatedly, and dried at 60 °C for 4 h and reused. The metal content of the recycled catalyst was measured by AAS after one model reaction. The results are given in Table 5.10. Catalyst showed outstanding recyclability without any significant loss of activity after four successive runs. The corresponding bar diagram is depicted in Figure 5.13.

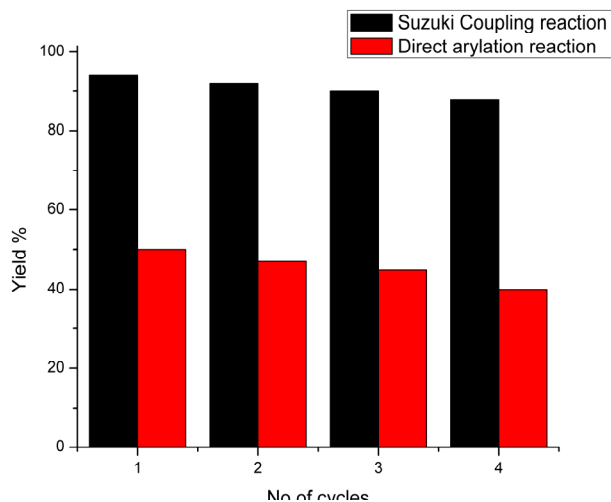


Fig. 5.13 Recycling study of IMD-Pd-MS in Suzuki coupling reaction and direct arylation reaction

Table 5.10 Metal content of the recycled catalyst

Entry	Reactions	Pd content after model reaction ^{a,b,c}
1	Suzuki coupling	1.58 mmol/g
2	Direct arylation	1.57 mmol/g

^a Atomic absorption analysis, ^b 1-iodobenzene (1 mmol), phenylboronic acid (1.2 mmol), 60 °C, DMF:H₂O (1:1), 2 h, K₂CO₃ (3 mmol), catalyst (1 mol%), ^c 3,4-(ethylenedioxythiophene), 4-bromobenzaldehyde, 90 °C, DMSO, 8 h, catalyst (4 mol%)

5.3 Conclusion

In conclusion, Palladium (II) complex with N-heterocyclic carbene ligand was synthesized. It was immobilized on thiol functionalized mesoporous silica. This novel silica supported catalyst showed excellent activity in Suzuki cross-coupling reaction of various aryl iodides and bromides with phenylboronic acid in DMF/water medium. Donor-Acceptor system like bis-arylated 3,4-(ethylenedioxythiophene) was synthesized via direct arylation reaction. This push-pull system may find application in

molecular electronics and optical devices. Catalyst showed outstanding recyclability without any significant loss of metal.

5.4 Experimental

5.4.1 Materials

All the solvents were purified according to the standard procedures. All reagents and solvents used in the preparation and modification of mesoporous silica were used as received. Amorphous silica was purchased from Loba Chemie Pvt. Ltd., India. Pd(OAc)₂ & Pd on activated charcoal were received from Sigma Aldrich. TLC was done on silica coated alumina plates (Merck, 60F254).

5.4.2 Synthesis of mesoporous silica particles and thiol functionalized mesoporous silica (MS-SH)

Mesoporous silica particles were synthesized according to the method reported by Grun et al.⁵¹ Detailed procedure for the synthesis of MS and MS-SH and references are given in chapter 2.

5.4.3 Synthesis of 1,3 bis(p-tolylimidazolium) chloride (IMD-Cl)

A solution of p-toluidine (10.72 g, 100 mmol) in 15 mL toluene, was added drop wise over 10 min to a suspension of paraformaldehyde (1.51 g, 50 mmol) in 15 mL toluene. When the addition was complete, the mixture was heated to 40 °C, 8.3 mL of aqueous 6 N HCl was slowly added to the reaction mixture, followed by 7.25 g of 40 % aqueous glyoxal. When the addition was complete, the reaction mixture was stirred for 5 minutes at room temperature and heated to 100 °C in an oil bath for 2 h. A dark solid was formed and it was allowed to cool to room temperature. Removal of

volatiles under vacuum yielded a dark solid. The solid was triturated in acetonitrile and solid was filtered off.

Yield 84 %; Black powder; LCMS (M+1) m/z 249; IR (KBr): $\bar{\nu}$ 3390, 3110, 2928, 2319, 1596, 1360, 756 cm^{-1} ; ^1H NMR (400 MHz, $\text{DMSO-}d_6$): δ 2.31(s, 6H), 7.49-7.52 (d, $J = 8.4$ Hz, 4H), 7.81-7.83 (d, $J = 8.4$ Hz, 4H), 7.29-7.35 (d, $J = 8$ Hz, 2H), 8.53 (s, 1H); ^{13}C NMR (100 MHz, $\text{DMSO-}d_6$): 20.4, 121.7, 122.7, 129.5, 130, 130.4, 137.

5.4.4 Preparation of N-heterocyclic carbene palladium complex (IMD-Pd)

1,3-bis(p-tolylimidazolium) chloride (0.133 g, 0.537 mmol) was added to a 50 mL Schlenk flask containing $\text{Pd}(\text{OAc})_2$ (0.06 g, 0.268 mmol), potassium carbonate (0.074 g, 0.537 mmol) and dry DMF (10 mL). The mixture was allowed to stir for 5 h at ambient temperature. The solvent was completely removed under vacuum. The residue was dissolved in dichloromethane. The organic layer was washed twice with water. After drying with anhydrous magnesium sulphate, the residue was washed with ether and subsequently with methanol. The air stable solid was filtered and dried under vacuum.

Yield 73 %; Black powder; IR (KBr): $\bar{\nu}$ 3370, 3120, 2928, 2319 1605, 1360, 829 cm^{-1} ; CHN analysis: C (60.7 %), N (7.2 %), H (4.01 %), O (4.1 %); Pd content (AAS): 24.5 %

5.4.5 Preparation of silica supported NHC-Pd complex (IMD-Pd-MS)

NHC-Pd complex (0.9 g, 1 mmol) was added to the thiol functionalized silica (2 g) in DMSO (40 mL), stirred and refluxed at 60 °C for 8 h. Silica supported NHC-Pd complex was filtered and washed with CH_2Cl_2 in a

Soxhlet extractor to remove unreacted Pd(OAc)₂, and dried under vacuum at 60 °C for 5 h.

Yield: 2.15 g; Brown powder; IR (KBr): $\bar{\nu}$ 3360, 3100, 2918, 2309, 1416, 1226, 1115, 720 cm⁻¹; CHN analysis: C (11.8 %), N (2.9 %), S (3.0 %), H (4.01 %); Pd content (AAS): 1.59 mmol/g

5.4.6 Preparation of Pd incorporated amorphous SiO₂ & MS I

MS I is a periodic mesoporous silica which was synthesized according to the procedure described in chapter 4. Pd activated on amorphous silica (Pd-SiO₂) and Pd-MS I were prepared by stirring Pd(OAc)₂ (1 mmol, 100 mg) with 1 g silica in toluene (25 mL) for 12 h. It was filtered, and washed with ethanol in a Soxhlet extractor and dried under vacuum.

5.4.7 Suzuki coupling reaction

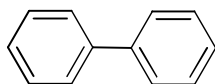
A 10 mL r. b flask was charged with the aryl halide (1 mmol), phenylboronic acid (1.2 mmol), and K₂CO₃ (317 mg, 3 mmol). The catalyst (7 mg) was added to it followed by DMF (2.5 mL) and water (2.5 mL) was added. The reaction mixture was stirred at 60 °C. The progress of the reaction was monitored by TLC on silica gel coated plates using hexane/ethyl acetate mixture (10:1). After the reaction was completed, catalyst was filtered and the reaction mixture was added to brine (15 mL) and extracted with diethyl ether. The solvent was concentrated under vacuum and the product was isolated by a short column on silica gel using hexane and ethyl acetate (10:1) as eluents. The products were characterized using GC-MS and ¹H NMR spectroscopy.

5.4.8 Procedure of direct arylation reaction

EDOT (0.048 g, 0.17 mmol), TBAB (0.112 g), Sodium acetate (0.1 g) and DMF (10 mL) were stirred at room temperature for 15 minutes. 4-Bromobenzaldehyde (0.1 g, 0.34 mmol) and catalyst (IMD-Pd-MS-25 mg or $(\text{CH}_3\text{COO})_2\text{Pd}$ - 76 mg) were added. The reaction mixture was stirred at 80 °C for 12 h. The reaction mixture was cooled and washed with cold methanol to separate the catalyst. The filtrate was poured into crushed ice and stirred well and the precipitate was filtered and dried and purified from petroleum ether/ethyl acetate mixture (3:1 v/v).

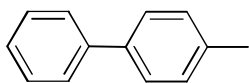
Characterization of the Suzuki products

Biphenyl (Table 5.7, Entry 1)



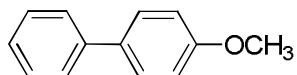
White solid, m.p 69-71 °C; GC-MS (M^+): 154; ^1H NMR (400 MHz, CDCl_3): δ 7.26-7.31 (m, 2H), 7.37-7.42 (m, 4H), 7.53-7.57 (m, 4H); ^{13}C NMR (100 MHz, CDCl_3): 127.20 (s, 5C), 128.79 (s, 5C).

4-Methyl biphenyl (Table 5.7, Entry 3)



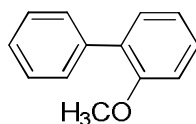
White solid, m.p 50-52 °C; GC-MS (M^+): 168; ^1H NMR (400 MHz, CDCl_3): δ 2.32 (s, 3H), 7.15(d, $J = 7.5$ Hz, 2H), 7.21- 7.29 (m, 1H), 7.33 (t, $J = 6.5$ Hz, 2H), 7.40 (d, $J = 8.3$, 2H), 7.51- 7.54 (m, 2H); ^{13}C NMR (100 MHz, CDCl_3): 21.14 (s, 1C), 127.02 (s, 5C), 128.75 (s, 2C), 129.52 (s, 2C), 137.06 (s, 1C) 138.39 (s, 1C), 141.19 (s, 1C).

4-Methoxy biphenyl (Table 5.7, Entry 4)



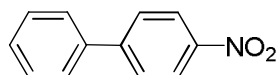
White solid, m.p 89-91 °C; GC-MS (M^+): 184; ^1H NMR (400 MHz, CDCl_3): δ 2.62 (s, 3H), 7.40-7.48 (m, 4H), 7.02- 7.68 (m, 4H), 8.1 (d, $J = 6.7$ Hz, 2H); ^{13}C NMR (100 MHz, CDCl_3): 55.38 (s, 1C), 114.26 (s, 2C), 126.71(s, 1C) 126.78 (s, 2C), 128.20 (s, 2C), 128.77 (s, 2C), 133.83 (s, 1C), 140.88 (s, 1C), 159.21 (s, 1C).

2-Methoxy biphenyl (Table 5.7, Entry 6)



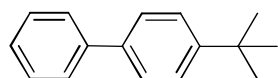
Colourless liquid, GC-MS (M^+): 184; ^1H NMR (400 MHz, CDCl_3): δ 2.60 (s, 3H), 7.41-7.48 (m, 4H), 7.02- 7.70 (m, 4H), 8.04 (d, $J = 6.60$ Hz, 2H); ^{13}C NMR (100 MHz, CDCl_3): 56.8 (s, 1C), 114.2 (s, 2C), 119 (s, 1C) 127.7 (s, 1C) 127.8 (s, 2C), 128.5 (s, 2C), 129 (s, 2C), 133.8 (s, 1C), 140.8 (s, 1C), 158.2 (s, 1C).

4-Nitro biphenyl (Table 5.7, Entry 8)



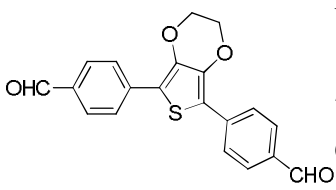
Pale yellow crystal, m.p 114-116 °C; GC-MS (M^+): 199; ^1H NMR (400 MHz, CDCl_3): δ 7.44 (m, 1H), 7.49 (m, 2H), 7.62 (m, 2H), 7.73 (d, $J = 8.84$ Hz, 2H), 8.26 (d, $J = 8.84$ Hz, 2H); ^{13}C NMR (100 MHz, CDCl_3): 123.09 (s, 2C), 126.37 (s, 2C), 126.78 (s, 2C), 127.89 (s, 1C) 128.13 (s, 2C), 137.77 (s, 2C), 146.62 (s, 2C).

4-*t*-butyl biphenyl (Table 5.7, Entry 10)



Liquid, GC-MS (M^+): 210; ^1H NMR (400 MHz, CDCl_3): δ 1.39 (s, 9H), 7.30-7.65 m, 9H); ^{13}C NMR (100 MHz, CDCl_3): 123.09 (s, 2C), 126.37 (s, 2C), 126.78 (s, 2C), 127.89 (s, 1C) 128.13 (s, 2C), 137.77 (s, 2C), 146.62 (s, 2C), 28.14 (s, 1C), 23.25 (s, 3C).

Characterization of the bis-arylated 3,4-(ethylenedioxythiophene) product



Yellow powder; LCMS (M+1): 351.2; m.p 278-280 °C; ¹H NMR (400 MHz, CDCl₃), δ 9.9 (2H, s, CHO), 7.87-7.94 (8H, m), 4.4 (s, 4H); ¹³C NMR (100 MHz, CDCl₃): 64.6, 116.3, 126.1, 130.2, 134.4, 138.5, 140.5, 191.4.

References

- [1] K. Ofele, *J. Organomet. Chem.*, 1968, **12**, 11.
- [2] H. J. Wanzlick and H. J. Schonherr, *Angew. Chem.*, 1968, **80**, 154.
- [3] C. W. K. Gstottmayr, V. P. W. Bohm, E. Herdtweck, M. Grosche and W. A. Herrmann, *Angew. Chem. Int. Ed.*, 2002, **41**, 1363.
- [4] H. Lebel, M. K. Janes, A. B. Charette and S. P. Nolan, *J. Am. Chem. Soc.*, 2004, **126**, 5046.
- [5] A. C. Chen, L. Ren, A. Decken and C. M. Crudden, *Organometallics*, 2000, **19**, 3459.
- [6] X. Wang, S. Liu and G. X. Jin, *Organometallics*, 2004, **23**, 6002.
- [7] D. Bourissou, O. Guerret, F. P. Gabba and G. Bertrand, *Chem. Rev.*, 2000, **100**, 39.
- [8] W. A. Herrmann, *Angew. Chem. Int. Ed.*, 2002, **41**, 1290.
- [9] W. A. Herrmann, M. Elison, J. Fischer, C. Köcher and G. R. J. Artus, *Angew. Chem. Int. Ed. Engl.*, 1995, **34**, 2371.
- [10] B. E. A. Kantchev and J. O. B. Christopher Brien, and M. G. Organ, *Angew. Chem. Int. Ed.*, 2007, **46**, 2768.
- [11] E. Peris and R. H. Crabtree, *Coord. Chem. Rev.*, 2004, **248**, 2239.
- [12] C. M. Crudden and D. P. Allen, *Coord. Chem. Rev.*, 2004, **248**, 2247.

- [13] W. A. Herrmann, K. Tfele, D. V. Preysing and K. S. Schneider, *J. Organomet. Chem.*, 2003, **687**, 229.
- [14] E. Negishi (Ed.), *Handbook of Organopalladium Chemistry for Organic Synthesis*, Wiley: New York, 2002.
- [15] A. de Meijere, F. Diederich (Ed.), *Metal-catalyzed cross-coupling reactions*, 2nd ed.; Wiley: New York, 2004.
- [16] A. J. Arduengo, R. L. Harlow and M. Kline, *J. Am. Chem. Soc.*, 1991, **113**, 361.
- [17] W. A. Herrmann, M. Elison, J. Fischer, C. Kechter and G. R. J. Arthus, *Angew. Chem.*, 1995, **107**, 2602.
- [18] G. M. Roberts, P. J. Pierce and L. K. Woo, *Organometallics*, 2013, **32**, 2033.
- [19] J. H. Kim, J. W. Kim, M. Shokouhimehr and Y. S. Lee, *J. Org. Chem.*, 2005, **70**, 6714.
- [20] S. C. Schurer, S. Gessler, N. Buschmann and S. Blechert, *Angew. Chem. Int. Ed.*, 2000, **39**, 3898.
- [21] J. W. Byun and Y. S. Lee, *Tetrahedron Lett.*, 2004, **45**, 1837.
- [22] C. Zhang, J. Liu and C. Xia, *Catal. Sci. Technol.*, 2015, **5**, 4750.
- [23] D. Y. Zhao, Q. S. Huo, J. L. Feng, B. F. Chmelka and G. D. Stucky, *J. Am. Chem. Soc.*, 1998, **120**, 6024.
- [24] J. C. Vartuli and T. F. Degnan, *Surf. Sci. Catal.*, 2007, **168**, 837.
- [25] O. Aksin, H. Turkmen, L. Artok, B. Cetinkaya, O. Buyukgungor and E. Ozkal, *J. Organomet. Chem.*, 2006, **691**, 3027.
- [26] E. B. Mubofu, J. H. Clark and D. J. Macquarrie, *Green Chem.*, 2001, **3**, 23.
- [27] E. Tyrrell, L. Whiteman and N. Williams, *J. Organomet. Chem.*, 2011, **696**, 3465.
- [28] K. Shimizu, S. Koizumi, T. Hatamachi, H. Yoshida, S. Komai, T. Kodama and Y. Kitayama, *J. Catal.*, 2004, **228**, 141.

- [29] A. F. Littke and G. C. Fu, *Angew. Chem. Int. Ed. Engl.*, 2002, **41**, 4176.
- [30] M. Miura, *Angew. Chem.*, 2004, **116**, 2251; *Angew. Chem. Int. Ed.*, 2004, **43**, 2201.
- [31] S. Kotha, K. Lahiri and D. Kashinath, *Tetrahedron*, 2002, **58**, 9633.
- [32] G. Park, S. Lee, S. J. Son and S. Shin, *Green Chem.*, 2013, **15**, 3468.
- [33] C. Liu, Q. Ni, F. Bao and J. Q. *Green Chem.*, 2011, **13**, 1260.
- [34] M. A. Zolfigol, T. Azadbakht, V. Khakyzadeh, R. Nejatyamid and D. M. Perrinb, *RSC Adv.*, 2014, **4**, 40036.
- [35] C. J. O. Brien, E. A. B. Kantchev, C. Valente, N. Hadei, G. A. Chass, A. Lough, A. C. Hopkinson, and M. G. Organ, *Chem. Eur. J.*, 2006, **12**, 4743.
- [36] R. K. Sharma, Y. Manavi, R. Gaur, Y. Monga and A. Adholeya, *Catal. Sci. Technol.*, 2015, **5**, 2728.
- [37] G. A. Grasa, M. S. Viciu, J. Huang, C. Zhang, M. L. Trudell, and S. P. Nolan, *Organometallics*, 2002, **21**, 2866.
- [38] N. Miyaura and A. Suzuki, *Chem. Rev.*, 1995, **95**, 2457.
- [39] N. Miyaura, (Eds.: A. dMeijere, F. Diederich), Vol. 1, 2nd ed.; Wiley-VCH, Weinheim, 2004, pp.41 – 123.
- [40] A. Suzuki, *Pure Appl. Chem.*, 1991, **63**, 419.
- [41] D. Alberico, M. E. Scott and M. Lautens, *Chem. Rev.*, 2007, **107**, 174.
- [42] G.P. McGlacken and L. M. Bateman *Chem. Soc. Rev.*, 2009, **38**, 2447.
- [43] K. Yoshinno, *Synth. Met.*, 1989, **28**, 669.
- [44] F. Garnier, G. Horowitz, X. Peng and D. Fichou, *Adv. Mater.*, 1990, **2**, 592.
- [45] Y. Fu, H. Cheng and R. L. Elsenbaumer, *Chem. Mater.*, 1997, **9**, 1720.
- [46] G.A Sotizg, T.A Thomas, J. R Reynolds and P.J. Steel, *Macromolecules*, 1998, **31**, 3750.

- [47] A. K. Mohanakrishnan, A. Hucke, M. A. Lyon, M. V. Lakshmikantham and M. P. Cava, *Tetrahedron*, 1999, **55**, 11745.
- [48] M. F. Peptide and S. S. Hardaker, R. V. Gregory, *Chem. Mater.*, 2003, **15**, 557.
- [49] H. Meng, D. Tucker, S. Chaffins, Y. Chen, R. Helgeson, B. Dunn and F. Wudl, *Adv. Mater.* 2003, **15**, 147.
- [50] T. Jeffery, *Tetrahedron*, 1996, **52**, 10113.
- [51] M. Grun, K. K. Unger, A. Matsumoto and K. Tsutsumi, *Microporous Mesoporous Mater.*, 1999, **27**, 207.

Chapter 6

POLYPEPTIDE FUNCTIONALIZED MESOPOROUS SILICA AS CATALYST IN AMINOLYSIS OF EPOXIDES

Contents	6.1 Introduction
	6.2 Results and Discussion
	6.3 Conclusion
	6.4 Experimental

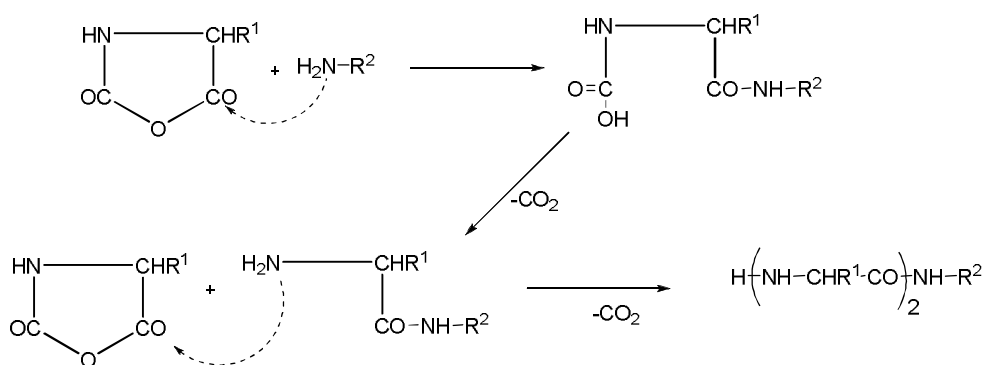
The surface of periodic mesoporous silica was modified by poly(L-phenylalanine) via the ring opening polymerization (ROP) of L-phenylalanine N-carboxyanhydride. Heterogeneous version of polypeptide functionalized silica catalyst is limited, even if it offers many advantages. The preparation was done using NCA polymerization chemistry and the synthesized catalyst was characterized by various techniques and its use in the synthesis of β -amino alcohols is discussed in this chapter.

6.1 Introduction

Polypeptides are considered to be emerging biomaterials possessing wide range of potentials such as chemical diversity, biodegradability, and high biocompatibility. So, they are extensively utilized in drug delivery, tissue engineering, sensing and catalysis.¹⁻⁴

N-carboxylic anhydrides (NCAs) of α -amino acids are a highly important class of cyclic monomers which are commonly used for the synthesis of polypeptides. The synthesis and polymerization of NCAs was first reported by Hermann Leuchs in 1906.⁵ NCAs are usually prepared by phosgenation

of side-chain protected α -amino acids. Among versatile polymerization methods,⁶⁻⁹ ring opening polymerization of NCAs is the most common one for the synthesis of polypeptides in large scale and with high molecular weight.¹⁰ Polypeptide with defined molecular weight was synthesized by ring opening polymerization of α -amino acid NCAs using suitable initiator such as aliphatic primary amine or bases such as triethylamine and sodium methoxide. Generally, NCA polymerization mechanism involves ring opening of NCA resulting in the release of one molecule of carbon dioxide and exposure of a primary amine, which behaves as the active species to open the next NCA monomer and the repetition of this step finally generates the polypeptides.¹¹ Normal route of primary amine-initiated NCA polymerization is shown in Scheme 6.1.



Scheme 6.1 Primary amine-initiated NCA polymerization mechanism¹¹

Grafting of polypeptides onto solid support has become an interesting area in materials chemistry. Y. Dai and coworkers investigated the biocompatibility of poly(L-phenylalanine) modified hydroxyapatite (HA) nanoparticles. HA was modified via the ring opening polymerization (ROP) of L-phenylalanine N-carboxyanhydride and authors considered ROP to be

an efficient surface modification method.¹² Polypeptide grafted silica nanoparticles are very important because, the ordered secondary structure of the polypeptide grafts impart novel functional properties onto the nanoparticle composite.¹³ Kar et al. studied the synthesis of a poly(L-lysine) silica nanoparticle hybrid using the grafting-to approach by employing a combination of NCA polymerization and click chemistry.¹⁴ In recent years, development and application of biomimetic strategies have been used successfully in organic synthesis. Tang et al. developed new covalent immobilization method for the preparation of silica-grafted poly(L-leucine) catalyst. It was achieved via polymerization of L-leucine NCA monomer on amine functionalized silica gel. The prepared catalyst showed good activity in asymmetric epoxidation of benzalacetophenone (Julia-Colonna reaction).¹⁵ Grafting of polypeptide to OMS (ordered mesoporous silica) through NCA chemistry was first reported by Shantz et al.¹⁶ It was achieved through the surface-initiated polymerization of N-carboxyanhydrides from amine-functionalized ordered mesoporous silica. Authors also studied the catalytic activity of the peptide-OMS in nitroaldol reaction (Henry reaction). To the best of our knowledge, there were only a few reports about the surface modification of silica by peptide and their application as heterogeneous catalyst in organic synthesis. So our aim was to synthesize polypeptide functionalized silica and extend its application as supported organocatalyst.

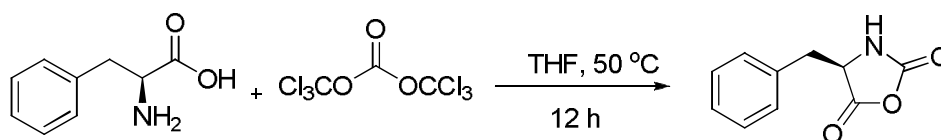
The present chapter discusses the synthesis and characterization of polypeptide functionalized mesoporous silica (MS). Ring opening polymerization (ROP) of NCA was adopted. The prepared material was used as Lewis base catalyst in the synthesis of β -amino alcohols. The

experimental parameters were optimized, scope of substrates, reusability of the catalyst and mechanism were studied.

6.2 Results and Discussion

6.2.1 Synthesis of L-phenylalanine N-carboxyanhydride (Phe-NCA)

L-phenylalanine N-carboxyanhydride (Phe-NCA) was prepared from a reaction of L-phenylalanine with triphosgene according to the reported method.¹⁷ Synthetic route is shown in Scheme 6.2. The product was a previously reported compound and was characterized by m. p, FTIR, and ¹H NMR spectroscopy. FTIR spectrum showed the appearance of two bands at 1840 cm⁻¹ and 1775 cm⁻¹ due to the asymmetric and symmetric stretching vibration of the carbonyl group of carboxyanhydride. ¹H NMR spectrum clearly showed the CH ($\delta = 4.47$ ppm) and NH ($\delta = 5.42$ ppm) signals of the NCA ring.



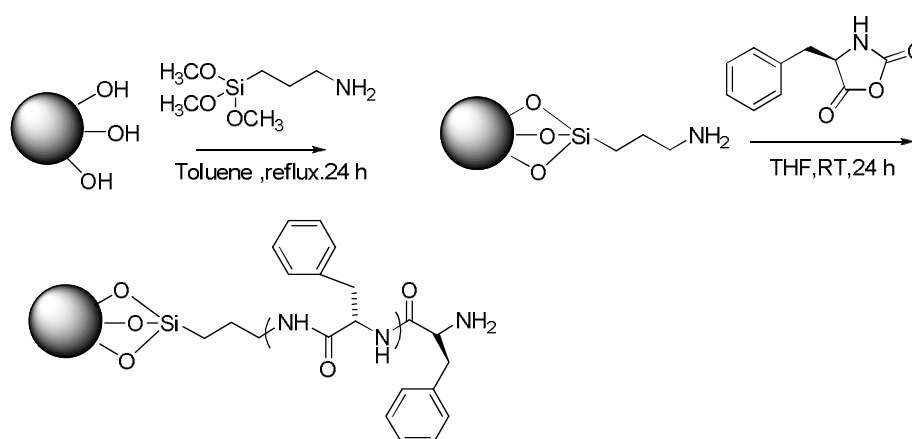
Scheme 6.2 Synthesis of L-phenylalanine N-carboxyanhydride (Phe-NCA)

6.2.2 Grafting of polypeptide onto silica surface

Polypeptide was grafted onto silica surface via ring opening polymerization of NCA via graft from approach. The silanol groups on the mesoporous silica do not act as initiator for the ring opening polymerization. Thus, silica surface was functionalized with 3-aminopropyl triethoxysilane (APTES) in toluene by post-grafting method. It acts as the initiator for polymerization. Three APTES functionalized silica materials were synthesized

with different loading capacity of 0.25 mmol of NH_2/g silica, 0.5 mmol of NH_2/g silica and 1 mmol of NH_2/g silica. The product obtained was designated as 0.25-MS- NH_2 , 0.5-MS- NH_2 and MS- NH_2 .

Using the silica-grafted primary amine, MS- NH_2 as an initiator, N-carboxyanhydride (NCA) of L-phenylalanine was polymerized in THF at room temperature for 24 h under nitrogen atmosphere which provided silica-grafted poly(L-phenylalanine) with degree of polymerization (n) (Scheme 6.3). A series of silica-grafted poly(L-phenylalanine) were prepared with NCA of L-phenylalanine in THF using 30:1 monomer:initiator ratio for the 0.25 mmol of NH_2/g silica, 20:1 and 15:1 for the 0.5 mmol and 1 mmol of NH_2/g silica substrates, respectively. CHN analysis was carried out to quantify the organic functionality on silica surface. The results are given in Table 6.1, which confirmed effective grafting of organic moiety on silica surface. It also showed that composition such as 0.25 mmol and 0.5 mmol of NH_2/g silica showed lower degree of functionalization after polymerization. So the representative catalyst was prepared by taking the initiator:monomer ratio of 1:15 for the 1 mmol of NH_2/g silica and designated as PPh@MS.



Scheme 6.3 Grafting of polypeptide onto silica surface

Table 6.1 Elemental composition of functionalized silica materials

Sample	C (%)	N (%)	H (%)
0.25-MS-NH ₂ /0.25-Pphe@MS	1.53/6.21	0.38/3.9	0.65/1.12
0.5-MS-NH ₂ /0.5-Pphe@MS	3.0/12.1	0.75/8.5	1.10/2.2
MS-NH ₂ / Pphe@MS	5.53/23.4	1.65/19.5	2.19/4.8

Amine capacity of the hybrid materials was measured by titration method and this shows good agreement with the result obtained from UV-Visible spectrophotometric analysis.¹⁸ Estimation of amino groups confirmed the drastic increase of the amount of amino group per gram of the silica. The results are shown in Table 6.2.

Table 6.2 Amine capacity of functionalized silica materials

Sample	NH ₂ content mmol/g ^a	NH ₂ content mmol/g ^b
MS-NH ₂	0.9	1.03
Pphe@MS	12.7	12.5

^aTitration ^b UV-Visible spectrophotometry

6.2.3 Characterization of polypeptide functionalized mesoporous silica catalyst

6.2.3.1 X-ray diffraction studies

Powder X-ray diffraction (PXRD) analysis was carried out to study the structural ordering of synthesized catalyst. XRD diagram of parent silica material was given in chapter 2. Polypeptide functionalized silica showed a diffraction in low angle region which confirmed the presence of mesophase in the synthesized sample (Figure 6.1). The intensity was significantly decreased after polymerization which confirmed successful grafting of polypeptide onto silica surface.

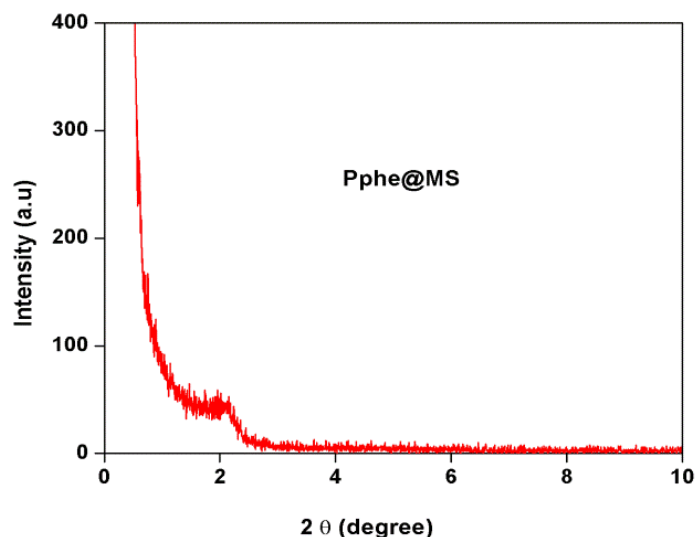


Fig. 6.1 XRD diagram of PPhe@MS

6.2.3.2 Surface area analysis

Nitrogen sorption measurements were performed to quantify the changes in porosity in the mesoporous silica resulting from functionalization (Figure 6.2). Amine-functionalized silica maintained its porosity with changes in the pore size and pore volume. The surface area, pore volume and pore diameter decreased dramatically after polymerization. The overall shape of the adsorption/desorption isotherms remained unchanged, and the pronounced steps of capillary condensation in primary mesopores were evident, indicating that the ordering of the MS support was not affected by the modification upto the polymerization step. A summary of the structural properties of these materials is shown in Table 6.3.

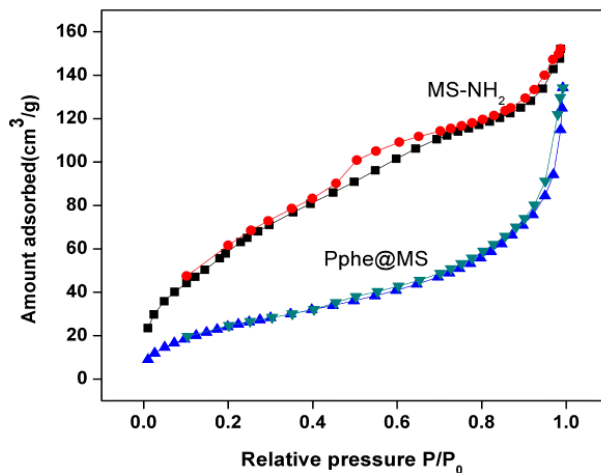


Fig. 6.2 N₂ adsorption/desorption isotherms of functionalized MS

Table 6.3 Structural properties of functionalized materials

Sample	S _{BET} (m ² /g)	V _p (cm ³ /g)	d _p (BJH) [nm]
MS	1039	0.75	2.8
MS-NH ₂	585	0.51	2.5
Pphe@MS	155	0.22	2.1

6.2.3.3 IR spectral studies

FTIR spectra of the amine functionalized silica and polypeptide functionalized silica are shown in Fig 6.3. It was used to verify the presence of the peptide functionality as manifested by the appearance of the amide bands. The silanol (Si-OH) and Si-O-Si bands from the parent silica material are observed at 3450 cm⁻¹ (broad) and 1080 cm⁻¹, respectively. The N-H stretching vibrations occur as two weak absorption bands in the 3500-3400 cm⁻¹ region. Here, the bands are masked by the bands of silanol groups.

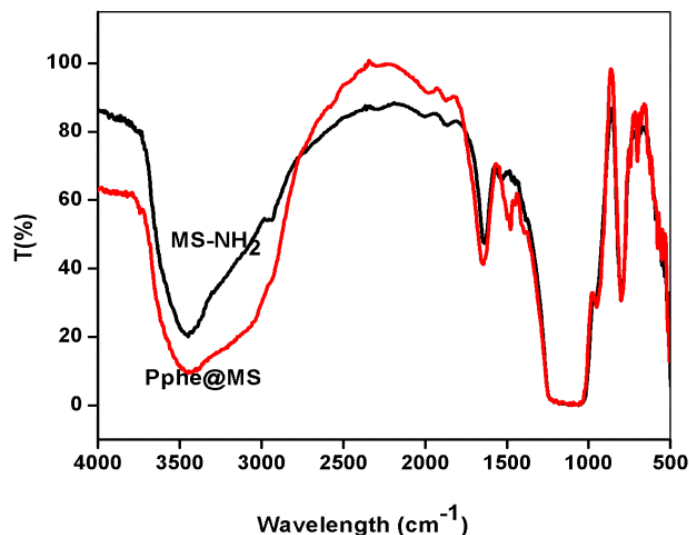


Fig. 6.3 IR spectra of MS-NH₂ and Pphe@MS

The N-H bending vibrations of primary amines are observed in the 1650-1580 cm⁻¹ region. The corresponding CO stretching and the N-H bending vibrations of amide are observed at 1651 cm⁻¹ and 1515 cm⁻¹, respectively. The amide peaks are more intense relative to those corresponding to the amine functionalized silica (MS-NH₂), suggesting that effective grafting of polypeptide was achieved.

6.2.3.4 Solid state ¹³C CP-MAS NMR spectroscopy

Solid state ¹³C CP-MAS NMR analysis was performed on polypeptide functionalized silica catalyst. It provides further evidence for covalent binding of peptide on silica framework (Figure 6.4). The peaks between 20-60 ppm are the characteristic peaks of aliphatic side chain carbon atoms and amide carbon was observed at 173-175 ppm. The peaks between 125-138 ppm are the aromatic carbons. Two of the aminosilane carbons are obscured by the resonances of the phenylalanine side chain. However, the

methyl carbon peak with reference to the silicon atom was observed at 9.4 ppm.^{19,20} Another interesting feature is the lack of any carboxylic acid carbon peak at 180 ppm. If peptide was formed in solution and merely adsorbed on the surface, this peak would be observed. It also confirmed an efficient covalent immobilization of peptide onto silica surface.

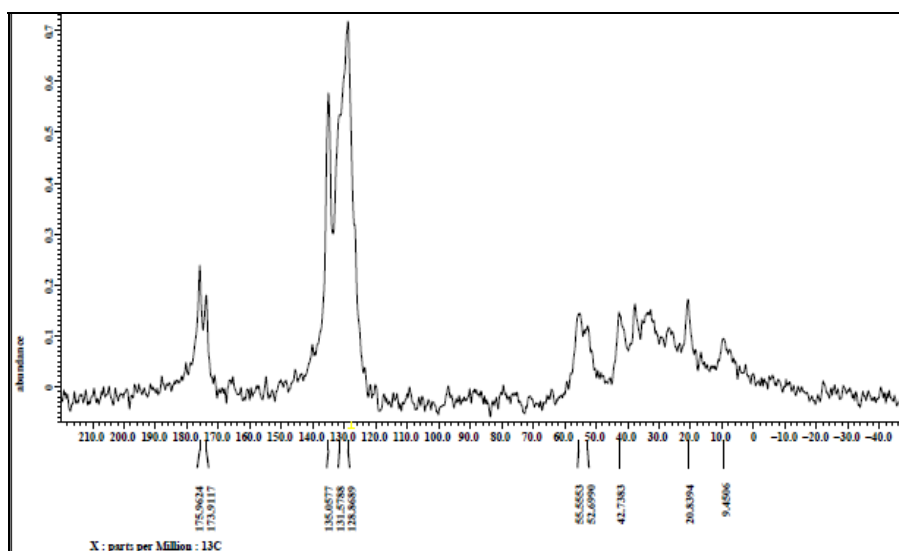


Fig. 6.4 ^{13}C CP-MAS NMR spectrum of Pphe@MS

6.2.3.5 TG-DTG analysis

The thermal stability of peptide functionalized silica system was studied by thermogravimetric analysis. TG plots of the Pphe@MS (Figure 6.5) showed first weight loss below 100 °C due to loss of physically adsorbed water. It showed a continuous mass loss in the range 200–600 °C, which was due to the removal of organic functionality on the silica surface. The decomposition between 200–300 °C corresponded to nearly 21 % mass loss,

which could be attributed to elimination of amine functionality as molecular nitrogen. The weight loss above 500 °C was due to the thermal degradation of the polymer backbone leading to the formation of hydrogen, carbon monoxide, carbon dioxide, methane, ammonia, hydrogen cyanide gas and other higher hydrocarbons.²¹

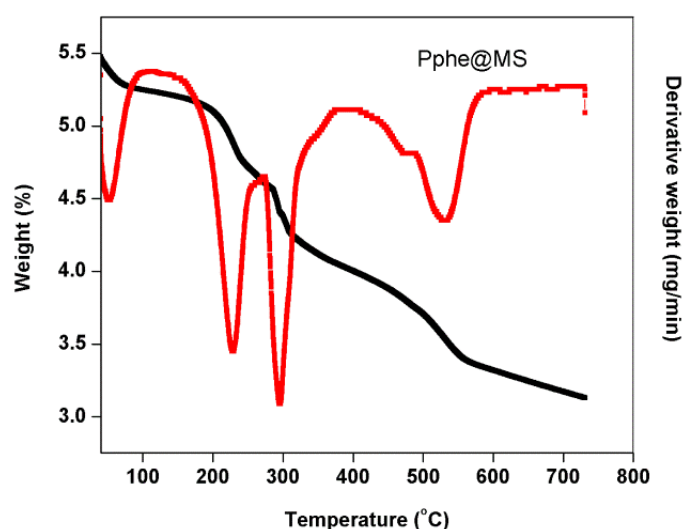


Fig. 6.5 TG-DTG plot of Pphe@MS

6.2.3.6 Gel permeation chromatography (GPC) analysis

GPC diagram of cleaved peptide from MS is depicted in Figure 6.6. The grafted peptide was cleaved from the silica surface according to the procedure described in literature.²² Polypeptide can be cleaved as fluorinated silane without decomposition and high organic loading was obtained.

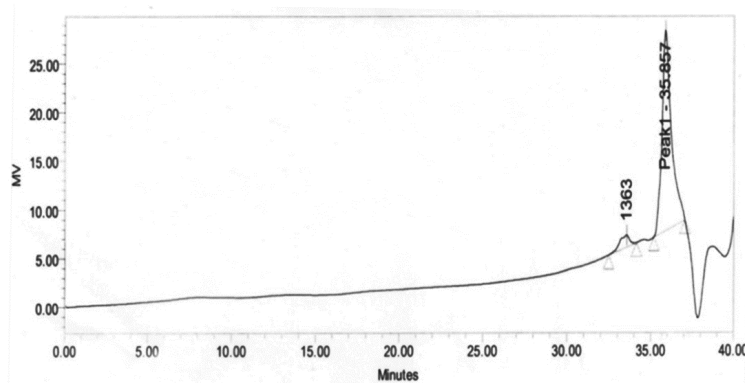


Fig. 6.6 GPC diagram of cleaved polypeptide

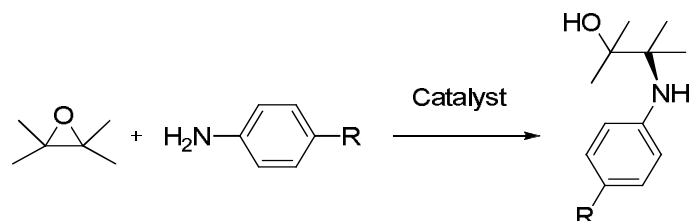
The average molecular weight (M_w) of the polypeptide was found to be 1511 with polydispersity index of 1.02, which confirmed that NCA polymerization resulted in a monodisperse polymer molecular weight.^{23,24} From the molecular weight, it is found that peptide length is limited to 8 monomer units.

6.2.4 Evaluation of catalytic performance

6.2.4.1 Aminolysis of epoxides (synthesis of β -amino alcohols)

Epoxides are small molecules with wide synthetic applications. They easily react with various nucleophiles regioselectively via ring opening reaction and leads to highly useful precursors which are used for the synthesis of new libraries of bioactive compounds. Among them, the reaction of epoxides with amines is particularly interesting, because it gives β -amino alcohols (Scheme 6.4).

β -amino alcohols are versatile intermediates in the synthesis of biologically active natural products, unnatural amino acids, β -blockers as well as insecticidal agent and chiral auxiliaries.²⁵⁻³⁰

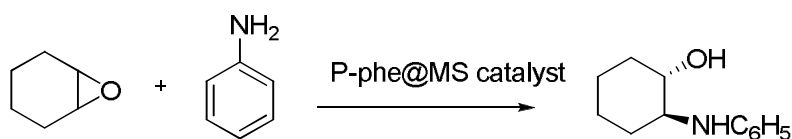


Scheme 6.4 Reaction of epoxide with amine

Classically, β-amino alcohols were synthesized by aminolysis of epoxides through heating with an excess of amine. This classical method has a number of limitations, such as the requirement of an excess of inorganic base, longer reaction times, low nucleophilicity in the case of deactivated aromatic amines, poor regioselectivity, elevated temperature.³¹ Some of these drawbacks have been overcome with the use of a variety of catalysts.³²⁻⁴⁰ There are still many limitations with these reported strategies such as the formation of bisalkylated products, longer reaction times, stoichiometric amounts of catalysts, harsh reaction conditions, moderate yields, use of air and moisture sensitive catalysts and problems in the recovery of the catalysts. Some of these methods are not applicable for aliphatic amines and lead to catalyst poisoning.⁴¹⁻⁴⁵ A new improved catalytic system has been reported recently using mesoporous Zr-Beta zeolites by Li et al.⁴⁶ The catalyst exhibited excellent activity and selectivity, but required high amount of catalyst loading. Recent advances in the asymmetric reactions of meso and racemic epoxides promoted by organocatalysts were reviewed recently. The organocatalyzed reactions of epoxides by chiral phosphoric acids, amino- and peptidylthioureas, and sulfinamides were discussed in detail.⁴⁷ Despite the large number of methodologies available for this purpose, there is a demand for better catalysts. Therefore, the development

of highly efficient, nonhazardous and easily separable catalyst is highly imperative for the synthesis of β -amino alcohols. In this sense, we have focused our attention to synthesize β -amino alcohols using high dense Lewis base catalyst: polypeptide supported on mesoporous silica.

A variety of β -amino alcohols have been synthesized in excellent yields by reaction of epoxides and amines using polypeptide functionalized mesoporous silica as supported Lewis base catalyst. The reaction condition was optimized by evaluating the effect of various reaction parameters, such as type of solvent, reaction temperature, catalyst concentration, etc., in the model reaction between cyclohexene oxide and aniline (Scheme 6.5).



Scheme 6.5 Aminolysis of epoxide by Pphe@MS catalyst

Initially, the influence of the amount of catalyst on the reaction was studied. The yield of the product was low when low amount of the catalyst was used. It was observed that, only 3 mol% of the catalyst was required for obtaining good yield. It is noted that large amount of catalyst did not improve the rate of the reaction and yield of the product. The reaction proceeded slowly at room temperature and took 5 h for completion. When the temperature was increased upto to 50 °C, the reaction was completed within 1 h and 100 % conversion to the product was obtained as observed from GC-MS. Further increase of temperature did not influence the yield and reaction rate. High accessibility of Lewis base site and ordered porous

nature of the support allowed use of small amount of catalyst and shorter reaction time.

To examine the influence of solvent, the model reaction between cyclohexene oxide and aniline was performed in various solvents under identical conditions and the results are shown in Table 6.4. It was observed that solvent has profound effect on yield of the product. The reaction proceeded best in dioxane compared to other solvents and 100 % conversion to the product was observed from GC-MS. The reaction in H₂O showed good result, because in water the peptide functionality on the support can be well dispersed and facilitated the reaction. Also, it is reported that epoxides react very efficiently in water with several nucleophiles, and the use of water as reaction medium is essential for realizing processes that cannot be performed alternatively in other reaction media.⁵¹ The reaction showed satisfying performance in chloroform and acetonitrile.

Table 6.4 Effect of solvent

Entry	Solvent	Yield (%) ^{a,b}
1	H ₂ O	89
2	THF	70
3	Dioxane	100
4	CH ₃ CN	76
5	CHCl ₃	72
6	No Solvent	68

^a Reaction conditions: 5 mmol cyclohexene oxide, 5.2 mmol aniline, 3 mol% of catalyst, 5 mL solvent, 50 °C, 1 h. ^b yield by GC-MS.

To establish the catalytic efficiency of the synthesized catalyst, the optimized condition was applied to a number of amines and epoxides. The results are presented in Table 6.5.

Table 6.5 Aminolysis of epoxides catalyzed by Pphe@MS

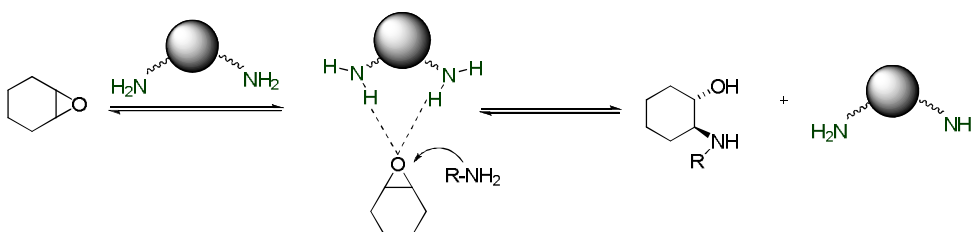
Entry	Epoxide	Amines	Time (h)	Yield (%) ^{a,b}
1	Cyclohexene oxide	Aniline	1	100
2	Cyclohexene oxide	3-chloroaniline	3	86
3	Cyclohexene oxide	2-methylaniline	3	90
4	Cyclohexene oxide	4-methylaniline	3	92
5	Cyclohexene oxide	4-methoxyaniline	2	93
6	Cyclohexene oxide	4-nitroaniline	5	85
7	Cyclohexene oxide	2-methyl 4-nitroaniline	5	82
8	Cyclohexene oxide	4-chloroaniline	2.5	90
9	Cyclohexene oxide	Benzylamine	5	95
10	Styrene oxide	Aniline	1	98
11	Styrene oxide	4-chloroaniline	2.5	92
12	Styrene oxide	2-methylaniline	1.5	95
13	Styrene oxide	4-nitroaniline	5	88
14	Styrene oxide	4-methoxyaniline	1.5	98
15	Styrene oxide	3-chloroaniline	3	86
16	Styrene oxide	Benzylamine	3	90

^a Reaction conditions: 5 mmol epoxide, 5.2 mmol aniline, 3 mol% of catalyst, 5 mL dioxane, 50 °C, ^b isolated yield.

It was observed that, the corresponding amino alcohols were obtained in all cases in excellent yields. Anilines with electron donating as well as electron withdrawing groups such as -CH₃, -OCH₃, -Cl, -NO₂ were well tolerated and gave the corresponding β-amino alcohols in quantitative yields. Amines such as o-methylaniline, o-methoxyaniline, also reacted smoothly. In the case of aminolysis of cyclohexene oxide with amines, the resultant product, racemic 2-amino cyclohexanol was identified as the trans-diastereoisomer on the basis of NMR spectral data. In the aminolysis of styrene oxide, the aromatic amine preferably attacked at the benzylic position (C_α) of epoxide whereas, aliphatic amine attacked at the less hindered methylene carbon (C_β) of the epoxide.

6.2.4.2 Reaction mechanism

The mechanism of the reaction involved activation of the epoxide via coordination with solid base catalyst through hydrogen bonding. It is followed by the attack of amine nucleophile, the resultant intermediate would then undergo a rapid proton transfer to give the desired product and the catalytic species. This can be represented as shown in Scheme 6.6. Similar double hydrogen bonding catalyzed ring opening of epoxides by nucleophiles was reported earlier.⁴⁹⁻⁵¹ The trans configuration of the product was confirmed from the determination of the H-H coupling constants for CH-NH in the corresponding ¹H NMR spectrum. This configuration of the products also supports the presented mechanism.



Scheme 6.6 Possible mechanism of aminolysis of epoxides

6.2.4.3 Effect of recycling on catalysis

The reusability and the activity of the catalyst was investigated. After completion of the reaction, the catalyst was washed with ethyl acetate repeatedly, and dried at 50 °C under vacuum for 4 h and reused directly for five subsequent runs. As shown in Figure 6.7, the yield of the product was decreased only slightly after four runs.

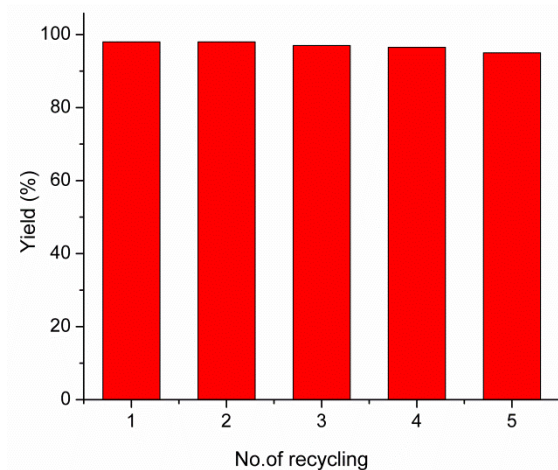


Fig. 6.7 Recycling study of Pphe@MS in aminolysis of epoxides

Reaction conditions: 5 mmol cyclohexene oxide, 5.2 mmol aniline, 3 mol% of catalyst, 5 mL solvent, 50 °C, 1 h, yield by GC-MS

6.3 Conclusion

To conclude, N-carboxyanhydride of L-phenylalanine was synthesized and characterized. NCA polymerization chemistry was used to synthesize polypeptide functionalized on mesoporous silica. Ordered mesoporous nature of the support was maintained after polymerization. This novel catalyst was used as supported organocatalyst in ring opening reaction of epoxides by amines. Various factors affecting the catalytic activity like amount of catalyst, solvent, temperature were studied in detail. The catalyst was recycled and reused without considerable loss of activity. High accessibility of Lewis base site and ordered porous nature of the support allowed use of small amount of catalyst and shorter reaction time. So this protocol combines the synergistic effect of green chemistry with functionalized mesoporous silica materials. Further investigation on application of this catalyst for other organic reactions is in progress.

6.4 Experimental

6.4.1 Materials

3-Aminopropyl triethoxysilane (APTES, Aldrich, 97 %) was used for post synthetic grafting which was distilled prior to use. Triphosgene and L-phenylalanine were received from Aldrich. All other reagents were purchased from local chemical suppliers and were used as received. All the solvents were purified according to the standard procedures. Hydrofluoric acid (48 wt% in water) was used for dissolution of silica framework.

6.4.2 Preparation of amine-functionalized MS (MS-NH₂)

Mesoporous silica (MS) was dried at 90 °C under vacuum for 12 h prior to use. MS (1 g) was suspended in dry toluene (30 mL) under N₂ atmosphere. To this, 0.25 mmol, 0.5 mmol or 0.75 mmol of distilled APTMS depending upon the desired degree of functionalization was added and stirred at room temperature for 24 h. The product was filtered, washed with toluene (5 mL × 3 times) and methanol (10 mL × 3 times) and dried at 60 °C overnight.

White powder; Yield 1.02 g; IR (cm⁻¹): $\bar{\nu}$ 3400 (N-H stretching), 2930 (C-H stretching), 1700-1400 (C-H bending), 1650-1580 (N-H bending); CHN analysis: C (5.53 %), N (1.65 %), H (2.19 %); Amine capacity of MS-NH₂: 0.965 mmol/g.

6.4.3 Preparation of L-phenylalanine N-carboxyanhydride (Phe-NCA)

L-phenylalanine N-carboxyanhydride (Phe-NCA) was synthesized according to the reported approach.¹⁷ L-phenylalanine (5 g, 30.3 mmol) was suspended in anhydrous THF (50 mL) and heated to 50 °C under nitrogen

atmosphere, triphosgene (3 g, 12.1 mmol) in anhydrous THF was added dropwise to the suspension. The reaction mixture was stirred for about 3 h at 50 °C till the suspension became a transparent solution. The solution was poured into petroleum ether (300 mL), stored in a freezer for 12 h; and white precipitate was formed. Finally, the white product was collected and recrystallized from a mixture of anhydrous ethyl acetate/petroleum ether.

Yield 80 %; White crystals; m. p 89-91 °C; LCMS (M+1): m/z 191.8.

IR (KBr): $\bar{\nu}$ 3250, 3100, 2859, 1840, 1775, 1585, 1400, 900 cm^{-1} ; ^1H NMR (CDCl_3 , 400 MHz): δ 2.87-2.93 (dd, $J = 9.2, 8.8$ Hz, 1H), 3.23-3.28 (dd, $J = 4.4$ Hz, 1H), 4.47 (m, 1H), 5.42 (bs, 1H), 7.12-7.31 (m, 5H); ^{13}C NMR (CDCl_3 , 100 MHz): 32.5, 60.6, 125.2, 125.7, 132.1, 148.1, 169.5.

6.4.4 Preparation of polypeptide functionalized silica (Pphe@MS)

Amine-functionalized MS (MS-NH₂) was dried at 80 °C under vacuum for 24 h prior to use. L-phenylalanine N-carboxyanhydride (2.8 g, 15 mmol) was dissolved in anhydrous THF (50 mL) under N₂ atmosphere and transferred to the dried MS-NH₂ (1 g) via cannula. The solution was vigorously stirred at room temperature for 24 h. After completion, the powder was filtered and stirred with THF (50 mL, 3 h), DMF (50 mL, 3 h) and finally washed with chloroform (15 mL x 2 times) and dried under vacuum at room temperature. Polypeptide functionalized silica with other compositions such as 0.25 mmol and 0.5 mmol of NH₂/g silica was prepared in the same manner.

Yield 1.35 g, Off white powder; IR (KBr): $\bar{\nu}$ 3454, 1651, 1515, 1401, 1116, 785 cm^{-1} ; CHN analysis: C (26.4 %), N (19.5 %), H (4.18 %); Amine capacity: 12.6 mmol/g; Solid state ^{13}C CP-MAS NMR (100 MHz): 9.49, 20.8, 42.3, 52.4, 55.5, 128.8, 133.5, 138.0, 173.9, 175.3 ppm.

6.4.5 Cleaving of grafted polypeptide from silica

Polypeptide from the silica surface was cleaved by dissolving 50 mg of silica in 10 mL of 1:1 solution of 48 wt% aqueous HF and THF respectively. The mixture was stirred for 24 h and evaporated to dryness in a Teflon petridish. The residue was decanted with THF and subjected to spectral analysis.

\bar{M}_n (GPC): 1511, PDI: 1.02; ^1H NMR (CDCl_3 , 400 MHz): δ 0.92 (t, CH_2 proton), 1.12 (m, CH_2 proton), 2.5 (m, CH_2 proton), 7.75 (bs, CO-NH proton), 3.95 (m, CH proton), 3.01-3.12 (d, CH_2 proton), 3.56 (m, CH), 4.95 (bs, NH_2 proton), 6.69-7.01 (m, aromatic).

6.4.6 Estimation of $-\text{NH}_2$ group capacity

The amine content of functionalized MS was estimated via aqueous HCl consumption using the acid–base titration method. Typically, 100 mg of functionalized MS was suspended in 30 mL of 0.1 M HCl solution and stirred at ambient temperature for 24 h. The filtrate was titrated with NaOH solution (0.1 M). The $-\text{NH}_2$ group capacity was further verified using UV-Visible spectrophotometric analysis.

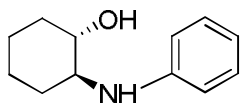
6.4.7 General procedure for the synthesis of β -amino alcohols

A 10 mL round bottom flask was charged with epoxide (5 mmol) and amine (5.2 mmol) and polymer supported catalyst. The amount of catalyst taken was such that each reaction mixture contained 0.15 mmol of the active sites (3 mol% with respect to the epoxide). 5 mL of dry dioxane was added and the reaction mixture was kept in an oil bath with the temperature preset at 50 °C with constant stirring. The progress of the reaction was

monitored by TLC on silica gel plate using hexane and ethyl acetate (25:1) as eluent. After the completion of the reaction, the catalyst was filtered off and washed with ethyl acetate. The filtrate and washings were combined and the solvent was removed under vacuum. The crude product was purified by column chromatography on silica gel using hexane-ethyl acetate (25:1) as eluent. All the products were previously reported compounds and were characterized using FTIR and ^1H NMR spectroscopy. The analytical data for the compounds are given below.

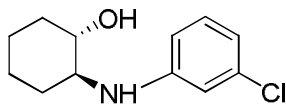
Characterization of β -amino alcohols

trans-2-(phenylamino) cyclohexanol (Table 6.5, Entry 1):



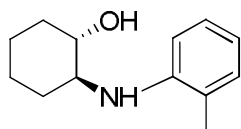
Purple solid, m.p 60-62 °C; GC-MS (M^+): 191; IR (KBr): $\bar{\nu}$ 3510, 3314, 2931, 2858, 1601, 1500, 1448, 1319, 1067 cm^{-1} ; ^1H NMR (CDCl_3 , 400 MHz): δ 6.63-7.12 (m, 5 H), 3.31 (ddd, $J = 4.8, 10.1$ and 10.2 Hz, 1H), 3.10 (ddd, $J = 4, 10.0$ and 9.8 Hz, 1H), 2.7 (m, 2H), 2.01-2.07 (m, 2H), 1.66-1.70 (m, 2 H), 1.18-1.31 (m, 4 H).

trans-2-(3-chlorophenylamino) cyclohexanol (Table 6.5, Entry 2):



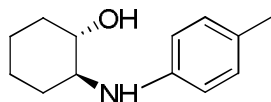
Light brown oil; GC-MS (M^+): 225; IR (neat): $\bar{\nu}$ 3525, 3475, 2956, 2878, 1631, 1520, 1476, 1343, 1087, 765 cm^{-1} ; ^1H NMR (CDCl_3 , 400 MHz): δ 6.73-7.24 (m, 4 H), 3.34 (ddd, $J = 4.6, 10.0$ and 10.1 Hz, 1H), 3.21 (ddd, $J = 3.9, 9.8$ and 9.8 Hz, 1H), 2.9 (m, 2H), 2.12-2.17 (m, 2H), 1.76-1.80 (m, 2H), 1.21-1.39 (m, 4H).

***trans*-2-(2-methylphenylamino) cyclohexanol (Table 6.5, Entry 3):**



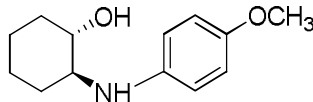
Light brown oil; GC-MS (M^+): 205; IR (neat): $\bar{\nu}$ 3537, 3400, 2945, 2335, 1609, 1564, 1450, 1326, 1073 cm^{-1} ; ^1H NMR (CDCl_3 , 400 MHz): δ 6.98 (m, 2H), 6.85 (d, $J = 8.0$ Hz, 1H), 6.67 (m, 1H), 3.38 (ddd, $J = 10.3, 9.2$ and 4.0 Hz, 1H), 3.18 (ddd, $J = 10.7, 9.2$ and 3.1 Hz, 1H), 2.2 (s, 3H), 2.15 (m, 2H), 1.3 (m, 2H), 1.4 (m, 3H), 1.1 (m, 1H).

***trans*-2-(4-methylphenylamino) cyclohexanol (Table 6.5, Entry 4):**



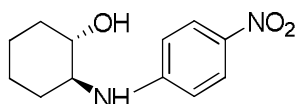
Light brown oil; GC-MS (M^+): 205; IR (neat): $\bar{\nu}$ 3517, 3380, 2845, 2275, 1567, 1504, 1412, 1301, 1052 cm^{-1} ; ^1H NMR (CDCl_3 , 400 MHz): δ 6.98 (d, $J = 8.2$ Hz, 2H), 6.89 (d, $J = 8.2$ Hz, 2H), 3.4 (ddd, $J = 10.1, 9.0$ and 4.0 Hz, 1H), 3.2 (ddd, $J = 10.6, 9.0$ and 3.0 Hz, 1H), 2.17 (s, 3H), 2.15 (m, 2H), 1.25 (m, 2H), 1.38 (m, 3H), 0.98 (m, 1H).

***trans*-2-(4-methoxyphenylamino) cyclohexanol (Table 6.5, Entry 5):**

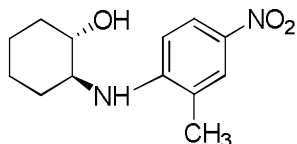


Brown solid, m.p 59-61 $^{\circ}\text{C}$; GC-MS (M^+): 221; IR (KBr): $\bar{\nu}$ 3509, 3366, 3013, 2938, 2861, 1612, 1512, 1465, 1450, 1239, 1221, 1067 cm^{-1} ; ^1H NMR (CDCl_3 , 400 MHz): δ 6.7 (d, $J = 8$ Hz, 2H), 6.6 (d, $J = 8$ Hz, 2H), 3.67 (s, 3H), 3.2 (ddd, $J = 9.5, 9.3$ and 3.9 Hz, 1H), 3.0 (ddd, $J = 10.9, 9.3$ and 3.8 Hz, 1H), 2.04 (m, 2H), 1.70 (m, 2H), 1.28 (m, 3H), 0.95 (m, 1H).

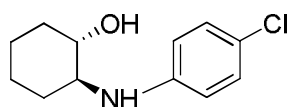
***trans*-2-(4-nitrophenylamino) cyclohexanol (Table 6.5, Entry 6):**



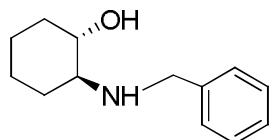
Yellow solid, m.p 120-121 $^{\circ}\text{C}$; GC-MS (M^+): 236; IR (KBr): $\bar{\nu}$ 3550, 3420, 2987, 2873, 1601, 1592, 1476, 1228, 1073 cm^{-1} ; ^1H NMR (CDCl_3 , 400 MHz): δ 7.76-7.81 (d, $J = 9.0$ Hz, 2H) 6.61 (d, $J = 9.0$ Hz, 2H), 4.82 (s, 2H), 3.41 (ddd, $J = 10.2, 10.2$ and 4.5 Hz, 1H), 3.25 (m, 1H), 2.00 (m, 2H), 1.70 (m, 2H), 1.25 (m, 4H).

trans-2-(2-methyl-4-nitrophenylamino) cyclohexanol (Table 6.5, Entry 7):

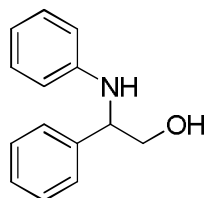
Brown oil; GC-MS (M^+): 250; IR (neat): $\bar{\nu}$ 3517, 3380, 2945, 2875, 1601, 1545, 1449, 1033, 890 cm^{-1} ; ^1H NMR (CDCl_3 , 400 MHz): δ 7.12 (m, 2H), 6.85 (d, $J = 8.0$ Hz, 1 H), 4.81 (s, 2H), 3.41 (ddd, $J = 10.0, 10.0$ and 4.53 Hz, 1H), 3.23 (m, 1H), 2.05 (m, 2H), 1.69 (m, 2H), 1.22 (m, 4H).

trans-2-(4-chlorophenylamino) cyclohexanol (Table 6.5, Entry 8):

Brown solid, m.p 74-76 $^{\circ}\text{C}$; GC-MS (M^+): 225; IR (KBr): $\bar{\nu}$ 3524, 3455, 2856, 2870, 1631, 1510, 1476, 1343, 1087, 765 cm^{-1} ; ^1H NMR (CDCl_3 , 400 MHz): δ 6.73-6.80 (d, $J = 8$ Hz, 2 H), 7.05-7.12 (dd, $J = 8$ Hz, 2 H), 3.31 (ddd, $J = 4.6, 10.0$ and 10.1 Hz, 1H), 3.18 (ddd, $J = 3.9, 9.8$ and 9.8 Hz, 1H), 2.7 (m, 2H), 2.12-2.15 (m, 2H), 1.76-1.82 (m, 2 H), 1.32-1.37 (m, 2H), 1.14-1.20 (m, 2H).

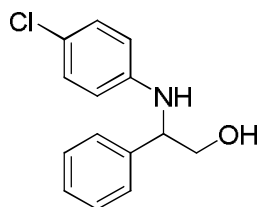
2-(benzylamino)cyclohexanol (Table 6.5, Entry 9):

Light brown solid, m.p 71-73 $^{\circ}\text{C}$; GC-MS (M^+): 205; IR (KBr): $\bar{\nu}$ 3539, 3376, 3021, 2988, 2861, 1632, 1512, 1465, 1455, 1245, 1227, 1067 cm^{-1} ; ^1H NMR (CDCl_3 , 400 MHz): δ 1.10-1.40 (m, 4H), 1.60-1.75 (m, 2H), 1.85-2.00 (m, 2H), 2.25 (bs, 1H), 3.20-3.30 (m, 1H), 3.40-3.50 (m, 1H), 3.85 (bs, 1H), 4.00 (s, 2H), 7.20-7.40 (m, 5H).

2-(phenylamino)-2-phenylethanol (Table 6.5, Entry 10):

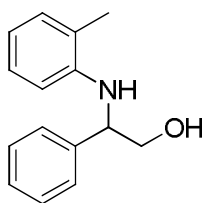
Yellow oil; GC-MS (M^+): 213; IR (neat): $\bar{\nu}$ 3493, 3354, 2931, 2353, 1601, 1500, 1443, 1319, 1037 cm^{-1} ; ^1H NMR (CDCl_3 , 400 MHz): δ 6.5-7.4 (m, 10H), 4.3 (dd, $J = 7.0, 4.0$ Hz, 1H), 3.90 (dd, $J = 11.0, 4.0$ Hz, 1H), 3.72 (dd, $J = 11.0, 7.0$ Hz, 1H).

2-(4-chlorophenylamino)-2-phenylethanol (Table 6.5, Entry 11):



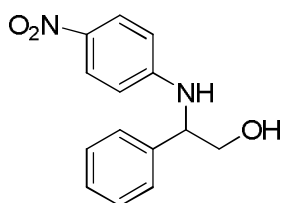
Yellow oil; GC-MS (M^+): 247; IR (neat): $\bar{\nu}$ 3497, 3374, 2951, 2373, 1641, 1550, 1463, 1339, 1047, 743 cm^{-1} ; ^1H NMR (CDCl_3 , 400 MHz): δ 6.73-7.24 (d, $J = 8$ Hz, 2H, d, $J = 8$ Hz, 2H), 6.8-6.9 (m, 5H), 4.3 (dd, $J = 7.0$, 4.0 Hz, 1H), 3.65 (dd, $J = 10.5$, 3.8 Hz, 1H), 3.55 (dd, $J = 10.5$, 6.6 Hz, 1H).

2-(2-methylphenylamino)-2-phenylethanol (Table 6.5, Entry 12):



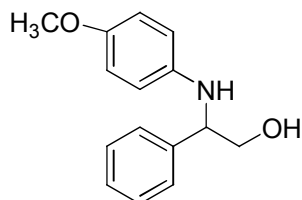
Yellow oil; GC-MS (M^+): 227; IR (neat): $\bar{\nu}$ 3500, 3394, 2990, 2888, 1613, 1511, 1446, 1321, 1087 cm^{-1} ; ^1H NMR (CDCl_3 , 400 MHz): δ 7.20-7.36 (m, 5 H), 6.9 (d, $J = 7.0$ Hz, 1H), 6.84 (t, $J = 7.4$ Hz, 1 H), 6.57 (t, $J = 7.4$ Hz, 1 H), 6.29 (d, $J = 8.1$ Hz, 1H), 4.50-4.56 (m, 1H), 3.94-4.01 (m, 1H), 3.73-3.80 (m, 1H), 2.23 (s, 3H).

2-(4-nitrophenylamino)-2-phenylethanol (Table 6.5, Entry 13):

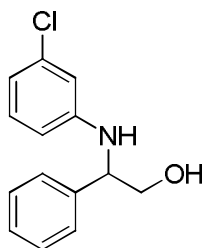


Yellow oil; GC-MS (M^+): 258; IR (neat): $\bar{\nu}$ 3517, 3380, 2945, 2875, 1601, 1592, 1523, 1349, 1073, 890 cm^{-1} ; ^1H NMR (CDCl_3 , 400 MHz): δ 7.31-7.46 (d, $J = 8.8$ Hz, 2H), 6.91-7.11 (d, $J = 8.8$ Hz, 2H), 6.8-6.9 (m, 5H), 4.6 (dd, $J = 7.2$, 4.0 Hz, 1H), 3.78 (dd, $J = 10.8$, 4.0 Hz, 1H), 3.55 (dd, $J = 10.8$, 6.8 Hz, 1H).

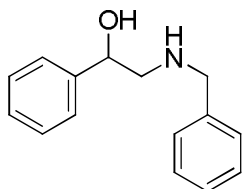
2-(4-methoxyphenylamino)-2-phenylethanol (Table 6.5, Entry 14):



Yellow oil; GC-MS (M^+): 243; IR (neat): $\bar{\nu}$ 3503, 3354, 2931, 2858, 1601, 1500, 1448, 1319, 1067 cm^{-1} ; ^1H NMR (CDCl_3 , 400 MHz): δ 7.40-6.50 (m, 9 H), 4.80 (dd, $J = 3.1$, 9.0 Hz, 1H), 3.69 (s, 3H), 3.45 (dd, $J = 12.0$, 3.1 Hz, 1H), 3.30 (dd, $J = 12.0$, 9.0 Hz, 1H).

2-(3-chlorophenylamino)-2-phenylethanol (Table 6.5, Entry 15):

Yellow oil; GC-MS (M^+): 247; IR (neat): $\bar{\nu}$ 3404, 3062, 3028, 2926, 2875, 1597, 1485 cm^{-1} ; ^1H NMR (400 MHz, CDCl_3): δ 3.89 (dd, $J = 6.6, 4.0$ Hz, 1H), 4.12 (dd, $J = 10.8, 4.0$ Hz, 1H), 4.05 (dd, $J = 10.8, 6.8$ Hz, 1H), 6.71-6.81 (m, 3H), 7.33 (t, $J = 2.1$ Hz, 1H), 7.25-7.36 (m, 5H).

2-(benzylamino)-1-phenylethanol (Table 6.5, Entry 16):

Yellow solid; m.p 98-100 $^{\circ}\text{C}$; GC-MS (M^+): 227; IR (KBr): $\bar{\nu}$ 3478, 3276, 3011, 2948, 2869, 1642, 1519, 1465, 1450, 1245, 1064 cm^{-1} ; ^1H NMR (CDCl_3 , 400 MHz): 3.50 (dd, 1H), 3.70 (dd, 1H), 3.95 (bs, 1H), 4.20 (s, 2H), 4.65 (t, 1H), 7.15-7.40 (m, 10H).

References

- [1] T. J. Deming, *Adv. Drug Delivery Rev.*, 2002, **54**, 1145.
- [2] X. Y. Wang, H. J. Kim, C. Wong, C. Vepari, A. Matsumoto and D. L. Kaplan, *Materials Today*, 2006, **9**, 44.
- [3] S. Dos Santos, A. Chandravarkar, B. Mandal, R. Mimna, K. Murat, L. Saucedo, P. Tella, G. Tuchscherer and M. Mutter, *J. Am. Chem. Soc.*, 2005, **127**, 11888.
- [4] R. J. Mart, R. D. Osborne, M. M. Stevens and R. V. Ulijn, *Soft Matt.*, 2006, **2**, 822.
- [5] H. Leuchs, *Chem. Ber.*, 1906, **39**, 857; (b) H. Leuchs and W. Manasse, *Chem. Ber.*, 1907, **40**, 3235; (c) H. Leuchs and W. Geiger, *Chem. Ber.*, 1908, **41**, 1721.
- [6] W. A. Braunecker and K. Matyjaszewski, *Prog. Polym. Sci.*, 2007, **32**, 93.
- [7] F. M. Veronese, *Biomaterials*, 2001, **22**, 405.

- [8] C. W. Bielawski and R. H. Grubbs, *Prog. Polym. Sci.*, 2007, **32**, 1.
- [9] D. Smith, E. B. Pentzer and S. T. Nguyen, *Polym. Rev.*, 2007, **47**, 419.
- [10] T. J. Deming, *Adv. Polym. Sci.*, 2006, **202**, 1.
- [11] H. R. Kricheldorf, C.V. Lossow and G. Schwarz, *Macromol. Chem. Phys.*, 2005, **206**, 282.
- [12] Y. Dai, M. Xu, J. Wei, H. Zhang and Y. Chen, *Appl. Surf. Sci.*, 2012, **258**, 2850.
- [13] R. V. Ulijn and A. M. Smith, *Chem. Soc. Rev.*, 2008, **37**, 664.
- [14] M. Kar, P. S. Vijayakumar, B. L. V. Prasad, and S. S. Gupta, *Langmuir*, 2010, **26**, 5772.
- [15] F. Yang, L.-M. He, H. Yi, G. Zou, J. Tang and M.-Y. He, *J. Mol. Catal. A: Chem.*, 2007, **273**, 1.
- [16] J. D. Lunn and D. F. Shantz, *Chem. Mater.*, 2009, **21**, 3638.
- [17] W. H. Daly and D. Poche, *Tetrahedron Lett.*, 1988, **29**, 5859.
- [18] C.O. Kim, *J. Colloid Interf. Sci.*, 2003, **24**, 374.
- [19] A. Enrico, C. Carlo, M. Giovanni and V. J. Paolo, *J. Chem. Soc., Perkin Trans. 1*, 1989, 105.
- [20] C. Anne, R. Gilbert and B. Daniel, *J. Org. Chem.*, 1997, **62**, 749.
- [21] S. K. Sahu, S. P. Panda, D. S. Sadafule, C. G. Kumbhar, S. G. Kulkarni and J. V. Thakur, *Polym. Degrad. Stab.*, 1998, **62**, 495.
- [22] Yu. Li and B. C. Benicewicz, *Macromolecules*, 2008, **41**, 21.
- [23] H. Y. Tian, C. Deng, H. Lin, J. Sun, M. Deng, X. Chen and X. Jing, *Biomaterials*, 2005, **26**, 4209.
- [24] K. Kataoka, A. Ishihara, A. Harada and H. Miyazaki, *Macromolecules*, 1998, **31**, 6071.

- [25] D. J. Ager, I. Prakash and D. Schad, *Chem. Rev.*, 1996, **96**, 835.
- [26] L. S. Goodman and A. Gilman, *The Pharmacological Basis of Therapeutics*, 6th ed.; Macmillan: New York, 1980, 1-6.
- [27] G. A. Rogers, S. M. Parson, D. C. Anderson, L. M. Nilsson, B. A. Bhar, W. D. Kornereich, R. Kaufman, R. S. Jacobs and B. Kirtman, *J. Med. Chem.*, 1989, **32**, 1217.
- [28] C. Auvin-Gutte, S. Rebuffat, V. Prigent and B. Bodo, *J. Am. Chem. Soc.*, 1992, **114**, 2170.
- [29] S. Wu, R. Takeya, M. Eto and C. Tomizawa, *J. Pestic. Sci.*, 1987, **12**, 221.
- [30] E. J. Corey, R. K. Bakshi, S. Shibata, C. P. Chen and V. K. Sing, *J. Am. Chem. Soc.*, 1987, **109**, 7925.
- [31] J. A. Deyrup and C. L. Moyer, *J. Org. Chem.*, 1969, **34**, 175.
- [32] J. Wu, and H. -G.Xiaa, *Green Chem.*, 2005, **7**, 708.
- [33] V. T. Kamble and N. S. Joshi, *Green Chem. Lett. Rev.*, 2010, **3**, 275.
- [34] T. Ollevier and G. Compin, *Tetrahedron Lett.*, 2004, **45**, 49.
- [35] Y. Harrak and M. D. Pujol, *Tetrahedron Lett.*, 2002, **43**, 819.
- [36] P. Van de Weghe and J. Collin, *Tetrahedron Lett.*, 1995, **36**, 1649.
- [37] G. Sekar and V. K. Singh, *J. Org. Chem.*, 1999, **64**, 287.
- [38] L. R. Reddy, M. A. Reddy, N. Bhanumati, K. R. Rao, *Synthesis*, 2001, **6**, 831.
- [39] M. Tajbakhsh, R. Hosseinzadeh, P. Rezaee, and H. Alinezhad, *J. Mex. Chem. Soc.*, 2012, **56**, 402.
- [40] G. Rajesh Krishnan and K. Sreekumar, *Polymer*, 2008, **49**, 5233.
- [41] J. R. Rodriguez and A. Navarro, *Tetrahedron Lett.*, 2004, **45**, 7495.
- [42] K. S. Babu, B. C. Raju, S. Praveen Kumar, S. G. Mallur, S. V. Reddy and J. M. Rao, *Synth. Commun.*, 2005, **35**, 879.

- [43] A. Kamal, R. Ramu, Mohd. A Azhar and G. B. Ramesh Khanna, *Tetrahedron Lett.*, 2005, **46**, 2675.
- [44] J. Iqbal and A. Pandey, *Tetrahedron Lett.*, 1990, **31**, 575.
- [45] F. Carree, R. Gil and J. Collin, *Tetrahedron Lett.*, 2004, **45**, 7749.
- [46] B. Tang, W. Dai, X. Sun, G. Wu, N. Guan, M. Hunger and L. Li, *Green Chem.*, 2015, **17**, 1744.
- [47] S. Meninno and A. Lattanzi, *Chem. Eur. J.*, 2016, **22**, 3632.
- [48] S. Bonollo, D. Lanari and L. Vaccaro, *Eur. J. Org. Chem.*, 2011, 2587.
- [49] J. Hine, S. -M. Linden and V. M. Kanagasabapathy, *J. Am. Chem. Soc.*, 1985, **107**, 1082.
- [50] S. J. Connon, *Synlett*, 2009, 354.
- [51] C. M. Kleiner, P. R. Schreiner, *Chem. Commun.*, 2006, 4315.

Chapter 7

SUMMARY AND CONCLUSION

Development of heterogeneous catalysts has become a major area of research in synthetic organic chemistry due to the potential advantages of these materials over homogeneous systems. Easy recovery, reusability, easy product isolation, enhanced selectivity and reactivity are some of the advantages of heterogeneous catalysts. Periodic mesoporous materials have attracted much interest because, these materials have regular pore morphologies, controllable pore sizes, and large surface area which enable these materials to be widely useful in the area of catalysis, separations, high performance composites etc. During the last two decades, hybrid mesoporous solids have been considered for a wide range of heterogeneous catalysis reactions. Chemically modified mesoporous silica are environmentally compatible materials. They are found to have enormously diverse potential as benign replacements for the many hazardous and environmentally threatening chemicals that we have used as catalysts in chemical manufacturing process.

The focus of this thesis was the design and synthesis of novel polyamine (Lewis base) and Lewis acid functionalized silica materials. Most of the works discussed in this field, used conventional synthetic strategies which resulted in low amount of organic functionality. So our prime

intention was to develop catalysts with high density of active sites on mesoporous material. Using the different synthetic strategies, we have achieved high amount of active sites on silica framework. The synthesis and characterization of functionalized mesoporous silica as well as tuning this organic/inorganic hybrid material for application in multicomponent reactions and C-C bond forming reactions have been described in this thesis.

The thesis was divided in to seven chapters. An overview of different types of periodic mesoporous silica, their synthesis and organically modified silica through diverse functionalization methods and a survey of recent literature on organic reactions catalyzed by functionalized mesoporous silica was given in **chapter 1**.

Chapter 2 has dealt with the synthesis and characterization of N,N-dialkylated polyamine mesoporous silica catalyst. Ring opening polymerization of epichlorohydrin by thiol functionalized mesoporous silica (MS) was carried out. High density of tertiary amine could be developed on the silica surface and catalytic activity was studied in the synthesis of α -amino nitriles in water. Various factors which control the reaction were studied and the mechanism was also proposed. A variety of carbonyl compounds, and amines have shown to undergo the reaction under mild experimental condition. The prepared catalyst showed higher turnover frequency in Strecker amino acid synthesis.

In **Chapter 3**, the synthesis and characterization of Ti-grafted polyamidoamine dendritic silica hybrid catalyst was explained. A simple, highly efficient and eco-friendly approach for the preparation of biologically

potent pyranopyrazoles and 3,4-dihydropyrimidin-2(*IH*)-ones were discussed in this chapter. The experimental parameters were optimized, scope of substrates and reusability of the catalyst were studied. The dual activation mechanism of the hybrid catalyst was also proposed. It was found that this dendritic silica hybrid catalyst exhibited high catalytic activity in the synthesis of 3,4-dihydropyrimidin-2-one under solvent free condition and pyranopyrazoles in aqueous medium. Dual nature of the hybrid catalyst played a vital role in the mechanism of both the reactions by activating the formation of intermediates resulting in the desired products in excellent yield within short period of time.

Chapter 4 has dealt with the synthesis and characterization of polyamine and chiral amine functionalized mesoporous silica (MS I). Novel N-alkylated polyamine functionalized mesoporous silica was synthesized via radical polymerization of α -methyl styrene within silica framework followed by post-functionalization method. The catalyst was found to be active for the synthesis of flavanone by the Claisen-Schmidt condensation of benzaldehyde and 2-hydroxyacetophenone under solvent free condition. Chiral amine functionalized silica catalyst was employed for asymmetric Mannich reaction. Various factors which control the reactions were studied and the mechanisms of both the reactions were also proposed. In flavanone synthesis, better selectivity and higher conversion was obtained under solvent free condition. Enantiomeric excess of the isolated product was found to be 60-90 % in asymmetric Mannich reaction. This novel supported organocatalyst allowed easy recovery and avoided significant leaching of active sites.

Chapter 5 has demonstrated the synthesis and characterization of mesoporous silica (MS)-supported N-heterocyclic carbene (NHC)-Pd complex. Catalytic applications of the NHC-Pd complex in Suzuki coupling and direct arylation reactions were described. The experimental parameters were optimized, scope of substrates, reusability of the catalyst and mechanism were studied. This novel silica supported catalyst showed excellent activity in Suzuki cross-coupling reaction of various aryl iodides and bromides with phenylboronic acid in DMF/water medium. Donor-Acceptor system like bis-arylated 3,4-(ethylenedioxythiophene) was synthesized via direct arylation reaction. This push-pull system may find application in molecular electronics and optical devices. Catalyst showed outstanding recyclability without any significant loss of activity.

In **Chapter 6**, the synthesis and characterization of polypeptide functionalized mesoporous silica (MS) was discussed. Ring opening polymerization (ROP) of N-carboxyanhydride (NCA) chemistry was applied in this chapter. This novel catalyst was used as supported organo catalyst in aminolysis of epoxides. The experimental parameters were optimized, scope of substrates, reusability of the catalyst and mechanism were studied. The catalyst was recycled and reused without considerable loss of activity.

In general, the thesis has described the synthesis, characterization and environmentally friendly catalysis by functionalized mesoporous silica. High accessibility of active site and ordered porous nature of the support allowed use of small amount of catalyst and shorter reaction time. All the synthesized catalysts exhibited negligible leaching of active sites after

recycling. So the proposed solid catalysts provided a prominent solution for boosting the activity of supported catalyst in many organic reactions. So the present thesis combines the synergistic effect of green chemistry with functionalized mesoporous silica materials and opens new possibilities for the development of environmentally friendly and efficient catalysts in synthetic organic chemistry. The prepared catalysts could also be used for similar MCR reactions and C-C bond forming reactions. Further investigations on the application of these catalysts for other organic reactions are in progress.

Publications

Papers Published in International Journals

- [1] Facile synthesis of pyranopyrazoles and 3,4-dihydropyrimidin-2(1*H*)-ones by Ti-grafted polyamidoamine dendritic silica hybrid catalyst via dual activation route, **P. S. Sinija** and K. Sreekumar, *RSC Adv.*, 2015, **5**, 101776.
- [2] Palladium(II) supported on polycarbosilane: Application as reusable catalyst for Heck reaction, K. Mangala, **P. S. Sinija** and K. Sreekumar, *J. Mol. Catal. A: Chem.*, 2015, **407**, 87.

Conferences Papers

- [1] **P. S. Sinija** and K. Sreekumar, Solvent free method for Biginelli reaction catalyzed by Ti(IV) incorporated polyamidoamine dendritic silica hybrids by a dual activation route. 27th Kerala Science Congress, 2015 Alapuzha.
- [2] **P. S. Sinija** and K. Sreekumar, Ti-grafted polyamidoamine dendritic silica hybrid catalyst in pyranopyrazole synthesis- An Ecofriendly approach. 24th Swadeshi Science Congress, Thunchathezhuthachan Malayalam University, Tirur, Kerala, ISBN: 978-81-928129-2-2.
- [3] **P. S. Sinija** and K. Sreekumar, N-alkylated polyamine functionalized mesoporous SBA-15 hybrid material as a solid Lewis base catalyst in flavanone synthesis-an ecofriendly approach. 14th Prof. K.V Thomas endowment national seminar, The Sacred Heart College, Thevara, Kochi.
- [4] **P. S. Sinija** and K. Sreekumar, Development of a Polyamine functionalized mesoporous SBA-15 hybrid material and its catalytic activity in Flavanone synthesis under solvent free condition. International Conference on Materials for the Millenium, Mat Con-2016, Department of Applied Chemistry, Cochin-22, ISBN: 978-93-800-95-738.